GLACIAL SUSPENDED PARTICULATE MATTER: CHARACTER, COMPOSITION AND ADSORPTION POTENTIAL IN FRESHWATER ENVIRONMENTS

A thesis submitted in partial fulfilment of the requirements for the Degree of Doctor of Philosophy in Water Resources Management at the University of Canterbury

by Phil Clunies-Ross

University of Canterbury

November 2017

Abstract

Suspended particulate matter (SPM) plays an important role in regulating the transport and bioavailability of toxic trace elements and nutrients in natural waters. This research addresses the absence of data on glacier-fed catchments, which are likely to undergo accelerated changes in water quality and SPM concentration as glacial recession proceeds into the future.

The glacier-fed Waitaki catchment has been subjected to intensive agricultural development in recent decades. The ability of the glacial SPM to adsorb phosphorus (P), cadmium (Cd) and copper (Cu), contaminants that are commonly associated with agrichemical applications, was determined with laboratory and modeling experiments. The SPM was first characterised in terms of its mineralogy and morphology, particle size, trace element content and degree of particle weathering. High concentrations of SPM occurred close to the glacial source, characteristically dominated by extremely fine inorganic particles (quartz, mica, feldspar) with a low degree of chemical weathering compared to the source rock. Major evolutions in SPM character occurred down-catchment. SPM concentrations declined significantly, becoming progressively weathered and enriched in organic matter, diatoms and aggregates, with corresponding reductions in the concentrations of reactive surface oxides and specific surface area (SSA).

The adsorption capability of the Waitaki SPM was determined by adsorption edge and isotherm experiments. The fresh glacial SPM was found to have the greatest capacity to adsorb P, which was attributed to the relatively high SSA and greater concentrations of reactive iron (Fe) oxides associated with the fine sediments. Down catchment, the SPM was found to have a greater capacity to adsorb Cu, which was attributed to the significant influence of organic matter. The low affinity of Cd for SPM throughout the catchment limited its adsorption generally. The novel measure of ‘adsorption potential’ conceived in this study, a function of the variable SPM concentrations and its adsorption capacity, indicated that SPM will readily adsorb Cu throughout the catchment. However, the adsorption of P and Cd will be highly constrained by the concentrations of SPM that remain in solution. Down catchment, the adsorption potential of the SPM declined by up to three orders of magnitude. As such, the SPM may not play an appreciable role in the attenuation of these

contaminants as land-use modification and climate change proceed into the future. Instead, the biogeochemical cycling of these elements is predicted to be largely controlled by adsorption onto surface sediments and uptake by aquatic biota.

The role of glacial SPM as a vector for the nutrient P was determined in the polar Onyx River catchment, Antarctica. The Onyx River is the largest meltwater stream in Antarctica, flowing inland and into the ultra-oligotrophic Lake Vanda. The system is generally considered to be P-limited and is one of the least biologically productive and clearest lakes in the world. Suspended particulate matter was collected from the Onyx River during the 2016/17 K802 sampling campaign with Antarctica New Zealand. The SPM was dominated by fine, inorganic particles (mica, smectite, chlorite, quartz) with a high degree of roundness. Sequential extractions indicated that the majority of the SPM P was associated with primary phosphorus-containing minerals (such as apatite) and is not expected to be readily bioavailable. Less than 20% was found to be associated with reactive metal oxides (Fe and Mn), clay minerals and organic matter. However, this may be liberated for metabolic uptake when incorporated into benthic mats, or exposed to the highly reducing conditions present in the bottom waters of Lake Vanda. In oxic waters, the SPM is predicted to be an efficient scavenger of dissolved P. The flux of SPM in the Onyx River catchment was predicted over a 20 year period with the generation of an SPM-discharge rating curve. This was applied to flow data collected by the McMurdo Long Term Ecological Research Network (LTER). The predicted SPM loads for the annual melt seasons were highly variable, ranging from 1.0 – 908.7 tonnes. So too were the predicted quantities of P, with loads varying from 0.6 – 515.2 kg of P. High flow events, such as those during the 2001/02 and 2008/09 austral summers, resulted in SPM loads up to three orders of magnitude greater than typical years. As such, the dominant source of P to the catchment is likely to be during these episodic events, which are predicted to have a long-lasting effect on the ecological productivity of the lake. An increase in the frequency of flood events caused by anthropogenic climate change may initiate a profound shift in the physicochemical characteristics of Lake Vanda, and its biological structure and diversity.

Table of Contents

Contents

List of Figures

List of Tables

Acknowledgements

First and foremost I would like to thank my supervisors Sally Gaw and Adam Hartland for their patience, encouragement and guidance throughout this research. My sincere gratitude goes to Sally for getting me going at UC, giving her time so generously, and providing an opportunity to take on the media. Cheers to Adam for his expertise and valuable critique of this research. It was fantastic to come work with you and the lovely Helen Turner in the "Tron". It's been a privilege.

I extend a very special and dedicated thank you to Suellen Knopick. Her daily enthusiasm, encouragement and advice has been absolutely invaluable throughout the duration of this work. I am also extremely grateful to Nik Lehto at Lincoln University, who provided exceptional training in the dark art of DGT, and general good chat. Thank you to John Revell, Emma McKenzie and Warwick Hill who have helped me enormously in the lab, and in the construction of the various gadgets used in this research. I am also indebted to Rob Stainthorpe, Nick Oliver and Wayne Mackay for all their help over in the chemistry department. Cheers also to Michael Sandridge and Rayleen Hendricks at engineering, and to Nancy Bertler and Uwe Morgenstern for allowing me to come to the GNS lab in Wellington and attack the Tasman Glacier ice-core.

A massive thanks to Paul Mason, James McKay and Emmanuel Buzobozi for joining me in the field and being patient through the crazy hours of collecting and filtering water! Cheers to Maria "Like Dis" Monteiro who joined me in the Dry Valleys, Antarctica and was a constant source of entertainment in the field. Thanks also to everyone at Antarctica New Zealand, who helped get us there and ensure our field event went without a hitch. You couldn't have offered more to look after us throughout the journey. Cheers to everyone at Waterways and Gateway Antarctica for your kindness and inspiration in and out of the lab. That includes you Tara McAllister, Qian Hu, Marlese Fairgray, Christian Wild, Rachel Innes, Gemma De Breit and Michelle Ryan. I am particularly grateful to Sean Waters who helped me along and provided me with methodology and sage advice.

I would like to express my gratitude to the University of Canterbury, the Waterways Centre and Meadow Mushrooms for your generous funding of this research. Grants from the Canterbury branch of the Royal Society and the Claude McCarthy Fellowship allowed me to attend international conferences in Hobart, Australia and Paris, France. Many thanks for your support.

I can't thank my family and friends enough for your endless support. I couldn't have done it without you. Last but not least, I thank Olivia Barclay for your love and endless enthusiasm.

Abbreviations

BD	Bicarbonate/dithionite
CEC	Cation Exchange Capacity
CIA	Chemical Index of Alteration
DGT	Diffuse Gradients in Thin-Films
DIC	Dissolved inorganic carbon
DLM	Diffuse Layer Model
DO	Dissolved oxygen
DRP	Dissolved reactive phosphorus
ECan	Environment Canterbury Regional Council
EDS	Energy-dispersive X-ray spectroscopy
HAO	Hydrous Aluminium Oxide
HFO	Hydrous ferric oxide
ICP-MS	Inductively coupled plasma- mass spectrometry
ICP-OES	Inductively coupled plasma- optical emission spectrometry
IEP	Isoelectric Point
K_d	Linear Partition Coefficient
LWGS	Lower Wright Glacier Stream
MDV	McMurdo Dry Valleys
NIWA	National Institute of Atmospheric and Water research
NOM	Natural Organic Matter
OLW	Onyx River at Lower Wright Weir
OVW	Onyx River at Vanda Weir
POM	Particulate Organic Matter
PSD	Particle Size Distribution
PZC	Point of Zero Charge
SCM	Surface Complexation Model
SEM	Scanning Electron Microscopy
SHM	Stockholm Humic Model
SI	Saturation index
SPM	Suspended Particulate Matter
SSA	Specific Surface Area
TIMS	Time-Integrated Mass-Flux Sampler
TOC	Total Organic Carbon
TP	Total phosphorus
UWV	Upper Wright Valley
WIP	Weathering Index of Parker
XRD	X-ray diffraction

1. Introduction

1.1 Motivation

The dissolved concentrations of toxic trace metals, nutrients and organic contaminants in surface waters are strongly influenced by sorption-desorption processes on the surfaces of suspended particulate matter (SPM) (Gregory, 2006). As many pollutants are more bioavailable to aquatic biota in their dissolved form, the binding of trace contaminants and nutrients onto SPM is an important process regulating their transport and toxicity (Florence et al., 1980; Tessier and Campbell, 1987).

Previous studies of lowland rivers and urban streams have confirmed the ability of SPM to adsorb dissolved trace metals and nutrients (Bibby and Webster-Brown, 2005; House et al., 1995; Webster-Brown et al., 2012). However, there has been little investigation of the role of glacial SPM in this regard. Glaciers are an important source of freshly eroded sediments to downstream water bodies. The finest sediments suspend in the melt-water and scatter light, giving glacier-fed streams and lakes their characteristic colours and turbidity (Gallegos et al., 2008). The weathering of these particles also has an important influence on the geochemical composition of downstream waters (Anderson, 2007; Brown, 2002). However, little is known about their adsorption capability and how this varies spatially in downstream water bodies. Many glacier-fed rivers, both in New Zealand and internationally, traverse highly developed agricultural and urban environments, and the attenuation of anthropogenic contaminants sourced from these settings may play a key role in regulating the quality of the water. Glacial SPM may also be a critical source of nutrients to extreme, ice-marginal ecosystems located in polar regions. However, glaciers have been retreating at an accelerated rate over the industrial period (since 1850 AD) (Gardner et al., 2013; Immerzeel et al., 2010; Oerlemans, 1994), and the current influence of glacial SPM on water quality and contaminant attenuation may be ephemeral. Understanding the physicochemical and adsorption characteristics of glacial SPM will provide much needed data that provides a benchmark against future assessments during a period of anthropogenic climate change and catchment modification.

1.2 Suspended Particulate Matter

1.2.1 SPM: What is it and where does it come from?

The term "suspended particulate matter" (SPM) refers to any particle that suspends in the water column of an aquatic environment. Suspended sediments are a common component and typically include quartz, aluminosilicates (such as feldspars and clays) and hydrous metal oxides. Organic components may include microorganisms (viruses, bacteria, diatoms and algae) and detritus originating from the biological breakdown of plant and animal remains (Gregory, 2006; Lead et al., 1999). The character and composition of the SPM is ultimately determined by the characteristics of the catchment. In lowland environments, SPM is commonly a heterogeneous mix of inorganic, organic and biological components (**Figure 1.1**). Much is sourced from erosion of the surrounding catchment, with significant quantities transported into the system during rainfall (Droppo, 2001; Van Rijn, 1993). In fresh glacial meltwaters, SPM is dominated by fine suspended inorganic particles (Anderson, 2007).

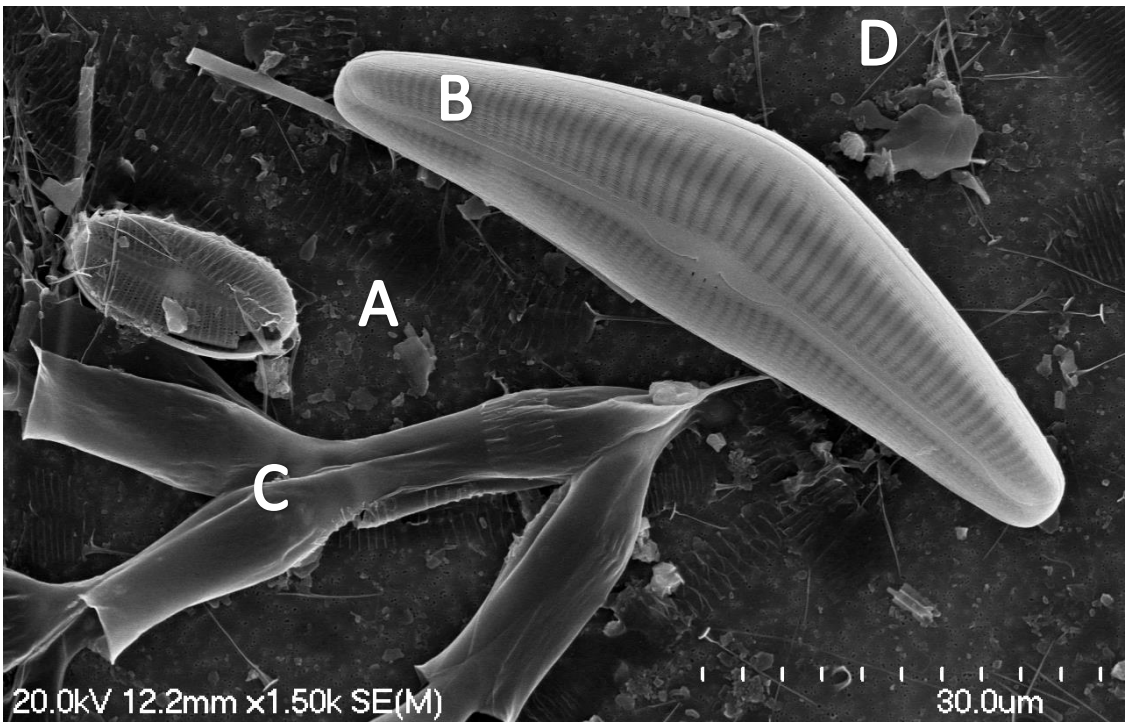

Figure 1.1. Suspended Particulate Matter (SPM) consisting of inorganic particles (A), diatoms (B), algae (C) and organic detritus (D). Sample collected from Lake Benmore, situated in the Lower Waitaki catchment, Canterbury, New Zealand. Image Credit: Phil Clunies-Ross

1.2.2 Glacial SPM

Glaciers are slow moving bodies of ice that are commonly located in alpine and polar environments where snowfall exceeds ablation. Due to sheer mass, glaciers have a considerable capacity to erode their underlying landscapes (Paterson, 1994). This process can result in the production of extremely fine-grained sediments which are entrained in the glacial ice and may be liberated during periods of glacial melt (Tranter, 2006). Glaciers can therefore function as storage reservoirs for both water and sediment (Jansson et al., 2003).

Glaciers have varying physical characteristics that are dependent on the geographic setting in which they are located (Benn and Evans 2010). The physicochemical characteristics of the SPM associated with glacial meltwaters can also vary. These characteristics are dependent on the environmental conditions under which the SPM is generated. An overview of the different glacial environments, and the associated mechanisms of SPM production is provided below.

Alpine Glaciers:

Glaciers in temperate alpine environments are typically "warm-based". This means that the ice sitting at the interface with the bedrock is above the pressure melting point, allowing for the subglacial flow of meltwater (Paterson, 1994). The presence of liquid water effectively lubricates the glacier and allows for basal sliding. This is a much faster and more efficient mode of glacial movement than internal ice deformation, where the glacial mass causes ice crystals to slide past one another (Anderson, 2007; Paterson, 1994). Warm based glaciers can therefore be highly erosive and generate massive volumes of fine grained sediments through the crushing and abrasion of rock (Clarke, 2004; Hallet et al., 1996). The rock may be derived from rock fall (avalanches, valley slips) or plucked from the underlying bedrock. Rock that becomes entrained in the glacial ice is subjected to reworking by glacial grinding (Boulton, 1978; Harvie, 2011).

The transport of sediment within the glacial environment is enhanced by the presence of meltwater. Water derived from snow- and ice-melt may flow through supraglacial channels and canyons that cut into the glacial surface. It may also plunge into the glacier via moulins and crevasses. Within the glacier, meltwater may travel slowly (<0.05 m s^{-1}) through permeable, subglacial sediments and cavities in the glacier. Rapid transport (up to 1 m s^{-1}) can also occur in channelized

systems incised into the basal ice layer (Hambrey and Glasser, 2014). In any case, the meltwater can accumulate and transport significant quantities of sediment from the subglacial environment to receiving water bodies. The quantities of which are highly variable and dependent on both seasonal and diurnal cycles (Brown, 2002).

Glacial sediments are subjected to considerable stresses during the process of glacial grinding. As a result, the fine sediments generated during this process have characteristic angular shapes and distinctive micro-features on their surfaces (Whalley and Krinsley, 1974). Such features (including striations, grooves, and troughs) may enhance the reactive surface area of the sediment and its susceptibility to chemical weathering (Anderson, 2007). Alpine glacial SPM is also typically deficient in attached bacteria and organic coatings compared to the particles found in productive aquatic ecosystems (Sommaruga and Kandolf, 2014).

Polar Glaciers

Glaciers in polar environments may be broadly categorised as being "polythermal" or "cold-based". Cold based glaciers have ice below the pressure melting point and are frozen to the underlying bedrock. As such, the movement of these glaciers is mostly constrained to internal ice deformation processes (Anderson, 2007; Paterson, 1994). Subglacial debris may be entrained in the glacial ice due to shearing processes occurring at the contact point of ice and substrate (Cuffey et al., 2000; Hambrey and Glasser, 2014; Hambrey and Fitzsimons, 2010). However, the erosive forces are comparatively low compared to alpine glacial movement and significantly reduces their capacity to generate fine sediments. Sediments derived from cold based glaciers do not typically have the same array of microfeatures characteristic of alpine glacial SPM. Instead, much of the sediment is sourced from aeolian deposition and has characteristic sub-rounded and sub-angular shapes (Mahaney, 2011).

Polythermal glaciers can exist in both polar and sub-polar environments. They are characterised by having a combination of both "cold-based" and "warm-based" ice. The entrainment of subglacial debris and bedrock commonly occurs where there is a transition from frozen bed to sliding bed conditions. Pressure melting and refreezing (regelation) may also result in the entrainment of debris, which is then subject to crushing, fracturing and abrasive processes at the ice/bedrock interface. Polythermal glaciers are erosive in nature (Hambrey and Glasser, 2012; Paterson, 1994).

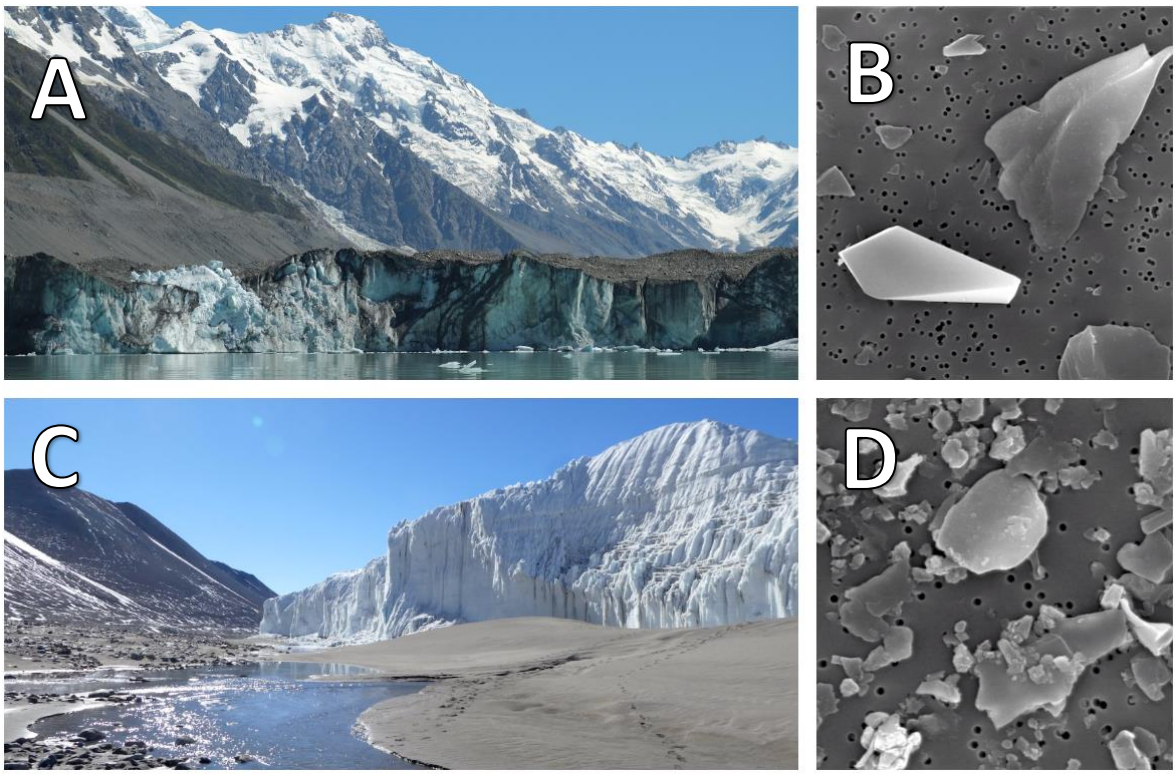

Figure 1.2. A) The Tasman Glacier is New Zealand's largest glacier. The glacier terminates into Lake Tasman, a large proglacial lake formed by glacial recession. B) Angular sediment from the Tasman Glacier ice. C) The Lower Wright Glacier, located in the Dry Valleys of Antarctica. This glacier feeds the Onyx River, Antarctica's largest meltwater stream. D) Rounded sediments from the Lower Wright Glacier ice. Image Credits: A) Wikimedia Commons. B-D) Phil Clunies-Ross

1.3 Effects of Climate Change on Proglacial Aquatic Environments

A warming climate is causing many of the glaciers around the globe to thin and recede at dramatic rates (Oerlemans, 1994; Roe et al., 2017). It is generally expected that the increase in melt will enhance stream flows in the short term (Casassa et al., 2009), with corresponding increases in the flux of suspended sediments, nutrients and dissolved trace elements to proglacial environments (Huss et al., 2017; Milner et al., 2017). However, the progressive wasting of glaciers will ultimately limit meltwater runoff and the production of glacial sediments (Milner et al., 2017). In many alpine locations, the recession of glaciers has exposed deep basins carved into the bedrock or sedimentary deposits. Proglacial lakes have rapidly formed in response and may act as sedimentary basins, capturing suspended sediments before it is transported to downstream environments (Bogen et al., 2015; Carrivick and Tweed, 2013; Geilhausen et al., 2013).

The ramifications of climate change on proglacial aquatic systems are likely to be profound. In alpine environments, greater loads of SPM may initially act as a source or sink for dissolved trace elements and nutrients. This will be dependent on the extent of particle weathering and the adsorption capacity of the SPM. However, a reduced flux of meltwater and suspended sediment is expected to shift the biogeochemical conditions and biodiversity of proglacial aquatic systems (Milner et al., 2017; Sommaruga, 2015). In polar settings, a warming climate is enhancing both the duration and quantities of meltwater discharged into proglacial environments (Fountain et al., 2014; Quayle et al., 2002). The productivity of these settings is commonly limited by the availability of water and bioavailable nutrients. It is therefore expected that an increasing flux of meltwater, trace elements and nutrients (i.e. phosphorus) will drive primary production in both freshwater (Green and Lyons, 2009) and marine environments (Martin et al., 1990).

1.4 Adsorption Processes: Mechanisms and Influences

1.4.1 General Overview

The process of adsorption involves the interaction of a dissolved substance (the adsorbate) with a reactive functional group on the surface of an adsorbent material. This definition generally covers the interaction of ions with charged surfaces that are typical of interactions with glacial SPM, although hydrophobic interactions and hydrogen bonding are also forms of adsorption. Adsorption may be broadly categorised as specific or non-specific. Specific adsorption results in the formation of strong "inner sphere complexes", and involves chemical bonding (e.g. covalent bonds) which overcome electrostatic repulsion. Non-specific adsorption occurs when ions of opposite charge (counter ions) form electrostatic interactions via coulombic interaction. The resulting "outer sphere complexes" are comparatively weak and are highly sensitive to variations in the solution chemistry (Stumm and Morgan, 1970). Important surface functional groups include hydroxyl (OH^-) groups on the reactive surfaces of metal oxides and clay minerals, and amine (NH^{3+}), carboxyl (COO^-), phenolic ($-OH^-$) and sulfhydryl (SH^-) groups on the surfaces of organic matter (Smith, 1999).

1.4.2 Factors Determining Adsorption

The partitioning of dissolved elements onto the surfaces of SPM is a complex process that is determined by both the biogeochemical conditions of the water body and the physicochemical characteristics of the SPM. The following section provides a brief overview of these important influences.

Solution Chemistry

The speciation of an adsorbate largely influences its behaviour, bioavailability and toxicity in natural waters. This is primarily influenced by the pH, redox-potential, ionic strength and temperature of the solution, and the presence of competing adsorbates and complexing agents (Ruthven, 1984). The pH is often stated to be the "master variable", largely controlling the speciation of the adsorbate and the surface charge of an adsorbent material. The attraction of a counter-ion to a surface of opposite charge is a key driver of adsorption (Smith, 1999; Warren and Haack, 2001). Many adsorbents have a 'point of zero charge' (PZC), the pH at which the net surface charge on the particle is equal to zero (Noh and Schwarz, 1989). The binding of cations typically occurs at a pH > PZC, while the opposite is true for anions. Many have a characteristic region in which the adsorption dramatically increases over 1-2 pH units. This region is known as the "adsorption edge". These adsorption profiles are characteristic of the adsorbate, its concentration in solution, and its affinity for the adsorbing surface (Ruthven, 1984; Stumm and Morgan, 1970).

Particle Characteristics and Composition:

Adsorption processes are also influenced by the physicochemical characteristics of the adsorbent. Certain materials are more effective adsorbents than others. Common adsorbents in natural waters include hydrated iron (Fe) and manganese (Mn) oxides, clay minerals, carbonates, natural organic matter (NOM) and the reactive surfaces of aquatic biota (Gregory, 2006; Lead et al., 1999; Warren and Haack, 2001). Iron oxide minerals and natural organic matter (NOM) are ubiquitous in aquatic environments and are generally considered to be the most important adsorbents in natural waters (Stumm and Morgan, 1970). SPM usually contains a heterogeneous mix of these adsorbing surfaces that are present as both particulates and surface coatings.

Iron oxides commonly exist as nanoparticles adsorbed to the surface of particulate matter (Poulton and Raiswell, 2005; Raiswell et al., 2006). Due to their prevalence, amphoteric nature and

large surface area they play a key role in the adsorption of dissolved ions (Cornell and Schwertmann, 2003; Dzombak and Morel, 1990). In general, less crystalline phases have a greater specific surface area (SSA) and a higher adsorption capacity. For example, the poorly ordered ferrihydrite ($(Fe^{3+})_2O_3$ $0.5H_2O$) has a SSA of ~600 m^2. The more crystalline goethite (FeO(OH)) has a significantly lower SSA of ~50 m^2 (Cornell and Schwertmann, 2003).

Natural organic matter commonly forms surface coatings on the surfaces on inorganic particles in the natural environment. The adsorption occurs mainly through the affinity of the acidic functional groups of NOM for the reactive hydroxyl groups (OH^-) on the mineral surfaces (Davis, 1982). The coatings possess a negative electrostatic charge at neutral pH (Hartland et al., 2013), which can make them an effective adsorbent of cationic trace metals (Davis, 1982; Tipping, 2002).

The adsorption capacity of clay minerals is generally considered to be less than that of both secondary metal oxides and organic matter. Layered clay minerals (e.g. smectite) have a negative 'constant surface charge' which is independent of the solution characteristics. This is due to non-stoichiometric isomorphous substitution of cations within their lattice structure (Smith, 1999). However, in natural settings, the charge characteristics and adsorption potential of clay minerals are commonly modified by coatings of metal oxides and NOM (Davis, 1982; Zhuang and Yu, 2002). However, the prevalence of clay minerals as a primary component of SPM means their potential for adsorption cannot be ignored.

Particle Size

The adsorption capacity of particulate matter generally increases with reducing particle size. This is due to an increase in SSA, which exposes a greater number of potential binding sites (Ruthven, 1984). Colloidal particles 1 nm - 1 µm in size are increasingly being recognised in playing an important role in the adsorption and transport of trace elements in aquatic environments, owing to their large surface areas and enhanced sites of reactivity (Hartland et al., 2013).

The relative size of particulates will commonly evolve throughout their residence in an aquatic environment. Fast moving and turbulent water can keep large particles in suspension. However, these will commonly undergo sedimentation in low flow and quiescent conditions (i.e. lakes). Particle aggregates will also commonly form in the water column through a combination of physical, chemical and biological processes. They are commonly comprised of a matrix of fine-grained inorganic particles within a network of organic matter, including substances derived from microbial metabolism

such as extracellular polymeric substances (EPS) and humic acids (Elliott et al., 2011). Natural organic material (NOM) is highly cohesive and can stabilise particles in suspension through charge repulsion (Hartland et al., 2013). However, NOM can also enhance the formation of composite particles (Droppo, 2001). Aggregated particles have different hydrodynamic and reactive properties compared to individual particles. The effective grain size, porosity, shape and density of the particles are altered and this may change their adsorption properties (Elliott et al., 2011).

Weathering

Weathering refers to the transformation of materials in the natural environment, and is caused by a plethora of physical and chemical processes that modify the chemical structure of the material (McLennan, 1993). Physical weathering is mediated by the degradation of materials by water, ice, pressure and wind. During chemical weathering, water acts as the reactant and transforms rock, sediments and other primary minerals via hydrolysis and carbonation (Stumm and Morgan, 1970; Stumm et al., 1992). For example, primary minerals such as micas and feldspars are converted to secondary clays (such as kaolinite and montmorillinite), metal oxy/hydroxides (gibbsite ($Al(OH_3)$), Ferrihydrite ($(Fe^{3+})_2O_3 \bullet 0.5H_2O$)) and goethite ($FeO(OH)$); and carbonates such as calcite ($CaCO_3$) and dolomite ($CaMg(CO_3)_2$). Elements resilient to dissolution, such as Al, Fe and Ti, are commonly conserved (Brown, 2002). New minerals may also form in the geochemical conditions encountered in proglacial environments. The process is gradual and will affect the character, composition and adsorption characteristics of SPM throughout its residence in a catchment.

Glacial environments may have rates of mechanical erosion greatly exceeding the rate of chemical weathering (Brown, 2002). The proglacial sediments are therefore likely to exhibit a composition which is closer to that of the parent rock and may have high concentrations of readily soluble elements such as Ca and Na still present. For this reason, glacial sediments may be geochemically reactive and primed for weathering on contact with dilute meltwaters (Brown et al., 1996).

Sediments that have undergone weathering can be examined for tell-tale signs of weathering processes. For example, angular sediments with sharp corners and edges are unlikely to have been transported over a great distance. By contrast, weathered sediments that have been transported over a

large distance, or sourced from surrounding soil material, have more rounded and smooth edges (Mahaney, 2011).

1.5 Geochemical Modelling

It is often not practical or indeed, possible to use laboratory methods to determine the complex, molecular scale processes and interactions that determine the character and behaviour of dissolved chemicals and adsorbing surfaces. Geochemical models are able to predict these processes and can be very useful in the interpretation of laboratory data. They are also commonly used to predict responses to environmental perturbations. A general overview of the modelling techniques used in this research is provided in the following section.

1.5.1 Geochemical Speciation Modelling

Geochemical modelling is able to predict the speciation of chemical constituents in natural waters. Modelling software, including Visual Minteq, PHREEQC and the Geochemist's Workbench© employ databases of thermodynamic and kinetic data derived from laboratory experiments. Models such as MINTEQA2, PHREEQC and WATEQ4F use this data to predict the distribution of aqueous species and the dissolution and precipitation of solid phases. All are frequently used to interpret both experimental and field data.

1.5.2 Empirical Adsorption Models

Empirical adsorption models describe the adsorption of an adsorbate onto a reactive surface. The linear partitioning coefficient (K_d) and the Freudlich and Langmuir isotherms are examples that are frequently applied to experimental datasets to describe the adsorption behaviour and/or capacity of an adsorbing surface for a sorbate (**Figure 1.2**). The major limitation of empirical models is that they are based on data collected under specific laboratory conditions and do not mechanistically represent the system in question. As such they are only applicable in the conditions for which they have been developed (Ruthven, 1984; Smith, 1999).

The linear partition coefficient (K_d) considers the ratio of an adsorbate bound to a known mass of adsorbent material. The resulting isotherm has a linear distribution and, due to its simplicity, has

been extensively applied to laboratory experimental data. Tabulations of K_d values are widespread and have been compiled for various adsorbents, adsorbates and conditions (e.g. lake water or sea water) (Ruthven, 1984; Smith, 1999). The Freudlich and Langmuir isotherms are non-linear models and account for the fact that the K_d value of an adsorbing surface will decrease as reactive functional groups become partially saturated with the adsorbate. Both models have been extensively used in the literature to describe the adsorption behaviour of metal oxy/hydroxides, clay minerals and mixed composition samples such as SPM, sediment and soils. The Freudlich isotherm may be applied to non-ideal sorption scenarios on heterogeneous surfaces, with multiple adsorption layers possible (Foo and Hameed, 2010). The model assumes a decaying adsorption capacity but does not have an upper limit. The more commonly applied Langmuir isotherm considers the upper adsorption limit, assuming the adsorbing surface has a finite number of adsorption sites and that adsorption is limited to a monolayer coverage on the adsorbent. The model can therefore be used to predict the adsorption capacity of the adsorbent. However, the Langmuir approach often under predicts adsorption due to poly-layer surface adsorption frequently observed in experimental systems (Foo and Hameed, 2010; Ruthven, 1984).

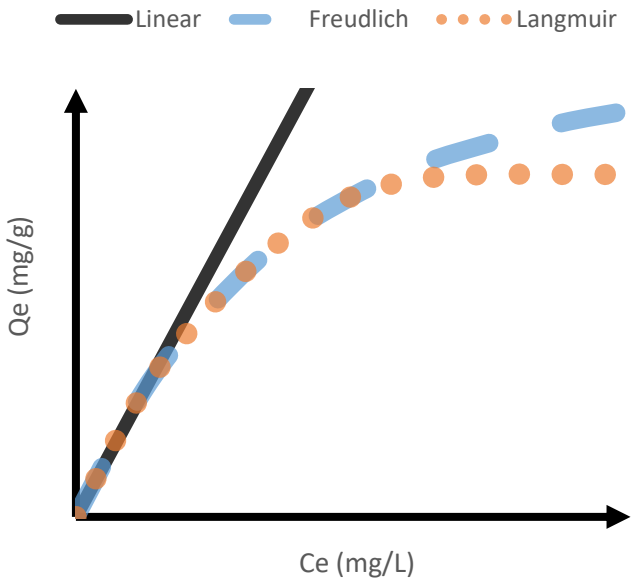

Linear Isotherm

$$q_e = K_d \cdot C_e \qquad (1.1)$$

Langmuir Isotherm

$$q_e = \frac{q_{max} K_L C_e}{1 + K_L C_e} \qquad (1.2)$$

Freudlich Isotherm

$$q_e = a_F C_e^{b_F} \qquad (1.3)$$

Figure 1.3. Schematic presenting the linear (black line), Freudlich (blue dashes) and Langmuir (orange dots) isotherms. The isotherms may be written with the corresponding equations (**1.1 – 1.3**) where Q_e = the concentration of bound P at equilibrium (mg/g); K_d = partition coefficient; C_e = equilibrium solution phase concentration of the adsorbate (mg/L) Qmax = Langmuir monolayer saturation capacity (mg/g); K_L = Langmuir isotherm constant (L/g); a_F = Freundlich isotherm constant; and b_F = Freundlich exponent.

1.5.3 Surface Complexation Models

Unlike empirical models, surface complexation models (SCMs) take a mechanistic approach that considers the physicochemical conditions of the solute, the associated chemical speciation and competitive effects that may arise in solution and on the adsorbing surface (Dzombak and Morel, 1990; Groenenberg and Lofts, 2014; Smith, 1999). They have been developed with experimental datasets which describe the thermodynamic behaviour of important reactive adsorbing phases (e.g. iron and aluminium oxy/hydroxides, organic matter, carbonates and clay minerals) with trace elements and nutrients whose mobility is of concern in the natural environment (Meeussen et al., 2009). Computational SCMs are commonly incorporated into geochemical modelling software. Surface complexation reactions are mathematically equivalent to aqueous reactions and can be solved using chemical thermodynamics in geochemical speciation models (including PHREEQC and MINTEQA2) to account for adsorption processes.

Surface complexation models consider the charge of both the adsorbate and adsorbing surface, and account for effects that may arise under variable solute conditions (Dzombak and Morel, 1990). For this reason, they may provide an advantage over empirical models when modelling outside-of-laboratory conditions (Groenenberg and Lofts, 2014). However, a thorough knowledge of the adsorbing surface is required before modelling can proceed. This is currently a challenging task in mixed composition samples such as SPM. Therefore, it is common practice to assume that a specific phase (e.g. iron oxide) is responsible for the majority of the adsorbing character (Dzombak and Morel, 1990). However, this often fails to account for many of the actual molecular scale mechanisms taking place on the particle surfaces. Surface complexation models can therefore be prone to significant error when compared to experimental data (Groenenberg and Lofts, 2014). Despite these limitations, SCMs are useful tools for predicting the behaviour, bioavailability and fate of contaminants in natural waters and as a tool for testing hypotheses in relation to the mechanics of adsorption in complex natural systems.

In recent years, major advancements have been made in the development and optimization of mechanistic models for important adsorbents such as Fe, Al and Mn oxides and organic matter. For Fe oxy/hydroxide, the generalized diffuse-layer model (DLM), first described by Dzombak and Morel (1990), is the most extensively developed and is widely used. The oxide/water interface is described as having two layers of charge. The first is an inner surface layer in which specifically adsorbed ions

(inner-sphere complexes) are assigned. The second is the diffuse layer which is occupied by non-specifically adsorbed ions (outer-sphere complexes), extending out from the particle surface and into solution. The charge on the adsorbing surface is limited by the number of binding sites and the pH of the solution (Dzombak and Morel, 1990). The constant capacitance, triple layer and charge distribution multi-site competitive adsorption model (CD-MUSIC) models are variations on the same theme, but have not been used herein and will not be described further in this thesis. In recent years the theoretical basis for the DLM has been applied to Al (Karamalidis and Dzombak, 2010) and Mn (Tonkin et al., 2004) oxides. Assemblage models combine SCMs to account for each of the reactive components (Groenenberg and Lofts, 2014), and are increasingly being used to predict the adsorption of dissolved ions onto more complicated mixtures of adsorbents such as SPM and sediments.

The modelling of adsorption processes onto the surface(s) of organic matter is complicated owing to its heterogeneous composition and variety of reactive functional groups. The WHAM (Tipping, 1994), NICA-Donnan (Kinniburgh et al., 1996), and Stockholm Humic (SHM) (Gustafsson, 2001) models are notable examples which are extensively utilised. All are comparable in the sense that they consider ions to adsorb to specific functional groups by electrostatic interactions. However, the models vary in the method of simulation, the heterogeneity and reactivity of adsorbing surfaces, and the associated site densities.

1.6 Research Rationale and Questions

Effective water quality monitoring requires a detailed understanding of the behaviour and fate of chemical contaminants. As suspended particulates significantly influence chemical speciation in natural waters, it is important that the physicochemical and adsorption characteristics of SPM are identified in different aquatic environments. This research will provide much-needed data on the character, composition and adsorption capability of glacial SPM, and how it may vary spatially in progressively downstream waters.

The primary aim of this research was to determine the character, composition and adsorption behaviour of glacial SPM in an alpine and polar environment. The alpine case study was conducted in the Waitaki River catchment, a large glacier-fed catchment located in Canterbury, New Zealand. The catchment is fed by a number of the country's most prominent glaciers that are currently in rapid retreat. The catchment has also been subject to rapid agricultural development in recent decades.

Between the years of 2003 – 2009, irrigation in the upper catchment had increased by 6000%, and has been further developed in recent years (**Figure 1.4)**. As associated increase in runoff and nutrient loading has resulted in the degradation of once pristine lakes located in the close vicinity of the developments (Clarke, 2015; Trolle et al., 2014). The ability of the glacial SPM to adsorb phosphorus (P), cadmium (Cd) and copper (Cu), pollutants that are commonly associated with agrichemical applications, was determined with laboratory and modelling experiments. The key questions addressed for this catchment were:

1. What is the character and composition of the SPM and how does this evolve down catchment?
2. Is the glacial SPM an effective adsorbent of P, Cd and Cu in the Waitaki catchment? What phases are implicated in the adsorption of these elements?
3. Can surface complexation models be used to predict the adsorption of Cd, Cu and P onto the glacial SPM?

The polar case study was conducted in the Onyx River catchment, located in the McMurdo Dry Valleys (MDVs) of Antarctica. The Onyx River is the largest meltwater stream in Antarctica and feeds the ultra-oligotrophic Lake Vanda, considered to be one of the least biologically productive and clearest lakes in the world (Canfield and Green, 1983). The adsorption of P onto the reactive surfaces of the SPM may play a key role in regulating the bioavailability of this limiting nutrient. However, little is known about the SPM, and its role as a vector for nutrients in the catchment. The key questions addressed for this catchment were:

1. What is the character and composition of the polar SPM in the meltwaters of the Onyx River catchment?
2. Is SPM an appreciable source of P to the ultra-oligotrophic Lake Vanda?
3. What is the speciation of the SPM P and is it likely to be bioavailable?

In both catchments, the evolution of the SPM was examined in progressively downstream sites from the glacial source. The weathering of the sediments associated with the SPM, and any changes to the adsorption capacity that may arise was determined using laboratory experiments. Empirical adsorption isotherms were used to predict the relative adsorption capacities of SPM throughout the catchments. Geochemical modelling in Visual Minteq (Gustafsson, 2014) was used extensively in this research to predict the speciation of chemical species in solution and assist in the interpretation of experimental data. Surface complexation models built into the software were used to assess the role

of metal oxides and organic matter in the adsorption of P, Cd and Cu. The data generated identified if key adsorption processes existed between glacial and non-glacial SPM. This in turn indicated whether models of contaminant adsorption and transport on SPM can be widely applied or need to be site specific.

Figure 1.4. Left – Agricultural developments in the direct vicinity of Lake Ruataniwha, a storage reservoir in the glacier-fed Waitaki catchment, New Zealand. The glacial influence of the water is evident from its brilliant blue hue. Right – The land surrounding the lower Waitaki River has been heavily modified for agricultural use. Image Credits: Google, DigitalGlobe 2017.

1.7 Thesis Outline

This thesis has been arranged into five main chapters (Chapters 2 – 6) which address the research aims and questions set out in Section 1.6. Chapters 2 – 4 focus on the character, composition and adsorption characteristics of SPM from the alpine Waitaki catchment. Chapters 5 and 6 focus on the Onyx River SPM, and its role as a transport agent for the nutrient P. Each chapter has been presented in the format of a scientific journal article. However, references have been made between chapters in an effort to avoid the repetitive description of laboratory methods that were used in both case studies. A final synthesis chapter incorporates the research findings and discusses limitations of the research and recommendations for future research and management of the catchments.

1.8 References

Anderson SP. Biogeochemistry of Glacial Landscape Systems. Annual Review of Earth and Planetary Sciences 2007; 35: 375-399.

Benn DI, Evans DJA. Glaciers and glaciation. London: Hodder Education, 2010.

Bibby RL, Webster-Brown JG. Characterisation of urban catchment suspended particulate matter (Auckland region, New Zealand); a comparison with non-urban SPM. Science of the Total Environment 2005; 343: 177-197.

Bogen J, Xu M, Kennie P. The impact of pro-glacial lakes on downstream sediment delivery in Norway. Earth Surface Processes and Landforms 2015; 40: 942-952.

Boulton GS. Boulder shapes and grain-size distributions of debris as indicators of transport paths through a glacier and till genesis. Sedimentology 1978; 25: 773.

Brown GH. Glacier meltwater hydrochemistry. Applied Geochemistry 2002; 17: 855-883.

Brown GH, Tranter M, Sharp MJ. Experimental Investigations of the Weathering of Suspended Sediment by Alpine Glacial Meltwater. Hydrological Processes 1996; 10: 579-597.

Canfield DE, Green WJ. Aspects of nutrient behavior in Lake Vanda. Antarctic Journal of the United States 1983; 18: p. 224-226.

Carrivick JL, Tweed FS. Proglacial lakes: character, behaviour and geological importance. Quaternary Science Reviews 2013; 78: 34-52.

Casassa G, López P, Pouyaud B, Escobar F. Detection of changes in glacial run-off in alpine basins: examples from North America, the Alps, central Asia and the Andes. Hydrological Processes 2009; 23: 31-41.

Clarke G. Upper Waitaki limit setting process. Predicting consequences of future scenarios: Lake water quality. Environment Canterbury, 2015.

Clarke GKC. Subglacial Processes. Annual Review of Earth and Planetary Sciences 2004; 33: 247-276.

Cornell RM, Schwertmann U. The Iron Oxides. Wiley, New York, 2003.

Cuffey KM, Conway H, Gades AM, Hallet B, Lorrain R, Severinghaus JP, et al. Entrainment at cold glacier beds. Geology 2000; 28: 351-354.

Davis JA. Adsorption of natural dissolved organic matter at the oxide/water interface. Geochimica et Cosmochimica Acta 1982; 46: 2381-2393.

Droppo IG. Rethinking what constitutes suspended sediment. Hydrological Processes 2001; 15: 1551-1564.

Dzombak DA, Morel FMM. Surface Complexation Modeling: Hydrous Ferric Oxide: Wiley, 1990.

Elliott AVC, Plach JM, Droppo IG, Warren LA. Comparative Floc-Bed Sediment Trace Element Partitioning Across Variably Contaminated Aquatic Ecosystems. Environmental Science & Technology 2011; 46: 209-216.

Florence TM, Batley GE, Benes P. Chemical Speciation in Natural Waters. C R C Critical Reviews in Analytical Chemistry 1980; 9: 219-296.

Foo KY, Hameed BH. Insights into the modeling of adsorption isotherm systems. Chemical Engineering Journal 2010; 156: 2-10.

Fountain AG, Levy JS, Gooseff MN, Van Horn D. The McMurdo Dry Valleys: A landscape on the threshold of change. Geomorphology 2014; 225: 25-35.

Gallegos CL, Davies-Colley RJ, Gall M. Optical closure in lakes with contrasting extremes of reflectance. Limnology and Oceanography 2008; 53: 2021-2034.

Gardner AS, Moholdt G, Cogley JG, Wouters B, Arendt AA, Wahr J, et al. A Reconciled Estimate of Glacier Contributions to Sea Level Rise: 2003 to 2009. Science 2013; 340: 852.

Geilhausen M, Morche D, Otto J-C, Schrott L. Sediment discharge from the proglacial zone of a retreating Alpine glacier. Zeitschrift f??r Geomorphologie, Supplementary Issues 2013; 57: 29-53.

Green WJ, Lyons WB. The Saline Lakes of the McMurdo Dry Valleys, Antarctica. Aquatic Geochemistry 2009; 15: 321-348.

Gregory J. Particles in Water: Properties and Processes. Boca Raton, Florida: CRC Press, Taylor and Francis Group, 2006.

Groenenberg JE, Lofts S. The use of assemblage models to describe trace element partitioning, speciation, and fate: A review. Environmental Toxicology and Chemistry 2014; 33: 2181-2196.

Gustafsson JP. Modeling the Acid–Base Properties and Metal Complexation of Humic Substances with the Stockholm Humic Model. Journal of Colloid and Interface Science 2001; 244: 102-112.

Gustafsson JP. Visual Minteq. KTH Royal Institute of Technology, KTH Royal Institute of Technology, 2014.

Hallet B, Hunter L, Bogen J. Rates of erosion and sediment evacuation by glaciers: A review of field data and their implications. Global and Planetary Change 1996; 12: 213-235.

Hambrey M, Glasser N. Sediment Entrainment, Transport, and Deposition. In: Singh V, Singh P, Haritashya U, editors. Encyclopedia of Snow, Ice and Glaciers. Springer Netherlands, 2014, pp. 984-1003.

Hambrey MJ, Fitzsimons SJ. Development of sediment–landform associations at cold glacier margins, Dry Valleys, Antarctica. Sedimentology 2010; 57: 857-882.

Hambrey MJ, Glasser NF. Discriminating glacier thermal and dynamic regimes in the sedimentary record. Sedimentary Geology 2012; 251-252: 1-33.

Hartland A, Lead JR, Slaveykova V, O'Carroll D, Valsami-Jones E. The Environmental Significance of Natural Nanoparticles. Nature Education Knowledge 2013; 4: 7.

Harvie ER. An integrated approach to landform genesis: case study of the Mueller Glacier (Thesis, Master of Science). University of Otago, 2011.

House WA, Denison FH, Armitage PD. Comparison of the uptake of inorganic phosphorus to a suspended and stream bed-sediment. Water Research 1995; 29: 767-779.

Huss M, Bookhagen B, Huggel C, Jacobsen D, Bradley RS, Clague JJ, et al. Toward mountains without permanent snow and ice. Earth's Future 2017; 5: 418-435.

Immerzeel WW, van Beek LPH, Bierkens MFP. Climate Change Will Affect the Asian Water Towers. Science 2010; 328: 1382.

Jansson P, Hock R, Schneider T. The concept of glacier storage: a review. Journal of Hydrology 2003; 282: 116-129.

Karamalidis AK, Dzombak DA. Surface Complexation Modeling: Gibbsite: John Wiley & Sons, Inc., 2010.

Kinniburgh DG, Milne CJ, Benedetti MF, Pinheiro JP, Filius J, Koopal LK, et al. Metal Ion Binding by Humic Acid: Application of the NICA-Donnan Model. Environmental Science & Technology 1996; 30: 1687-1698.

Lead JR, Hamilton-Taylor J, Davison W, Harper M. Trace metal sorption by natural particles and coarse colloids. Geochimica et Cosmochimica Acta 1999; 63: 1661-1670.

Mahaney WC. SEM Analysis of Glacial Sediments. In: Singh VP, Singh P, Haritashya UK, editors. Encyclopedia of Snow, Ice and Glaciers. Springer Netherlands, Dordrecht, 2011, pp. 1016-1027.

Martin JH, Fitzwater SE, Gordon RM. Iron deficiency limits phytoplankton growth in Antarctic waters. Global Biogeochemical Cycles 1990; 4: 5-12.

McLennan SM. Weathering and Global Denudation. The Journal of Geology 1993; 101: 295-303.

Meeussen JCL, Van Der Sloot HA, Dijkstra JJ, Kosson DS. Review of Thermodynamic and Adsorption Databases. International Atomic Energy Agency, 2009.

Milner AM, Khamis K, Battin TJ, Brittain JE, Barrand NE, Füreder L, et al. Glacier shrinkage driving global changes in downstream systems. Proceedings of the National Academy of Sciences 2017; 114: 9770-9778.

Noh JS, Schwarz JA. Estimation of the point of zero charge of simple oxides by mass titration. Journal of Colloid and Interface Science 1989; 130: 157-164.

Oerlemans J. Quantifying Global Warming from the Retreat of Glaciers. Science 1994; 264: 243-245.

Paterson WSB. The Physics of Glaciers (Third Edition). Pergamon, Amsterdam, 1994, pp. 158-172.

Poulton SW, Raiswell R. Chemical and physical characteristics of iron oxides in riverine and glacial meltwater sediments. Chemical Geology 2005; 218: 203-221.

Quayle WC, Peck LS, Peat H, Ellis-Evans JC, Harrigan PR. Extreme Responses to Climate Change in Antarctic Lakes. Science 2002; 295: 645.

Raiswell R, Tranter M, Benning LG, Siegert M, De'ath R, Huybrechts P, et al. Contributions from glacially derived sediment to the global iron (oxyhydr)oxide cycle: Implications for iron delivery to the oceans. Geochimica et Cosmochimica Acta 2006; 70: 2765-2780.

Roe GH, Baker MB, Herla F. Centennial glacier retreat as categorical evidence of regional climate change. Nature Geosci 2017; 10: 95-99.

Ruthven DM. Principles of adsorption and adsorption processes: John Wiley & Sons, 1984.

Smith KS. Metal sorption on mineral surfaces: an overview with examples relating to mineral deposits. The Environmental Geochemistry of Mineral Deposits. Part B: Case Studies and Research Topics 1999; 6: 161-182.

Sommaruga R. When glaciers and ice sheets melt: consequences for planktonic organisms. Journal of Plankton Research 2015.

Sommaruga R, Kandolf G. Negative consequences of glacial turbidity for the survival of freshwater planktonic heterotrophic flagellates. Scientific Reports 2014; 4.

Stumm W, Morgan JJ. Aquatic chemistry; an introduction emphasizing chemical equilibria in natural waters, 1970.

Stumm W, Sigg L, Sulzberger B. Chemistry of the Solid-Water Interface: Processes at the Mineral-Water and Particle-Water Interface in Natural Systems: Wiley, 1992.

Tessier A, Campbell PGC. Partitioning of trace metals in sediments: Relationships with bioavailability. Hydrobiologia 1987; 149: 43-52.

Tipping E. WHAMC—A chemical equilibrium model and computer code for waters, sediments, and soils incorporating a discrete site/electrostatic model of ion-binding by humic substances. Computers & Geosciences 1994; 20: 973-1023.

Tipping E. Cation Binding by Humic Substances. Cambridge: Cambridge University Press, 2002.

Tonkin JW, Balistrieri LS, Murray JW. Modeling sorption of divalent metal cations on hydrous manganese oxide using the diffuse double layer model. Applied Geochemistry 2004; 19: 29-53.

Tranter M. Sediment and Solute Transport in Glacial Meltwater Streams. Encyclopedia of Hydrological Sciences. John Wiley & Sons, Ltd, 2006.

Trolle D, Spigel B, Hamilton D, Norton N, Sutherland D, Plew D, et al. Application of a Three-Dimensional Water Quality Model as a Decision Support Tool for the Management of Land-

Use Changes in the Catchment of an Oligotrophic Lake. Environmental Management 2014; 54: 479-493.

Van Rijn LC. Principles of sediment transport in rivers, estuaries and coastal seas: Aqua Publications, 1993.

Warren LA, Haack EA. Biogeochemical controls on metal behaviour in freshwater environments. Earth-Science Reviews 2001; 54: 261-320.

Webster-Brown JG, Dee TJ, Hegan AF. Metal removal via particulate material in a lowland river system. Water Sci Technol 2012; 66: 1439-45.

Whalley WB, Krinsley DH. A scanning electron microscope study of surface textures of quartz grains from glacial environments. Sedimentology 1974; 21: 87-105.

Zhuang J, Yu G-R. Effects of surface coatings on electrochemical properties and contaminant sorption of clay minerals. Chemosphere 2002; 49: 619-628.

2. Glacial SPM: Character, Composition and Behaviour in the Waitaki Catchment, New Zealand

2.1 Introduction

Suspended particulate matter (SPM) sourced from alpine glaciers may play an important role in regulating of the quality of downstream waters. The freshly abraded mineral surfaces may have a high reactive surface area and a large capacity to adsorb dissolved ions, including nutrients such as phosphate, toxic trace elements and organic molecules (Gregory, 2006; Lead and Wilkinson, 2007). However, there has been limited investigation of the role of glacial SPM in this regard and its evolution through a catchment. Many glacier-fed rivers, both in New Zealand and internationally, traverse highly developed agricultural catchments. The ability of glacially derived SPM to regulate the concentrations of dissolved pollutants in the run-off from pastures may be an important consideration in the environmental management of these catchments.

The glacier-fed Waitaki catchment is located in Canterbury, New Zealand, and is highly valued for its cultural, ecological recreational and commercial values (Williams, 2015). The system is sustained by turbid pro-glacial meltwater (**Figure 2.2A**) from a number of the country's most prominent glaciers, all of which are steadily retreating (Dykes et al., 2010). The lands in the Upper Waitaki Basin, commonly known as the MacKenzie Country, are characteristically arid. Land-use in the basin has historically been low-intensity, dryland sheep farming. However, in recent decades the land has increasingly been converted to more intensive uses such as dairy farming (Gray, 2015; Norton et al., 2009). Between the years of 2003 – 2009, irrigation in the upper catchment increased by 6000% (Trolle et al., 2014) (**Figure 2.2B**), and has been further developed in recent years. This has been termed the "greening of the MacKenzie". The development of the land has resulted in increasing losses of nutrients to the rivers, groundwater and lakes and has been associated with the degradation of the water quality (Clarke, 2015; Norton et al., 2009).

The primary aim of this study was to determine the previously unknown physicochemical characteristics of SPM in the glacial-fed Waitaki catchment. The setting provided a natural transect, whereby the influence of the glacial SPM could be determined in progressively downstream sites. Five large hydroelectric lakes increase the residence time of the water in the catchment (Snelder et al.,

2005), optimizing the opportunity to detect active weathering and compositional changes to the SPM. Further down the catchment land use is predominantly agricultural, allowing for a direct comparison between SPM in the upper glacier-fed catchment versus the lower, agricultural catchment. Particular attention has been paid to particle size and mineralogy, and how this evolves down the catchment. The water quality throughout the catchment was monitored to investigate possible influences on the SPM composition. The differences in the likely adsorptive capability of the glacial SPM, compared to lowland river SPM are discussed.

2.2 Methodology

2.2.1 Catchment Description

The upper Waitaki River catchment has its headwaters in the Aoraki/Mt Cook National Park, located in the Southern Alps of the South Island of New Zealand (**Figure 2.1**). The geology of the upper catchment is dominated by the Torlesse Supergroup greywacke (Mackinnon, 1983), which gives way to alluvial gravels on the plains between the mountains and the coast. The region has an extensive glacial coverage with numerous peaks of > 3000 meters above sea level (masl). Glacial meltwaters transport sediments from the actively melting glacier faces. The Tasman, Hooker and Mueller Glaciers lie on the East side of the Southern Alps at the head of the Waitaki River catchment. Each glacier is in a sparsely vegetated alpine environment and terminates at a glacial lake, filled with cold, turbid meltwater. All glaciers are currently in a period of fast retreat (Dykes et al., 2011). Lake Hooker feeds the single channelled Hooker River which flows into the proglacial Lake Mueller and then onto the confluence with the Tasman River, fed by the glacier-fed Lake Tasman. The levels of these glacial rivers are highly variable due to variations in daily and seasonal meltwater flow (Hambrey and Ehrmann, 2004). The combined river flows south for approximately 4 km across the Tasman River plains before entering Lake Pukaki. This lake is a storage reservoir in the Waitaki hydroelectric scheme. Meltwater has an estimated residence time of 484 days in Lake Pukaki (Snelder et al., 2005), and it has been estimated that 23% of the annual water input into Lake Pukaki is from snow and ice melt (Kerr, 2013). The turbid grey waters of Lake Tasman evolve to a bright turquoise in Lake Pukaki and then to a clear state in the lower lakes. The upper catchment is relatively arid but has been subject to ongoing agricultural intensification with irrigation over the last 10-15 years (Trolle et al., 2014).

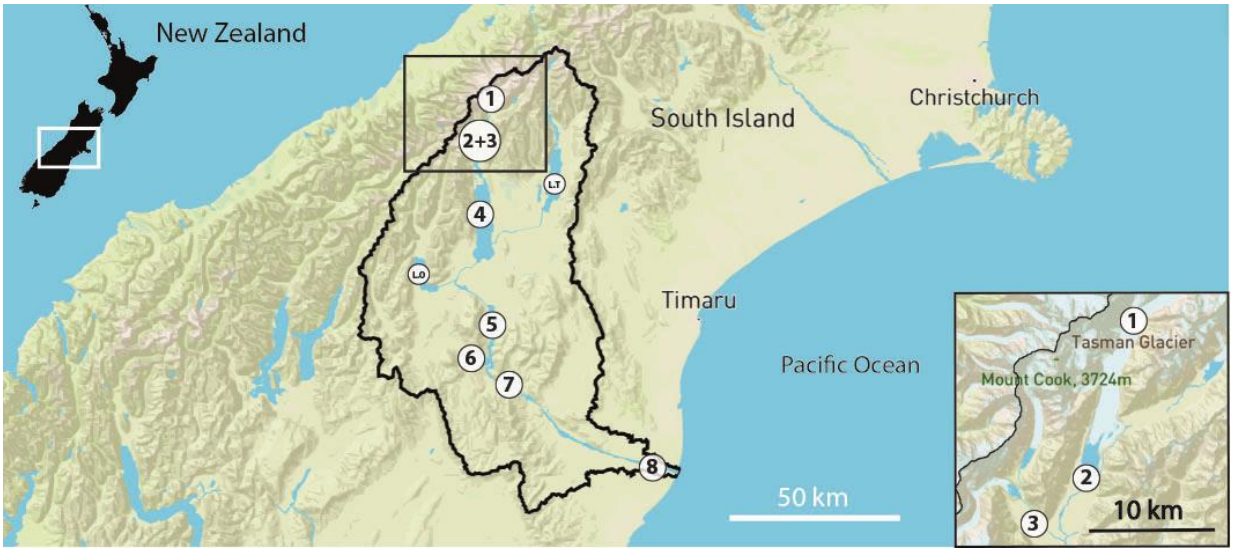

Figure 2.1. Sampling locations in the Waitaki River Catchment, South Island, New Zealand. Sample site 1 = Tasman Plateau; 2 = Lake Tasman; 3 = Hooker River; 4 = Lake Pukaki; 5 =Lake Benmore – Haldon Arm; 6 Lake Benmore – Ahuriri Arm; 7 = Lakes Aviemore and Waitaki; 8 = Waitaki River; LO = Lake Ohau; LT = Lake Tekapo. Map credit: Phil Clunies-Ross

Downstream of Lake Pukaki, artificial canals feed water through a number of storage lakes and power generators, and water from neighbouring Lakes Tekapo and Ohau is also diverted to this scheme for hydroelectricity generation. The storage reservoirs are Lakes Ruataniwha (not shown, residence time of 1.4 days), Benmore (58 days), Aviemore (14 days) and Waitaki (1.1 days) (Snelder et al., 2005). All lakes have naturally low concentrations of dissolved nutrients and organic carbon (Gallegos et al., 2008). Glacial sediment can be seen to influence the colour of water through to Lake Benmore (**Figure 2.2**). Finally, the Waitaki River drains from the outlet of Lake Waitaki and flows east to the Pacific Ocean. Flow is artificially controlled in the lower river; normally low during winter months, increasing significantly in spring due to snow and ice melt in the glacial headwaters. The average residence time of water in the whole Waitaki River system is approximately two years (Snelder et al., 2005).

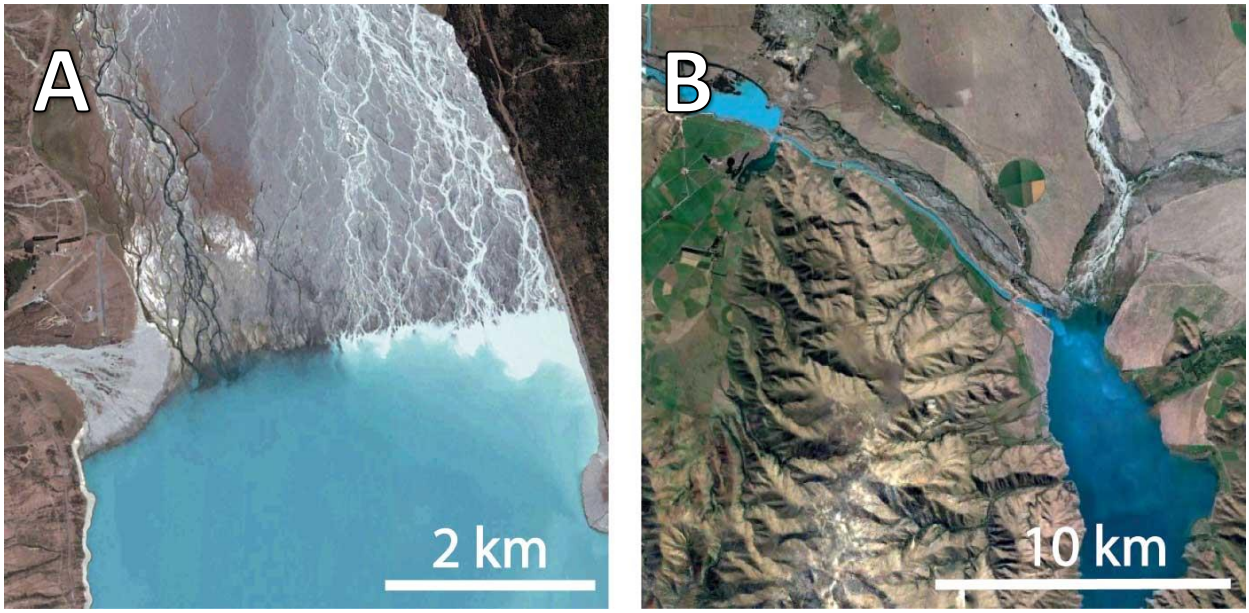

Figure 2.2. A) Satellite image of the turbid Tasman River (top) flowing into Lake Pukaki. B) Meltwater is channelled for the purposes of hydroelectric generation before entering Lake Benmore. Note the reduction in sediment concentrations in both images. Satellite imagery credit: Google, DigitalGlobe 2017.

While the coarse glacially-derived sediment is trapped in the proglacial lakes, fine suspended sediments are swept further down the catchment. The total input from the upper catchments into the next major reservoir, Lake Benmore, has been estimated to be between 87,000 – 170,000 t sediment/year (Pickrill and Irwin, 1986). A total of 175,000 – 264000 t from all sources has been estimated to enter Lake Benmore annually, 85% of which is glacial SPM. Bed sediment accumulates at a rate of 3mm per year, ranging from silt-sand sized particles at the head of the lake to clay sized particles 5km down the lake (Pickrill and Irwin, 1986). The dominant source rock area is the Torlesse Supergroup greywacke containing quartz, feldspar (5:1 plagioclase to potassium), mica (illite and biotite), and microcline. Minor contributions from titanite, epidote-clinozoisite, hornblende, apatite, zircon, garnet are present in the source rock (Mackinnon 1983). Up to 3% of the source rock composition is calcite (Templeton et al., 1998).

Figure 2.3. Lake Tasman. Panoramic photo looking North-East from the South-West viewing platform. The large proglacial lake is formed at the terminus of the Tasman Glacier (shown top left). High concentrations of fine SPM give this water its characteristic grey hue. Image credit: Phil Clunies-Ross.

2.2.2 Sample collection and preparation

Water and SPM were collected during spring (25th – 27th October, 2015) and autumn (13th – 14th March, 2016, and 26th Feb – 2nd March 2017) during base flow conditions. The sites were Lake Tasman (**Figure 2.3)**, Hooker River, Lake Pukaki, Lake Benmore – Haldon Arm, Lake Benmore – Ahuriri Arm, Lake Aviemore and the Waitaki River (**Figure 2.1)**. Note that Site 8 (Waitaki River), nearest the coast, is above the tidal-affected zone of the river. Sediment entrained in the glacial ice was obtained for comparative purposes with the SPM. Tasman Glacier ice was subsampled from an ice core (**Figure 2.4**) which had been collected from the Tasman Saddle in October, 2004 by Morgenstern et al. (2006), and stored in the GNS ice-core facility in Wellington, New Zealand. Six, one-meter long sections of glacier core were taken, from depths of between 5 and 43 m, and a single 20 cm block cut from each section targeting ice with visible entrained sediment. The ice was washed with ultrapure, deionised water in a clean laboratory, before being placed into enclosed acid washed plastic containers to melt at room temperature.

At each site, water conductivity, dissolved oxygen, pH and temperature were measured *in situ* with a Hach HQ40d portable field meter and turbidity using an Orion AQ4500 turbidimeter. Water was filtered through a 0.45 µm cellulose nitrate filter membrane into new 50 ml polypropylene tubes for analysis of major ions and nutrients. Nutrient samples were stored frozen until they could be analysed. Unfiltered samples were collected for total carbon (TC) and total organic carbon (TOC), SPM and particle size analysis.

Larger quantities of SPM were collected by filtering 20 - 40 l of water through pre-weighed GF/F and 0.45 µm nitrocellulose filters using a vacuum pump. Particulates adhered to the

nitrocellulose membranes were liberated by sonication before being freeze-dried. It is noted that particles of < 0.45 µm were also collected on the membrane once an initial layer of sediment had formed. SPM was also collected by filtering water through 0.22 µm Nucleopore membrane filters, which were air dried in clean petri dishes for later SEM analysis.

Surface sediments were collected from four depositional environments at: the Tasman River below Lake Tasman; Lake Pukaki; Lake Benmore – Ahuriri; Lake Aviemore; Waitaki River. These sediments were used as an analog for SPM in analytical procedures where insufficient SPM was available. The top 1cm of oxic sediment was collected into acid-washed 200 ml polycarbonate jars with the use of a telescopic pole. Sediments were freeze dried and sieved through acid washed 63 µm mesh, with this fraction retained for subsequent analysis. The character and composition of the material was tested in parallel with the SPM to determine if the substitution is appropriate. The results of these findings are presented in **Appendix B**.

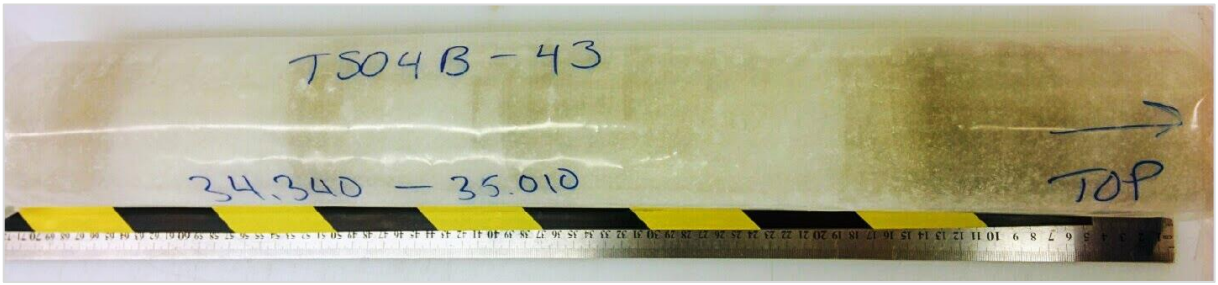

Figure 2.4. Tasman Glacier Ice-Core courtesy of GNS Science, Wellington. This section was retrieved from a depth of 34.3 – 35.0 m. The dark bands show high concentrations of glacial sediment entrained in the ice. Image credit: Phil Clunes-Ross

2.2.3 Water Analysis

Concentrations of suspended particulates were determined by filtering 1000 ml of water through a pre-dried, pre-weighed Millipore nitrocellulose filter membrane. Dissolved reactive phosphorus (DRP) and total P (after a persulphate digestion) were measured using the ascorbic acid method (APHA, 2005), with a detection limit of 0.005 mg P/l. Calibration curves for these analyses were constructed using standards (0 – 0.2 mg/l) made with a fresh stock potassium phosphate (KH_2PO_4) stock solution diluted with accurately weighed additions of ultrapure water.

Total carbon (TC), inorganic carbon (TIC) and organic carbon (TOC, by difference) were determined by IR analysis of CO_2, following combustion of samples at 680°C using a Shimadzu TOC-

L instrument. The instrument was calibrated with a series of analytical standards solutions (0, 0.1, 1, 5, 10, 25, 100 mg C/l) of potassium hydrogen phthalate ($C_8H_5KO_4$) for TC; and a combined sodium carbonate (Na_2CO_3) and sodium bicarbonate ($NaHCO_3$) standard for TIC analysis. The detection limit was 0.1 mg/l TOC. Dissolved inorganic carbon (DIC) was determined by Li-Cor Infra-Red Gas Analyser (IRGA). The DIC concentration was calculated from peak height after calibration of the instrument with standard solutions (0, 5, 10, 50, 100 and 250 mg/l) of $NaHCO_3$.

Cation concentrations were determined using an Agilent 7500cx inductively coupled plasma-mass spectrometer (ICP-MS) with detection limits of: 0.1 µg/l for sodium (Na), manganese (Mn), copper (Cu), cadmium (Cd) and lead (Pb); 1 µg/l for magnesium (Mg), aluminium (Al), iron (Fe), zinc (Zn) and arsenic (As); 10 µg/l for potassium (K); and 100 µg/l for calcium (Ca). Major anion concentrations were determined by high pressure ion chromatography (HPIC) using a Dionex ICS-2100 with detection limits of 0.1 mg/l for chloride (Cl), sulphate (SO_4) and nitrate (NO_3). All major ion balances were within 10%. Analytical blanks with ultrapure water were included in all analyses. The concentrations of ions detected in these samples were below detection limits.

Quality control and assurance procedures were included for all analyses. Blanks of ultrapure water and analytical standards (made with fresh stock solutions) were run with every analysis. Replicate samples were also tested where possible. This ensured that the results of the analytical procedures were consistent, comparable and accurate. The procedures also ensured that instruments were calibrated and functioning within their specified limits of precision. Meters used for the physical characterisation of water samples were calibrated frequently and checked with standard solutions. For major ion and trace metal analyses, a dedicated calibration was performed for every batch of samples analysed. The quality of these analyses was checked with the inclusion of a blank and standard samples for every ten samples analysed.

2.2.4 SPM analysis

All analyses of SPM were conducted on samples collected during periods of low rainfall in the autumn months. This was chosen to distinguish between the sediment likely to be contributed by glacial melt rather than rain runoff. Seasonal variation of the SPM composition has not been considered in this study.

2.2.4.1 Particle Size Distribution and Zeta-Potential

Particle size distributions of the SPM was measured using a Horiba LA-950V2 laser diffractometer with a range of 10 nm – 3.0 mm, on chilled samples within 48 hours of collection. The instrument was zeroed on deionized water and calibrated to a refractive index of 1.56 (the refractive index of pure water multiplied by 1.17 + 0.0001) as recommended by Andrews et al. (2010) and Charters et al. (2015). Suspensions were measured before and after ultrasonication for 20 seconds to determine possible particle aggregation. Water samples from Lake Benmore, Lake Aviemore and the Waitaki River did not have sufficient SPM for direct analysis, so were pre-concentrated by resuspending SPM collected by filtration from 2 L of water, into 50 ml sample water. A comparison of particle size distributions (PSDs) from original and pre-concentrated samples from Lake Tasman, the Tasman River and Lake Pukaki showed no significant difference in particle size distribution arising as a result of this pre-concentration method. Sediment in the meltwater from the ice-core was allowed to settle for 5 minutes before sampling the supernatant. This was done to measure the PSD of particles likely to remain in suspension in proglacial environments.

The PSDs of the SPM were specifically examined after pre-digestion of organic matter and biogenic silicates. Organic matter was oxidized by adding 0.1g of SPM to 10 ml of 6% hydrogen peroxide solution and heating to 80°C. This was repeated until effervescence has subsided (Gee and Or, 2002). Biogenic silicates were removed by adding 10 ml of 10% KOH to samples previously treated with H_2O_2 and then heating to 80°C for 30 min (Tiit, 2008). The residual SPM was washed thoroughly with deionized water, resuspended and dispersed with 1% sodium hexametaphosphate ($(NaPO_3)_6$) prior to analysis (Gee and Or, 2002). In addition, untreated samples were analysed to determine the extent of particle flocculation during transportation. Particle size distributions were collected in volume mode and converted to a number distribution for comparison with SEM imagery. The median particle size (D50) is reported along with the sizes in which 10% (D10) and 90% (D90) of particles pass, respectively. The zeta (ζ) potentials of SPM in the water samples were measured with a Zetasizer Nano ZS with a voltage of 150 V at the University of Canterbury. The measured electrophoretic mobility was converted to zeta-potential by instrument's software (Zetasizer Ver. 5 Malvern Instruments Ltd., UK).

2.2.4.2 SPM Composition

SPM mineralogy was determined by X-ray Diffraction (XRD) using an Empyrean diffractometer at the University of Waikato. The morphology and chemical composition of the SPM was determined using scanning electron microscopy (SEM) and energy dispersive X-ray (EDS) analysis. Nucleopore filters bearing SPM were coated with carbon for EDS analysis and with platinum for high resolution imagery. The particle morphology (particle appearance, surface textures and shapes) and mineralogy were recorded in systematically selected areas of the filter membranes. Elemental mapping was used to pinpoint minerals with high concentrations of target elements. The chemical composition of SPM (as weight, oxide and atomic %) was determined with EDS analysis.

Suspended particulate matter was digested to quantify the acid-soluble oxide phases. An accurately weighed quantity of SPM was digested in hot analytical grade 1+1 HNO_3/HCl as per standard method 3030F (APHA, 2005). The concentrations of acid-extractable metals in the digest were determined by inductively coupled plasma-mass spectrometry (ICP-MS) with detection limits of: 0.1 µg/l for Mn, Cu and Pb; and 1 µg/l for Al, Fe, Zn, and As. A PACs-2 reference marine sediment was used to determine the trace element recoveries during every sediment digestion. Recoveries of 80 – 106% were typically measured in the reference sediment (n= 3). This data is tabulated in **Appendix B**. Blank controls without the addition of SPM were used to measure possible contamination during the digestion process.

Total phosphorus concentrations were determined in sediments after an autoclave-assisted digestion with persulphate followed by the ascorbic acid method (APHA, 2005). Potassium phosphate (KH_2PO_4) standards (0.01 – 1 mg/l) and solution blanks were included to calibrate the procedure. A certified PACs-2 marine sediment was included as a reference standard, with TP recoveries ranging from 89.9 – 92.4% (n= 3). The total organic carbon content of the SPM (weight %) was determined with the combustion of freeze-dried SPM with a Shimadzu SSM-5000A coupled to the TOC-L described in **Section 2.2.3**.

2.2.4.3 Specific Surface Area

The most common method for determining the specific surface area (SSA) of sediment is the BET nitrogen adsorption method (Nelsen and Eggertsen, 1958). The use of ethylene glycol (EG), ethylene glycol monoether (EGME), and para-nitrophenol is also reported in the literature. However, it was not possible to use these methods due to the limited quantities of SPM available for analysis.

The methylene blue (MB) method was instead used to determine the relative SSA of SPM due to its high sensitivity, with the techniques used by Kahr and Madsen (1995), Santamarina et al. (2002) and Hähner et al. (1996) modified to account for the small quantities of SPM. Freeze-dried SPM was introduced to deionized water to make a 100 mg/l suspension. The solution was sonicated for 30 seconds to loosen aggregates prior to refrigeration for 48 hours to rehydrate the particulate matter. Five ml of the SPM suspension was then transferred to clean 15 ml centrifuge tubes and 5-100 µl of freshly made 0.05 g/l methylene blue solution was added to each tube. These were spun on an end-over-end mixer for 3 hours. Samples were rested overnight to equilibrate prior to spectrophotometric determination at 665 nm. Deionized water blanks with methylene blue additions were ran in parallel to calibrate the experiment. The SSA was calculated from the "point of complete cation replacement", the point at which the SPM can no longer adsorb all methylene blue from solution. The SSA is then calculated by **Equation 2.1**:

$$\boldsymbol{SSA = \frac{m_{mb}}{319.87}\, A_{av} A_{mb} \frac{1}{m_s}} \qquad (\mathbf{1.1})$$

where: m_{mb} = the mass (g) of adsorbed MB at the point of complete cation replacement; A_{av} is Avogadro's number (6.02×10^{23}/mol); A_{MB} is the area covered by one methylene blue molecule (130 $Å^2$, or 13 nm^2); m_s = the mass of SPM in the sample.

The suitability of the proposed method was then tested by comparing the SSA of surface sediments with para-nitrophenol (pNP), using the method detailed by Hedley et al. (2000), and the BET method (Nelsen and Eggertsen, 1958). The results of these comparisons are detailed in **Appendix B**.

The methylene blue adsorption data may also be applied to effectively approximate the cation exchange capacity (CEC) of the SPM (Yukselen and Kaya, 2008) and provides a quick estimation of the adsorptive potential of the SPM. At the "point of complete cation replacement" the CEC can be calculated using **Equation 2.2**:

$$\boldsymbol{CEC = \frac{100}{m_s}\, V_{cc} N_{mb}} \qquad (\mathbf{2.2})$$

where: m_s = Weight of SPM in sample (g); V_{cc}= volume of MB solution added (ml); N_{mb} = Normality of MB in solution (meq/ml) and CEC is given in meq/100 g SPM.

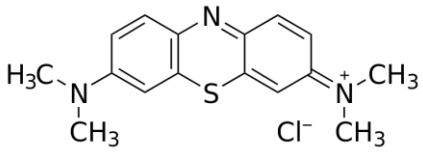

Figure 2.5. Chemical structure of methylene blue used to determine specific surface area (SSA) and cation exchange capacity (CEC).

2.2.5 Weathering Indices

Two common chemical weathering indices were used to assess the degree of sediment weathering:

i. The Chemical Index of Alteration (CIA; Nesbitt and Young (1982) assesses the breakdown of feldspar minerals to clays, assuming that aluminium (Al) is a resilient, immobile phase while mobile ions such as K, Na and Ca are lost (**Equation 2.3**). Unweathered feldspar has a CIA value of 50, while muscovite-illite CIA = 75 and gibbsite CIA = 100. Fedo et al. (1995) described the systematic progression in weathering as low (50 – 60), intermediate (60- 80) and extreme (> 80). The measurements of P_2O_5 was subtracted from CaO values, as per the method of McLennan (1993), to correct for apatite that may be present in samples.

$$\boldsymbol{CIA = 100\,x\frac{Al_2O_3}{Al_2O_3 + CaO + Na_2O + K_2O}} \qquad (\mathbf{2.3})$$

ii. The Weathering Index of Parker (WIP) measures the degree of weathering in silicate rocks, using the proportions of the most labile major elements; Na, K, Mg and Ca, weighted by their bond strength with oxygen (Parker, 1970) (**Equation 2.4**). WIP use in highly weathered sediments is limited as it relies on labile elements that may already be diminished in weathered minerals (Price and Velbel, 2003). Decreasing index scores indicate a greater degree of sediment weathering.

$$\boldsymbol{WIP = 100\,x\frac{2Na_2O}{0.35} + \frac{MgO}{0.9} + \frac{2K_2O}{0.25} + \frac{CaO}{0.7}} \qquad (\mathbf{2.4})$$

2.2.6 Point of Zero Charge (PZC) and Isoelectric Point (IEP) Determination:

The pH at which the SPM has a net neutral charge is the point of zero charge (PZC). The isoelectric point (IEP) is the point of zero net charge at the shear plane, and is commonly determined with zeta potential analysis (Adamson, 1990). A zeta potential titration and the 'immersion technique', both detailed by Bourikas et al. (2003), were combined in a novel method to investigate these properties. To begin, SPM was rehydrated in 0.01 M KNO_3 to a concentration of 100 mg/l for 48 hours. The suspension was adjusted to pH 10 with small aliquots of KOH and then left to equilibrate for 30 minutes. The pH was then reduced with 1-10 µl additions of 1 M HNO_3 and 10 ml aliquots taken every 0.5 – 1 pH unit. All pH measurements were accurately recorded. The samples were placed on an end-over-end mixer for 24 hours to equilibrate before the pH was re-measured in each tube. The change in pH (ΔpH) required for the immersion technique was determined by subtracting the initial pH – final pH values. The initial pH was plotted against the associated ΔpH value, and the point of zero charge identified where the minimum ΔpH is plotted. The zeta-potential of the SPM was then determined in each sample with the use of a Zetasizer Nano ZS as described in Chapter 2. The resulting PZC and IEP values were compared to literature values (**Table 2.10)** in order to predict important adsorbing phases on the SPM.

2.2.7 Statistics

Statistical analysis was performed with XLSTAT ver. 19. A Pearson's correlation matrix was prepared with the descriptive data obtained from the characterization experiments. Significance was tested at the 5% level ($p = < 0.05$).

2.3. Results

2.3.1 Water chemistry trends down catchment

A summary of the physical and chemical measurements obtained for the ice and water samples is presented in **Table 2.1**. The concentration of sediment entrained in the glacier ice core varied considerably, with sections > 30m in depth containing concentrated bands of glacial sediment. The melt from these samples had a very high turbidity, clearly demonstrating the source of glacial sediment in the meltwaters running off the glaciers. The proglacial meltwater samples collected from Lake

Tasman and the Hooker River were characterised by relatively low temperatures (<6^{0}C), and highly turbid waters (often >100 NTU). Sediment concentrations were up to an order of magnitude higher during the warm autumn sampling campaign compared to those collected in the cooler spring. By Lake Pukaki temperatures had increased to be more reflective of air temperatures, and there was little change down the catchment. Turbidity had decreased substantially by Lake Pukaki and continued to decrease in downstream lakes and river water. The conductivity of the core ice sample was very low (<10 µS/cm). Meltwater collected below the glacier was of moderate conductivity (<100 µS/cm) and was relatively consistent throughout the catchment. The glacial melt, lake and river waters were all well aerated near the surface (no deep lake samples were collected), and pH did not show a significant change down the catchment.

Table 2.1. Water quality parameters for study sites. Unless a single value is given, a range over 3 sampling visits (spring and autumn) is given. "n.a" is "not analysed". * The concentrations measured in the ice-core samples were a range between 3 core-section depths (5, 14 and 42 m).

Site	Location	pH	Temp (°C)	Conductivity (µS/cm)	DO (mg/l)	Turbidity (NTU)	SPM (mg/l)
1*	Tasman ice core	6.6	n.a	5.3 - 9.5	n.a	< 1 - >1000	< 1 - 4300
2	Lake Tasman	7.1 - 8.5	2.4 - 5.5	56.7 - 64.4	11.8 - 12.3	27 - 362	22 - 226
3	Hooker River	7.8	3.4 - 4.8	62.3 - 65.2	11.6 – 11.8	80 - 210	128 - 190
4	L. Pukaki	7.0-7.7	9.3 - 18.6	55.3 - 60.9	8.8 - 10.7	1.9 - 4.7	2.5 - 7.5
5	L. Benmore -Haldon	6.9 - 7.6	11.4 – 18.8	52.8 – 60.0	10.4 - 10.5	0.1 - 1.8	0.8 – 2.0
6	L. Benmore -Ahuriri	7.5 - 8.1	11.6 - 18.9	48.9 - 53.4	9.1 - 10.6	0.3 - 1.7	0.7 – 2.0
7	Lake Aviemore	7.2 - 7.9	9.1 - 19.0	55.0 - 61.2	8.4 - 10.8	0.1 - 0.8	0.5 – 1.0
8	Waitaki River	6.8 - 7.9	8.5 - 16.9	62.5 - 80.8	8.4 - 11.4	0.5 - 3.9	1.0 - 4.0

A summary of dissolved major ion and nutrient concentrations is presented in **Table 2.2**. The concentrations of major ions were found to be either very low or below detection limits in the melted Tasman ice core. All were measurable in the proglacial meltwaters. No significant changes were observed in downstream samples over the 3 sampling visits. However, concentrations of major cations generally increased with increasing distance from the glacier terminus. The exception was SO_4, with the greatest concentrations measured at Lake Tasman and the Hooker River, in close proximity to the glacier terminus. Nitrate concentrations were consistently low throughout the catchment. DRP was below detection limit throughout the catchment except for a low detectable concentration (0.03 mg/l) on one occasion. The concentrations of DIC were also stable throughout the catchment. However, increasing concentrations of TOC were measured with increasing distance from the glacier source.

Table 2.2. Major ion, nitrate and total organic carbon (TOC) concentrations (mg/l) for study sites. Unless a single value is given, a range over 3 sampling visits (spring and autumn) is given. "na" is "not analysed". DRP was <DL for all except site 9 (Waitaki River) on one occasion (0.03 mg/l). * The concentrations measured in the ice-core samples were a range between 3 core-section depths (5, 14 and 42 m).

Site	Na	K	Mg	Ca	Cl	SO4	NO3	DIC	TOC
1*	< DL - 0.1	0.1 - 0.25	0.01 - 0.07	<DL - 0.3	<DL	< DL	< DL	na	< DL
2	1.21 - 1.88	0.67 - 1.1	0.45 - 0.88	9.5 - 10.6	0.2 - 0.4	7.2 - 8.4	< DL - 0.1	22 – 25	<DL - 0.9
3	1.52 - 1.9	0.70 - 1.0	0.51 - 0.57	9.9 - 10.5	0.2 - 0.4	7.2 - 7.4	< DL - 0.1	22 – 29	<DL - 1.1
4	1.46 - 2.05	0.60 - 0.96	0.49 - 0.70	8.4 - 10.2	0.3 - 0.5	5.2 - 5.7	< DL - 0.1	22 – 25	<DL - 1.9
5	1.56 -1.67	0.53 - 0.59	0.62 - 0.65	7.9 - 9.5	0.4 - 0.5	4.5 - 4.7	< DL - 0.1	23 – 27	0.5 - 2.1
6	2.18 - 2.86	0.44 - 0.80	0.79 - 1.05	6.1 - 7.4	0.3 - 0.7	2.7 - 3.2	< DL - 0.1	23 – 24	0.2 - 2.9
7	2.07 - 2.30	0.53 - 0.90	0.81 - 0.88	8.7 - 10.5	0.2 - 0.6	3.3 - 4.7	< DL	20 – 29	0.3 - 2.8
8	2.91 - 3.05	0.90 - 1.16	1.07 - 1.28	9.9 - 11.0	0.2 - 0.8	4.8 - 6.0	0.2 - 0.5	24 – 29	0.9 - 3.2

The associated concentrations of dissolved trace elements are presented in **Table 2.3**. The concentrations determined in the ice-core varied significantly with depth. In general, greater concentrations of all analytes were detected in core sections of increasing depth and sediment concentrations. The greatest differences were determined for Al, Mn and Fe, with concentrations of ranging from 0.2, 0 and 1 µg/l in the 5m deep core section, to 84.5, 4.88 and 145.8 µg/l for the 43 m deep section respectively. In general, low concentrations of the toxic trace elements (Cu, Zn, As, Cd, Sb and Pb) were detected.

In the water samples, the greatest concentrations of dissolved analytes were typically measured in the upper catchment samples. High concentrations of Al and Fe were detected in the upper catchment, with the Lake Tasman and Hooker River samples ranging from 41.9 – 104.2 and 21.7 – 56.1 µg/l respectively. These were generally an order of magnitude higher than the concentrations measured in the lower catchment. The concentrations of toxic trace elements (Zn, As, Cd, Sb and Pb) were low throughout the catchment. The concentrations of Zn, Cd, Sb and Pb were below the most conservative trigger values (99% level of protection) detailed by the Australian and New Zealand Guidelines for Fresh and Marine Water Quality. The concentrations of As were below the 95% trigger value (ANZECC, 2000).

Table 2.3. Dissolved cations (µg/l) in filtered (0.45 µm) water samples at study sites. Unless a single value is given, a range over 3 sampling visits (spring and autumn) is given. * The concentrations measured in the ice-core samples were a range between 3 core-section depths (5, 14 and 42 m).

Site	Al	Mn	Fe	Cu	Zn	As	Cd	Sb	Pb
1*	0.2 - 84.5	0 - 4.88	1.0 - 145.8	0.01 - 0.55	0.24 - 3.0	0 - 0.24	0 - 0.01	0 - 0.01	0 - 0.35
2	41.9 - 71.9	0.60 - 1.78	21.7 - 52.8	0.11 - 0.19	0.57 - 0.63	2.76 - 4.00	0.00 - 0.01	0.39 - 0.48	0.07 - 0.13
3	62.6 - 104.2	1.02 - 1.41	44.8 - 56.1	0.17 - 0.27	0.53 - 0.67	2.84 - 4.34	0.01 - 0.01	0.44 - 0.45	0.13 - 0.22
4	9.2 - 31.0	0.29 - 0.54	1.7 - 18.1	0.22 - 0.37	0.01 - 1.46	1.13 - 1.63	0.01 - 0.06	0.25 - 0.44	0.02 - 0.04
5	6.1 - 6.6	0.28 - 0.31	1.9 - 4.6	0.15 - 0.18	0.0 - 0.04	0.88 - 1.04	0 - 0.01	0.13 - 0.29	0.0 - 0.01
6	1.6 - 7.0	0.20 - 5.1	7.0 - 14.6	0.20 - 0.33	0.02 - 0.42	0.57 - 1.67	0 - 0.02	0 - 0.19	0.0 - 0.06
7	4.0 - 7.9	0.54 - 1.34	3.8 - 6.2	0.17 - 0.26	0.06 - 0.34	0.77 - 1.49	0 - 0.06	0.16 - 0.36	0.02 - 0.04
8	3.6 - 7.9	0.69 - 0.83	2.9 - 10.7	0.17 - 0.39	0.05 - 0.33	0.65 - 0.93	0 - 0.01	0.08 - 0.30	0.01 - 0.02

2.3.2 SPM Character and Composition

2.3.2.1 SPM - Particle Size Distributions, Surface Area and Charge

A summary of SPM PSD data generated for both number and volume distributions is presented in Table 2. The PSD data from the ice core shows that smaller particles 2 – 5 µm in size remained in suspension once settled. The volume distributions for Lake Tasman and the Hooker River demonstrates that larger particles 0.2 - 7 µm are prominent in the suspension. However, the number distribution indicates that the majority of particles were 0.1 – 0.3 µm. The PSDs of SPM collected from Lake Pukaki and all downstream sites were noticeably different. The fine particles < 0.3 µm measured at Lake Tasman and the Hooker River were no longer detected. At Lake Pukaki, the volume and number distributions increased to 2.7 – 10.3 µm and 1.4- 6.0 µm respectively. The PSD volume distributions increased to between 4.7 – 29.5 µm for Lakes Benmore – Haldon, Benmore – Ahuriri and Aviemore. The number distribution indicated that most particles were between 1.8 – 12.2 um in size. The PSD at the Waitaki River indicated a general decrease in size with a volume and number distribution of 3.5 – 15.5 µm and 2.2 – 8.9 µm respectively.

The specific surface area (SSA) of the pre-settled ice-core sediment was 124 m^2/g. Lake Tasman and Hooker River SPM had the greatest SSA's with 353 – 361 m^2/g respectively. SPM collected from downstream lakes progressively declined from 214 m^2/g (Lake Pukaki) to 66 m^2/g (Lake Aviemore), and then increased to 181 m^2/g in the lowland Waitaki River. The same trend was observed for the cation exchange capacities with the greatest CEC's of 68.0 and 66.5 meq/100g SPM

obtained for Lake Tasman and the Hooker River respectively. A gradual decline was measured down catchment with the lowest CEC, 2.5 meq/100g SPM, measured at Lake Aviemore.

The zeta potentials of the ice-core melt and water samples collected in autumn 2016 are presented in **Table 2.4**. The smallest zeta potential of -12 mV was measured in the melt from the ice-core. The greatest zeta potentials of – 20.1 to -26.4 mV were measured in samples collected from in close proximity to the glacier source. A general decline in zeta-potential was measured in all downstream sites below Lake Pukaki.

Table 2.4. Particle size distributions (PSD's), zeta-potentials (ζ), specific surface areas (SSA's) and cation exchange capacities (CEC's) for study sites. The PSD's are presented as the size in which 10% (D10), 50% (D50) and 90% (D90) of particles pass for volume and number analysis. The associated: zeta-potential (ζ) measurements are reported in mV; SSA in m^2/g SPM; and CEC in millieqivilents (meq) per 100 g SPM.

Site	Distance (km)	Volume Particle Size (µm)			Number Particle Size (µm)			ζ (mV)	SSA (mb)	CEC (mb)
		D10	D50	D90	D10	D50	D90			
1*	Ice-core	2.1	3.2	4.9	1.5	2.4	3.5	-12	286	4.7
2	5	0.3	2.3	7.1	0.1	0.2	0.3	-26.4	1130	43.8
3	6	0.2	3.1	4.7	0.1	0.2	0.3	-21.7	1145	44.4
4	45	2.7	5.8	10.3	1.4	2.5	6.0	-20.1	573	11.1
5	95	5.8	10.0	16.5	3.6	6.9	10.9	-14.8	399	5.8
6	125*	4.7	10.2	23.4	1.8	3.2	7.3	-14.5	573	11.1
7	140	7.1	13.3	29.5	3.9	6.8	12.2	-18.2	256	2.5
8	210	5.3	9.7	16.8	2.2	4.5	8.9	-17.7	557	10.8

A scatter graph showing the relationship between the PSD median volume (D50) and the SSA obtained with methylene blue is presented in **Figure 2.6**. A strong negative correlation ($R^2 > 0.85$) is evident between the two variables.

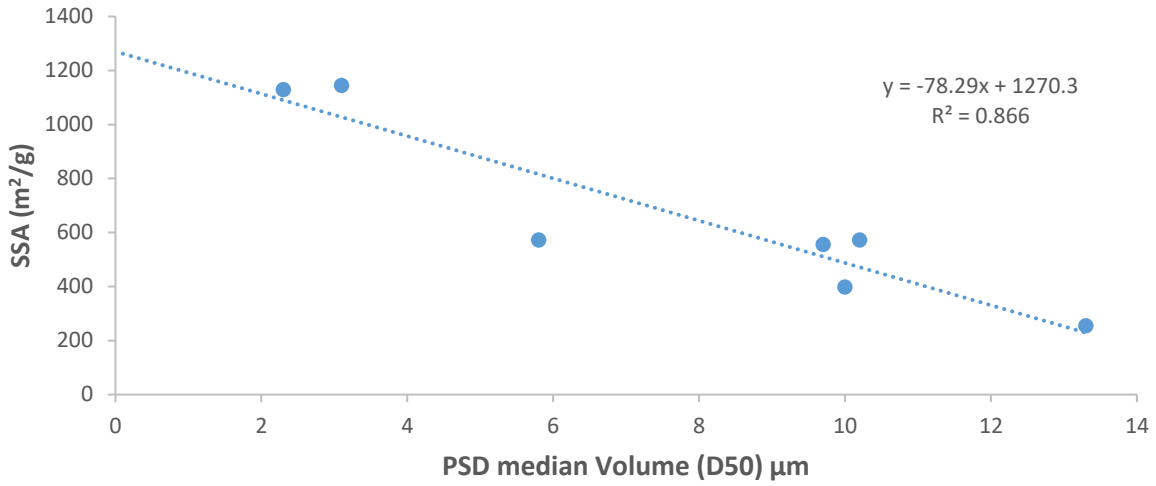

Figure 2.6. Scatter graph plotting the relationship between SSA (m^2/g by methylene blue) and PSD median volume (D50).

The PSD profiles (volume analysis) of SPM chemically dispersed with $(NaPO_3)_6$ are presented in **Figure 2.7**. The PSD of the resuspended ice core sediment has a single distinct mode, grouped between 6 – 10.5 µm. Once allowed to settle for 5 minutes, the PSD of the suspended particles remaining in solution shifted to 2-5 µm (Figure 2.6). SPM collected from Lake Tasman and the Hooker River had bimodal PSD's. Notable peaks lay between 0.1 – 0.5 µm and 2 – 10 µm. PSD's obtained from samples collected below these sites were considerably different. All remaining PSD's had a single mode with consistent peaks at 2 – 10 µm. The PSD profiles of SPM not subjected to chemical dispersion are provided in **Appendix B**. The fresh glacial SPM from Lake Tasman and the Tasman and Hooker River was unaffected. However, the downstream sites were significantly different with bimodal PSD's with peaks between 3 – 30 µm and 100 - 300 µm.

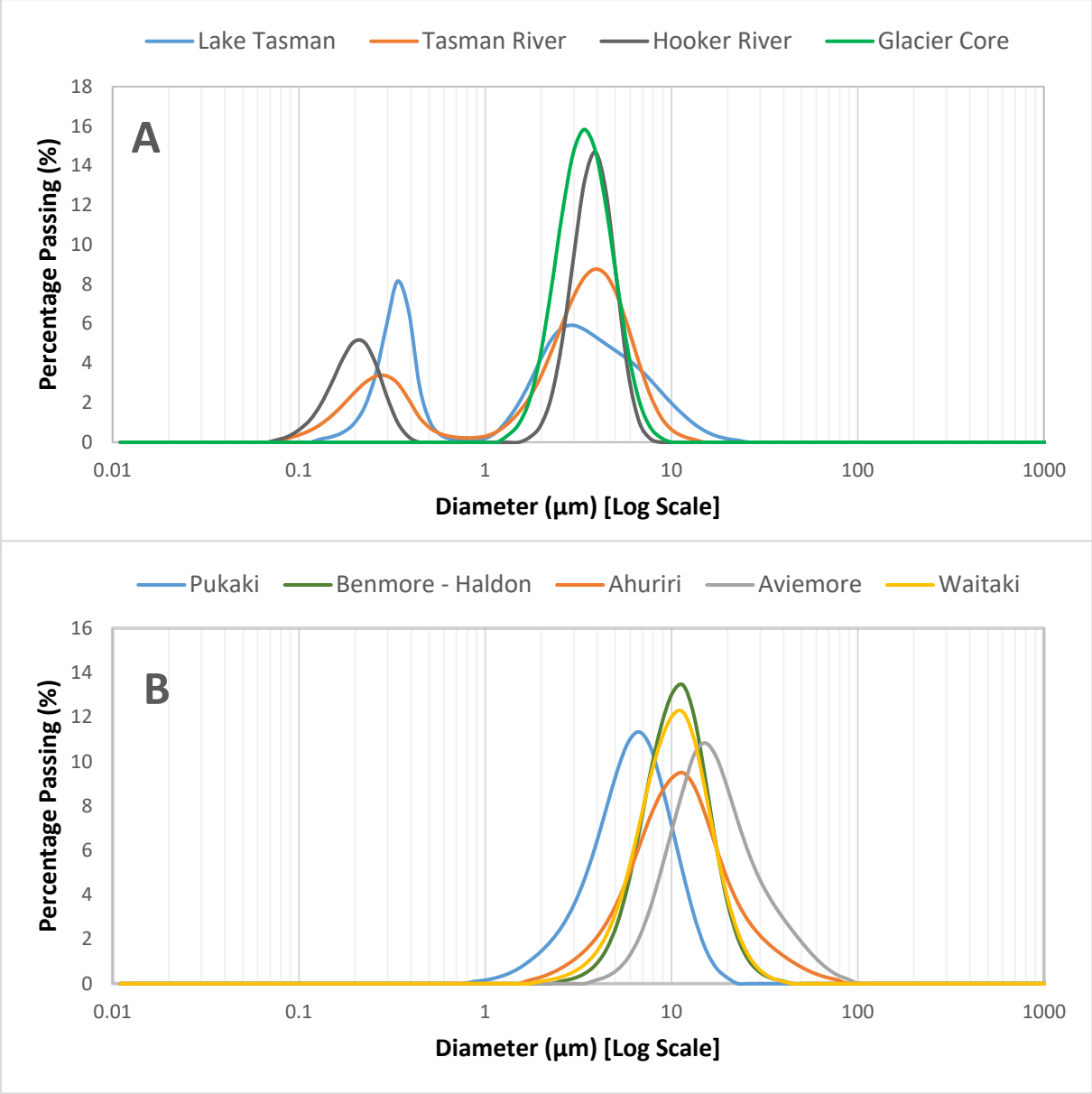

Figure 2.7. Particle size distributions of chemically dispersed SPM ((NaPO3)6) in the upper Waitaki catchment (a) and lower catchment (b).

The PSD D50's (median volume) for the untreated, dispersed and digested SPM are presented in **Table 2.5 and Figure 2.8**. The data demonstrates the considerable influence of these treatment processes. No significant differences were detected in the upper catchment SPM. However, reductions in the SPM D50s were detected in all SPM samples from Lake Pukaki. The H_2O_2 digestion step was found to significantly reduce the D50 of Lake Pukaki SPM from 5.8 to 1.9 µm. All other down catchments had minor reductions with this method (0.3 - 1 µm). The additional digestion step with

NaOH further reduced the D50 of the lower catchment SPM. Only a minor reduction of 0.5 µm was determined in the Lake Pukaki SPM. However, reductions of between 2.2 – 9.9 µm were determined in the lower catchment samples. The greatest reductions of 7, 5.5 and 9.9 µm were determined in Lakes Benmore – Haldon Arm, Benmore - Ahuriri Arm and Aviemore respectively.

Table 2.5. PSD Median volumes (D50) for untreated, dispersed, and digested SPM collected throughout the Waitaki Catchment.

Site	Distance	Untreated	Dispersed $(NaPO_3)_6$	H_2O_2	H_2O_2 + NaOH
	(km)		D50 (µm)		
1*	0	7.7*	3.2**	n.a	n.a
2	5	2.3	2.3	2.3	2.3
3	6	3.1	3.1	3.1	3.1
4	45	11.6	5.8	1.9	1.4
5	95	14.1	10.0	9.1	2.1
6	125	13.4	10.2	9.9	4.4
7	140	14.2	13.3	12.9	3.0
8	210	25.6	9.7	8.7	7.5

*** Mixed ice-core sample. ** Ice-core sediment pre-settled for 5 minutes. Aliquot from supernatant taken and chemically dispersed.**

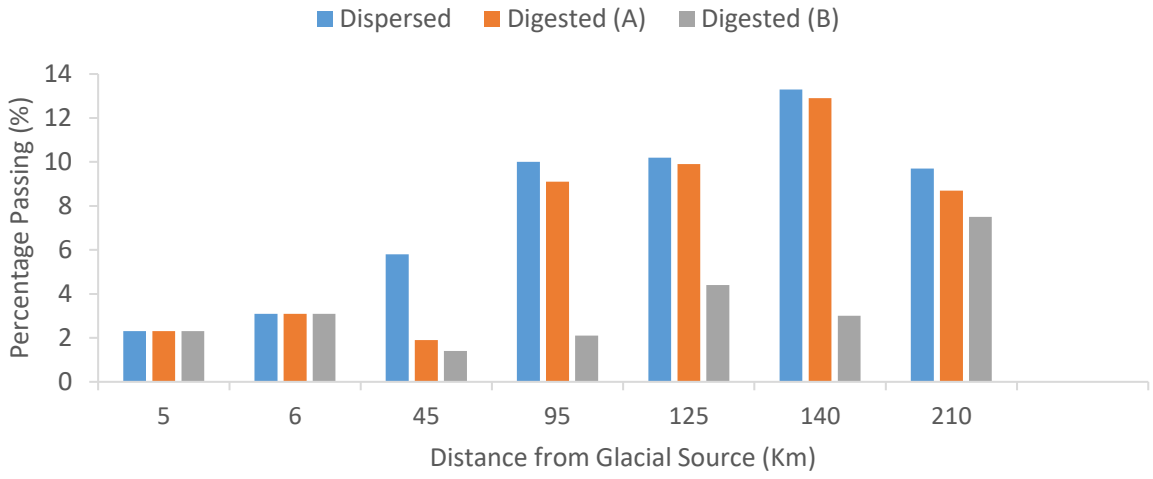

Figure 2.8. Plot of the PSD median volumes (D50) for chemically dispersed ($(NaPO_3)_6$), H_2O_2 treated (A), and NaOH treated (B) SPM collected throughout the catchment.

2.3.2.2 SPM - Morphology

SEM imaging supports the PSD data, demonstrating that the majority of inorganic particles were 0.1 – 10 um in size. Particles observed in the ice-core, Lake Tasman and the Hooker River samples were almost exclusively individual single mineral particles. Some aggregation of particles were observed in the glacier core sample, but most aggregation occurred downstream of Lake Pukaki (Figures 3 and 4). Freshwater diatoms (including *Cyclotella, Asterionella, Dinobryon, Eunotia, Fragilaria, Cymbella and Surirella*) and detrital organic matter were identified in samples collected from Lake Pukaki and all other downstream sites (**Table 2.6 and Figures 2.9 – 2.11**).

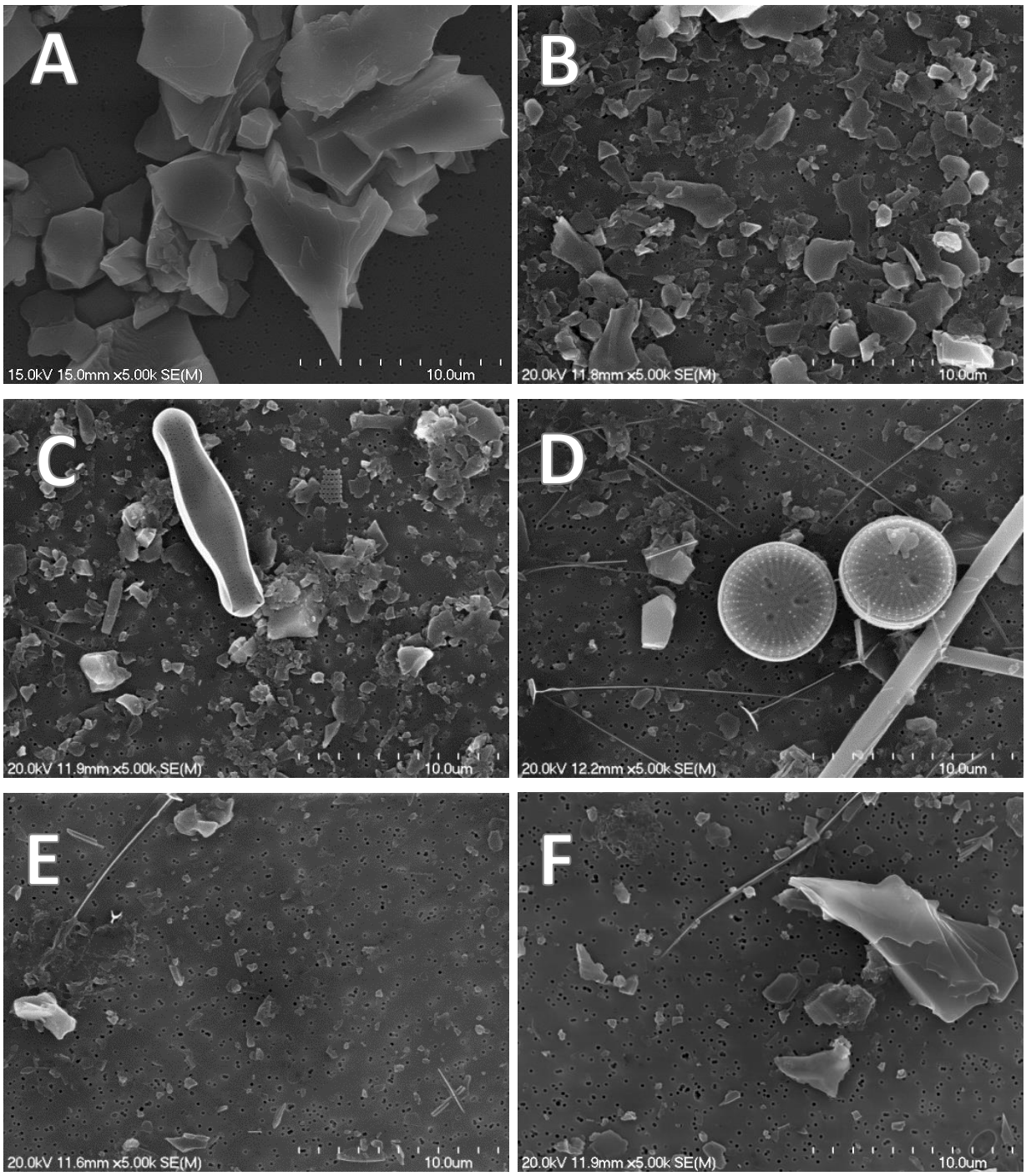

Figure 2.9. SEM images of SPM retrieved from sites progressing down the length of the Waitaki Catchment. 5000x magnification to allow size comparison (full scale bar is 10 μm): (A) Sediment from the Tasman Glacier Core; (B) Lake Tasman; (C) Lake Pukaki; (D) Lake Benmore – Haldon Arm; (E) Lake Aviemore; (F) Waitaki River.

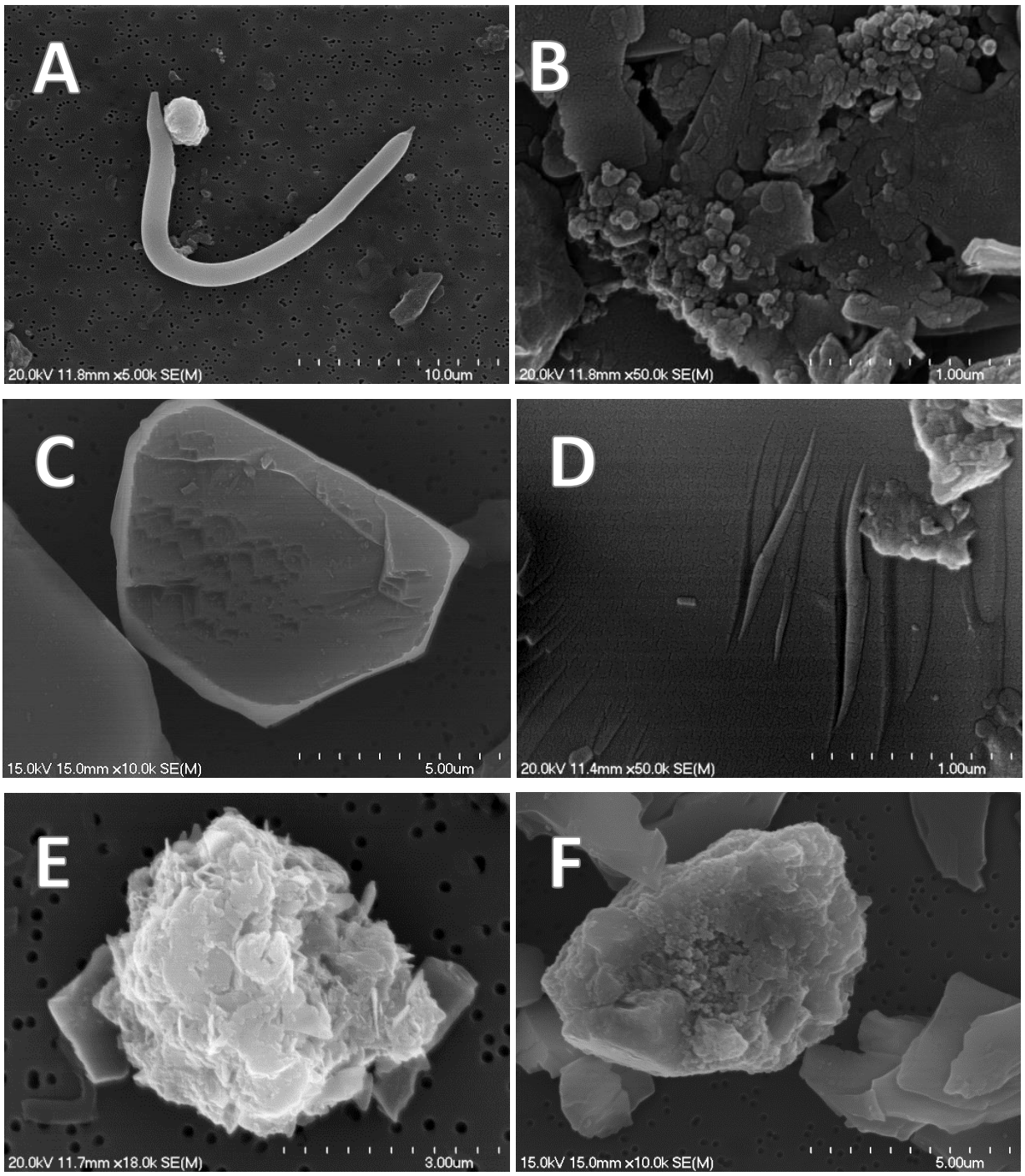

Figure 2.10. SEM images from of particles isolated from the ice-core. (A) Unidentified organism, possibly a nematode, isolated from a core section at 34 m depth; (B) Surface precipitate on mineral particle from ice core (C); Evidence of glacial grinding on quartz particle (D); Micro-striations on surface of quartz particle from the ice core (E) Particle aggregate in ice-core; (F) Plagioclase (anorthite) with iron rich surface coating. Note the variation in scale. 1,000 – 50,000 X magnification. Full scale bar ranging from 1 – 10 µm.

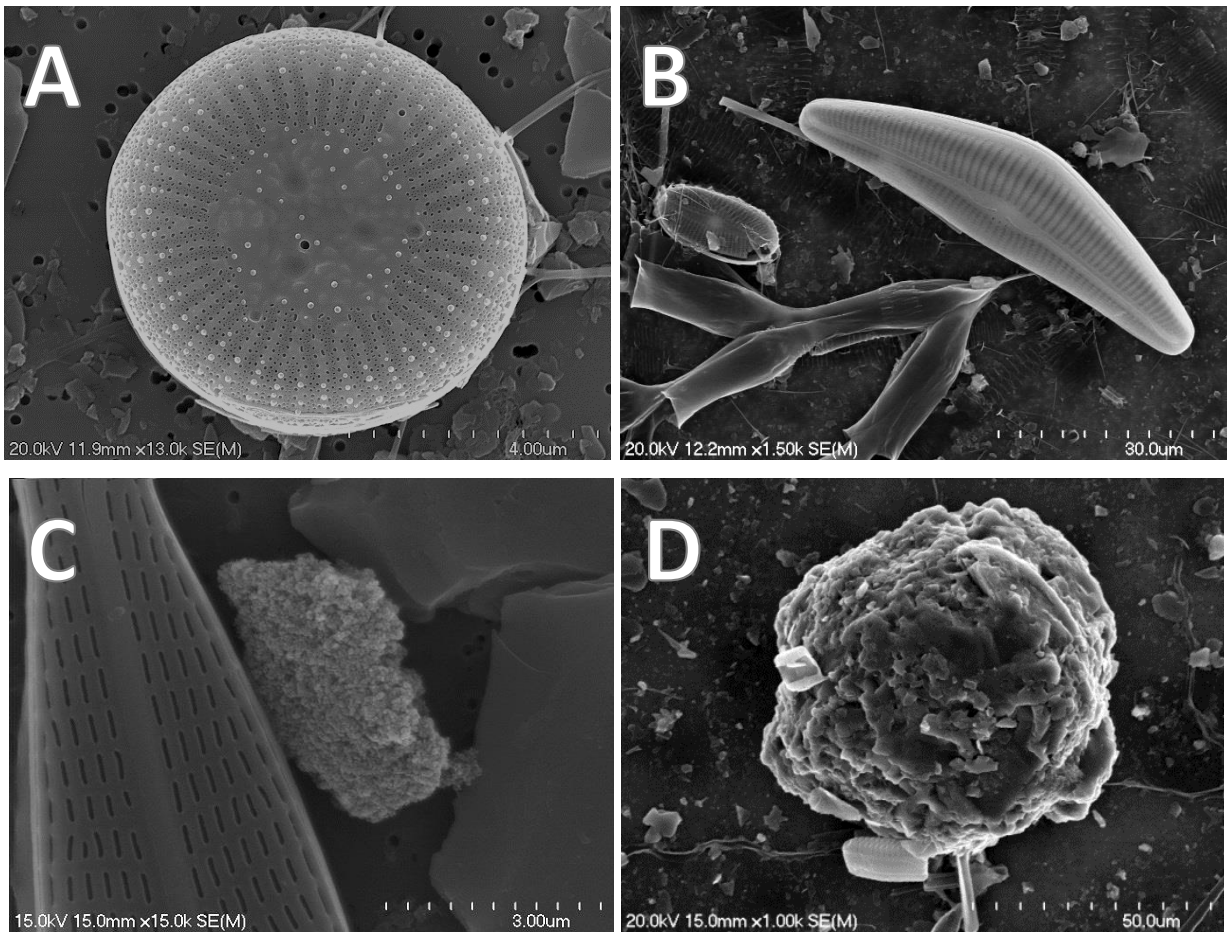

Figure 2.11. SEM images from of particles encountered in the Waitaki Catchment. (A) *Cyclotella*, from Lake Pukaki; (B) SPM from Lake Benmore (C) An aluminosilicate particle with extremely rough surface texture (D) large aggregate from Lake Benmore – Ahuriri Arm. Note the variation in scale. 1,000 – 15,000 X magnification. Full scale bar ranging from 3 – 50 µm.

2.3.2.3 SPM - Composition

Analysis of Lake Tasman SPM by XRD indicated the mineralogy was dominated by quartz, albite, illite, and minor kaolinite (**Table 2.6**). EDS analysis identified illite, quartz and albite as the dominant minerals throughout the catchment. Diatoms and filamentous algae and/or cyanobacteria became increasingly present in samples from Lake Pukaki, and were the dominant particles in Lakes Benmore and Aviemore. Minor quantities of anorthite, biotite, titanite and hydroxyapatite were also detected throughout the catchment. The weathering product kaolinite was only detected in Lake Aviemore with EDS. A model spectra of hydroxyapatite is presented in **Figure 2.12**.

Table 2.6. SPM composition and mineralogy at sites throughout the Waitaki Catchment. Major phases (> 80% particles) identified with combination of XRD and SEM/EDS analysis. Minor phases were not identifiable in the XRD analysis. These were characterised with EDS mapping and targeted point analysis.

Site	Particles identified (in order of abundance)		Character*
	Major phases identified by XRD + SEM/EDS	**Minor phases observed by SEM/EDS**	
1*	Illite, albite, quartz	anorthite, biotite, titanite and hydroxyapatite	A, B
2	Illite, albite, quartz	anorthite, biotite, titanite and hydroxyapatite	A
3	Illite, albite, quartz	anorthite, orthoclase, biotite, titanite, hydroxyapatite	A
4	Illite, albite, quartz, diatoms	biotite, diatoms, hydroxyapatite, orthoclase	A, B, C, D
5	Diatoms, illite, quartz	biotite, albite, kaolinite	A, B, C, D, E
6	Diatoms, illite, albite, quartz	biotite, titanite and hydroxyapatite	A, B, C, D, E
7	Diatoms, quartz, illite	kaolinite and orthoclase	A, B, C, D, E
8	Illite, albite, quartz, diatoms	muscovite, anorthite, titanite and chlorite	A, B, C, D

***Particle Character Classification System: A = Single Particles; B = Aggregates; C = Diatoms; D = Organic Detritus or Pollen; E = Filamentous algae &/or cyanobacteria**

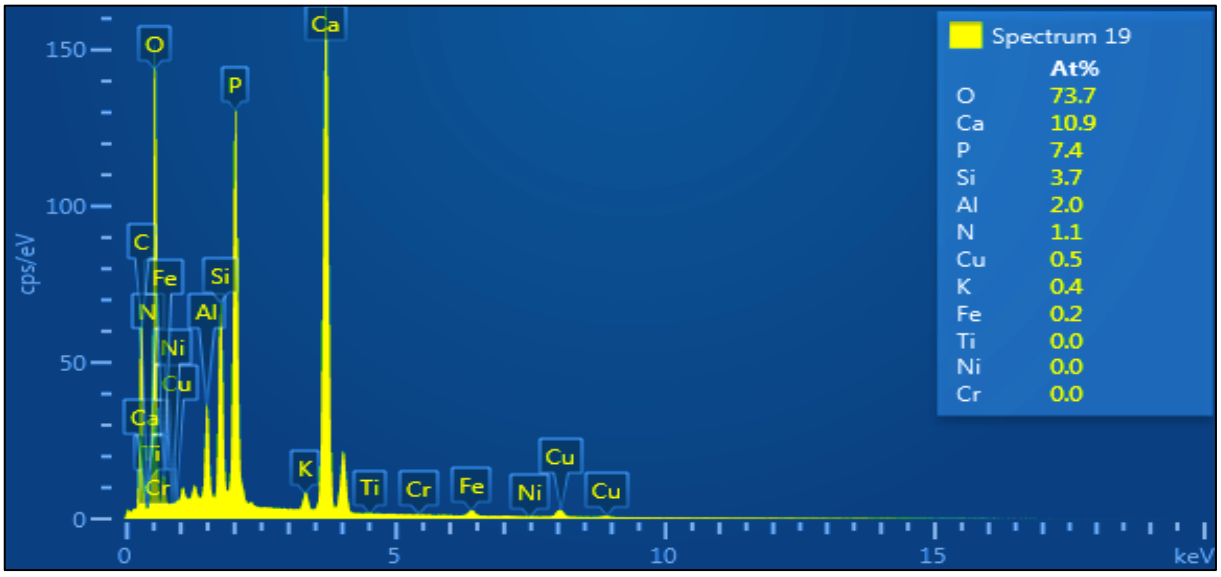

Figure 2.12. SEM/EDS spectra for hydroxyapatite particle generated on Oxford Aztec© EDS software.

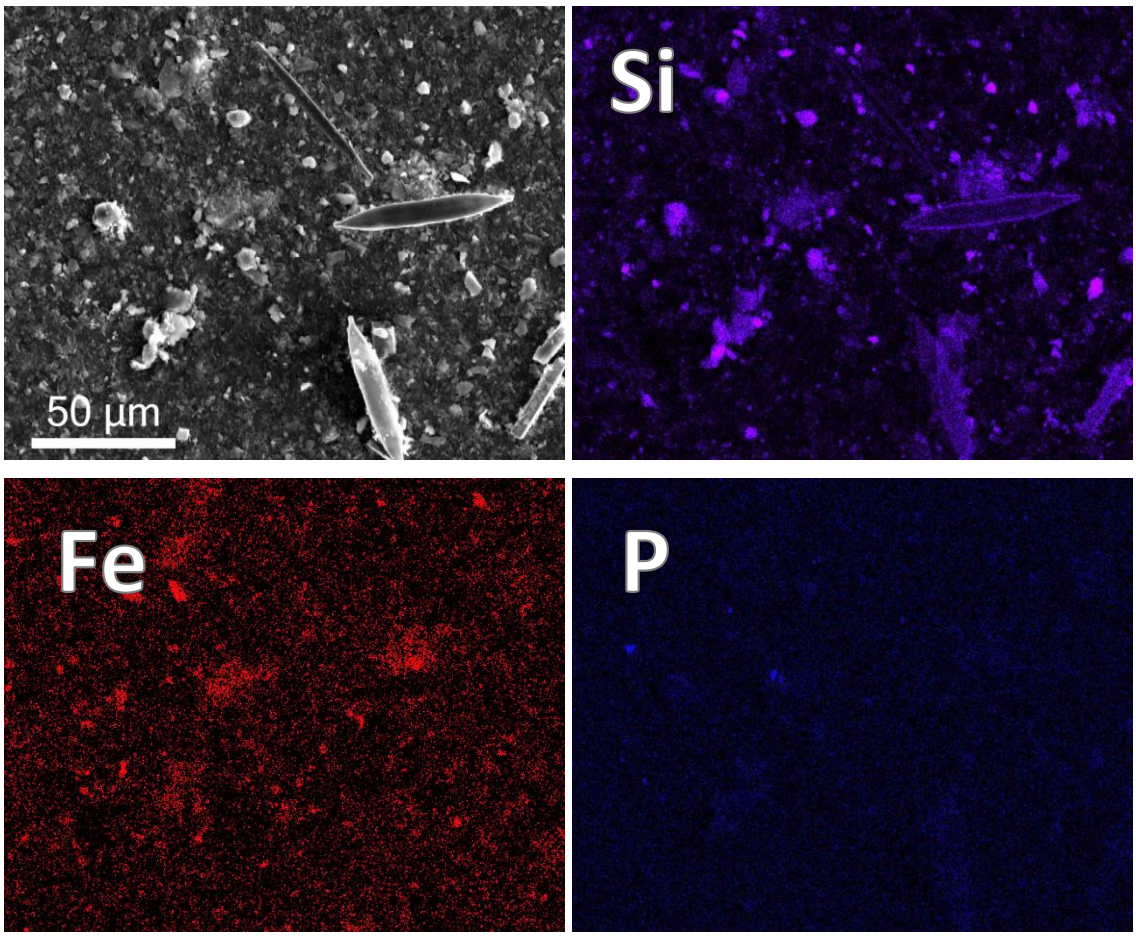

Figure 2.13. SEM/EDS mapping was used to characterise minerals in the SPM. Biogenic silicates (such as diatoms) and organic matter were identified with Si profiles. Minor phases were identified from "elemental hotspots", such as the presence of: Fe-oxide phases associated with SPM throughout the samples; and hydroxyapatite identified from the bright blue spots on the P map.

The proportions of major elements, determined by SEM/EDS, are presented in **Table 2.7 and Figure 2.14**. A general decrease in the proportions of K, Mg, Fe and Al (weight %) was detected in SPM collected with increasing distance from the glacier source. No trend was observed for Na, Ca and S, but a substantial decrease in Si relative to other elements was recorded in Lakes Ahuriri and Aviemore. SPM collected from Lake Tasman and the Hooker River were 0.22 – 2.8 % organic carbon by weight. This increased significantly down catchment with the corresponding increase in diatoms. Organic carbon made up 9.9 – 63.2 % of SPM weight in the catchment lakes. Between 8.3 – 19.6 % was measured in SPM collected from the Waitaki River.

Table 2.7. Elemental composition of SPM obtained by 400 x 400 µm scan showing: weight % from SEM/EDS analysis of SPM. TC (% weight SPM) determined by combustion.

Site	Na	K	Mg	Ca	Fe	Al	Si	S	TOC
1*	1.1	3.5	1.6	0.8	3.5	8.7	16.1	0.6	0.2
2	2.1	3.9	1.8	1	4.9	11	24.2	< 0.1	0.8
3	1.7	4.3	1.8	1.2	5.6	11.5	25.7	< 0.1	1.5
4	2.8	2.9	1.1	1.5	3.6	9.9	23.9	0.2	9.9
5	1.8	2	1.1	0.8	3.5	7.1	18.2	0.2	26.7
6	1.4	1.7	1.1	0.7	3.5	6.8	16.5	0.2	24.0
7	1.4	1	0.9	0.5	1.9	4.9	13.5	< 0.1	31.7
8	3.3	2.3	1.2	2.3	3.6	11.4	28	0.4	8.3

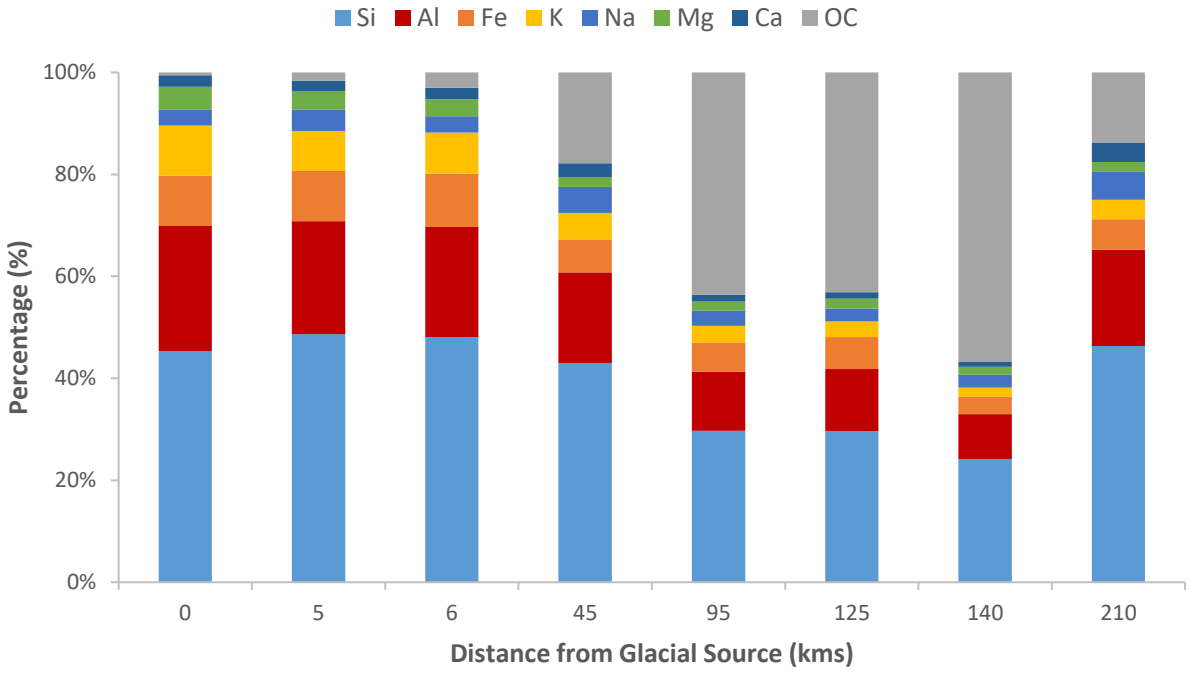

Figure 2.14. Collective elemental composition (weight %) of SPM collected with increasing distance from the glacial source in Waitaki Catchment. Only the major elemental components have been included, and have been normalized to 100%.

Large differences were detected in the acid-soluble Al, Mn and Fe concentrations detected in between samples collected in the upper and lower catchment (**Table 2.8**). Significantly higher proportions of Al and Fe, ranging from 2.3 – 3.1 and 3.0 – 4.2 weight % respectively, were measured in the upper catchment samples. This declined to 0.8 – 1.2 and 1.1 – 3.0 weight % for Al and Fe in the lower catchment respectively. Interestingly, higher proportions of Mn (1474 – 2409 mg/kg) were

detected in SPM at Lakes Ahuriri and Aviemore compared to the remainder of the catchment (576 – 738 mg/kg). SPM collected from Lake Benmore – Ahuriri Arm was enriched in Cd relative to other sites. The total digested phosphorus concentrations in the upper catchment glacial SPM ranged from 247 mg/kg in the ice-core to 342 mg/kg at Lake Tasman. The concentrations were comparatively low to all downstream sites. The greatest concentrations, of 3103 and 5593 mg/kg, were determined in samples from Lakes Benmore – Haldon Arm and Aviemore respectively.

Table 2.8. Acid soluble composition of SPM in mg/kg after digestion in hot concentrated nitric acid. *Total phosphate in mg/kg after autoclave assisted persulphate digestion.

Site	Al_{as} (Wt %)	Fe_{as} (Wt %)	Mn_{as}	Co_{as}	Ni_{as}	Cu_{as}	Zn_{as}	As_{as}	Cd_{as}	Pb_{as}	TP_{as}*
1*	2.3	3.3	576	11.7	17.2	13.6	59	4.1	0.02	28.7	247
2	3.1	4.2	738	23.9	24.8	43.7	230.9	12.5	<DL	57.5	342
3	2.9	3.5	650	20	25.3	25.6	107.8	19.1	0.06	42.5	339
4	2.4	3.0	620	16.2	24.2	52.5	183.8	24.2	0.42	47.6	784
5	1.0	1.1	581	< DL	34.8	53.4	255.4	16.7	<DL	67.5	3103
6	1.2	3.0	2409	16.8	10.8	31.8	162.4	31	8.15	28.8	1090
7	0.8	1.3	1474	7.9	7.4	6.2	117.6	14.7	<DL	17.3	5593
8	1.0	1.6	679	8	7.1	24.6	94.7	7.5	<DL	15.4	1546

2.3.2.4 SPM - Weathering

A comparison of the CIA and WIP weathering index scores, as a function of distance down the catchment, is presented in **Table 2.9.** The WIP generally declines with increasing distance from the glacier source. The exception is a single outlier measured for the Ahuriri Arm of Lake Benmore (125 km). The greatest decrease (WIP score 69 – 56) was observed in the first 45 km. An increase was also observed in the final Waitaki River sample (210 km). Only minor fluctuations (67 – 72) were measured with the CIA throughout the catchment (**Figure 2.15)**.

Table 2.9. Chemical index of alteration (CIA) and Weathering Index of Parker (WIP) scores calculated for SPM collected with progressive distance from the glacial source in the Waitaki River catchment. An increase in weathering is indicated by: an increasing CIA value; and a decreasing WIP value.

Site (kms)	1 (0)	2 (5)	3 (6)	4 (45)	5 (95)	6 (125)	7 (140)	8 (210)
CIA	71.8	70	70.8	68.9	69.7	72.6	72.2	67.6
WIP	69.3	64.7	62.1	55.2	55.7	51.1	47.7	54.2

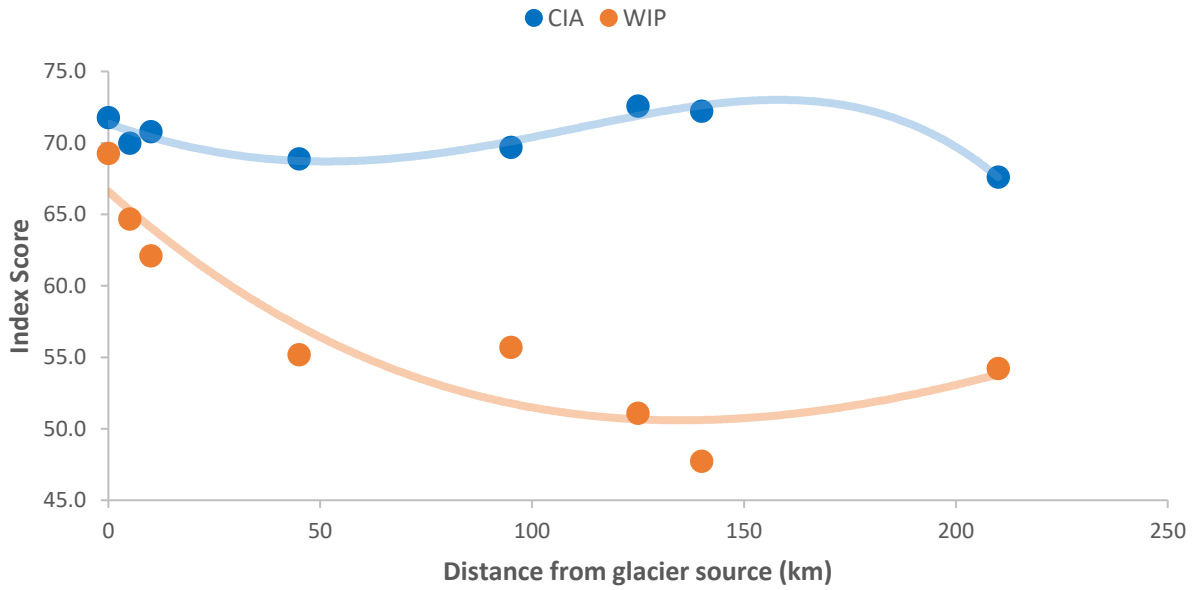

Figure 2.15. Plot of Chemical index of alteration (CIA) and Weathering Index of Parker (WIP) scores determined for SPM collected with progressive distance from the glacial source in the Waitaki River catchment.

2.3.2.5 Point of Zero Charge and Isoelectric Point

The IEP, the point at which the zeta potential was equal to 0 mV, was found to be located at ~pH 2 for all samples. The greatest zeta potential of -50 mV was measured in the Lake Tasman SPM between pH 6-9, while the Waitaki and Waikato River SPM were found to have the lowest zeta potential (-30 mV) in the same pH region. Common IEP values for primary and secondary minerals are provided in **Table 2.10** for comparison.

The PZCs determined with the immersion technique was comparable for all SPM samples (pH ~6.5 – 7). The greatest pH changes were measured at initial pH values of 5 and 9, with ΔpH of ~1 and 2 units respectively. The lowest ΔpH was measured at pH 2 and 6-7, where little pH drift was detected.

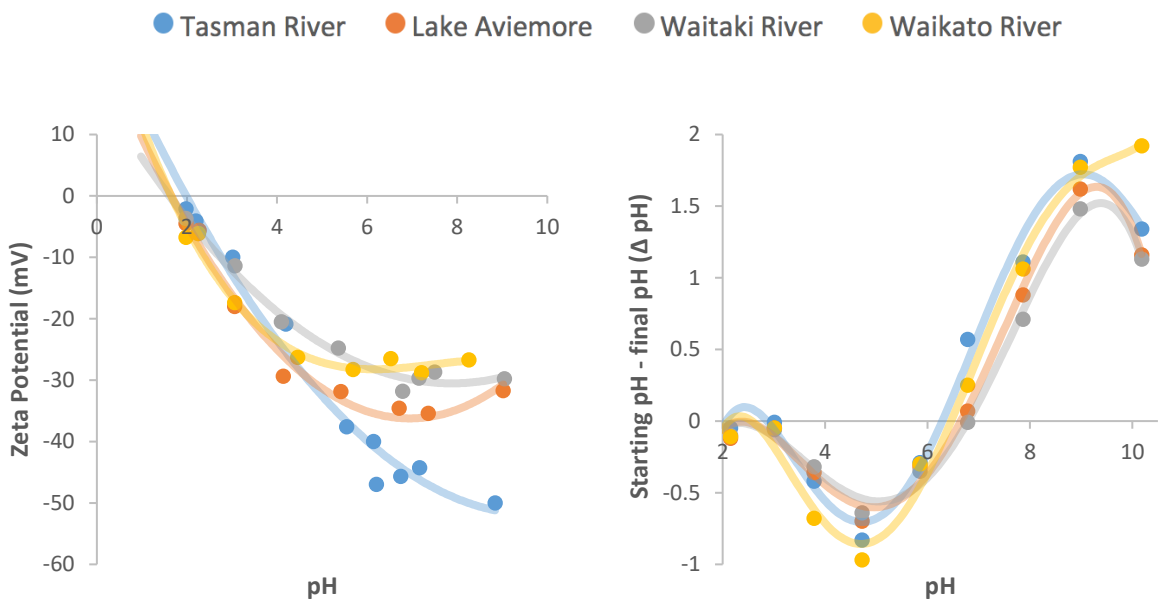

Figure 2.16. The isoelectic point as determined by zeta Potential (left) and immersion technique results (right).

Table 2.10. Published Isoelectric Point (IEP) values for common primary and secondary minerals. Values compiled by Kosmulski (2011).

Primary Minerals		**Secondary Minerals**	
Name	**IEP**	**Name**	**IEP**
Quartz	< 2	Kaolinite	~3
K-feldspar	< 3	Gibbsite	9.6
Na-Feldspar	< 2	Ferrihydrite (2-line)	7.1 - 8.6
Mica	< 3	Goethite	7.3 - 9.2
Biotite	6.5	Calcite	7.5 - 8.8

2.3.3 Statistical Analysis

Key correlations calculated with the Pearson correlation matrix included: the distance from the glacial source and the PSD median size (D50); the PSD D50 and TOC and TP content; concentrations of Cu, Zn and Pb; and Mn and Cd concentrations. Key inverse correlations of interest include: distance from the glacial source and the concentrations of acid-soluble Al and Fe; PSD D50 and concentrations of acid-soluble Al and Fe; PSD D50 and SSA (**Table 2.11**).

Table 2.11. Pearson correlation matrix with resulting values ranging from -1 (red) to 1 (green). Significant values at the 5% (p= <0.05) are highlighted in **bold**.

	km	µm	m^2/g	wt %			mg/kg				
Variables	**Distance**	**D50**	**SSA**	**TOC**	**Al**	**Fe**	**Mn**	**Cu**	**Zn**	**Pb**	**TP**
Distance	**1.00**										
D50	**0.86**	**1.00**									
SSA	-0.45	-0.64	**1.00**								
TC	0.65	**0.93**	-0.58	**1.00**							
Al	**-0.88**	**-0.96**	**0.74**	**-0.83**	**1.00**						
Fe	**-0.76**	**-0.86**	0.68	-0.68	**0.90**	**1.00**					
Mn	0.39	0.53	-0.18	0.70	-0.44	-0.05	**1.00**				
Cu	-0.20	-0.20	0.31	-0.14	0.23	0.12	-0.25	**1.00**			
Zn	-0.10	0.05	0.24	0.17	0.04	-0.03	-0.01	**0.85**	**1.00**		
Pb	-0.55	-0.40	0.39	-0.28	0.42	0.23	-0.40	**0.83**	**0.83**	**1.00**	
TP	0.56	**0.84**	-0.57	**0.81**	**-0.74**	**-0.81**	0.26	-0.30	0.08	-0.24	**1.00**

2.4 Discussion

2.4.1 Changing Water Characteristics down Catchment:

High concentrations of glacial SPM remained suspended in the cold proglacial meltwater from Lake Tasman and Hooker Rivers throughout the year, giving rise to its turbid grey hue (Figure 3). However, only a small proportion (2 - 6 %) of the SPM remained suspended in the samples collected from Lake Pukaki. Most will undergo sedimentation on entry into Lake Pukaki. Chikita et al. (2000) demonstrated that the cold sediment-rich meltwater plunges on entry into Lake Pukaki. Beyond Lake Pukaki, SPM concentrations were found to increasingly decline. This will be due to sedimentation and may be enhanced by aggregation processes in the quiescent conditions (Droppo, 2001). Minor increases in SPM concentration were detected in the Lower Waitaki River. This may be due to the resuspension of river bed sediments and minor inputs from downstream tributaries.

Despite the highly modified character and extensive agricultural developments in the lower catchment, the water quality of the glacier-fed Waitaki catchment remained of a high quality throughout the catchment. The composition of the glacial meltwater was typical of an alpine, glacial fed catchment. The meltwater was found to be enriched in Ca^{+}, HCO_3^{-} and SO_4^{2-} which may be due to the weathering of sediments in the subglacial environment. This process may also account for the elevated trace element concentrations (e.g. As from sulphide weathering) closer to the glacial source

(Brown, 2002; Tranter, 2007). Significant differences in the concentrations of "dissolved" cations were detected in the fresh glacial melt. The concentrations were typically 1-2 orders of magnitude greater than samples collected in the lower catchment. However, it is likely that these increases are attributable to the greater concentration of fine particles < 0.45 μm in size in these waters, which are known to pass through filter membranes (Horowitz et al., 1996). No appreciable enrichment of the toxic trace elements was detected in the developed lower catchment. The concentrations of dissolved nitrate remained low, and DRP concentrations were typically below detection limits. The concentrations of organic carbon were found to increase with progressive distance from the glacial source. This trend is attributable to the evolution of the rivers surroundings from its sparse, alpine headwaters to the predominantly agricultural character in the lower catchment.

2.4.2 Changing SPM Characteristics Down Catchment:

The particles isolated from the Tasman Glacier ice-core were almost exclusively inorganic mineral particles and highly angular (**Figures 2.9 -2.11**). The SPM had surface textures characteristic of freshly abraded glacial sediments such as the distinct striations present on a particle of quartz (**Figure 2.10**). Evidence of both chemical weathering and mineral precipitation was observed on particles, demonstrating the dynamic modifications of the sediment taking place within the glacial environment. The predominant minerals identified in the ice-core were illite, quartz and albite which is consistent with the primary mineral phases found in the Torlesse greywacke source (Mackinnon, 1983). A number of organisms, including diatom frustules and an unidentified nematode, were also discovered in the ice-core sediment (**Figure 2.10**). Previous research has demonstrated that glaciers sustain simple ecosystems that are mainly dominated by fungi, protists, bacteria and viruses (Hodson et al., 2008). The findings from this research provide additional evidence that glaciers can support niche ecosystems. Aggregated particles were also found in the ice-core sediments which have previously been suggested to form in the subglacial environment (Woodward et al., 2002).

The morphology and mineralogy of particles isolated from Lake Tasman and the Hooker River were similar to those in the ice-core. Illite, quartz and albite remained the dominant mineral phases, and the SPM had a low proportion of organic matter. The major difference was that the particles were considerably finer (**Figure 2.9**). This was evident in the distinctly bimodal PSD and dominance of sub-micron particles seen in SEM imagery. Some rounding of the particles was observed and may be attributable to weathering taking place within the glacier and in the proglacial lakes. The greatest zeta

potentials were also determined in these samples, demonstrating the high dispersive stability for these particles. In general, the mineralogy and morphology of the fresh glacial SPM collected in this study was found to be comparable to previous investigations of fresh glacial SPM (Chanudet and Filella, 2006; Finger et al., 2006; Sommaruga, 2015), and may indicate that adsorption studies with glacial SPM could be broadly applied.

SPM collected from Lake Pukaki had a greater proportion of diatoms and organic matter, with a corresponding increase in TOC and TP concentrations. The SPM lost its bimodal character in the PSD, and the associated D10, 50 and 90 increased by almost an order of magnitude. The significant reduction in size after the digestive treatments suggests that the presence of larger, voluminous diatoms acted to shift the particle size distribution. Fine mineral particles were still present in the SPM (**Figure 2.9 -2.11**), but were often associated with large aggregates. Filella and Buffle (1993) showed that fine particulates (< 1 µm) undergo rapid coagulation in lake environments, and it is likely that aggregation processes have resulted in a significant reduction in these particles (Droppo, 2001). Illite, quartz and albite remained the major inorganic phases in the SPM. The dominance of illite clay in the SPM has been proposed to account for the high reflectance and bright blue colour (**Figure 2.2**) of the lake (Gallegos et al., 2008). Chanudet and Filella (2007) reported the character and composition of SPM in the proglacial Lake Brienz, a large lake in Switzerland fed by the Aare and Lütschine Rivers. The majority (~ 80%) of the SPM were large individual particles > 2µM in size that had not yet undergone aggregation. The larger particles were found to undergo sedimentation slower than predictions based on Stokes law. It is possible that the large illite plates in Lake Pukaki behave in a similar fashion, assisting them to stay in suspension for their long residence (> 400 days) in this reservoir.

Diatoms and large aggregates became increasingly prevalent in the SPM collected downstream of Lake Pukaki (**Figure 2.9**). The large increases in TP and TOC, and general decline in the proportion of Na, K, Mg, Fe and Al is a testament to the increased presence of the biological particles. A corresponding increase in the D50s associated with the PSD data demonstrates the influence of these particles. Significant reductions in the PSD D50's of the SPM were detected after digestion in NaOH. This demonstrated that biogenic silicates (such as diatoms) played a key role in influencing the particle size distributions of the SPM. Illite, quartz and albite remained the major inorganic particles in the lower catchment lakes. The decline of the zeta potential (ZP) indicated that the SPM may be more susceptible to particle aggregation. Zhuang and Yu (2002) found that organic matter can decrease the

zeta potential of clay minerals. Particle aggregates were certainly more frequent in the lower catchment and the increased presence of organic matter may be enhancing particle aggregation and instability.

The Lower Waitaki River SPM had a greater proportion of inorganic particles relative to the upstream Lakes Benmore and Aviemore. Illite, quartz and albite were once again the dominant minerals, demonstrating that the mineralogy of inorganic particles remained consistent throughout the catchment despite the lengthy opportunity for sorting, sedimentation and weathering to occur. These observations are consistent with recent observations in the Rhone River in France, where the SPM mineral composition was found to remain unchanged in the varying size fractions throughout the catchment (Slomberg et al., 2016).

In general, the mineralogy and morphology of the fresh glacial SPM collected in this study was found to be comparable to previous investigations of glacial SPM. Chanudet and Filella (2006) reported SPM from Lake Brienz, Switzerland to mainly consist of aluminosilicate particles coated with iron oxy/hydroxides. The major mineral phases were biotite, muscovite, quartz and orthoclase with minor quantities of titanite, apatite, kaolinite, barite and calcite. Finger et al. (2006) also reported a PSD range of 3.4 – 8 µm for SPM in the same lake. A more recent investigation from the Austrian Alps reported glacial SPM to be mainly muscovite/illite, chlorite, quartz and calcite, with and PSD range 0.7 – 4 µm (Sommaruga and Kandolf, 2014).

2.4.3 SPM Weathering

Active chemical weathering of the glacial SPM occurs during its residence in the Waitaki Catchment. The most significant changes appear to have occurred in the transition from the ice-core sediment to the proglacial SPM, where an immediate decline in the WIP was determined. There was also direct evidence of pitting on the surface of the ice-core sediment. Kirkbride and Spedding (1996) previously stated that glacial debris is weathered during fluvial transport within the englacial conduits of the Tasman glacier. Reactive components of the freshly abraded mineral surfaces will undergo solubilisation on contact with dilute ice- and snowmelt (Tranter et al., 2002). Carbonates and sulphide bearing minerals are only present in trace quantities in the greywacke bedrock (Mackinnon, 1983; Templeton et al., 1998). However, both carbonate and sulphide oxidation processes can play a key role in the weathering of sediment in glacial environments, forming important secondary minerals such as hydrous ferric oxides (HFO) (Tranter et al., 2002). Higher proportions of SO_4^{2-} were detected

in the ice-core sediment compared to the proglacial SPM. The highest concentrations of SO_4^{2-} and Ca^{2+} were also measured in the meltwaters nearest the glacial source, suggesting that active sulphide and carbonate weathering has occurred. SPM continued to be weathered down catchment as demonstrated by a decline in the WIP and gradual increases in the concentrations of Na, K and Mg. Only the SPM from the Waitaki River deviated from the trend, with WIP scores more characteristic of the upper catchment SPM. It is possible that the resuspension of bed sediment more characteristic of the unweathered source rock, or the input of fresh sediment via a lowland tributary is contributing to this result.

Two indices - the CIA and WIP were used to assess particle weathering. Only the WIP was found to show a clear decline in the index score (and therefore increased weathering) with increasing distance from the glacier source. The CIA demonstrated no clear trend. A depletion of the labile Ca, Na and K relative to Al will increase the calculated CIA value during the conversion of primary feldspar minerals to clays. It is likely that the enrichment of diatoms in the SPM, with their silicon rich frustules, have obscured this relationship. SEM imaging also indicates that many of the primary minerals are still present in high proportions throughout the catchment, indicating that the use of aluminium as a resilient, immobile phase may not be applicable in this instance. The WIP allows for the mobility of aluminium (Price and Velbel, 2003) and was found to be applicable in this study.

2.4.4 Adsorption Capability

The SPM collected in close proximity to the glacial source was dominated by fine, sub-micron particles. These particles were found to have a large capacity to adsorb methylene blue relative to the lower catchment. The associated SSAs and CECs were comparable to clay rich soils reported by Hang (1970), Yukselen and Kaya (2008), and highly adsorptive sediments by Lin and Chen (1998). A high degree of surface roughness was observed on these particles, and it is possible that this has enhanced the associated surface area and adsorption capability (Mahaney and Kalm, 2000). The glacial SPM was also found to have greater proportions of acid soluble Al and Fe concentrations compared to the lower catchment samples. The higher concentrations were attributed to the digestion of reactive surface oxides, such as ferrihydrite and gibbsite, which are known to be efficient scavengers of dissolved ions (Dzombak and Morel, 1990; Parfitt et al., 1975). The combination of these properties indicates that the freshly abraded glacial SPM may have a large adsorption capacity for dissolved ions.

The SPM from the lower catchment lakes was found to have a greater proportion of biogenic particles with larger particle sizes. This SPM also had lower acid-soluble Al and Fe concentrations, and a significantly lower capacity to adsorb methylene blue compared to the upper catchment SPM. These results suggest that the lower catchment SPM may have a lower capacity to adsorb dissolved ions relative to the upper catchment SPM. However, the greater concentrations of organic matter may complicate this relationship. Contrary to this research, Lin and Chen (1998) demonstrated that non-glacial sediments from Taiwan had positive correlations between the organic matter content, the associated CECs and the adsorptive capacity for Cu, Cr, Zn and Pb. Bibby and Webster-Brown (2006) also demonstrated that the organic matter content of SPM in the non-glacial Waikato River played an important role in the adsorption of Cu, while the surface oxides played important roles in the adsorption of Zn and Pb.

An additional insight into the adsorption characteristics of the SPM was generated with the determination of the PZC. Most iron oxide minerals, including ferrihydrite, goethite and hematite, have PZC values in the range of pH 6-8 (Kosmulski, 2011). The PZC of the SPM samples were determined in the same range, and strongly indicates that one, or a combination of these phases, plays a key role in controlling the charge characteristics of the glacial SPM.

2.5 Review of Analytical procedures:

This research has utilised a variety of analytical techniques to determine both the character, composition and adsorption capability of SPM throughout the Waitaki catchment. An extremely limited amount of SPM was able to be recovered at the lower catchment sites due to the extremely low concentrations of SPM in suspension. It was therefore not possible to use some of the more common analytical procedures used to characterise the particulate material. The following section describes the strengths and weaknesses of the analytical methods used.

2.5.1 Surface Sediments:

Surface sediments are commonly used as an analog for SPM when sufficient quantities of SPM cannot be collected. In this research, the surface sediments had a very different character and composition to the SPM. In the upper catchment, the surface sediments were course and were found to have low SSAs and CECs compared to the SPM sample. In the lower catchment, the surface sediments had a greater proportion of inorganic particles and concentrations of reactive oxides; and a

lower concentration of biogenic particles, TOC and TP compared to the SPM. Based on these results, it is predicted that the surface sediments collected near the glacial source will have a lower adsorption capacity than the SPM, while the opposite is true for the lower catchment. It is therefore not recommended that surface sediments are used as a substitute for SPM in adsorption studies.

2.5.2 Specific Surface Area (SSA) Analysis

To date, there is still no standard method for the determination of the SSA of SPM when only small quantities of material are available. The BET is commonly used to determine the SSA of particulate matter. However, the test requires a large sample mass which was not possible to collect in this study. There have also been questions about its suitability as an effective determinant of SSA in aquatic samples. The method uses material in a dry state, which may limit the reactivity and the accessibility of the reactive functional groups accessible in the aqueous phase. Additionally, the compaction of fine SPM, especially clay minerals, may inhibit the penetration of nitrogen molecules onto potential adsorption sites (Shelden et al., 1993).

The novel methylene blue method used in this study has proven to be an effective tool to determine the relative SSA, CEC and adsorption capability of SPM. The molecule may adsorb to the interlayer surfaces of clay minerals and micropores of organic matter (Heister, 2014; Santamarina et al., 2002). However, Li et al. (2011) has stressed caution in using the methylene blue technique for SSA measurements, pointing to the fact that methylene blue may achieve a multiplicity of different molecular configurations during adsorption that can contribute to errors in the final calculations. They also determined that the charge density, rather than the SSA, was of greater importance for the adsorption of methylene blue and that the technique could be used to provide a reliable determination of the CEC. In any case, the technique has been used effectively in this research to provide an assessment of the likely SSA and adsorption capability of the SPM.

2.5.3 Particle Size Distribution

Laser diffraction analysis has proven to be a rapid, cost-effective tool to investigate particle size distributions. However, care must be taken with the analysis of results. SPM is often a heterogeneous mix of particles determined by the biogeochemical features of the catchment. The size of particles may vary from tiny colloids to large aggregates, with varying complexity of shape. These attributes increase the potential for error and results should always be compared with microscopic

analysis (Andrews et al., 2010). In this study, it was deemed to be important to classify the difference between the number and volume distribution data. The conversion of the volume data to a number basis provided an indication of how numerous the different particle size classes were.

The PSD's obtained from fresh, untreated SPM was found to differ markedly from the chemically dispersed and digested SPM. PSD's obtained without treatment with the chemical dispersant ($(NaPO_3)_6$) had greater PSD D_{50} values, which indicates the possibility of particle aggregation when transported to the laboratory. The digestion of organic matter and biogenic silicates also demonstrated the importance of the masking effect these particles play in particle size distributions, confirming the potential for interpretive error if laser diffraction is used solely for particle size analysis. Based on these learnings, it is recommended that: 1. SPM is treated with a dispersant, as suggested by Gee and Or (2002), to avoid interpretive errors in the first instance; 2. Separate samples are analysed after digestion of organic matter and biogenic particulates. This will provide an indication of the relative importance these particles play in the overall PSD; 3. A combination of techniques, such as SEM and laser diffraction, are utilized to gain a full picture into the character of SPM in natural systems.

2.6 Conclusions

The results from this study suggest that the freshly eroded glacial SPM has a large capacity to adsorb dissolved contaminants and nutrients. High concentrations of SPM remain suspended in the proglacial lakes that have formed at the termini of the glaciers. This SPM was dominated by extremely fine inorganic particles with high SSAs and CECs as determined by methylene blue adsorption. The particles also had a low degree of chemical weathering compared to the source rock and were relatively enriched in Al- and Fe- surface oxides. Further down the catchment, the concentrations of SPM were found to significantly decline. The SPM remaining was found to become progressively weathered and enriched in organic matter and diatoms. This resulted in an increase in the overall particle size distribution, and decreases in the relative SSAs, CECs and concentrations of reactive surface oxides. Based on this data, it is predicted that the fine SPM generated at the top of the catchment will have a greater adsorption capacity for nutrients such as phosphate and trace elements than SPM from the lower catchment, although the degree of cation or anion adsorption will also be a function of solution chemical composition and pH. SPM in the lower lakes is predicted to have the lowest adsorption capacity. SPM in the lower Waitaki River is expected to have a moderate adsorptive

capacity owing to its greater proportion of inorganic particles and reactive surface oxides. Additional studies that test the adsorption of specific pollutants will be required to validate this hypothesis and determine the variation that may arise from compositional differences. Such information will be increasingly important in assessing changes in water quality in these systems as land-use modification and climate change proceed into the future.

2.7 References

Adamson AW. Physical chemistry of surfaces: Wiley, 1990.

Anderson SP. Biogeochemistry of Glacial Landscape Systems. Annual Review of Earth and Planetary Sciences 2007; 35: 375-399.

Andrews S, Nover D, Schladow SG. Using laser diffraction data to obtain accurate particle size distributions: the role of particle composition. Limnology and Oceanography: Methods 2010; 8: 507-526.

ANZECC (2000). National Water Quality Management Strategy. Australian and New Zealand Guidelines for Fresh and Marine Water Quality.

APHA APHA. Standard methods for the examination of water and wastewater. American Public Health Association, Washington, D.C., 2005.

Bibby RL, Webster-Brown JG. Trace metal adsorption onto urban stream suspended particulate matter (Auckland region, New Zealand). Applied Geochemistry 2006; 21: 1135-1151.

Bourikas K, Vakros J, Kordulis C, Lycourghiotis A. Potentiometric Mass Titrations: Experimental and Theoretical Establishment of a New Technique for Determining the Point of Zero Charge (PZC) of Metal (Hydr)Oxides. The Journal of Physical Chemistry B 2003; 107: 9441-9451.

Brown GH. Glacier meltwater hydrochemistry. Applied Geochemistry 2002; 17: 855-883.

Chanudet V, Filella M. Particle size and mineralogical composition of inorganic colloids in glacier-melting water and overlying ice in an Alpine glacier, Oberaargletscher, Switzerland. Journal of Glaciology 2006; 52: 473-475.

Chanudet V, Filella M. The fate of inorganic colloidal particles in Lake Brienz. Aquatic Sciences 2007; 69: 199-211.

Charters FJ, Cochrane TA, O'Sullivan AD. Particle size distribution variance in untreated urban runoff and its implication on treatment selection. Water Research 2015; 85: 337-345.

Chikita AK, Halstead I, Carter G. Sedimentary environments in Lake Pukaki, New Zealand. Journal of the Sedimentological Society of Japan 2000; 51: 55-66.

Clarke G. Upper Waitaki limit setting process. Predicting consequences of future scenarios: Lake water quality. Environment Canterbury, 2015.

Clarke GKC. Subglacial Processes. Annual Review of Earth and Planetary Sciences 2004; 33: 247-276.

Droppo IG. Rethinking what constitutes suspended sediment. Hydrological Processes 2001; 15: 1551-1564.

Dykes RC, Brook MS, Robertson CM, Fuller IC. Twenty-First Century Calving Retreat of Tasman Glacier, Southern Alps, New Zealand. Arctic, Antarctic, and Alpine Research 2011; 43: 1-10.

Dykes RC, Brook MS, Winkler S. The contemporary retreat of Tasman Glacier, Southern Alps, New Zealand, and the evolution of Tasman proglacial lake since AD 2000. Erdkunde 2010; 64: 141-154.

Dzombak DA, Morel Fo. Surface complexation modeling: hydrous ferric oxide. New York: Wiley, 1990.

Fedo CM, Wayne Nesbitt H, Young GM. Unraveling the effects of potassium metasomatism in sedimentary rocks and paleosols, with implications for paleoweathering conditions and provenance. Geology 1995; 23: 921-924.

Filella M, Buffle J. Factors controlling the stability of submicron colloids in natural waters. Colloids and Surfaces A: Physicochemical and Engineering Aspects 1993; 73: 255-273.

Finger D, Schmid M, Wüest A. Effects of upstream hydropower operation on riverine particle transport and turbidity in downstream lakes. Water Resources Research 2006; 42: n/a-n/a.

Gallegos CL, Davies-Colley RJ, Gall M. Optical closure in lakes with contrasting extremes of reflectance. Limnology and Oceanography 2008; 53: 2021-2034.

Gee GW, Or D. Particle Size Analysis. Methods of Soil Analysis, 2002, pp. 255-293.

Gray D. Upper Waitaki catchment flows, water quality and ecology: state and trend. Investigations and Monitoring Group. Environment Canterbury, Christchurch, New Zealand, 2015.

Gregory J. Particles in Water: Properties and Processes. Boca Raton, Florida: CRC Press, Taylor and Francis Group, 2006.

Hähner G, Marti A, Spencer ND, Caseri WR. Orientation and electronic structure of methylene blue on mica: A near edge x-ray absorption fine structure spectroscopy study. The Journal of Chemical Physics 1996; 104: 7749-7757.

Hallet B, Hunter L, Bogen J. Rates of erosion and sediment evacuation by glaciers: A review of field data and their implications. Global and Planetary Change 1996; 12: 213-235.

Hambrey MJ, Ehrmann W. Modification of sediment characteristics during glacial transport in high-alpine catchments: Mount Cook area, New Zealand. Boreas 2004; 33: 300-318.

Hang PT. Methylene blue absorption by clay minerals - determination of surface areas and cation exchange capacities. Clays and Clay Minerals 1970; 18: 203 - 212.

Hedley CB, Saggar S, Theng BKG, Whitton JS. Surface area of soils of contrasting mineralogies using para-nitrophenol adsorption and its relation to air-dry moisture content of soils. Soil Research 2000; 38: 155-168.

Heister K. The measurement of the specific surface area of soils by gas and polar liquid adsorption methods—Limitations and potentials. Geoderma 2014; 216: 75-87.

Hodson A, Anesio AM, Tranter M, Fountain A, Osborn M, Priscu J, et al. Glacial Ecosytems. Ecological Monographs 2008; 78: 41-67.

Horowitz AJ, Lum KR, Garbarino JR, Hall GEM, Lemieux C, Demas CR. The Effect of Membrane Filtration on Dissolved Trace Element Concentrations. In: Chow W, Brocksen RW, Wisniewski J, editors. Clean Water: Factors that Influence Its Availability, Quality and Its Use: International Clean Water Conference held in La Jolla, California, 28–30 November 1995. Springer Netherlands, Dordrecht, 1996, pp. 281-294.

Kahr G, Madsen FT. Determination of the cation exchange capacity and the surface area of bentonite, illite and kaolinite by methylene blue adsorption. Applied Clay Science 1995; 9: 327-336.

Kerr T. The contribution of snowmelt to the rivers of the South Island, New Zealand. Journal of Hydrology (New Zealand) 2013; 52: 61-82

Kirkbride M, Spedding N. The Influence of Englacial Drainage on Sediment-Transport Pathways and Till Texture of Temperate Valley Glaciers. Annals of Glaciology 1996; 22: 160-166.

Kosmulski M. The pH-dependent surface charging and points of zero charge. Journal of Colloid and Interface Science 2011; 353: 1-15.

Lead JR, Wilkinson KJ. Environmental Colloids and Particles: Current Knowledge and Future Developments. Environmental Colloids and Particles. John Wiley & Sons, Ltd, 2007, pp. 1-15.

Li Z, Chang P-H, Jiang W-T, Jean J-S, Hong H. Mechanism of methylene blue removal from water by swelling clays. Chemical Engineering Journal 2011; 168: 1193-1200.

Lin J-G, Chen S-Y. The relationship between adsorption of heavy metal and organic matter in river sediments. Environment International 1998; 24: 345-352.

Mackinnon TC. Origin of the Torlesse terrane and coeval rocks, South Island, New Zealand. Geological Society of America Bulletin 1983; 94: 967-985.

Mahaney WC, Kalm V. Comparative scanning electron microscopy study of oriented till blocks, glacial grains and Devonian sands in Estonia and Latvia. Boreas 2000; 29: 35-51.

McLennan SM. Weathering and Global Denudation. The Journal of Geology 1993; 101: 295-303.

Morgenstern U, Mayewski PA, Bertler N, Ditchburn RG. Ice core research in the New Zealand Southern Alps. Geochimica et Cosmochimica Acta 2006; 70: A430.

Nelsen FM, Eggertsen FT. Determination of Surface Area. Adsorption Measurements by Continuous Flow Method. Analytical Chemistry 1958; 30: 1387-1390.

Nesbitt HW, Young GM. Early Proterozoic climates and plate motions inferred from major element chemistry of lutites. Nature 1982; 299: 715-717.

Norton N, Spigel B, Sutherland D, Trolle D, Plew D. Lake Benmore Water Quality: a modelling method to assist with assessments of nutrient loadings. Environment Canterbury, Environment Canterbury, 2009.

Parfitt RL, Atkinson RJ, Smart RSC. The Mechanism of Phosphate Fixation by Iron Oxides. Soil Science Society of America Journal 1975; 39: 837-841.

Parker A. An Index of Weathering for Silicate Rocks. Geological Magazine 1970; 107: 501-504.

Pickrill RA, Irwin J. Circulation and sedimentation in Lake Benmore, New Zealand. New Zealand Journal of Geology and Geophysics 1986; 29: 83-97.

Price JR, Velbel MA. Chemical weathering indices applied to weathering profiles developed on heterogeneous felsic metamorphic parent rocks. Chemical Geology 2003; 202: 397-416.

Santamarina JC, Klein KA, Wang YH, Prencke E. Specific surface: determination and relevance. Canadian Geotechnical Journal 2002; 39: 233-241.

Shelden RA, Caseri WR, Suter UW. Ion Exchange on Muscovite Mica with Ultrahigh Specific Surface Area. Journal of Colloid and Interface Science 1993; 157: 318-327.

Slomberg DL, Ollivier P, Radakovitch O, Baran N, Sani-Kast N, Miche H, et al. Characterisation of suspended particulate matter in the Rhone River: insights into analogue selection. Environmental Chemistry 2016

Snelder T, Spigel B, Sutherland D, Norton N. Assessment of effects of increased nutrient concentrations in streams and lakes of the Upper Waitaki Basin due to catchment land use changes. NIWA client report CHC2005-003. National Institute of Water and Atmospheric Research, Christchurch, New Zealand, 2005.

Sommaruga R. When glaciers and ice sheets melt: consequences for planktonic organisms. Journal of Plankton Research 2015.

Sommaruga R, Kandolf G. Negative consequences of glacial turbidity for the survival of freshwater planktonic heterotrophic flagellates. Scientific Reports 2014; 4.

Templeton AS, Chamberlain CP, Koons PO, Craw D. Stable isotopic evidence for mixing between metamorphic fluids and surface-derived waters during recent uplift of the Southern Alps, New Zealand. Earth and Planetary Science Letters 1998; 154: 73-92.

Tiit V. Grain-size Analysis of Lacustrine Sediments: A Comparison of pre-treatment Methods. Estonian Journal of Ecology 2008; 57: 231-243.

Tranter M. Glacial Chemical Weathering, Runoff Composition and Solute Fluxes. Glacier Science and Environmental Change. Blackwell Publishing, 2007, pp. 71-75.

Tranter M, Sharp MJ, Lamb HR, Brown GH, Hubbard BP, Willis IC. Geochemical weathering at the bed of Haut Glacier d'Arolla, Switzerland—a new model. Hydrological Processes 2002; 16: 959-993.

Trolle D, Spigel B, Hamilton D, Norton N, Sutherland D, Plew D, et al. Application of a Three-Dimensional Water Quality Model as a Decision Support Tool for the Management of Land-Use Changes in the Catchment of an Oligotrophic Lake. Environmental Management 2014; 54: 479-493.

Williams E. The Cultural Health of the Waitaki Catchment Enviornment Canterbury, 2015.

Woodward JC, Porter PR, Lowe AT, Walling DE, Evans AJ. Composite suspended sediment particles and flocculation in glacial meltwaters: preliminary evidence from Alpine and Himalayan basins. Hydrological Processes 2002; 16: 1735-1744.

Yukselen Y, Kaya A. Suitability of the methylene blue test for surface area, cation exchange capacity and swell potential determination of clayey soils. Engineering Geology 2008; 102: 38-45.

Zhuang J, Yu G-R. Effects of surface coatings on electrochemical properties and contaminant sorption of clay minerals. Chemosphere 2002; 49: 619-628.

3. Phosphorus Adsorption on SPM in the Glacier-Fed Waitaki Catchment, New Zealand

3.1 Introduction:

Phosphorus (P) is an essential nutrient that is required by all living organisms. For this reason, its presence in aquatic environments can be a primary driver of biological activity (Tiessen, 2008; Withers and Jarvie, 2008). However, an excess of bioavailable P can have severe impacts on the quality of natural waters. Runoff from anthropogenic activities is often a primary cause of enrichment. Point source discharges in urban environments are commonly enriched in sediment, detergents, fertilisers and effluents rich in P. In agricultural settings, phosphate fertilisers are used on massive scales to enhance plant growth and yields. Enhanced P concentrations can result in the proliferation of nuisance periphyton and diatoms in fast moving rivers. In slower moving rivers and lakes, the growth of algae and phytoplankton may result in reduced light penetration, the deoxygenation of water, and the release of toxins (Withers and Jarvie, 2008). These effects are collectively referred to as eutrophication (Eby, 2004), and can ultimately impact the amenity, recreational, ecological and cultural values of the system. The incidence of these events have been increasing in recent decades, largely due to rapid urban and agricultural development and a general increase in global temperatures caused by anthropogenic climate change (Anderson et al., 2002; O'Neil et al., 2012).

The cycling of P in aquatic environments is primarily influenced by its speciation and the rates of in situ processes such as adsorption, weathering and biological uptake (Tiessen, 2008). The adsorption of P onto sediment and SPM largely controls the mobility, distribution and bioavailability of P in freshwater environments (House, 2003; Spivakov et al., 1999). A variety of studies have characterised P adsorption characteristics and capacity of primary and secondary minerals (Dzombak and Morel, 1990) (Tanada et al., 2003) (Edzwald et al., 1976), soils (Olsen and Watanabe, 1957) and sediments (Boström et al., 1988a; Zhou et al., 2005). However, studies examining the adsorption of P onto glacial SPM are limited (Hodson et al., 2004). The Waitaki Catchment lakes have been subject to rapid agricultural development in recent decades. A corresponding increase in nutrient runoff and leaching has contributed to the degradation of these previously pristine deep lakes (Clarke, 2015; Norton et al., 2009; Trolle et al., 2014). The attenuation of P by SPM in the system is therefore an important consideration in the management of these lakes.

The primary aim of this study was to determine the adsorption capability of the Waitaki SPM for phosphorus. To achieve this aim, the adsorption characteristics of the SPM were determined with adsorption edge and isotherm experiments. Geochemical modelling and sequential extractions were used to assist in the identification of key phases implicated in P adsorption. The Diffuse Layer surface complexation model, assuming hydrous ferric oxide (HFO) to be the only adsorbing surface, was applied in this study to assess whether the adsorption of P can be predicted onto the SPM.

3.2 Methods

3.2.1 Sample collection and preparation

Please refer to **Chapter 2** for a detailed account of the collection and preparation of SPM throughout the Waitaki Catchment. In addition, SPM collected from the lowland Waikato River, a large non-glacial system in the North Island of New Zealand, was included in a number of the experimental procedures detailed below. This was added to compare the adsorption behaviour of the glacial SPM with that from a lowland riverine environment. The SPM has previously been described by Dr Rebecca Bibby (Bibby and Webster-Brown, 2005).

3.2.2 Materials and Experimental Procedures

The SPM solutions used in the procedures were prepared by rehydrating an accurately weighed quantity in 0.01 M $NaNO_3$ for 48 hours at 4°C prior to experimentation. This step was undertaken to allow surface oxide/hydroxide groups to rehydrate and equilibrate. A 50.03 mg/l stock solution of potassium phosphate (KH_2PO_4) was prepared in ultrapure H_2O for the purposes of PO_4-P additions in adsorption experiments. All pH adjustments were made with analytical grade NaOH and ultrapure HNO_3 with concentrations ranging from 0.01 – 1.00 M. Dissolved reactive phosphorus (DRP) was determined using the ascorbic acid method (APHA, 2005) with a detection limit of 0.005 mg P/l. Total phosphorus was also determined with this method after an autoclave assisted persulfate digestion (APHA, 2005). An exception was made for the determination of redox-reactive phosphorus, detailed in **method 3.2.7**, which was unable to be analysed with this method due to interference from CO_2 generation. In this instance, the redox-reactive P, Al, Fe and Mn was determined with a Varian 720 ES inductively coupled plasma optical emission spectrometer (ICP-OES) at Lincoln University with

a detection limit of 0.005 mg/l for P, and 0.02, 0.005 and 0.001 mg/l for Al, Fe and Mn respectively. For all analyses, solution blanks and standards were run in parallel with the analytical procedure as described in **Chapter 2, Section 2.2.3**.

3.2.3 Batch Adsorption Isotherms:

The P adsorption capacity of SPM was determined using adsorption isotherms. The methods detailed by Tanada et al. (2003), Edzwald et al. (1976) and Zhou et al. (2005) were modified to account for the small quantities of SPM available for experimentation. 100 mg/l rehydrated SPM and sediment solutions were first prepared and the pH adjusted to 7 with small additions of 0.1 M NaOH while stirring. After 30 minutes, an accurately weighed aliquot (12 ml) of the SPM solution was transferred into individual 15 ml centrifuge tubes. The P concentration was adjusted in each tube by accurately weighed additions of 50 mg/l KH_2PO_4. Sample blanks with deionised water were ran in parallel during the procedure. The final concentrations were 0, 0.01, 0.025, 0.05, 0.075, 0.1 and 0.2 mg/l PO_4-P. Samples were transferred to a temperature-controlled environment (25°C) and spun on an end-over-end mixer for 24 hours, a suitable period for the adsorption of P to reach equilibrium (Edzwald et al., 1976; Zhou et al., 2005). After 24 hours, the tubes were removed and pH immediately recorded with the use of a HACH HQ40d pH probe. The samples were then centrifuged at 4000 rpm for 20 minutes. A 10 ml aliquot was removed and filtered through a 0.22 µm nitrocellulose filter membrane, accurately weighed and PO4-P was determined with the ascorbic acid method (APHA, 2005) as described in **Chapter 2**.

The phosphate sorption isotherms were fitted with Langmuir and Freudlich models by non-linear regression. The total concentration of adsorbed P at equilibrium was determined with **Equation 4.1**:

$$\boldsymbol{q_e = q'_e + q^0_e} \qquad (\mathbf{4.1})$$

Where q_e = the concentration of bound P at equilibrium (mg/g); q'_e = the apparent concentration of P adsorbed during the isotherm experiment (mg/g); and q_e^0 = the native concentration of P on the SPM/sediment without P additions (mg/g). The Langmuir isotherm was then calculated using **Equation 4.2**:

$$q_e = \frac{q_{max} K_L C_e}{1 + K_L C_e} \quad (4.2)$$

Where q_{max} = Langmuir monolayer saturation capacity (mg/g); K_L = Langmuir isotherm constant (L g^{-1}) – corresponds to the affinity of the adsorbate for the solid; and C_e = equilibrium solution phase concentration of the adsorbate (mg L^{-1}). The Freudlich isotherm was also modelled using **Equation 4.3**:

$$q_e = a_F C_e^{b_F} \quad (4.3)$$

Where a_F = Freundlich isotherm constant; and b_F = Freundlich exponent.

3.2.4 Adsorption Potential

A novel measure of the theoretical "adsorption potential" of the Waitaki catchment water was developed in this research. It combines the variable SPM concentrations detected throughout the catchment and the associated adsorption capacity for P. To do this, it was first necessary to determine the SPM concentration range throughout the Waitaki catchment under varying conditions. Very little SPM concentration data has been collected outside of this research. However, turbidity data (as NTU) has been collected under a range of flows throughout the catchment by the Environment Canterbury Regional Council (ECan) during the period of 1983 – 2017 (n= 215). This data is available on the ECan Open Data Portal (http://data.ecan.govt.nz).

Regression analysis of the turbidity and SPM concentration data collected throughout the duration of this research (n=32) resulted in the generation of two linear models. These models were then used to calculate SPM concentrations from turbidity data mined from the online data portal. The first model (**Equation 4.4)** was generated for low turbidity samples (NTU < 30) and was found to have a high coefficient of determination (R^2 = 0.92).

$$\text{SPM Concentration (mg / l)} = (\text{Turbidity [NTU} < 30] * 0.75) + 0.84 \quad (4.4)$$

The second model (**Equation 4.5)** included high turbidity samples (NTU > 30) was also found to have a high coefficient of determination (R^2 = 0.93).

$$\text{SPM Concentration (mg / l)} = (\text{Turbidity [NTU} > 30] * 0.79) + 5.5 \quad (4.5)$$

The mined turbidity data was transformed to SPM concentrations using **Equations 4.4 and 4.5**. The mean, minimum and maximum SPM concentrations were then calculated. This data was multiplied by the maximum adsorptive capacity of the SPM (determined with the Langmuir isotherm) to predict the maximum adsorption potential (mg P/l) of the water throughout the catchment. It must be noted that the resulting value is a relative indication of the maximum capacity of the water to adsorb P. In actual fact, the adsorption potential may be much lower under environmentally relevant scenarios.

A description of the data and methods used to generate these relationships is provided in **Appendix C.** It is important to note that these models were used for estimation purposes only. The dataset is limited, and relationships between nephelometric turbidity units (NTU) and SPM concentrations may have a high degree of uncertainty. This is due to the significantly different scattering abilities of inorganic sediments, organic matter and biogenic particles. The relationship may also break down in turbulent environments and flood conditions when suspended particle sizes can significantly increase (Pfannkuche and Schmidt, 2003). In the Waitaki catchment, the flow of water is regulated by hydroelectric dams which can regulate such fluctuations. In any case, the relationships generated have proven to be a useful indicator of SPM concentrations when only turbidity data is available.

3.2.5 Adsorption Edge Experiments:

The effect of pH on the adsorption of P by the SPM was tested with batch adsorption edge experiments. Rehydrated 100 mg/l SPM and sediment solutions were adjusted to pH ~10.5 with small additions (1 – 10 µl) of 1 M NaOH while mixed with a magnetic flea. A sample blank was collected before an accurately weighed quantity of KH_2PO_4 was added to make a total solution concentration of 0.1 mg/l PO_4-P. Exact weights of all additions were recorded. The solution was left to equilibrate for an additional 30 minutes before a 12 ml aliquot was taken for analysis at time zero. The pH of the solution was then progressively lowered with small additions (1 – 10 µl) of 1 M HNO_3. Aliquots were drawn for every change in 0.5 – 1 pH unit, down to a final pH of 2 – 2.5. The resulting aliquots were transferred to an end-over-end mixer for 24 hours in a 25°C temperature-controlled environment. After this period, the pH of the solutions was re-measured before tubes were centrifuged at 4000 rpm for 20 minutes. The supernatant was recovered, filtered through pre-cleaned 0.22 µm nitrocellulose filter membranes and analysed for DRP as described above. Exact weights of all samples and reagents

were recorded throughout the procedure to ensure accuracy when calculating PO_4-P concentrations. For select experiments, 5 ml aliquots were also recovered for later analysis of dissolved Al, Fe and Mn concentrations by ICP-MS. This was undertaken to investigate the dissolution of labile mineral phases throughout the pH range, which was hypothesised to provide useful information on the potential adsorption phases associated with the SPM.

3.2.6 SEM/EDS

Scanning electron microscopy (SEM) with energy dispersive X-ray (EDS) mapping analysis was used to investigate P adsorption and the possible formation of phosphate bearing minerals during the adsorption experiments. The SPM remaining from the adsorption experiments was transferred onto Nucleopore filters and carbon-coated prior to inspection by SEM using the methods detailed in **Chapter 2, Section 2.2.4.2**. Imagery and EDS data were exported in both TIFF and CSV format for later analysis with FIJI version 2.0, an ImageJ software package used for the detailed analysis of microscopic data and imagery.

3.2.7 Sequential Extractions

The sequential extraction method by Rydin (2000) and optimised by Waters (2016) was used to characterise the forms of P associated with surface bed sediments collected in this study. It was not possible to use SPM in this procedure due to the insufficient quantities available for the procedure. Surface sediments collected from the Waitaki catchment were found to primarily be fine inorganic particles of glacial origin (**Appendix B**). Samples were therefore used to provide an important first insight into the speciation and likely bioavailability of P associated with the glacial sediments. A lowland, non-glacial Waikato River sediment sample was included for comparison with the glacial material. The sediment samples were subjected to a succession of differing chemical conditions which optimise the dissolution of P from different phases of the material (**Table 3.1)**. To begin, an accurately weighed aliquot of dry sediment (~0.5 g) was transferred to clean 50 ml polypropylene centrifuge tubes. A 25 ml aliquot of 1 M NH_4CL was then added to each tube and weighed before rotating on an end-over-end mixer for the appropriate time period. All mixing was performed in a temperature-controlled environment at 25°C. The tubes were removed after the period and centrifuged at 4000 rpm for 15 minutes before the supernatant was removed by pipette, diluted accordingly and analysed by

ascorbic acid analysis (APHA, 2005) or ICP-OES. The next step of the procedure was then performed with the remaining material. A PACS-2 certified marine reference sediment was included to determine the efficiency of the sequential extraction procedure. The recovery of P by the sequential extraction procedure was 93.5%.

Table 3.1. Details of the Rydin/Waters sequential extraction procedure.

Step	Extraction Solution	Conditions	Phosphorus Fraction	Description
1	1 M NH_4Cl	2 hours, pH 7	"Exchangeable P"	Competitive ion-exchange in the NH_4Cl solution may liberate loosely bound and soluble P by competitive ion-exchange.
2	0.11M bicarbonate/dithionate ($NaHCO_3/Na_2S_2O_4$)	1 hour, pH 6.9	"Redox-reactive P"	The reducing environment in this step releases redox-sensitive P, such as that bound to reactive Fe and Mn oxy/hydroxides that undergo dissolution in reducing conditions.
3	0.1 M NaOH	16 hours, pH 10.	"NaOH-reactive P"	The high pH environment results in the dissolution of surface Al-oxy/hydroxide phases and associated P. It may also liberate P adsorbed to resilient Fe and Mn phases, and clay minerals through competition exchange with OH^-.
4	0.1M NaOH + persulphate digestion	As above	"Organic P"	The persulphate digestion liberates easily degradable organic P. This may include hydrolysable organic P and polyphosphates which are generally considered to be bioavailable.
5	0.5 M HCl	16 hours, pH < 2.	"HCl-reactive P"	The acidic environment in this step liberates P associated with Ca-phosphates (apatite) and carbonates. It may also release P from refractory metal oxy/hydroxides that were unaffected in the previous steps.
6	70% HNO_3	As per method 4500- P B (APHA, 2005).	"Residual P"	The use of HNO_3 in this step was recommended by Waters (2016) for its superior ability to dissolve the remaining organic and highly inert P associated with inorganic phases.

3.2.8 Geochemical Modelling

Geochemical modelling was performed with the software package Visual MINTEQ 3.1 (Gustafsson, 2014). The software was used extensively to predict the thermodynamically favoured distribution of aqueous species in solution. It was also used to predict mineral formation and dissolution reactions implicated in phosphorus speciation and adsorption. The software package utilises the thermo_minteq database which has the most up to date and comprehensive data relevant to phosphorus speciation. Unless specifically stated, the model was programmed to operate at 25^0C and in oxic conditions (pE = 9) consistent with conditions applied in the literature. Ion balance error was < 10%.

Speciation Modelling

The speciation of dissolved P and the dissolution of phosphate bearing minerals were first modelled to assist in the interpretation of the adsorption experiments. The speciation of the dissolved P was first modelled in the pH range of 2-11, using water chemistry data determined in the filtered Waitaki Catchment samples (**Appendix C**). The dissolution of hydroxylapatite was modelled in the same pH range as an 'infinite phase', assuming equilibrium with the solution conditions.

The dissolution profiles of Fe and Al oxides were also modelled in the pH range of 2-11. Ferrihydrite, goethite and gibbsite were specified as a 'possible' mineral phases. The quantities of Fe and Al applied in the model were derived from the acid-soluble concentrations detected by ICP-MS at pH 2 during the adsorption edge experiments. The details of this method are described in section **3.2.6.**

Surface Complexation Models

The adsorption of P onto glacial SPM was modelled onto Fe- and Al-oxide surfaces using the diffuse layer model (DLM) (Dzombak and Morel, 1990) and the gibbsite (Karamalidis and Dzombak, 2010) surface complexation models (SCMs) incorporated into Visual Minteq. Organic matter is not expected to adsorb any appreciable quantities of P owing to predominant negative charge under normal environmental pH. It was therefore excluded from this analysis.

An important consideration was determining the concentrations of reactive adsorbing surface input into the model. A common method to determine this is by subtracting the concentrations of

reactive metals measured in a filtered (0.45 µm) water sample from that measured in an unfiltered sample. In this study, this approach was found to grossly over predict the adsorption capacity of the SPM. Specific details are provided in **Appendix C**. An alternative approach was used, whereby the concentrations of Fe, Al and Mn liberated by the SPM at pH 2 for 24 hours was utilised. This was hypothesised to dissolve reactive oxides that participate in the adsorption process, without liberating ions from resilient phases of the mineral assemblage. Similar methods with weak acids have been previously utilised (Groenenberg and Lofts, 2014). The concentrations were determined by ICP-MS during the adsorption edge experiments and are detailed in **Table 3.2**.

Ferrihydrite and gibbsite were specified as 'possible' mineral phases in Visual Minteq and a pH range of 2-11 was configured using the multi-problem/sweep function. The HFO or gibbsite adsorbing surface was then established in the model and was connected to the 'possible' formation of ferrihydrite and gibbsite respectively. A novel modelling approach was used in this study, whereby the adsorption capacity of the SCMs were compared to the experimental isotherm capacities determined in **Section 3.3.1.** This provided an indication of the discrepancies that may exist between the modelled and experimental data. To do so, the model was programmed to progressively increase the solution concentration of P in 25 µg/l aliquots using the multi-problem/sweep function.

Table 3.2. Concentrations of Al, Fe and Mn liberated from the SPM after treatment in a weak HNO_3 solution at pH 2 for 24 hours. * A non-glacial, lowland river SPM from the Waikato River has been included for comparison with the Waitaki Catchment SPM.

Site # and Location	Concentration (µg/l)		
	Al	Mn	Fe
2. L. Tasman	649.1	12.3	667.1
4. L. Pukaki	549.22	10.5	286.8
6. L. Benmore – Ahuriri	75.1	53.3	116.9
7. L. Aviemore	144.0	34.0	156.4
8. Waitaki River	280.9	12.5	307.5
*** Waikato River**	292.9	200.1	1499.0

3.3 Results:

3.3.1 Adsorption Isotherms

The adsorption of P was found to progressively decline with increasing P concentrations (**Table 3.3**). The Langmuir model was found to provide a good fit to the experimental data with corresponding high coefficients of determination (R^2 = 0.93 – 0.99). Lake Aviemore was found to have the greatest affinity for P, with a K_L value of 275.6, up to an order of magnitude greater than the values determined for the other sites. The upper catchment SPM from Lakes Tasman and Pukaki had the lowest affinities, with K_L values of 20.6 and 38.3 respectively. However, these samples had the greatest adsorption capacities (0.27 - 0.28 mg P/g SPM) as predicted with the Langmuir model (**Figure 3.1)**. The lowest capacity was measured with the lower catchment Lake Aviemore SPM with just 0.17 mg P/g SPM. Both the Langmuir and Freudlich models provided a good fit to the experimental adsorption data with corresponding high coefficients of determination (R^2 > 0.9). The non-glacial Waikato River SPM was found to have a relatively low affinity (K_L = 25) and capacity for P (0.13 mg P/g SPM) compared to the Waitaki SPM.

Table 3.3. Coefficients of determination (R^2) reported for Freudlich (F) and Langmuir (L) models fitted to the experimental adsorption isotherms for phosphorus (P) onto SPM. The Langmuir constant K_L corresponds to the affinity of P for the SPM. The maximum adsorption capacity of the SPM was determined with the Langmuir model (L. Qmax).* A non-glacial SPM sample from the Waikato River has been included for comparison.

#	Site Name	Langmuir K_L	Langmuir QMax (mg P/g SPM)	Langmuir R^2	Freudlich R^2
2	L. Tasman	20.6	0.26	0.99	0.96
4	L. Pukaki	38.3	0.28	0.96	0.98
6	L. Benmore -Ahuriri	54.3	0.22	0.99	0.95
7	L. Aviemore	275.6	0.16	0.94	0.98
8	Waitaki River	88.1	0.22	0.93	0.98
*	Waikato River	25	0.13	0.96	0.89

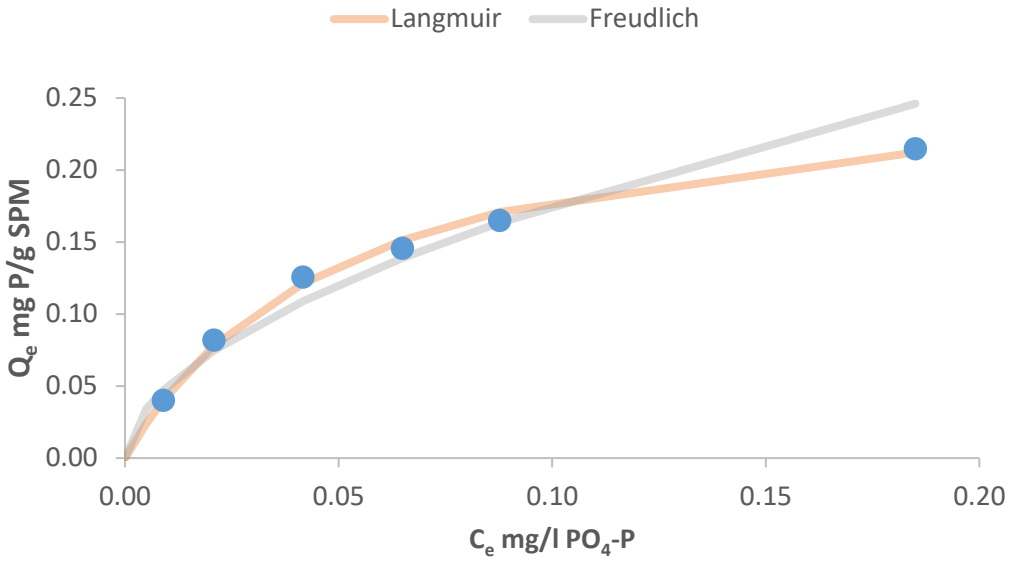

Figure 3.1. Phosphorus adsorption isotherms for Lake Tasman SPM. Ce = equilibrium solution concentration. Qe = mg P adsorbed per g SPM. The lines indicate the Langmuir and Freudlich model fits. Experiment undertaken at pH 7, 25^0C for a 24 hour equilibrating period.

3.3.2 Theoretical Adsorption Potential

The theoretical adsorption potential of the Waitaki catchment water for P is presented in **Figure 3.2**. The greatest potential is predicted for the meltwater collected from Lake Tasman, with a theoretical ability to adsorb between 0.006 – 0.076 mg P/l. The mean adsorption potential was 0.035 mg P/L. A significant decrease was calculated down catchment. For Lakes Benmore – Ahuriri (125 km) and Lake Aviemore (140 km), the adsorption potential declined to a range of 0.0002 – 0.0024 mg P/l. A slight increase was predicted for the Lower Waitaki River (210 km) with an adsorption potential ranging from 0.0005 – 0.0065 mg P/l. Specific values are detailed in **Appendix C**.

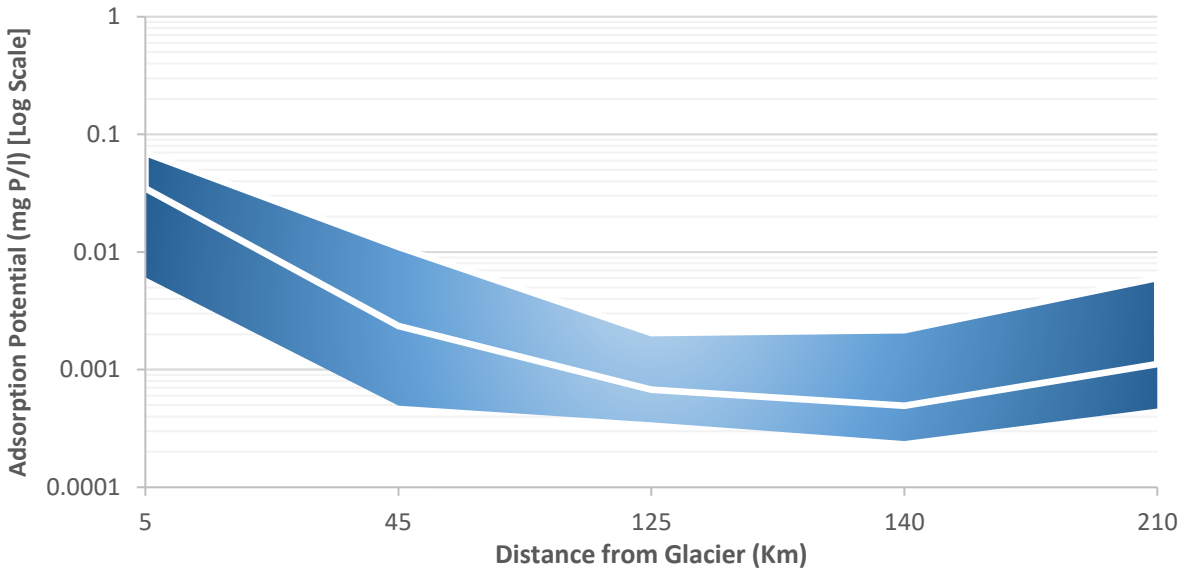

Figure 3.2. Adsorption Potential of the Waitaki Catchment water – a function of the variable SPM concentrations in the Waitaki Catchment and its maximum adsorption capacity for P. Units are mg P/l water. The white line corresponds to the mean adsorption potential. Note, the Y-axis is a logarithmic scale.

3.3.3 Adsorption Edge Experiments

The adsorption of P onto the glacial SPM had a complex relationship with pH (**Figure 3.3**). All Waitaki samples had a similar adsorption profile. However, major differences in the adsorption capacity of the SPM at varying pH were detected. The greatest adsorption occurred in the pH range of 4.5 – 7. Very little P (<0.05 mg P/g SPM) was adsorbed in the pH range of 8-11. Below pH 4, P was typically liberated into solution from the SPM, with increasing concentrations detected with decreasing pH.

The lowland Waikato river sample was found to differ from that observed in the glacial SPM. A generally reduced capacity to adsorb P was detected. There was also a distinct lack of P liberation into solution as measured in the Waitaki Catchment. Instead, the adsorptive capacity was found to increase with progressively declining pH.

The concentrations of Al, Fe and Mn detected in solution during the adsorption edge procedure are plotted in **Figure 3.4.** At near neutral pH values (6-8) very low concentrations of Al, Fe and Mn were detected in solution. At pH > 8 Al was found to be progressively liberated into solution. Both Al and Fe were detected at pH < 5 with increasing concentrations measured with declining pH. The

concentrations of Mn increased as the pH declined but were found to remain low throughout the titrations. These same dissolution profiles were typical in the Waitaki Catchment SPM. However, the concentrations detected were highly variable, and generally declined down catchment. The concentrations measured at pH 2 are detailed in **Table 3.2**.

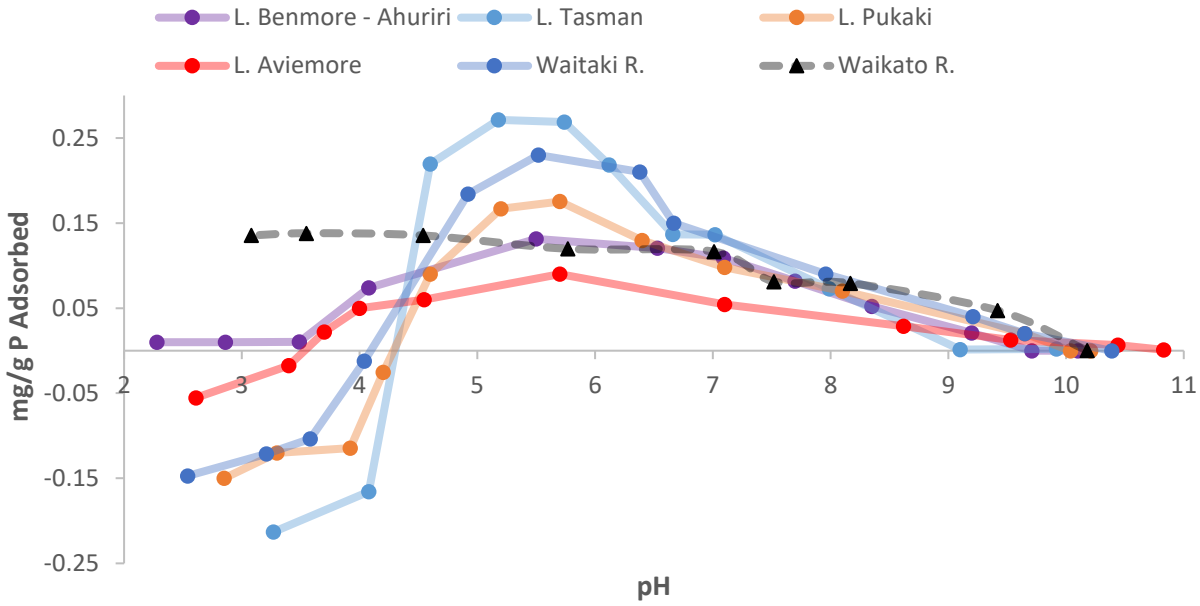

Figure 3.3. Adsorption edge profile for P adsorption onto Waitaki catchment SPM. Experiments undertaken in 0.01 mg/l PO_4-P, pH range 2 – 11, 25^{0}C and a 24-hour equilibration period.

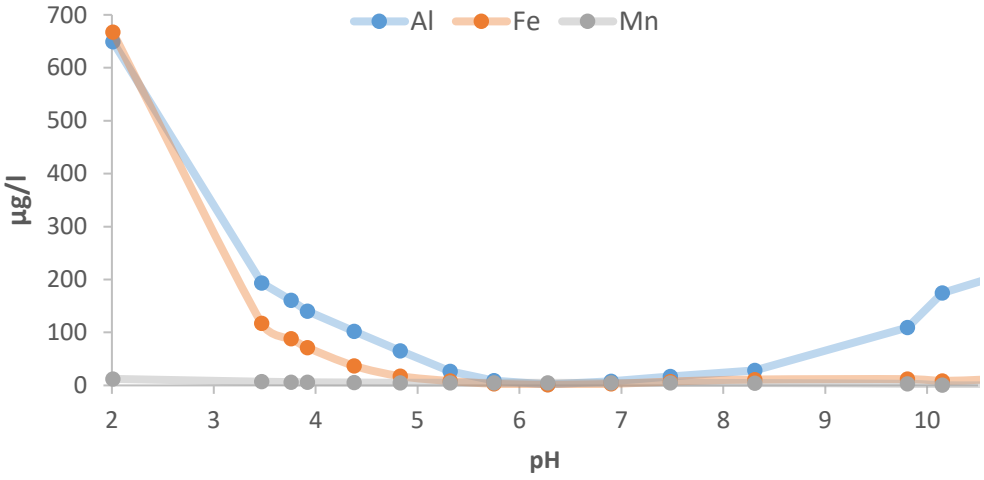

Figure 3.4. Concentrations of dissolved Al, Fe and Mn measured in 100 mg/L Lake Tasman SPM in 0.01 mol/l $NaNO_3$ during an adsorption edge experiments. The solution concentrations were measured in filtered samples by ICP-MS after the 24-hour experimentation period.

3.3.4 SEM/EDS Characterisation

Elemental mapping with SEM/EDS indicated the presence of P on the SPM surfaces after exposure for 24 hours in the isotherm procedure. Phosphorus was detected on all particle surfaces. However, very little was observed on organic particles present in the SPM. Phosphorus 'hotspots' were determined in locations where detrital apatite was present (**Figure 3.5**). A highly concentrated area of P was also detected on a feldspar particle (albite), and was not associated with any particular mineral phase (**Figure 3.6**).

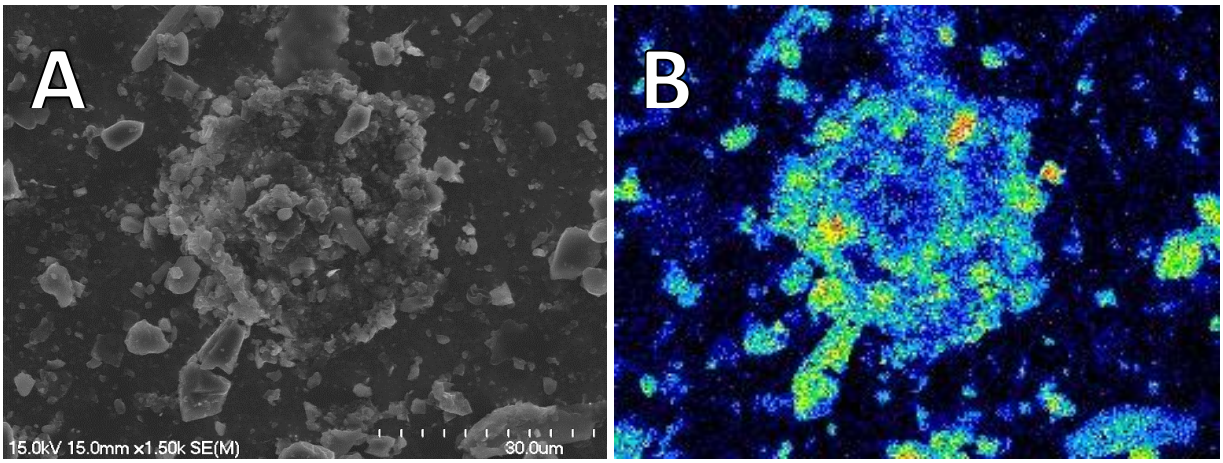

Figure 3.5. A) Lake Tasman SPM. B) The associated phosphorus map determined with SEM/EDS. The degree of P intensity is displayed with 16 colour lookup table. Black = no detection and red = high intensity.

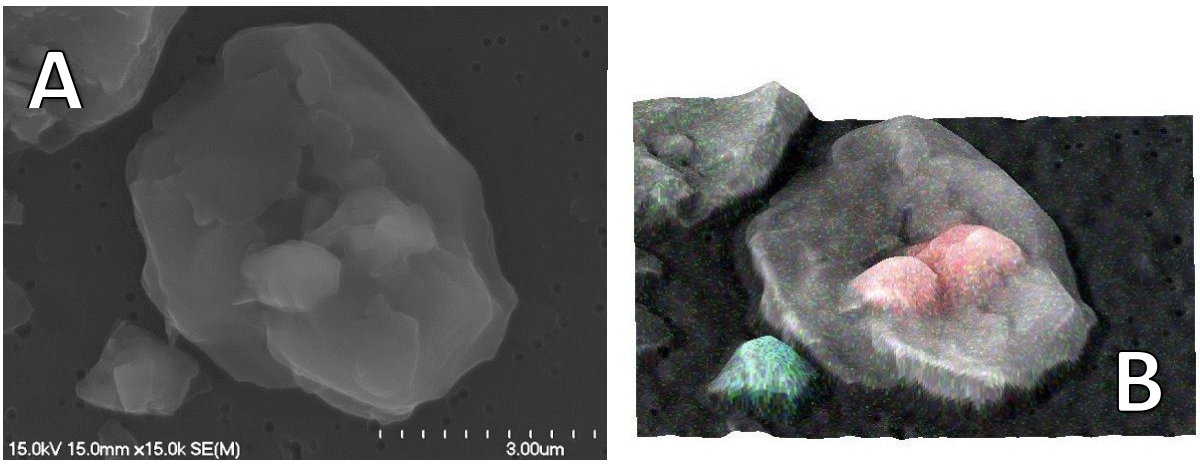

Figure 3.6. A) Feldspar (albite) particle in Lake Aviemore SPM after 24 hour treatment with 0.1 mg/l P. B) 3D surface model of the particle with corresponding SEM/EDS mapping data overlaid. Red area is phosphorus rich. The green and blue particle is titanite.

3.3.5 Sequential Extractions

The greatest proportions of SPM P (48 – 86%) was associated with the HCl-reactive fraction for the Waitaki sediments (**Figure 3.7, Table 3.4**). Lake Tasman was found to have the greatest proportion (86.3%). The remaining P was associated with the NaOH-reactive (4.3%) and residual (6%) P fractions. Only minor proportions of exchangeable, redox-reactive and organic P were detected. The sample from Lake Pukaki was comparable but was found to have a greater proportion of organic-P (14.3%). Considerable changes were detected at the lowland Lakes Benmore - Ahuriri and Aviemore. The sediment was found to have 40-60 % greater total P concentrations with 615 – 748 mg/kg P relative to the 445 – 481 mg/kg P determined in the upper catchment. Most of this enrichment was associated with the redox-reactive, NaOH and organic P fractions. The Ahuriri Arm of Lake Benmore was found to have a reduced quantity of HCl-reactive P relative to other sites. The sediment from the Waitaki River was characteristic of the upper catchment, with reduced proportions of redox-reactive, NaOH-relative and organic P relative to the adjacent lakes.

The lowland Waikato River SPM had a very different character to the glacial SPM. The HCl – apatite fraction was determined to be a minor component (13.2%). The greatest proportions of P were associated with the redox-reactive, NaOH and organic fractions. Very little exchangeable P was measured in all samples. The greatest proportion (0.8%) was measured in the Waitaki River sediment.

After equilibration with a 0.1 mg/l P solution, both the Lake Tasman and Lake Aviemore SPM were found to have minor enrichment in redox-reactive and NaOH-P (**Table 3.4)**.

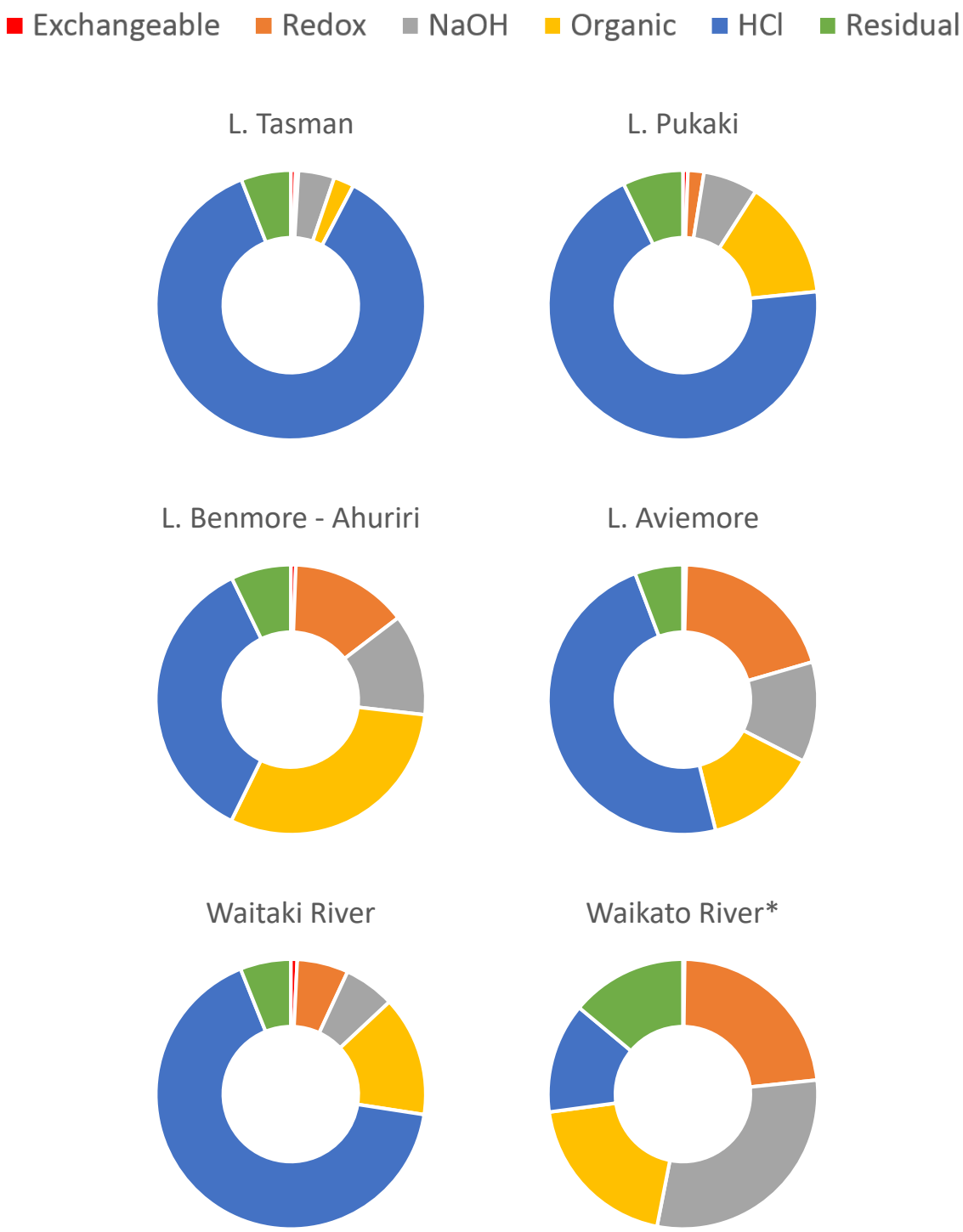

Figure 3.7. Donut charts presenting the P fractions associated with glacial sediment/SPM from the Waitaki Catchment. Note* Non-glacial SPM from the lowland Waikato River has been included for comparison.

Table 3.4. Proportions of P associated with different sequential extraction fractions for surface sediments from the Waitaki catchment. A PACS-2 reference marine sediment was included for experimental control. Units in mg/kg. Percentage of total P in brackets. *The non-glacial Waikato River has been included for comparison.

Sampling Site	mg/kg (%)						
	Exchangeable	**Redox-P**	**NaOH-P**	**Organic-P**	**HCl-P**	**Residual -P**	**Total**
L. Tasman	2.6 (0.6)	1.5 (0.3)	19.3 (4.3)	10.9 (2.4)	385.0 (86.3)	26.6 (6.0)	**445.9**
L. Tasman + P**	2.6 (0.6)	8.8 (1.9)	31.8 (6.9)	7.7 (1.7)	390.2 (85.2)	17.0 (3.7)	**458.2**
L. Pukaki	2.9 (0.6)	9.2 (1.9)	31.5 (6.5)	68.9 (14.3)	333.7 (69.4)	34.8 (7.2)	**481.0**
L. Benmore - Ahuriri	3.7 (0.6)	86.4 (14.0)	74.9 (12.2)	187.7 (30.5)	218.8 (35.5)	44.3 (7.2)	**615.9**
L. Aviemore	3.0 (0.4)	150.4 (20.1)	90.1 (12.0)	101.7 (13.6)	360.4 (48.1)	43.1 (5.8)	**748.6**
L. Aviemore + P**	3.8 (0.5)	159.4 (20.3)	98.0 (12.5)	95.9 (12.2)	378.0 (48.2)	49.0 (6.2)	**784.1**
Waitaki River	4.5 (0.8)	35.7 (6.2)	35.5 (6.1)	83.7 (14.4)	386.4 (66.5)	35.3 (6.0)	**581.1**
PACs-2	1.6 (0.2)	96.7 (11.2)	55.0 (6.4)	108.9 (12.7)	500.5 (58.2)	97.6 (11.3)	**860.2**
Waikato River*	1.6 (0.2)	172.8 (23.1)	222.4 (29.7)	148.0 (19.8)	98.6 (13.2)	104.2 (13.9)	**747.5**
****Note:** - Additional samples exposed to 0.01 mg/l PO_4-P solution in 0.01 M $NaNO_3$ for 24 hours.							

The concentrations of Fe and Mn liberated during the reducing bicarbonate/dithionate (BD) step are presented in **Table 3.5.** In general, greater concentrations of redox-reactive Fe were detected from sediment samples collected with progressive distance from the glacial source. The exception was the lower Waitaki River sample, which was found to have the lowest concentrations of reactive Fe and Mn.

Table 3.5. Concentrations of redox-reactive Al, Fe, and Mn (mg/kg) detected in solution after treatment with 0.11 M bicarbonate/dithionate solution.

	L. Tasman	**L. Pukaki**	**L. Benmore - Ahuriri**	**L. Aviemore**	**Waitaki River**	**PACs-2**	**Waikato River**
Fe	1527	2347.9	2569.9	6028.7	931.2	4586.6	7524.5
Mn	64.1	99.5	620.3	396	5.1	3.8	236.2

3.3.7 Geochemical Modelling

Phosphorus Speciation

The PO_4-P speciation model generated in Visual Minteq indicates that $H_2PO_4^-$ and HPO_4^{2-} are the dominant species over the pH range of 2-11 (**Figure 3.8).** $H_2PO_4^-$ is predicted to be the primary

species from pH 3-7. HPO_4^{2-} becomes increasingly prevalent from pH 7-9. The modelled dissolution of hydroxyapatite has been included in the plot. Dissolution is predicted to occur below pH 4 and progresses with decreasing pH.

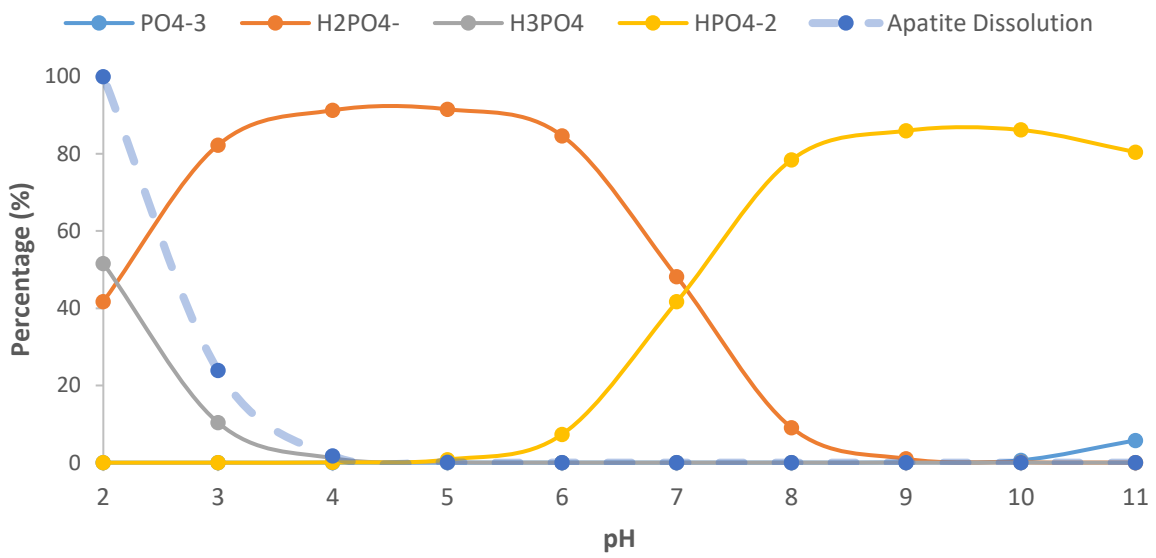

Figure 3.8. Modelled phosphorus speciation in the pH range of 2 – 11. Modelled in Visual Minteq (0.1 mg PO_4-P in 0.01 M $NaNO_3$ at 25^0C). Percentage (%) dissolution of hydroxyapatite is included for reference.

Dissolution of Oxide Surfaces

The concentrations of Al and Fe measured during the adsorption edge with the Lake Tasman SPM are plotted in **Figure 3.9**. The modelled dissolution curves of gibbsite and ferrihydrite are included for comparison. The model predicts the dissolution of gibbsite in the pH range of < 5 and > 9, and this was found to closely resemble the experimental data. The progressive dissolution of ferrihydrite was predicted at pH < 4 and was also found to closely resemble the experimental data. The profiles of goethite and hematite did not provide a good fit and have therefore been omitted from the plots.

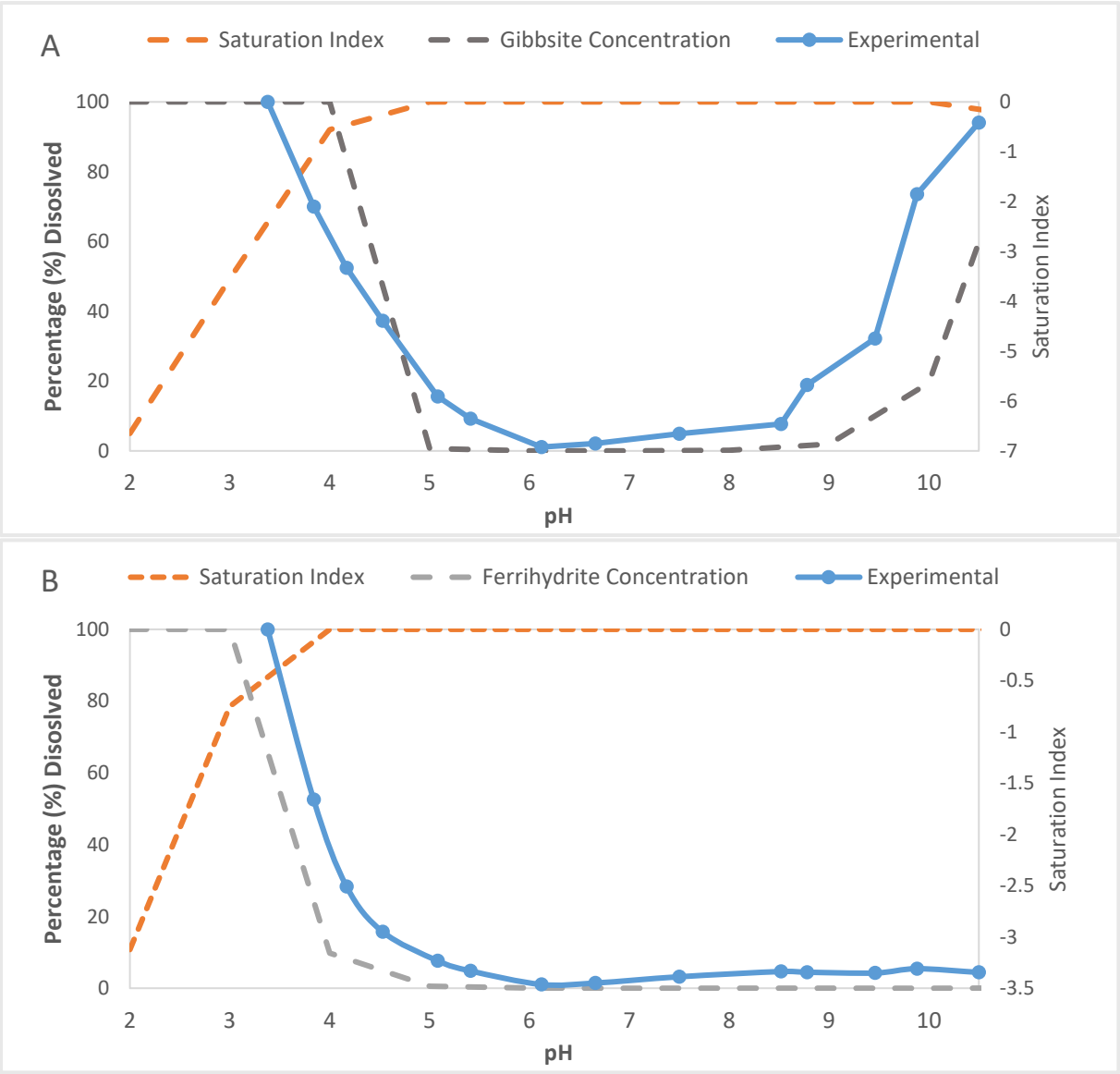

Figure 3.9. The dissolution of gibbsite (A) and ferrihydrite (B) were modelled in Visual Minteq 3.1 using the concentrations of "reactive" metal oxides determined by ICP-MS after treatment of the SPM at pH 2 for 24 hours. The dissolution profiles obtained for the experimental data are included for comparison. The modelled saturation indices indicate whether the solutions are likely to dissolve gibbsite or ferrihydrite. A negative value indicates the mineral may dissolve.

3.3.6 Surface Complexation Modelling

The modelled adsorption capacities of the Waitaki SPM, assuming HFO to be the only adsorbing surface, is presented in **Figure 3.10.** The concentrations determined with the gibbsite and manganese surface complexation models were comparatively low. These results are detailed in **Appendix C**. In general, the adsorption profiles of the model were similar to that observed in the

experimental adsorption edges in the pH range of 5-10 (**Section 3.3.3**). On first glance, the models appear to grossly over-predict P adsorption. However, the values predicted at the environmentally relevant pH of 6-8 were not dissimilar (**Table 3.6**). The predicted error ranged from 16- 56%. The greatest error was associated with the Lake Pukaki SPM.

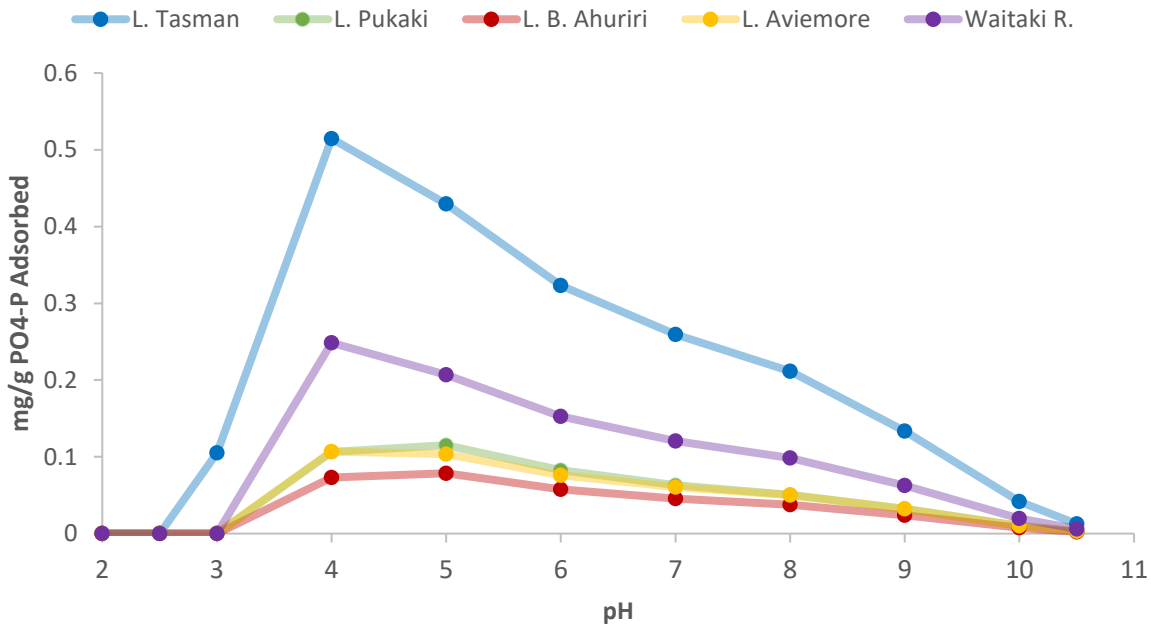

Figure 3.10. Modelled adsorption capacity of the SPM for P throughout Waitaki Catchment, generated with the diffuse layer model (DLM) in Visual Minteq 3.1. Model conditions: 0.01 M $NaNO_3$, 25^0C, pE = 9, PO_4-P = 0.1 mg/L. The concentrations of "reactive" Fe oxide were determined by ICP-MS after treatment of the SPM at pH 2 for 24 hours.

The modelled adsorption capacities of the SPM were comparable to those determined with the adsorption isotherm experiments at circumneutral pH in **Section 3.3.1**. The modelled adsorption capacity for the Lake Tasman SPM was comparable that determined by the Langmuir isotherm (0.26 mg P/g SPM) (**Table 3.6**). However, significant differences were detected down catchment, with the SCM under predicting adsorption by up 0.1 mg P/g SPM.

Table 3.6. Comparison of P adsorption determined in adsorption edge and isotherm experiments (**Section 3.3.3**) and that predicted with the diffuse layer model (HFO). Adsorption edge data in the environmentally relevant pH range of 6-8 is presented. The modelled adsorption capacity is presented with that calculated from the Langmuir isotherms (L. Qmax). Units in mg P/g SPM.

	Adsorption Edge - pH 6-8		Adsorption Isotherm - pH 7	
Site	**Experimental Data**	**Modelled Data**	**L. Qmax**	**Modelled**
	mg/g		**mg/g**	
2. L. Tasman	0.14 – 0.27	0.21 - 0.32	0.26	0.26
4. L. Pukaki	0.07 – 0.18	0.04 - 0.08	0.28	0.11
6. L. Benmore – Ahuriri	0.08 – 0.12	0.04 - 0.06	0.22	0.05
7. L. Aviemore	0.03 – 0.1	0.05 - 0.08	0.16	0.06
8. Waitaki River	0.09 – 0.21	0.1 - 0.15	0.22	0.12

3.4 Discussion:

3.4.1 Glacial SPM: An Effective Adsorbent for Dissolved Phosphorus?

In this research, the fresh glacial SPM collected in close proximity to the glacial source was found to have the greatest adsorption capacity and potential for P. This was attributed to the greater proportion of fine inorganic particles, large specific surface areas (SSA) and the greater concentrations of reactive surface oxides associated with the glacial SPM relative to SPM collected down catchment (**See Chapter 2 for details)**.

The P adsorption capacity of the Waitaki SPM (0.16 - 0.28 mg P/g SPM) was greater than organic rich SPM from the Three gorges reservoir in China (0.08 mg/g) and glacial SPM collected from collected from the Austre Brøggerbreen (0.04 – 0.07 mg/g) and Midre Lovenbreen (0.04 – 0.1 mg/g) in Svalbard (Hodson et al., 2004). For the latter, the low adsorption capacity of the SPM was attributed to a short residence time in the glacial environment, minimising the development of important adsorption phases including Fe/Al oxy/hydroxides and fine clay minerals. In the Waitaki Catchment, these minerals were found to be prominent in the SPM. The Tasman glacier, the source of much of the SPM, is the longest glacier in NZ (~24 km) and the long residence of sediments in the glacial environment may enhance the generation of important adsorption phases.

The adsorption capacities of the Waitaki SPM were comparable to previous reports for lowland sediments collected in the United Kingdom (0.036 – 0.141 mg/g) (House and Denison, 2000)

and China 0.24 – 0.59 mg/g (Zhou et al., 2005). This indicates that the glacial SPM does have an appreciable adsorption capacity. However, it is not exceptional compared to these lowland sediments.

The novel measure of 'adsorption potential' generated in this research has demonstrated that the water in close proximity to the glacial source has a significant potential to adsorb P (0.03 – 0.08 mg P/l) from the water column. This is primarily due to the high concentrations of SPM associated with the meltwater. However, the adsorption potential dramatically declined down catchment and was attributed to the significant reductions in SPM concentrations and their lower adsorption capacities. The calculated adsorption potential (< 0.003 mg P/l) in the lower Lakes Benmore and Aviemore is lower than the median 0.004 mg/l DRP that is typically measured in the 30 tributaries that feed into these lakes. The land in the vicinity has been subjected to the rapid intensification of agriculture in recent years. Concentrations of DRP ranging from 0.01 - 0.036 mg/l have been detected in spring-fed waters flowing into Lake Benmore (Gray, 2015). The measure of adsorption potential in this study indicates that the SPM in the Waitaki water cannot attenuate such concentrations. The remaining DRP may be readily available for uptake by aquatic biota prior to geochemical cycling with SPM and surface sediments.

3.4.2 Phosphorus Enrichment in the Waitaki Glacial Sediments

In **Chapter 2** it was shown that both the Waitaki SPM and sediment samples became progressively enriched in P with increasing distance from the glacial source. This not only provided an insight into its adsorptive potential, but also its potential to be a reservoir for bioavailable P in depositional environments. The sequential extractions used in this research have provided key insights into the forms of phosphorus associated with the sediments, the phases implicated in the adsorption of P, and its likely reactivity and bioavailability as described below.

The dominant P fraction in the Waitaki catchment sediments was HCl-reactive P. This is consistent with previous analysis of glacial sediment by Hodson et al. (2004) and Burrus et al. (1990). This fraction is typically comprised of calcium phosphate bearing minerals, the most common and stable form is apatite, a calcium phosphate mineral ($(Ca_4(PO_4)_3(OH,Cl,F)$) which has an average concentration in the continental crust of 665 µg/kg (Hans Wedepohl, 1995). Detrital apatite was identified in all Waitaki Catchment SPM samples (**Chapter 2**) and will be sourced from the glacial

grinding of the greywacke source rock. Despite its prevalence, apatite is not considered to be readily bioavailability owing to its low reactivity in normal environmental conditions (Mindl et al., 2007).

Down catchment, the sediments were found to be relatively enriched in exchangeable, redox-reactive and NaOH-reactive P. The significant enrichment in the redox-reactive fraction indicated that Fe and/or Mn oxides may be actively adsorbing dissolved P in the lower catchment. The associated P is not directly bioavailable. However, it may be liberated in reducing and/or alkaline conditions. Such conditions are common in eutrophic and anoxic waters (Stumm and Morgan, 1970); and the internal micro-environments of benthic biota (Borovec et al., 2010; Stal, 1995).

The enrichment of the NaOH fraction may be attributed to the adsorption of P by Al oxides (such as gibbsite), clay minerals and/or Fe and Mn oxide minerals resilient to the redox treatment. NaOH-reactive P has been shown to be directly bioavailable to algae (Boström et al., 1988b) and may be utilised by aquatic biota in the Waitaki catchment. The low concentrations (19.3 mg/kg) measured in the upper Lake Tasman SPM were comparable to the concentrations (1 – 23 mg/kg) reported for fresh glacial SPM in Northern Hemisphere catchments (Hodson et al., 2004). Burrus et al. (1990) reported the proportions of "non-inorganic" P for the upper Rhone River, a developed glacial-fed catchment in Switzerland. This fraction will include the exchangeable, redox-reactive and NaOH-reactive fractions. In any case, the reported values (46.7 – 128 mg/kg) were comparable (23.4 – 165 mg/kg) to sediments in this study. The exception was the sample from Lake Aviemore which was relatively enriched (303.8 mg/kg)

The progressive increase in organic-P measured in the Waitaki sediments is likely due to the increasing proportion of biogenic particles that were evident in both the SPM and sediment (**Chapter 2, Section 2.3.2.2**). The concentrations determined in the lower catchment (102 – 187 mg/kg) were higher than concentrations reported for the upper Rhone (46.7 and 128 mg/kg) (Burrus et al., 1990). Biotic forms of P include polyphosphates, phospholipids, phosphonates and nucleic acids which may be incorporated into the structural features of both live and dead organisms. Organic-P can be recycled in situ by resident microbes and other aquatic organisms, using enzymatic processes to hydrolyse P from the organic complex and liberating bioavailable P to the water column (Correll, 1998).

3.4.3 Adsorption Characteristics and Phases

The adsorption of P onto natural sediments and SPM is a complex process, involving multiple phases that may evolve in different environments and varying conditions. Despite this challenge, the complementary techniques used in this research have provided key insights into the adsorption surfaces of the SPM. This information was used to inform the modelling process. The sequential extractions provided a first insight into the likely phases implicated in adsorption. The redox-reactive and NaOH-reactive P fractions were found to become enriched when sediments from Lakes Tasman and Aviemore were exposed to a 0.1 mg/l phosphate solution for 24 hours. The P associated with the redox-reactive fraction will be associated with reactive Fe and Mn oxide surfaces. Both were found to undergo dissolution during the procedure. The P associated with the NaOH fraction is expected to be adsorbed to more crystalline Fe and Mn phases that are resilient to the reducing procedure.

Additional evidence of the adsorbing phases was provided by the adsorption edge experiments. The adsorption edge curves had a complex relationship with pH and were not comparable to the adsorption of P onto single mineral phases (Dzombak and Morel, 1990). However, the greatest adsorption capacity for P was consistently measured in the pH range of 4.5 – 6. This indicated that a key phase of the SPM was responsible for the adsorptive capacity in all samples. At this pH, the dissolved phosphate was predicted to be in the form of the dihydrogen phosphate ($H_2PO_4^-$), an anion that will adsorb to a positively charged surface. The dramatic increase in adsorption at pH < 7 strongly indicates that iron-oxide mediate the adsorption, which has a point of zero charge (PZC) of ~7 (Kosmulski, 2011). Below the PZC the oxide surface gains a net positive charge which will attract $H_2PO_4^-$. The dissolution profiles of Fe and Al during the procedure were comparable to the model profiles of ferrihydrite and gibbsite, indicating that these phases are prevalent in the SPM. These will largely be present as surface coatings on the primary and clay minerals present in the SPM. It is likely that these phases have formed during the rapid weathering of the immature glacial sediments (Tranter et al., 2002).

A prominent feature of the Waitaki catchment samples was the liberation of P into solution at pH < 4.5. Modelling in Visual Minteq indicated that the source of this P was the dissolution of hydroyxlapatite, which dissolves in acidic conditions, liberating Ca^{2+} and PO_4-P into solution (Dorozhkin, 1997) (**Equation 4.5**).

$$Ca_{10}(PO_4)_6(F,OH)_2 + 14H^+ \leftrightarrow 10Ca^{2+} + 6H_2PO_4^- + 2HF, H_2O \qquad (\mathbf{4.5})$$

Quartz, illite and albite constituted the major mineral phases of the SPM and all were found to have a coating of P with SEM/EDS analysis (**Figure 3.5).** However, these minerals are not expected to play a direct role in the adsorption of P owing to their negative charge characteristics at low pH values (Kosmulski, 2011). Instead, it is likely that the adsorption capacity of these minerals for P are primarily influenced by surface coatings of Fe, Al and Mn oxides, which have been previous reported in the literature (Edzwald et al., 1976; Wang et al., 2009). Organic coatings (such as fulvic and humic acids) may inhibit adsorption on these minerals due to competitive adsorption and charge repulsion effects (Guppy et al., 2005).

3.4.4 Can phosphorus adsorption onto glacial SPM be accurately predicted with Surface Complexation Modelling?

The similarities of the experimental and modelled adsorption profiles indicate that SCMs can be usefully applied in the modelling of P adsorption onto fresh glacial SPM. The primary adsorbing phase was determined to be amorphous Fe oxide (ferrihydrite), and the addition of the DLM alone was found to accurately describe P adsorption in the environmentally relevant pH range of 6 – 10. Below this pH, the relationship was obscured by the dissolution of both the adsorbing phases and hydroxyapatite liberating P into solution. The accuracy of the model declined down catchment, where significant differences in P adsorption were determined. It is likely that the increasing complexity of the SPM down catchment has obscured the relationship.

Determining the quantity of reactive adsorbent applied in a surface complexation model is a highly challenging task (Groenenberg and Lofts, 2014). In this study, an acid treatment at pH 2 was used to liberate reactive Fe, Al and Mn oxides from the SPM into solution. This proved to be a relatively simple procedure and can be easily applied as a means of estimating reactive phases contributing to P adsorption. However, this method was not suitable in determining the adsorption capacity and behaviour of the non-glacial Waikato River SPM. A significant concentration of Fe was liberated from the sample during the acid treatment. In spite of this, the adsorption capacity was comparatively low, suggesting that the adsorption behaviour of this lowland SPM was very different. This may be due to the presence of competing adsorbates, or a more crystalline adsorbing surface (e.g. goethite). Further analysis could explain the discrepancy and may also determine if the use of the diffuse layer SCMs is appropriate in other glacier-fed catchments. It is recommended that any future

studies monitor the concentrations of Al, Fe and Mn in solution during adsorption experiments, as it provides valuable information on the behaviour and composition of the adsorbing phases.

Despite the challenges faced in this research, the results have demonstrated that simple SCMs can be used to predict P adsorption onto glacial SPM. In a regulatory context, the models could be useful in predicting the attenuation of P from runoff. The models may also be used to determine the mobility of P when exposed to perturbations in biogeochemical conditions (i.e. pH, redox potential, temperature and ionic strength) which are commonly encountered in natural waters.

3.5 Conclusions

The collective findings of this study have demonstrated that glacial SPM has a significant potential to adsorb P. The freshly abraded particles collected in close proximity to the glacial source were found to have a greater adsorption capacity for P compared to the organic rich SPM collected down catchment. This was attributed to the greater concentrations of reactive Fe oxides associated with the glacial SPM, which were determined to have a dominant influence on the adsorption of P. A Diffuse Layer SCM, assuming HFO to be the only adsorbing surface, was used to model the adsorption of P. The model provided a good fit to the adsorption character and capacity of the fresh glacial SPM. However, the accuracy of the model declined for the down catchment SPM, which was attributed to the increasingly complexity of the SPM and possible competitive effects.

The ‘adsorption potential’ of the Waitaki catchment water, a function of the variable SPM concentrations and its adsorption capacity, was greatest in the SPM rich meltwaters of the upper catchment. However, this declined rapidly decreased down catchment, owing to the declining influence of the glacial sediments and the significantly lower SPM concentrations in the water. For this reason, glacial SPM is not predicted to play an important role in the attenuation of P loads that may result from the continuing development of the catchment.

3.6 References:

Anderson DM, Glibert PM, Burkholder JM. Harmful algal blooms and eutrophication: Nutrient sources, composition, and consequences. Estuaries 2002; 25: 704-726.

APHA APHA. Standard methods for the examination of water and wastewater. American Public Health Association, Washington, D.C., 2005.

Bibby RL, Webster-Brown JG. Characterisation of urban catchment suspended particulate matter (Auckland region, New Zealand); a comparison with non-urban SPM. Science of the Total Environment 2005; 343: 177-197.

Borovec J, Sirová D, Mošnerová P, Rejmánková E, Vrba J. Spatial and temporal changes in phosphorus partitioning within a freshwater cyanobacterial mat community. Biogeochemistry 2010; 101: 323-333.

Boström B, Andersen JM, Fleischer S, Jansson M. Exchange of phosphorus across the sediment-water interface. Hydrobiologia 1988a; 170: 229-244.

Boström B, Persson G, Broberg B. Bioavailability of different phosphorus forms in freshwater systems. Hydrobiologia 1988b; 170: 133-155.

Burrus D, Thomas RL, Dominik B, Vernet JP, Dominik J. Characteristics of suspended sediment in the upper rhone river, switzerland, including the particulate forms of phosphorus. Hydrological Processes 1990; 4: 85-98.

Clarke G. Upper Waitaki limit setting process. Predicting consequences of future scenarios: Lake water quality. Environment Canterbury, 2015.

Correll DL. The Role of Phosphorus in the Eutrophication of Receiving Waters: A Review. Journal of Environmental Quality 1998; 27: 261-266.

Dorozhkin SV. Surface Reactions of Apatite Dissolution. Journal of Colloid and Interface Science 1997; 191: 489-497.

Dzombak DA, Morel Fo. Surface complexation modeling: hydrous ferric oxide. New York: Wiley, 1990.

Eby GN. Principles of environmental geochemistry. Pacific Grove, California: Thomson-Brooks/Cole, 2004.

Edzwald JK, Toensing DC, Leung MCY. Phosphate adsorption reactions with clay-minerals. Environmental Science & Technology 1976; 10: 485-490.

Gray D. Upper Waitaki catchment flows, water quality and ecology: state and trend. Investigations and Monitoring Group. Environment Canterbury, Christchurch, New Zealand, 2015.

Groenenberg JE, Lofts S. The use of assemblage models to describe trace element partitioning, speciation, and fate: A review. Environmental Toxicology and Chemistry 2014; 33: 2181-2196.

Guppy CN, Menzies NW, Moody PW, Blamey FPC. Competitive sorption reactions between phosphorus and organic matter in soil: a review. Soil Research 2005; 43: 189-202.

Gustafsson JP. Visual Minteq. KTH Royal Institute of Technology, KTH Royal Institute of Technology, 2014.

Hans Wedepohl K. The composition of the continental crust. Geochimica et Cosmochimica Acta 1995; 59: 1217-1232.

Hodson A, Mumford P, Lister D. Suspended sediment and phosphorus in proglacial rivers: bioavailability and potential impacts upon the P status of ice-marginal receiving waters. Hydrological Processes 2004; 18: 2409-2422.

House WA. Geochemical cycling of phosphorus in rivers. Applied Geochemistry 2003; 18: 739-748.

House WA, Denison FH. Factors influencing the measurement of equilibrium phosphate concentrations in river sediments. Water Research 2000; 34: 1187-1200.

Karamalidis AK, Dzombak DA. Surface Complexation Modeling: Gibbsite: John Wiley & Sons, Inc., 2010.

Kosmulski M. The pH-dependent surface charging and points of zero charge. Journal of Colloid and Interface Science 2011; 353: 1-15.

Mindl B, Anesio AM, Meirer K, Hodson AJ, Laybourn-Parry J, Sommaruga R, et al. Factors influencing bacterial dynamics along a transect from supraglacial runoff to proglacial lakes of a high Arctic glacieri. FEMS Microbiology Ecology 2007; 59: 307-317.

Norton N, Spigel B, Sutherland D, Trolle D, Plew D. Lake Benmore Water Quality: a modelling method to assist with assessments of nutrient loadings. Environment Canterbury, Environment Canterbury, 2009.

O'Neil JM, Davis TW, Burford MA, Gobler CJ. The rise of harmful cyanobacteria blooms: The potential roles of eutrophication and climate change. Harmful Algae 2012; 14: 313-334.

Olsen SR, Watanabe FS. A Method to Determine a Phosphorus Adsorption Maximum of Soils as Measured by the Langmuir Isotherm1. Soil Science Society of America Journal 1957; 21: 144-149.

Pfannkuche J, Schmidt A. Determination of suspended particulate matter concentration from turbidity measurements: particle size effects and calibration procedures. Hydrological Processes 2003; 17: 1951-1963.

Rydin E. Potentially mobile phosphorus in Lake Erken sediment. Water Research 2000; 34: 2037-2042.

Spivakov BY, Maryutina TA, Muntau H. Phosphorus Speciation in Water and Sediments. Pure and Applied Chemistry. 71, 1999, pp. 2161.

Stal LJ. Physiological ecology of cyanobacteria in microbial mats and other communities. New Phytologist 1995; 131: 1-32.

Stumm W, Morgan JJ. Aquatic chemistry; an introduction emphasizing chemical equilibria in natural waters, 1970.

Tanada S, Kabayama M, Kawasaki N, Sakiyama T, Nakamura T, Araki M, et al. Removal of phosphate by aluminum oxide hydroxide. Journal of Colloid and Interface Science 2003; 257: 135-140.

Tiessen H. Phosphorus in the global environment. In: White PJ, Hammond JP, editors. The Ecophysiology of Plant-Phosphorus Interactions. Springer Netherlands, Dordrecht, 2008, pp. 1-7.

Tranter M, Sharp MJ, Lamb HR, Brown GH, Hubbard BP, Willis IC. Geochemical weathering at the bed of Haut Glacier d'Arolla, Switzerland—a new model. Hydrological Processes 2002; 16: 959-993.

Trolle D, Spigel B, Hamilton D, Norton N, Sutherland D, Plew D, et al. Application of a Three-Dimensional Water Quality Model as a Decision Support Tool for the Management of Land-Use Changes in the Catchment of an Oligotrophic Lake. Environmental Management 2014; 54: 479-493.

Wang Y, Shen Z, Niu J, Liu R. Adsorption of phosphorus on sediments from the Three-Gorges Reservoir (China) and the relation with sediment compositions. Journal of Hazardous Materials 2009; 162: 92-98.

Waters AS. Phosphorus dynamics in a shallow, coastal lake system, Canterbury, New Zealand. Waterways Centre for Freshwater Management. PhD. University of Canterbury, University of Canterbury, 2016.

Withers PJA, Jarvie HP. Delivery and cycling of phosphorus in rivers: A review. Science of The Total Environment 2008; 400: 379-395.

Zhou A, Tang H, Wang D. Phosphorus adsorption on natural sediments: Modeling and effects of pH and sediment composition. Water Research 2005; 39: 1245-1254.

4. Cadmium and Copper Adsorption onto SPM in the Glacier-Fed Waitaki Catchment, New Zealand

4.1 Introduction

Suspended particulate matter plays an important role in regulating the transport, speciation and bioavailability of trace metals in urban and lowland environments e.g. (Bibby and Webster-Brown, 2006; Lu and Allen, 2001; Webster-Brown et al., 2012). However, the role of glacial SPM in this regard has to date not been well characterised. In the glacier-fed Waitaki catchment, the predominant sources of contamination are from aquaculture, agricultural runoff and wastewater treatment effluent (Clarke, 2015). Trace metals are commonly associated with these sources. Their adsorption by SPM may determine their availability to aquatic biota, and their transport and accumulation in the catchment.

Cadmium (Cd) is a toxic trace element that is a common impurity in phosphate fertilizers extensively used in agricultural applications. In New Zealand, the use of superphosphate ($CaH_4P_2O_8$) fertilisers is widespread. Substantial quantities were manufactured from Cd-rich rock from Nauru and imported into the country, which has resulted in the contamination of topsoil's around the country (Taylor, 1997). Cadmium is highly mobile and is toxic to humans, aquatic organisms and plants (Wright and Welbourn, 1994). Its mobility in the environment is therefore a concern for regulators. Iron (Fe) and manganese (Mn) oxy/hydroxides are the predominant adsorbing surfaces for Cd on sediments in aquatic environments (Davies-Colley et al., 1984; Fu and Allen, 1992; Laxen, 1983).

Copper is used in a variety of agrichemical applications including pesticides, herbicides, fungicides and animal remedies. High concentrations may also be present in sewage effluent (Flemming and Trevors, 1989; Harrison and Bishop, 1983). Dissolved copper is a potent pollutant in freshwater environments. Extremely low concentrations can induce behavioural responses in aquatic biota, and at higher doses Cu can be acutely toxic (Flemming and Trevors, 1989). Copper is known to strongly adsorb to natural organic matter (NOM, either in the dissolved phase or as a coating on particles (Davis, 1982; Davis, 1984; Tipping, 1981).

The primary aim of this research was to determine the adsorption capability of the Waitaki catchment SPM for Cd and Cu and investigate how this evolves throughout the catchment. Adsorption edge and isotherm experiments were first used to determine the adsorption behaviour and capacity of the SPM. Geochemical modelling was used to assist in the interpretation of these experimental results. A key consideration was the determination of phases implicated in the adsorption process. The Diffuse Layer (DLM) and Stockholm Humic model (SHM) were applied in this study to assess whether the adsorption of Cd and Cu can be predicted onto the reactive surfaces of Fe oxide and organic matter respectively.

4.2 Methods

4.2.1 Sample collection and preparation

Please refer to **Chapter 2, Section 2.2.2** for a detailed account of the collection and preparation of SPM throughout the Waitaki Catchment. Rehydrated SPM samples in 0.01 M $NaNO_3$ from Lakes Tasman, Benmore – Ahuriri Arm and Aviemore and the Waitaki River were used in this study. These samples were selected for their situation in the catchment and their varying characteristics.

4.2.2 Materials and Experimental Procedures

The SPM solutions used in the procedures were prepared in the same manner described in **Chapter 3, Section 3.2.2**. TraceCERT® reference Cd (1000 mg/l in 2% HNO_3) and Cu (1000 mg/l in 2% HNO_3) standard solutions were used in the adsorption experiments. Stock solutions of 10 and 50 mg/l were prepared by dilution with ultrapure H_2O. All pH adjustments were made with analytical grade NaOH and HNO_3 with concentrations ranging from 0.01 – 1.00 M. The pH of the Cd and Cu solutions were adjusted to pH 5 with 1-10 µl additions of NaOH. This pH value was selected to minimise the acidic degradation of the SPM when transferred to the batch vessel, while preventing precipitation at a higher pH. The dissolved concentrations of trace metals in the filtered samples were determined with the use of ICP-MS as described in **Chapter 2, Section 2.2.4.2**. Solution blanks and standards were run in parallel with every analysis.

4.2.3 Adsorption Edge Experiments:

The effect of pH on the adsorption of Cd and Cu onto SPM was determined with batch adsorption edge experiments. The method detailed by Bibby and Webster-Brown (2006) was used to design the experimental procedure. Rehydrated SPM (100 mg/l) solutions were adjusted to pH ~3 with small additions (1 – 10 µl) of 1M NaOH while mixed with a clean magnetic flea in an acid-washed 250 ml polypropylene jar. A sample blank was collected before an accurately weighed aliquot of Cu or Cd stock solution was added to make a primary concentration of 50 µg/l**.** The solution was left to equilibrate for an additional 30 minutes before a 12 ml aliquot was transferred to a separate 15 ml polypropylene centrifuge tube for analysis at time zero. The pH of the solution was then progressively increased with small additions (1 – 10 µl) of 1M NaOH. Aliquots were drawn for every change in 0.5 – 1 pH unit, up to a final pH of 10 – 10.5 and transferred to separate 15 ml tubes. These were next transferred to an end-over-end mixer for 24 hours in a 25°C temperature-controlled environment. After this period, the pH of the solutions were re-measured before tubes were centrifuged at 4000 rpm for 20 minutes. The supernatant was recovered, filtered through 0.22 µm nitrocellulose filter membranes and analysed for trace metals (Cd, Cu, Fe, Al and Mn) by ICP-MS. Analytical controls without the addition of SPM were included in the analysis.

4.2.4 Batch Adsorption Isotherms:

The adsorption capacities of the SPM samples for Cd and Cu were determined with adsorption isotherms. First, 10 ml aliquots of rehydrated SPM solution were transferred into separate 15 ml polypropylene centrifuge tubes. The concentrations of Cd and Cu were adjusted in each tube with accurately weighed additions of the stock solutions. The final concentrations were 0, 10, 50, 100, 250, 500, 1000, 2500, 5000, 10,000 and 25,000 µg/l Cu or Cd. Analytical controls with no SPM were ran in parallel. Samples were spun on an end-over-end mixer for 24 hours in a temperature-controlled environment (25°C). After 24 hours, the tubes were removed and pH immediately recorded with the use of a HACH HQ40d pH probe. The samples were then centrifuged at 4000 rpm for 20 minutes. The supernatant was recovered, filtered through 0.22 µm nitrocellulose filter membranes and analysed for trace metals by ICP-MS. The experimental data was fitted with Langmuir and Freudlich models by non-linear regression to determine the maximum adsorption capacity/site densities. These models have been extensively used in the literature to describe the adsorption of Cd and Cu onto metal

oxy/hydroxides, clay minerals and mixed composition samples such as SPM, sediment and soils (Laxen, 1983). The methodology and equations used to fit the isotherms are detailed in **Chapter 3, Section 3.2.4**.

4.2.5 Theoretical Adsorption Potential

The theoretical adsorption potential was calculated for the Waitaki catchment water, combining the SPM concentrations detected throughout the catchment with their associated adsorption capacities for Cd and Cu, were determined in this study. The Langmuir isotherms reported in **Section 4.3.4** were used to determine the SPMs adsorption capacity when Cd or Cu is present as a solution concentration of 1 µg/l. This concentration is 1 – 3 orders of magnitude greater than the concentrations of Cd and Cu measured in the system (**Chapter 2, Section 2.3.1**). However, the scenario has been applied to determine the relative adsorption potential of the water in the event of contamination. The resulting values, in µg Cd or Cu/g SPM, were multiplied by the varying concentrations of SPM predicted in the catchment. Additional details of the methods used to calculate the adsorption potential are provided in **Chapter 3, Section 3.2.5** and **Appendix D**.

4.2.6 Geochemical Modelling

Geochemical speciation modelling was performed with the software package Visual MINTEQ 3.1. The effect of pH on the speciation of Cd and Cu in solution was first modelled for the analytical (0.01 M $NaNO_3$ solution, 25°C, pE = 9, Cd or Cu = 50 µg/l). The model was configured to allow for the precipitation of 'possible' mineral phases under the thermodynamic constraints. For cadmium these included cadmium hydroxide ($Cd(OH)_{2\,(S)}$ and otavite ($CdCO_3$). Copper compounds included copper hydroxide ($Cu(OH)_{2(s)}$), tenorite ($CuO_{(s)}$), malachite ($Cu_2(OH)_2CO_{3(s)}$) and azurite ($Cu_3(OH)_2(CO_3)_{2(s)}$).

The adsorption of Cd and Cu onto the SPM surfaces was predicted with surface complexation models (SCMs) incorporated into the software. Surface complexation models were combined (hereby referred to as assemblage models) to investigate cumulative adsorption onto particle surfaces. The reactive concentrations of Fe, Mn, Al and organic matter applied in the models are presented in **Table 4.1**. Adsorption onto hydrous ferric oxide (HFO) was predicted with the double layer model (DLM) (Dzombak and Morel, 1990) and hydrous aluminium oxide (HAO) with the gibbsite SCM

(Karamalidis and Dzombak, 2010). The concentrations of reactive surface oxides (HFO, HAO) applied in the model were derived from concentrations liberated by the SPM at pH 2 as detailed in **Chapter 3, Section 3.2.5.** The influence of particulate organic matter (POM) was also predicted with the incorporation of the Stockholm Humic Model (SHM) (Gustafsson, 2001) incorporated into Visual Minteq. The adsorption of trace metals by organic matter is a highly complex process due to the diverse nature of organic matter and its associated functional groups. A key consideration is determining the quantities of "reactive" organic matter contributing to adsorption. It was not possible during this research to specifically analyse the character and quantities of humic substances associated with the SPM. Therefore, the following assumptions were made in order to calibrate the model: 1) The reactive organic matter was limited to fulvic acids, the dominant humic species in natural waters (Boggs Jr et al., 1985) for which complexation data is available; 2) The concentration of reactive FA was 2 – 5% of the SPM TOC content, based on preliminary optimisation of the model.

The adsorption capacity of the adsorbent (HFO, gibbsite, organic matter) was determined for comparison with the experimental isotherm data in **Section 4.3.4**. This provided an indication of the discrepancies that may exist between the modelled and experimental data. To do so, the models were programmed to progressively increase the solution concentration of dissolved Cd or Cu in 100 µg/l aliquots using the multi-problem/sweep function in the software.

Table 4.1. Parameters used in the surface complexation models applied in Visual Minteq: HFO = hydrous ferric oxide double layer model (DLM); HAO = hydrous aluminium oxide gibbsite model; HMO = hydrous manganese oxide model; POM = reactive particulate organic matter applied in the Stockholm model (SHM).

Site	HFO	HAO	HMO	POM 2 %	POM 5 %
	µg/l			g/l	
L. Tasman	667.1	649.1	12.3	0.00002	0.00004
L. Benmore -Ahuriri	175.4	112.7	80.3	0.0005	0.0012
L. Aviemore	156.4	144	34.0	0.0006	0.0016
Waitaki River	307.5	280.9	12.5	0.0002	0.0004

4.2.7 Statistics

Statistical analysis was performed with XLSTAT version 19. A Pearson's correlation matrix was prepared with the descriptive data obtained from the characterization experiments. Significance was tested at the 5% level ($p \leq 0.05$).

4.3 Results:

4.3.1 Adsorption Edge Profiles

The adsorption edge profiles for the sorption of Cd and Cu onto the Waitaki SPM (100 mg/l) are presented in **Figure 4.1.** The adsorption of Cd had a high dependence on pH. Almost all Cd was detected in solution under acidic conditions (pH < 5). The majority of Cd sorption occurred in the pH range of 6-8 and all samples had a well-defined adsorption edge. The associated pH_{50} values (pH at which 50% of the metal initially present has been adsorbed to the SPM) for the SPM were similar, ranging from pH 6.8 – 7.2 **(Table 4.3)**. The control sample (no SPM added) was found to have a higher pH_{50} value (8.8). Approximately 5-10% of the Cd remained in an unbound, dissolved state in the experiments.

Significant differences in both the character and position of the adsorption edge curves were detected for Cu. In general, the adsorption edge was less defined, occurring in the pH range of 4-8 for the SPM samples and 6-8 for the control. The Cu adsorption edge curves for the SPM from Lakes Tasman, Benmore and Aviemore were comparable, with the greatest increase in adsorption occurring in the pH range of 6-7. The Waitaki River SPM had a broader profile, with adsorption progressively increasing in the pH range of 4-7. The highest pH_{50} for Cu was determined for SPM collected from Lake Tasman (6.6), and progressively declined with increasing distance from the glacial source.

The dissolved concentrations of Al, Fe and Mn measured during the adsorption edge experiments are plotted in **Figure 4.2**. Significant differences were detected throughout the pH range. At neutral pH (6-8) very low concentrations of Al and Fe were detected in solution. Al was liberated into solution in both acidic (pH < 5) and alkaline (pH > 8) conditions. Fe was only liberated under acidic conditions. The concentrations of Al and Fe decreased in the order: Lake Tasman SPM > Waitaki River > Lake Benmore > Lake Aviemore. The concentrations of Mn progressively increased in acidic conditions. The concentrations decreased in the order Lake Benmore > Lake Aviemore > Waitaki River > Lake Tasman.

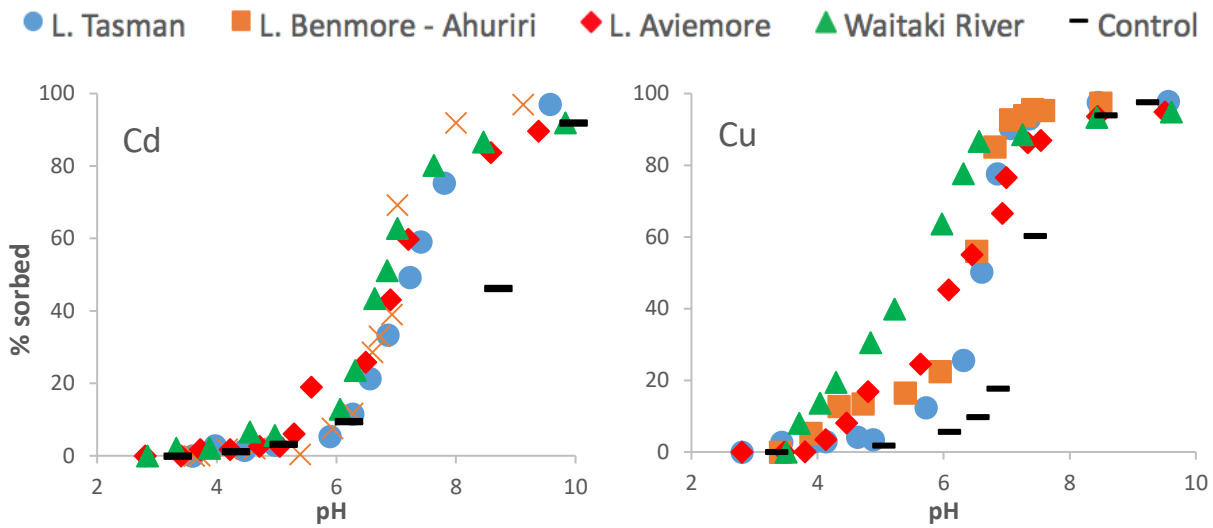

Figure 4.1. Cadmium (Cd) and Copper (Cu) adsorption as a function of pH on Waitaki catchment SPM. Concentration of Cd and Cu was 50 µg/l. SPM concentration was 100 mg/l in 0.01 M $NaNO_3$. No SPM was added to control samples.

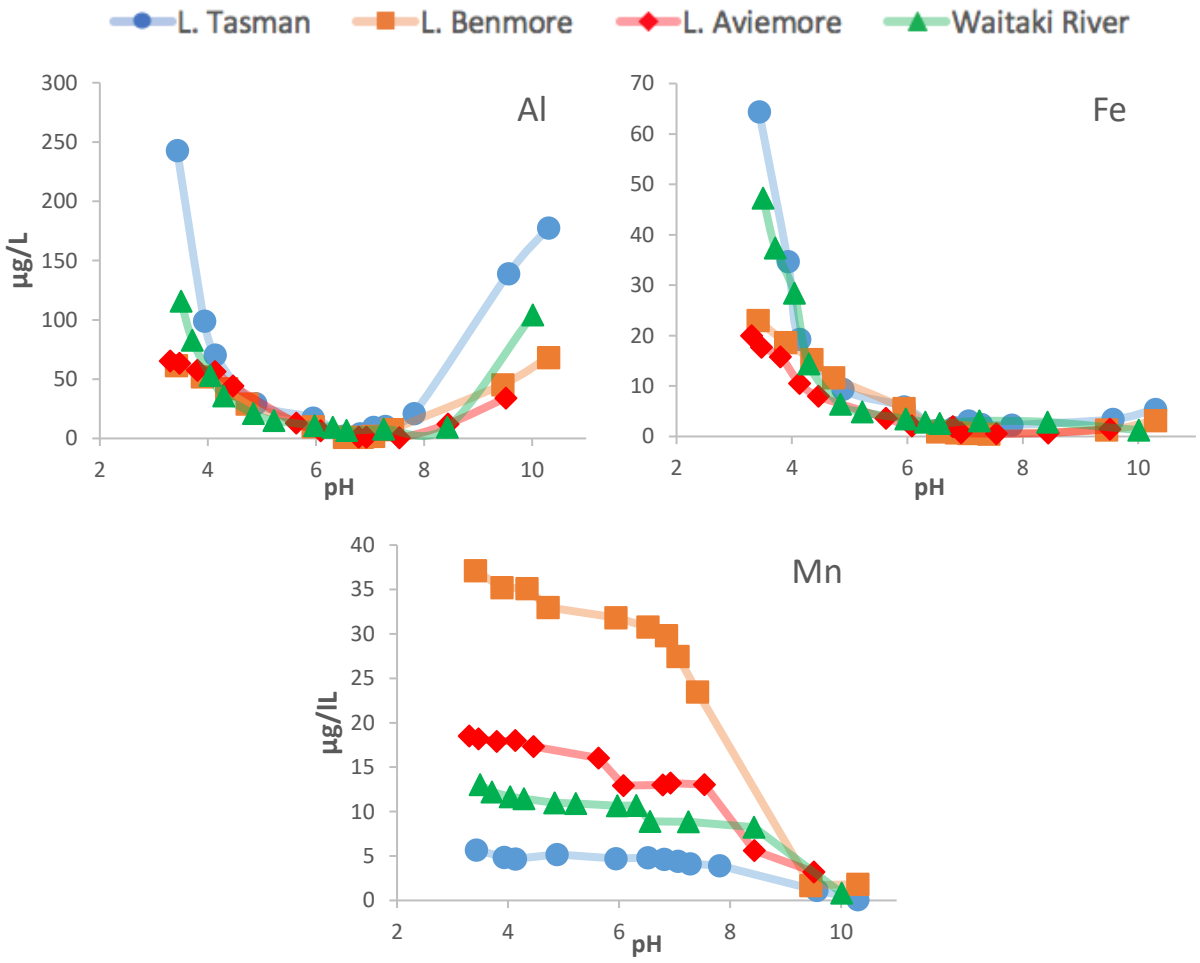

Figure 4.2. Concentrations of dissolved Al, Fe and Mn detected in solution during the adsorption edge experiments. Concentration of SPM was 100 mg/l in 0.01 M $NaNO_3$.

4.3.2 Adsorption Edge Models

A comparison of the adsorption edge data from **Section 4.3.1** and the modelled adsorption capacities of the SPM generated with the DLM, gibbsite and SHM surface complexation models (SCMs) is presented in **Figures 4.3 and 4.4**. For Cd, the combination of the DLM (HFO) and SHM (POM) SCMs were found to provide the best fits for the experimental data. The DLM and gibbsite (HAO) SCMs were generally found to poorly predict the experimental adsorption edge, with modelled pH_{50} values between 1 – 3 pH units higher than the experiment data (**Table 4.2**). The SCMs did not provide a good fit of the experimental data for the Lake Tasman SPM. The best modelled pH_{50} was 8.4, 1.2 pH units higher than what was observed in the laboratory experiment (pH 7.2). For Lakes Benmore and Aviemore, the addition of the SHM (2% POM) resulted in comparable adsorption edge models with similar pH_{50} values (< 0.2 pH unit's difference) to the experimental data. For the Waitaki River sample, a better fit was modelled with the addition of the SHM (5% POM), with the pH_{50} 0.3 units greater than the experimental data.

For Cu, the combination of the DLM and SHM models provided the most accurate fits to the experimental data. For Lake Tasman, no appreciable differences were detected between the SCMs. All were found to a good fit with pH_{50} values (6.7) just 0.1 units greater than the experimental data. Once again, for Lakes Benmore and Aviemore the best model fits for Cu were generated with the combined HFO and SHM models with the addition of 2% POM. The resulting pH_{50} values were <0.2 units greater than the experimental data. For the Waitaki River SPM, the addition of 5% POM resulted in a model fit and pH_{50} (5.5) comparable to the experimental data.

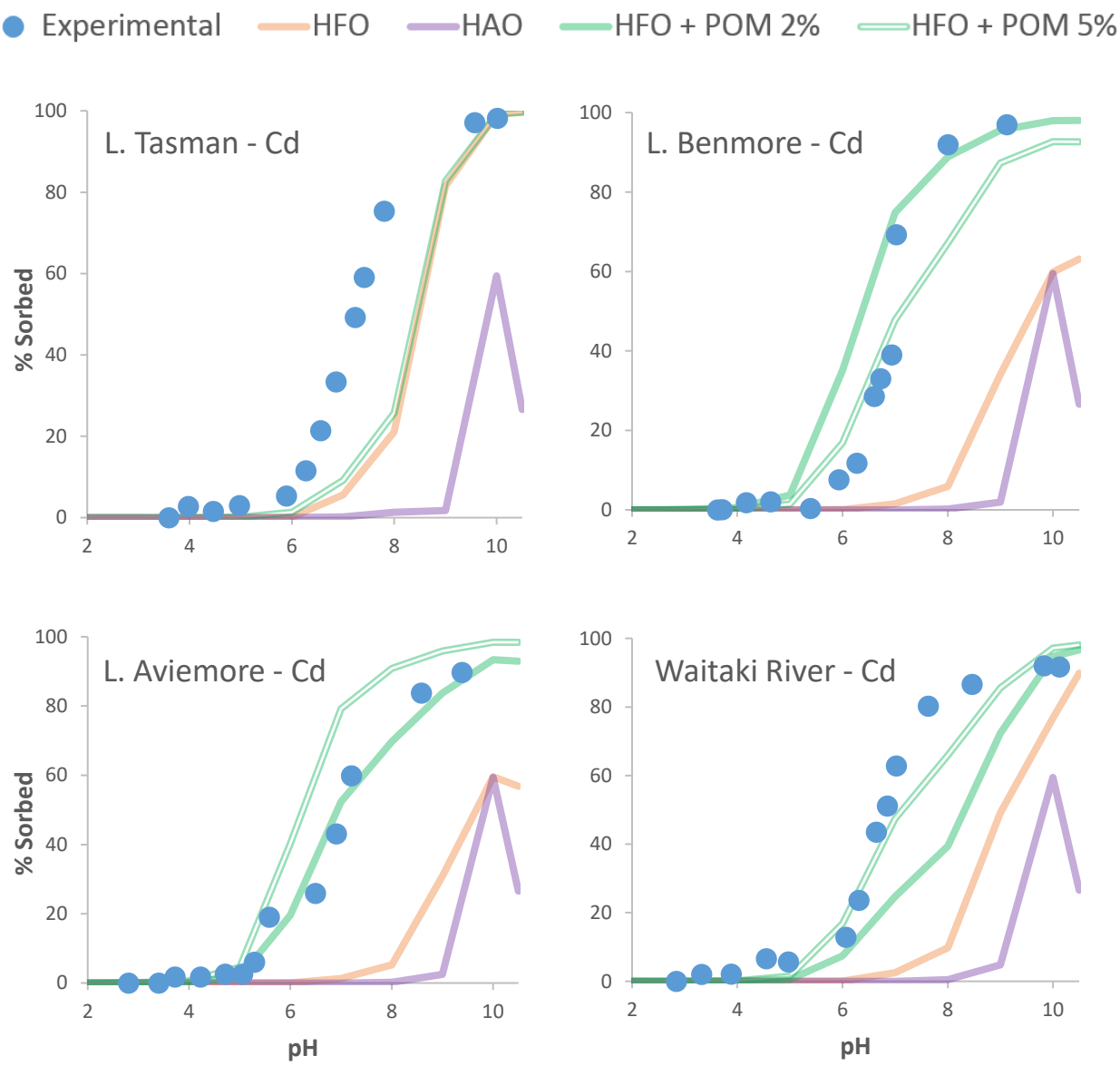

Figure 4.3. Cd adsorption as a function of pH onto different SCMs incorporated in Visual Minteq. SPM concentration was 100 mg/l in 0.01 M $NaNO_3$. Lines indicate model fits for: Orange – HFO double layer model; purple – gibbsite (HAO) model; blue – combined HFO and HAO model; solid green - HFO + SHM model using 2% reactive particulate organic matter (POM); and double green – HFO + 5% reactive POM. Models calculated using parameters shown in **Table 4.1**.

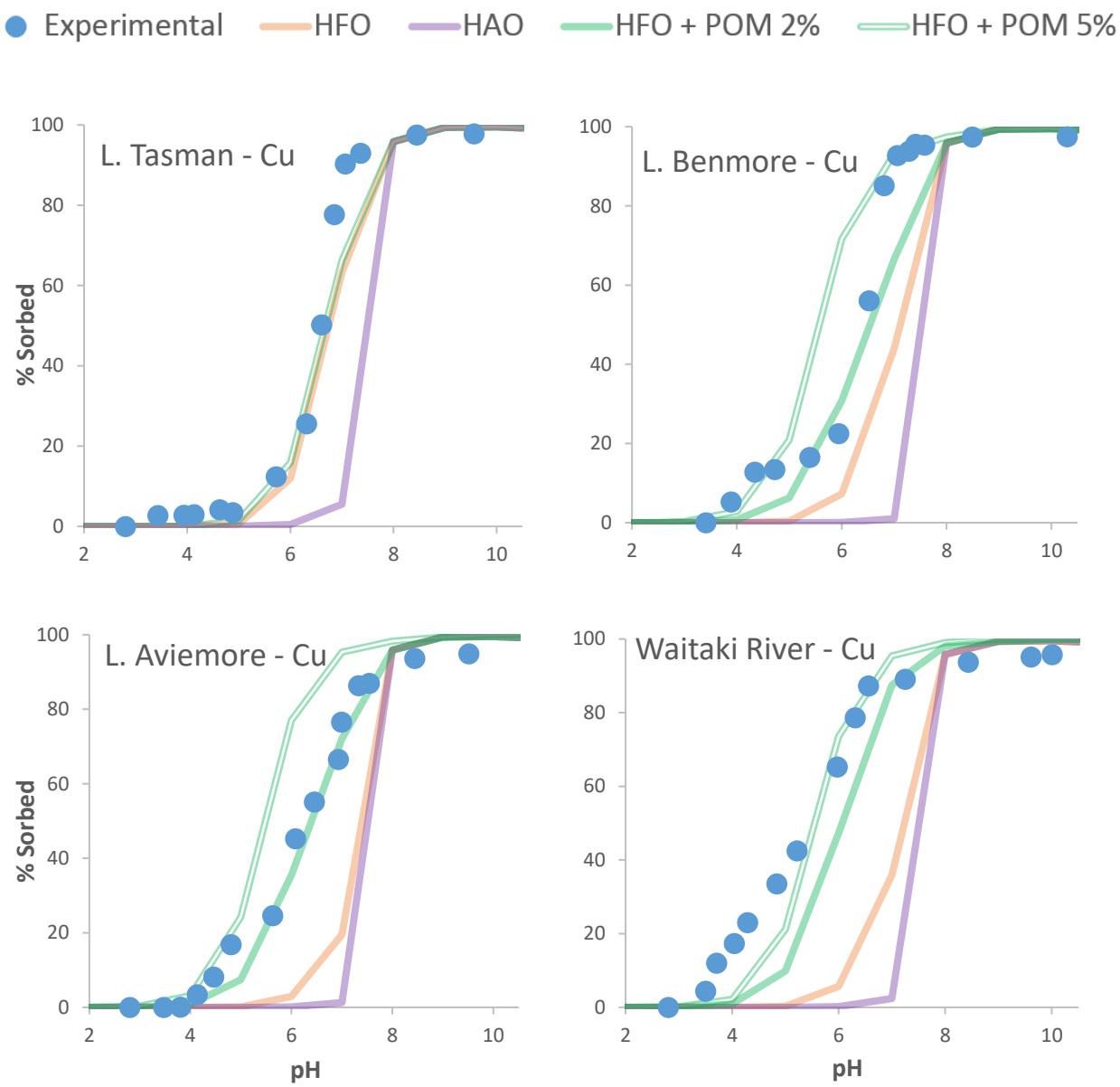

Figure 4.4. Cu adsorption as a function of pH onto different SCMs incorporated in Visual Minteq. SPM concentration was 100 mg/l in 0.01 M $NaNO_3$. Lines indicate model fits for: Orange – HFO double layer model; purple – gibbsite (HAO) model; blue – combined HFO and HAO model; solid green - HFO + SHM model using 2% reactive particulate organic matter (POM); and double green – HFO + 5% reactive POM. Models calculated using parameters shown in **Table 4.1**.

Table 4.2. The experimental and modelled pH values at which 50% of the dissolved Cd and Cu is adsorbed (pH_{50}) to SPM in the Waitaki catchment.

	Cadmium pH_{50}				Copper pH_{50}			
Site	**Experimental**	**HFO**	**HFO + POM 2%**	**HFO + POM 5 %**	**Experimental**	**HFO**	**HFO + POM 2%**	**HFO + POM 5 %**
L. Tasman	**7.2**	8.4	8.4	8.4	**6.6**	6.7	6.7	6.7
L. Benmore -Ahuriri	**6.9**	9.6	7.1	6.4	**6.2**	6.6	6.3	5.8
L. Aviemore	**7**	9.7	6.9	6.2	**6.2**	7.4	6.4	5.5
Waitaki River	**6.8**	9	8.3	7.1	**5.5**	7.2	6.1	5.5
Control	**8.8**	-	-	-	**7.2**	-	-	-

4.3.3 Controls

In the experimental controls, both Cd and Cu appeared to be removed by precipitation in the pH range of 8-10 (**Figure 4.5**). Geochemical speciation modelling in Visual Minteq predicted Cd to be dissolved from pH 2-10. Cd^{2+} is predicted to be the dominant ion (92 – 98%) in the pH range of 2 – 9. $CdOH^{+}$ (14 – 29%) and $Cd(OH)_{2\,(aq)}$ (17 – 82%) become the dominant ions at pH > 10. At pH > 10, $Cd(OH)_{2\,(s)}$ reached saturation, with precipitation removing dissolved Cd from solution. The model did not reproduce the experimental results, whereby the majority of dissolved Cd was removed from the solution phase in the pH range of 7 – 9. This data is tabulated in **Appendix D**.

The dissolved Cu speciation model was found to more closely reproduce the experimental results, with precipitation occurring in the pH range of 7-9. The model predicts that the Cu is the dominant aqueous ion (95 – 98%) at pH 2 - 7. At pH > 7, $CuCO_3$ (15 – 41%), $CuOH^{+}$ (16 – 36%) and $Cu(OH)_{2\,(aq)}$ (6 – 65%) are the dominant dissolved species. At pH values ≥ 8, tenorite ($CuO_{(s)}$) and malachite ($Cu_2(OH)_2CO_{3(s)}$) are predicted to reach saturation precipitates, removing dissolved Cu from solution by precipitation. At pH 9 copper hydroxide $Cu(OH)_2(s)$ reached saturation.

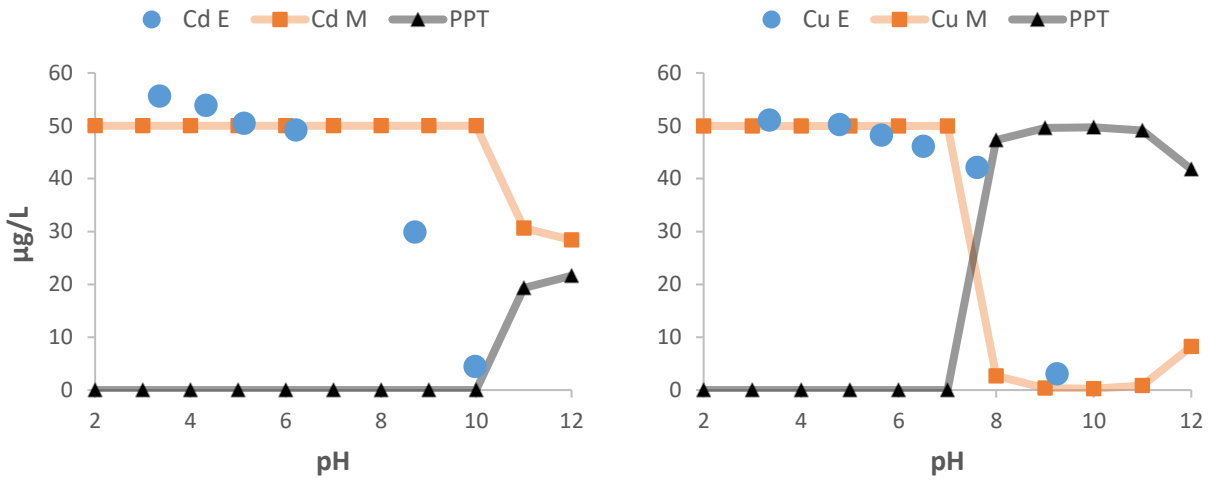

Figure 4.5. Comparison of the concentrations of dissolved Cd (left) and Cu (right) detected in solution in the experimental controls (blue markers), and that predicted by Visual Minteq (orange line). The concentrations of precipitates (PPT) predicted by the model are represented by the black line.

4.3.4 Adsorption Isotherms:

The adsorption of Cd by the Waitaki SPM was linear in the concentration range of 0 – 1000 µg/l (**Figure 4.6**). At progressively higher concentrations the curves flattened, with the Langmuir model found to provide a good fit to the experimental data with corresponding high coefficients of determination (R^2 = 0.97 – 0.99) **(Table 4.3)**. The Lake Aviemore SPM had the greatest associated affinity for Cd with a K_L value of 1.03. This was significantly greater than values of 0.48, 0.40 and 0.17 for the Waitaki River, Lake Tasman and Lake Benmore SPM respectively. The greatest adsorption capacity for Cd determined with the Langmuir isotherm was 7.27 mg/g for the Lake Tasman SPM. The Waitaki River, Lake Benmore and Lake Aviemore had capacities of 5.84, 5.6 and 4.5 mg/g respectively. The Freudlich model had a comparatively poor fit to the experimental data (R^2 = 0.84 – 0.92).

The Cu adsorption isotherms are reported for the concentration range of 0 – 1000 µg/L. A significant increase (> 500%) of Cu was found to be sequestered from solution in the concentration range of 2500 – 25,000 µg/l. This was attributed to the precipitation of copper containing minerals and the data was excluded. In the lower concentration range, the isotherm curves flattened with progressive increases in Cu concentration. The Langmuir model provided a good fit to the experimental data (R^2 = 0.94 – 0.99). The SPM from Lakes Tasman and Aviemore were found to have the greatest associated affinity for Cu, with K_L values of 22.2 and 21.6 respectively. The values for

the Waitaki River and Lake Benmore were 17.3 and 14.8 respectively. The greatest adsorption capacity was 4.36 mg/g for the lowland Waitaki River SPM. SPM from Lakes Benmore, Aviemore and Tasman were found to have reduced adsorption capacities of 2.67, 2.65 and 2.03 mg/g respectively. The Freudlich model provided a good fit of the experimental data (R^2 = 0.94 – 0.97).

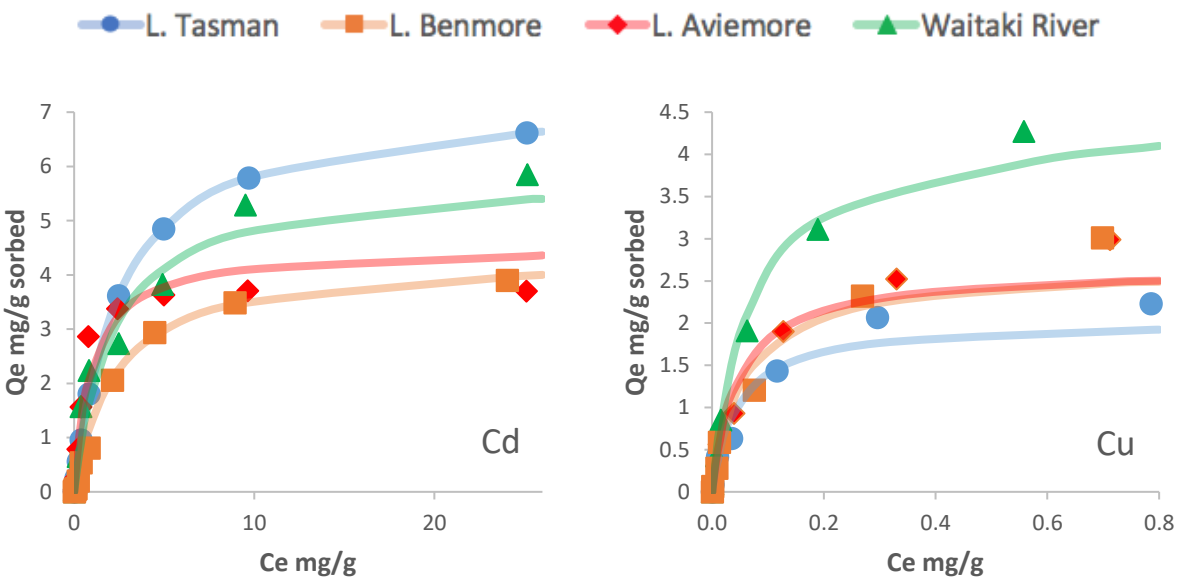

Figure 4.6. Cd (left) and Cu (right) adsorption isotherms for Waitaki catchment SPM. Ce = equilibrium solution concentration. Qe = mg Cu or Cd adsorbed per g SPM. The lines indicate the Langmuir model fits.

Table 4.3. Coefficients of determination (R^2) reported for Freudlich (F) and Langmuir (L) models fitted to the experimental adsorption isotherms with cadmium (Cd) and copper (Cu) onto SPM in the Waitaki catchment. The Langmuir constant K_L corresponds to the affinity of Cd and Cu for the SPM. The maximum adsorption capacity of the SPM was determined with the Langmuir model (L. Qmax).

	Cadmium				Copper			
Site	**F. R^2**	**L. R^2**	**K_L**	**L. QMax (mg/g)**	**F. R^2**	**L. R^2**	**K_L**	**L. QMax (mg/g)**
L. Tasman	0.86	0.98	0.40	7.27	0.94	0.96	22.2	2.03
L. Benmore -Ahuriri	0.92	0.99	0.17	5.60	0.97	0.96	17.3	2.67
L. Aviemore	0.9	0.95	1.03	4.50	0.95	0.94	21.6	2.65
Waitaki River	0.84	0.97	0.48	5.84	0.94	0.99	14.8	4.36

The adsorption capacities of the SPM determined with the DLM (HFO) and SHM (POM) SCMs in Visual Minteq are presented in **Table 4.4**. The gibbsite SCM did not result in the appreciable adsorption of Cd or Cu and has been omitted from the table. See **Appendix D** for details. The lowest

adsorption capacities were generated with the HFO SCM. However, the addition of POM with the SHM model enhanced the adsorption capacity. The modelled capacities of the Lake Tasman and Waitaki Catchment SPM for Cd and Cu were significantly lower than the experimental data. However, the adsorption capacities generated by the combined HFO and SHM models were comparable to the experimental data for SPM from Lakes Benmore and Aviemore.

Table 4.4. Comparison of the adsorption capacities of the SPM, as determined by adsorption isotherms and surface complexation models. HFO = double layer model; POM = Stockholm humic model (SHM) with 2% or 5% reactive particulate organic matter (POM).

Site	L. Tasman	L. Benmore -Ahuriri	L. Aviemore	Waitaki River
		Cadmium (mg/g SPM adsorbed)		
Experimental	7.27	5.6	4.5	5.84
HFO	0.32	0.2	0.07	0.15
HFO + POM 2%	0.35	1.5	1.77	0.71
HFO + POM 5%	0.4	3.77	4.61	1.56
		Copper (mg/g SPM adsorbed)		
Experimental	2.03	2.67	2.65	4.36
HFO	0.63	0.39	0.43	0.29
HFO + POM 2%	0.81	1.19	1.36	0.76
HFO + POM 5%	0.85	2.74	3.3	1.34

4.3.5 Theoretical Adsorption Potential

The adsorption potential of the Waitaki catchment water for Cd and Cu is presented in **Figure 4.7**. The meltwater from Lake Tasman, collected in close proximity to the glacial source (5 km), had the greatest adsorption potential with theoretical capacities to adsorb 0.27 – 0.59 µg Cd/l and 5.7 – 12.2 µg Cu/l. Down catchment, the adsorption potentials decreased by up to three orders of magnitude. For Lakes Benmore – Ahuriri (125 km) and Lake Aviemore (140 km), the adsorption potential declined to 0.009 – 0.05 µg Cd/l and 0.17 – 1.0 µg Cu/l. The adsorption potentials in the lower Waitaki River were slightly greater, ranging from 0.02 – 0.1 µg Cd/l and 0.3 – 2.5 µg Cu/l. The specific values are detailed in **Appendix D**.

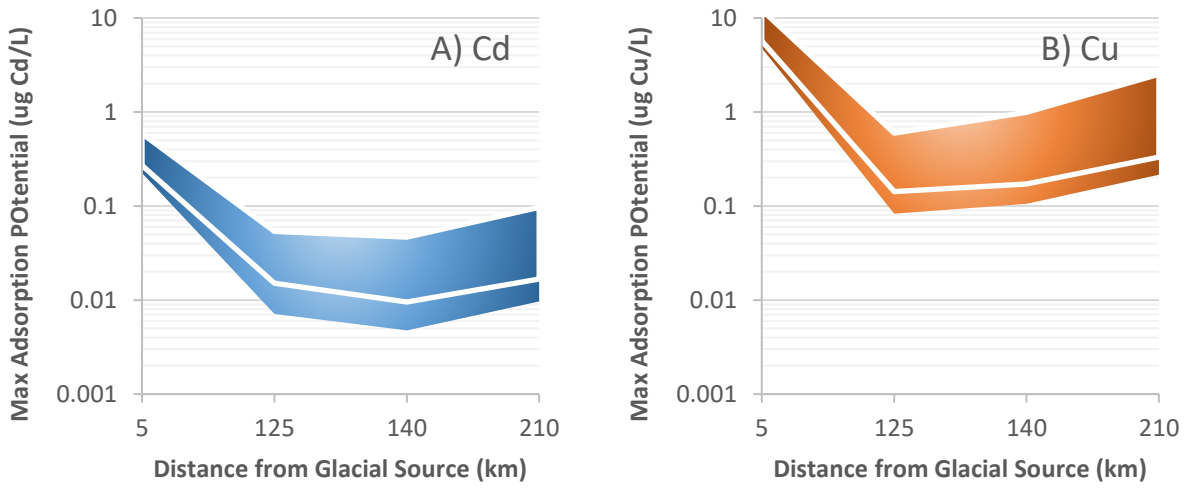

Figure 4.7. Adsorption potentials of the Waitaki Catchment water – a function of the SPM concentrations in the Waitaki Catchment and its maximum adsorption capacity for Cd (A) and Cu (B). Units are µg Cd or Cu/L water. The white line corresponds to the median adsorption potential. Note, the Y-axis is a logarithmic scale.

4.3.6 Correlation Analysis

The maximum adsorption capacity of Cd was highly correlated with the SSA and acid soluble concentrations of Fe and Al associated with the SPM (**Table 4.5**). It was also strongly inversely correlated with the PSD D_{50} and TC content. No significant correlations with the SPM or solution characteristics were determined for the adsorption capacity with Cu.

Table 4.5. Pearson correlation analysis of the compositional and adsorption characteristics associated with the Waitaki SPM. Strong correlations and inverse correlations are dark green and red respectively.

	µm	m²/g	µg/l (pH 2)			wt %			Langmuir (mg/g)	
Variables	**PSD D_{50}**	**SSA**	**Fe_{as}**	**Al_{as}**	**Mn_{as}**	**TC**	**pH_{50} Cd**	**pH_{50} Cu**	**Cd max**	**Cu max**
PSD D_{50}	**1.00**									
SSA	**-1.00**	**1.00**								
Fe_{as}	**-0.97**	0.94	**1.00**							
Al_{as}	-0.94	0.91	**1.00**	**1.00**						
Mn_{as}	0.42	-0.34	-0.61	-0.67	**1.00**					
TC	0.90	-0.88	-0.92	-0.90	0.66	**1.00**				
pH_{50} Cd	-0.67	0.64	0.72	0.73	-0.28	-0.38	**1.00**			
pH_{50} Cu	-0.44	0.46	0.35	0.33	0.34	0.00	0.81	**1.00**		
Cd max	-0.93	0.91	**0.96**	0.95	-0.67	**-0.99**	0.48	0.10	**1.00**	
Cu max	-0.04	0.07	-0.06	-0.10	0.00	-0.33	-0.71	-0.66	0.22	**1.00**

Values in bold are different from 0 with a significance level alpha=0.05

4.4 Discussion:

4.4.1 Adsorption of Cd and Cu by Glacial SPM

The glacial SPM was found to have a high adsorption capacity for Cd (7.27 mg/g). This was greater than the organic rich SPM collected in the lower catchment (4.5 – 5.6 mg/g), and that typically reported for SPM and sediment in non-glacial environments (Duddridge and Wainwright, 1981; Jain and Sharma, 2002; Wright and Welbourn, 1994). The greater adsorption capacity of the glacial SPM was attributed to the greater proportion of fine inorganic particles, large specific surface areas (SSA) and the greater concentrations of adsorbing surface oxides relative to SPM collected down catchment (**See Chapter 2 for details).** However, it must be noted that Cd was found to have a low affinity for SPM throughout the catchment, with most Cd remaining in the solution phase.

The affinity of Cu for the glacial SPM was significantly greater (~20x). However, the fresh glacial SPM was found to have the lowest adsorption capacity compared to the organic rich SPM in the lower catchment. The reported capacities in this study were comparable, but lower than those reported for SPM from Nanhu Lake in China (4.5 mg/g) (Hua et al., 2012), and SPM from the Susquehanna River, Delaware, USA (12.6 mg/g) (Shi et al., 1998).

The adsorption of both Cd and Cu in the Waitaki catchment water will be highly constrained by the concentrations of SPM in the water. The 'adsorption potential' was highest for both elements in the SPM rich, turbid meltwater of the upper catchment. In the theoretical scenario applied in this study (1 µg/L Cd or Cu solution concentration), between 5 – 59 % of the Cd may be adsorbed by the glacial SPM at Lake Tasman. However, the adsorption potential declined by up to 3 orders of magnitude down catchment, with less than 5% of the Cd is expected to be adsorbed onto the SPM. For Cu, 100% is predicted to be adsorbed in the upper catchment. The adsorption potential did significantly decline down catchment. However, a greater proportion (between 9.5 – 100%) of the Cu is still predicted to be adsorbed by the SPM.

4.4.2 Adsorption Characteristics and Phases

The adsorption of dissolved Cd and Cu was highly dependent on pH. For Cd, the Waitaki SPM had comparable, well-defined adsorption edges occurring in the pH range of 6 – 8. This adsorption was in the same vicinity of the SPMs point of zero charge (PZC), which was determined to be pH

~6.5 – 7 for all SPM samples (**Chapter 2, Section 2.3.5)**. At pH < 7, the SPM surface will become progressively protonated and electronic repulsions will prevent Cd partitioning onto the particle surface. At pH > 7 the SPM will gain a net negative charge in the presence of OH^-, allowing for the electrostatically favourable adsorption of Cd.

The adsorption of Cd was linear in the concentration range of 10 – 1000 µg/l. This is significantly greater than concentrations typically measured in environmental samples (0.001 – 1 µg/l) (Laxen, 1984; Wright and Welbourn, 1994). This shows that adsorption will not be limited by the number of adsorbing sites present on the SPM, but rather the Cd's affinity for the sites (Benjamin and Leckie, 1981). Laxen (1983) reported Cd adsorption onto individual mineral surfaces follows the order Mn > Fe (amorphous) > chlorite > Fe (crystalline) = illite = humics = > kaolinite > silica. Additional studies later confirmed that Fe- and Mn- oxy/hydroxides are often the dominant adsorbing phases on particulate matter in freshwater environments (Davies-Colley et al., 1984; Fu and Allen, 1992; Laxen, 1983). In this study, the adsorption capacity of the fresh glacial SPM was highly correlated ($p < 0.05$) to the concentrations of reactive Fe oxide associated with the particles. As these characteristics were lost in the downstream SPM, so too did its adsorption capacity. Iron oxides were shown to form in the pH range of 4-6 in this study (**Figure 4.2**), which is characteristic of ferrihydrite (**Chapter 3, Section 3.3.5**). For the lower catchment SPM, organic matter was predicted to be an increasingly dominant adsorbent. Organic matter is generally recognised as a weak adsorbent of Cd (Davis, 1984). However, the substantial proportions associated with the lower catchment SPM have been determined to play an important role in this study.

The adsorption character of Cu varied significantly throughout the catchment. The SPM from Lake Tasman had a steep adsorption profile in the pH range of 6 – 7, which was once again characteristic of adsorption onto a Fe oxide surface. However, the adsorption edges became less defined down catchment, with Cu removed from solution over a broader pH range. Dissolved Cu strongly adsorbs to organic surface functional groups (Davis, 1984; Lu and Allen, 2001), which are commonly associated with sediments and SPM as surface coatings (Davis, 1982; Tipping, 1981). The broad adsorption edge is consistent with the progressive development of surface charges on functional groups with a range of pKa values (Davis, 1984). Organic matter was a dominant component of the SPM and the application of the organic SCM indicated that it plays a key role in the adsorption of both Cd and Cu onto the organic rich SPM in the lower Waitaki.

It must be noted that both dissolved Cd and Cu may precipitate in solution, and was shown to occur without the presence of SPM at higher pH values for both Cd and Cu. This is a potential source of error that could influence the experimental data, especially the adsorption isotherms where high concentrations of Cd and Cu were used. Care was taken to control the pH to mitigate such effects in this study. However, the precipitation of Cu was detected at concentrations > 1000 μg/L and the data was excluded from analysis. In natural waters the concentrations of these pollutants are significantly lower (<100 μg/L), and their speciation will be largely controlled by adsorption processes and complexation with organic matter in circumneutral pH conditions (Namieśnik and Rabajczyk, 2010).

4.4.3 Can Surface Complexation Models Predict Cd and Cu Adsorption onto glacial SPM?

The SCMs used in this study were not able to accurately simulate the adsorption character and capacity of the fresh glacial SPM for Cd and Cu. Many possible reasons could explain this difference (including experimental and model input errors, precipitation reactions and competitive effects). However, the large discrepancies in this study indicate that the models have failed to account for additional, important surface functional groups present on the fine-grained SPM. The use of SCMs often fails to predict the adsorption behaviour of trace metals onto mixed composition samples such as SPM (Bibby and Webster-Brown, 2006; Groenenberg and Lofts, 2014). For the glacial SPM, Cu and Cd may directly adsorb onto reactive groups on the surface on the clay sized particles (Sposito et al., 1999). Recent progress has been made in modelling the adsorption of dissolved ions onto clay minerals such as illite (Lackovic et al., 2003), montmorillonite (Gu et al., 2010) and kaolinite (Gu and Evans, 2008). It possible that their inclusion would optimize the model. However, this is beyond the scope of this study.

Down catchment, the SCMs were found to more accurately predict both the adsorption character and capacity of the SPM. Much of the adsorption capacity was attributed to the organic content of the SPM. However, these results were generated with the assumption that the reactive organic matter was a small proportion (2 – 5%) of the TOC content. In reality, the determination of the reactive organic component of the SPM presents a major challenge. The composition of organic matter is complex and is both difficult and time consuming to quantify. Additionally, the composition of organic matter, and its associated adsorption properties, will vary both spatially and temporally in aquatic systems (Tipping, 2002).

The inclusion of organic matter with the SHM SCM did not assist in the modelling of Cd and Cu adsorption onto glacial SPM. However, for the organic rich SPM in the lower catchment, the addition of the SHM SCM resulted in predictions of both the adsorption behaviour and capacity that were much more reflective of the experimental data. This indicates that the inclusion of an organic SCM should be an important consideration in the modelling of trace metals onto SPM where appreciable concentrations of organic matter is present. Specific analysis of the reactive fraction of the SPM TOC content would assist in optimising these the models in future studies, providing important insights that will enhance the modelling of Cd and Cu onto SPM in years to come.

4.5 Conclusion

The adsorption capability of SPM collected throughout the glacier-fed Waitaki Catchment was determined for Cd and Cu in this research. The fresh glacial SPM collected from the upper catchment was found to have a greater adsorption capacity for Cd relative to the organic-rich SPM in the lower catchment. This was attributed to the greater proportion of fine inorganic particles associated with the fresh glacial SPM which had greater concentrations of reactive Fe-oxides. However, the affinity of Cd for all SPM samples was low, which will limit its adsorption throughout the catchment. The opposite trend was detected for Cu. Copper was found to have a relatively high affinity for the SPM. The organic-rich SPM collected in the lower catchment also had the greatest adsorption capacity. This was attributed to the dominant influence of organic matter in the adsorption of Cu. For both contaminants, the ‘adsorption potential’ was greatest in the turbid meltwaters of the upper catchment, where significantly greater concentrations of SPM are detected. It was predicted that Cu will be readily attenuated by SPM throughout the catchment. However, the SPM may not play an appreciable role in the attenuation of Cd in the Waitaki catchment waters.

Surface complexation modelling was not found to accurately predict the adsorption of Cd and Cu onto the fresh glacial SPM. It is likely that additional adsorbing surfaces, including crystalline Fe oxides and the reactive surfaces of clay minerals, enhance the adsorption capability of the glacial SPM. Additional research will be required to elucidate these mechanisms, which could assist in the optimisation of the future models that consider contaminant adsorption onto glacial SPM. The novel inclusion of the Stockholm Humic (SHM) did, however, optimise the modelling of Cd and Cu adsorption onto the organic-rich SPM collected in the lower Waitaki catchment. This technique could

be used to optimise adsorption models in catchments where organic matter is an important component of the SPM.

4.6 References

Benjamin MM, Leckie JO. Multiple-site adsorption of Cd, Cu, Zn, and Pb on amorphous iron oxyhydroxide. Journal of Colloid and Interface Science 1981; 79: 209-221.

Bibby RL, Webster-Brown JG. Trace metal adsorption onto urban stream suspended particulate matter (Auckland region, New Zealand). Applied Geochemistry 2006; 21: 1135-1151.

Boggs Jr S, Livermore D, Seitz M. Humic substances in natural waters and their complexation with trace metals and radionuclides: a review. Argonne National Lab., 1985.

Clarke G. Upper Waitaki limit setting process. Predicting consequences of future scenarios: Lake water quality. Environment Canterbury, 2015.

Davies-Colley RJ, Nelson PO, Williamson KJ. Copper and cadmium uptake by estuarine sedimentary phases. Environmental Science & Technology 1984; 18: 491-499.

Davis JA. Adsorption of natural dissolved organic matter at the oxide/water interface. Geochimica et Cosmochimica Acta 1982; 46: 2381-2393.

Davis JA. Complexation of trace metals by adsorbed natural organic matter. Geochimica et Cosmochimica Acta 1984; 48: 679-691.

Duddridge JE, Wainwright M. Heavy metals in river sediments—calculation of metal adsorption maxima using Langmuir and Freundlich isotherms. Environmental Pollution Series B, Chemical and Physical 1981; 2: 387-397.

Dzombak DA, Morel Fo. Surface complexation modeling: hydrous ferric oxide. New York: Wiley, 1990.

Flemming CA, Trevors JT. Copper toxicity and chemistry in the environment: a review. Water, Air, and Soil Pollution 1989; 44: 143-158.

Fu G, Allen HE. Cadmium adsorption by oxic sediment. Water Research 1992; 26: 225-233.

Groenenberg JE, Lofts S. The use of assemblage models to describe trace element partitioning, speciation, and fate: A review. Environmental Toxicology and Chemistry 2014; 33: 2181-2196.

Gu X, Evans LJ. Surface complexation modelling of Cd(II), Cu(II), Ni(II), Pb(II) and Zn(II) adsorption onto kaolinite. Geochimica et Cosmochimica Acta 2008; 72: 267-276.

Gustafsson JP. Modeling the Acid–Base Properties and Metal Complexation of Humic Substances with the Stockholm Humic Model. Journal of Colloid and Interface Science 2001; 244: 102-112.

Harrison FL, Bishop DJ. Review of the impact of copper released into freshwater environments, 1983, pp. Medium: X; Size: Pages: 94.

Hua X, Dong D, Liu L, Gao M, Liang D. Comparison of trace metal adsorption onto different solid materials and their chemical components in a natural aquatic environment. Applied Geochemistry 2012; 27: 1005-1012.

Jain CK, Sharma MK. Adsorption of Cadmium on Bed Sediments of River Hindon: Adsorption Models and Kinetics. Water, Air, and Soil Pollution 2002; 137: 1-19.

Karamalidis AK, Dzombak DA. Surface Complexation Modeling: Gibbsite: John Wiley & Sons, Inc., 2010.

Lackovic K, Angove MJ, Wells JD, Johnson BB. Modeling the adsorption of Cd(II) onto Muloorina illite and related clay minerals. Journal of Colloid and Interface Science 2003; 257: 31-40.

Laxen DPH. Cadmium adsorption in freshwaters - a quantitative appraisal of the literature. Science of The Total Environment 1983; 30: 129-146.

Laxen DPH. Cadmium in freshwaters: concentrations and chemistry. Freshwater Biology 1984; 14: 587-595.

Lu Y, Allen HE. Partitioning of copper onto suspended particulate matter in river waters. Science of The Total Environment 2001; 277: 119-132.

Namieśnik J, Rabajczyk A. The speciation and physico-chemical forms of metals in surface waters and sediments. Chemical Speciation & Bioavailability 2010; 22: 1-24.

Shi B, Allen HE, Grassi MT, Ma H. Modeling copper partitioning in surface waters. Water Research 1998; 32: 3756-3764.

Sposito G, Skipper NT, Sutton R, Park S-h, Soper AK, Greathouse JA. Surface geochemistry of the clay minerals. Proceedings of the National Academy of Sciences 1999; 96: 3358-3364.

Taylor MD. Accumulation of cadmium derived from fertilisers in New Zealand soils. Science of The Total Environment 1997; 208: 123-126.

Tipping E. The adsorption of aquatic humic substances by iron oxides. Geochimica et Cosmochimica Acta 1981; 45: 191-199.

Tipping E. Cation Binding by Humic Substances. Cambridge: Cambridge University Press, 2002.

Webster-Brown JG, Dee TJ, Hegan AF. Metal removal via particulate material in a lowland river system. Water Science and Technology 2012; 66: 1439-1445.

Wright DA, Welbourn PM. Cadmium in the aquatic environment: a review of ecological, physiological, and toxicological effects on biota. Environmental Reviews 1994; 2: 187-214.

5. Character, Composition and Behaviour of SPM in the Onyx River Catchment, Antarctica

5.1 Introduction

The Onyx River catchment is located in the McMurdo Dry Valleys (MDVs), the largest ice-free area on the Antarctic continent and a true polar desert with some of the lowest rates of precipitation on Earth (Fountain et al., 2010). Despite the name, the valleys can transform into temporary oases during the warmest months of the austral summer. Melting glaciers feed ephemeral streams that flow for short periods, providing connectivity between the soils and sediments to the streams, lakes and ocean (Gooseff et al., 2011). The Onyx River is the largest meltwater stream in Antarctica, and its waters are typically extremely dilute (Brown, 2002; Stumpf et al., 2012). The meltwater does however carry SPM into the proglacial aquatic systems (Chinn and Mason, 2015), which may play a key role as a vector for trace elements and nutrients to the extreme, ice-marginal ecosystems which are "hotspots of life" in an otherwise barren landscape (Hodson et al., 2004; McKnight et al., 1999). The source of the SPM is distinct from alpine glacial catchments. Polar glaciers are typically frozen to the underlying bedrock and are generally assumed to be weakly erosive (Anderson, 2007). The subfreezing temperatures (−20 °C) of the lowermost ice does not allow for basal melting to occur, greatly limiting the speed of glacial flow and the associated production of fine grained glacial sediments (Hodson et al., 2004). It is therefore possible that the polar SPM has very different physicochemical characteristics to that in alpine catchments. Various studies have reported the characteristics of soils and sediments from the catchment, and it is commonly thought that the weathering of these materials is a key source of dissolved nutrients (Green et al., 2013; Green et al., 2005; Marra et al., 2017; Nezat et al., 2001; Prestrud Anderson et al., 1997). However, there has been little investigation of the role of the polar SPM in this regard.

The aim of this chapter was to determine the previously unknown physicochemical characteristics of SPM in the Onyx River catchment. The setting provides unique conditions under which glacial SPM can be studied. The streamflow is derived entirely from the melt of glaciers that flank the valley, and anthropogenic influence and contamination is minimal. Meltwater flows inland and is the sole source for the ultra-oligotrophic Lake Vanda, considered to be one of the least biologically productive and clearest lakes in the world (Canfield and Green, 1983). The

physicochemical characteristics of water and SPM samples collected throughout the Onyx River catchment during the 2016/17 K802 sampling campaign are first described. The weathering state and adsorption capacity of the SPM has been investigated and will be discussed in terms of its possible role in influencing the biogeochemical conditions of the proglacial aquatic environment

Figure 5.1. A waterfall flowing off the North-Western tip of the Lower Wright Glacier, McMurdo Dry Valleys Antarctica. This is a primary source of meltwater and SPM to the Onyx River.

5.2 Methodology

5.2.1 Catchment Description

The MDVs are glacial-carved landforms that were formed during the erosion of pre-existing river valleys on retreat of the East Antarctic ice-sheet 10 – 15 million years ago (Denton et al., 1984). It is the largest ice-free area in Antarctica, covering an area of approximately 4500 km^2 and has been referred to as an 'oasis' in a desert of ice (Chinn and Mason, 2015). The Onyx River catchment is located in the Wright Valley (**Figure 5.2**), located between the Taylor and Victoria Valleys. The neighbouring valleys are separated by the steep walls of the Asgard and Olympus mountain ranges, with multiple peaks reaching 2,500 masl. Precipitation is extremely low and always falls as snow,

with most sublimating before settling (Fountain et al., 2010). The eastern side of the valley is bordered by the Wright Lower and Wilson Piedmont Glaciers. These glaciers are the primary source of flow to the Onyx River (Chinn and Mason, 2015). During the warmer weeks of the austral season (December – February), the glacial surface is warmed by extended hours of solar radiation which results in glacial melt. Meltwater flows along the northern edge of the Wright Lower Glacier before it enters Lake Brownworth, an ice-capped lake situated at the western snout of the glacier (**Figure 5.2**). During the same period, water may overflow from the western outlet to form the ephemeral Onyx River, flowing west through permafrost gravels and boulder-fields (Chinn and Mason, 2015). The flow may be supplemented during warm weather from glaciers that flank the valley on both the northern and southern sides on the stream. However, the Clark, Meserve and Bartley Glaciers are the only glaciers observed to contribute appreciable flows (Chinn and Mason, 2015). The meltwater flows inland for approximately 29 km before it enters the 'Boulder Pavement', a 1.5 km stretch of the river that is characterized by large flat rocks rich in algae and cyanobacterial growth. The reduced velocity of flow and interaction with the local ecology acts to "strip" the meltwater of nutrients (Canfield and Green, 1983; Green et al., 2005). The meltwater continues to flow west to the Bull Lake, a large ponding area formed from a glacial depression which has yet to be filled with bedload alluvium from the Onyx River (Chinn and Mason, 2015). Meltwater continues to flow west before entering Lake Vanda, a highly stratified, closed-basin lake (Green et al., 1993; Green et al., 2005). The lake is approximately 8 km long and 1.5 km wide with a maximum depth of 69 m deep in the western depression. It is covered by a four meter-thick permanent ice layer which forms an open moat at the shoreline during the melt season. The water above 54 m is fresh. Below this water becomes progressively saline with increasing depth. The bottom waters are depleted in oxygen, strongly reducing and hypersaline, rich in Ca^{2+} and Cl^{-} and approximately four times saltier than average seawater (Green and Lyons, 2009). Solar energy penetrating the ice-cap is stored in stratified layers, producing a distinct thermocline in the lake with bottom water temperatures maintained at approximately 25^{0}C (Vincent and Laybourn-Parry, 2008).

The flow period of the Onyx River is intermittent and diurnal, typically lasting for 6-8 weeks (Chinn and Mason, 2015). During this period approximately 2.5 – 5.5 x 10^6 m^3 of meltwater enters Lake Vanda. This value can vary significantly from year to year. No flows were recorded during the 1977/78 and 93/94 field seasons, and the largest floods recorded to date occurred in the 1994/95 and 2001/02 seasons when discharge exceeded 20 x 10^6 m^3 of meltwater. The permafrost-patterned ground

typically results in no-gain or loss to groundwater, and there is no outflow from the lake. Therefore, the process of evaporation and ice sublimation acts to maintain the water balance (Chinn and Mason, 2015). However, the level of Lake Vanda abruptly began to rise in the early 1930s and levels have risen over 15 m since monitoring began in 1947 (Castendyk et al., 2016).

The basement geology of the MDVs includes schist, hornfels, and marble metasediments. Granite intrusions, and lamprophyre and granitic dykes are prominent crosscutting features. The basement rocks are overlain by Beacon sandstones and dolerite sills (Green et al., 1993; Maurice et al., 2002). The valley floors are typically covered with 'desert pavement' consisting of sedimentary, igneous and metamorphic rocks including granite, marble, gneiss, dolerite and sandstone. The soils and sediments in the Wright Valley are dominated by quaternary lacustrine and glacial drift deposits, and aeolian deposits. The aeolion processes are an important transport agent in the MDVs, distributing sediments, nutrients and organic matter onto the surfaces of glaciers and the hyporheic zones of meltwater streams. Soils in the valley are typically low in organic content but contain salts originating from the marine environment or derived from the weathering of rocks. Previous analysis of Onyx River SPM by X-ray diffraction determined that the majority of clay-size particles were quartz, feldspar and amorphous aluminosilicates. Specific components were identified as illite (64 – 67%), chlorite (25 – 30%), montmorillonite (5.9 – 6.6%) and minor quantities of kaolinite (Green et al., 1993). Webster-Brown and Webster (2007) investigated the trace metal content of cyanobacteria, phytoplankton and sediments in the Lake Vanda region, and identified fine quartz, feldspar, smectite, kaolinite and mica incorporated in the biological matrix of the cyanobacterial mats.

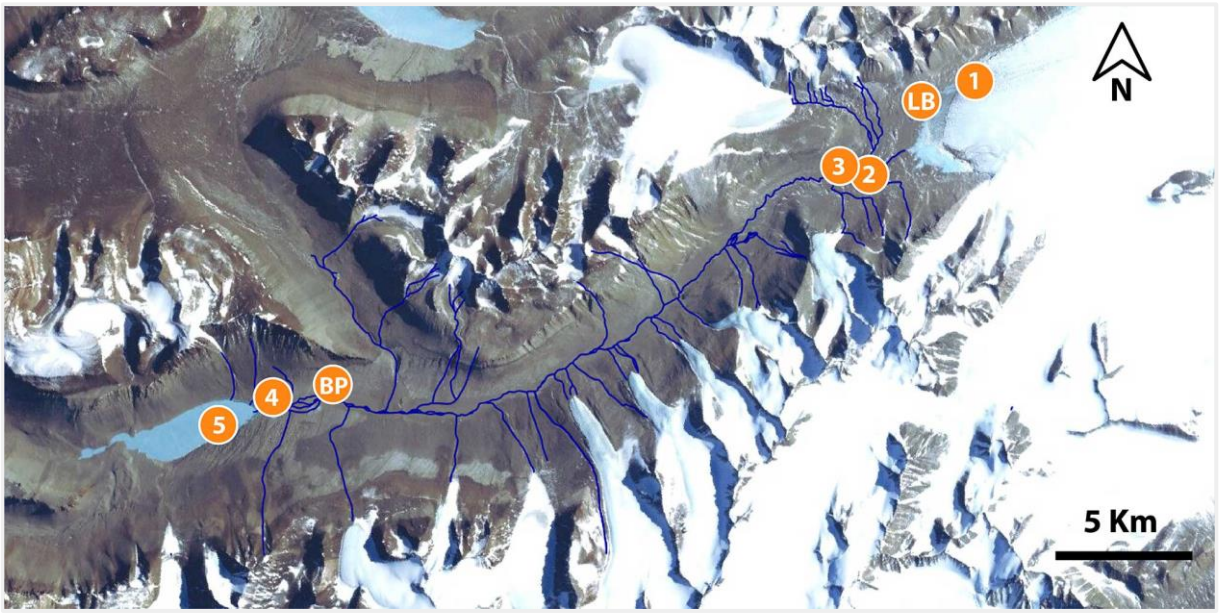

Figure 5.2. Sampling locations in the Onyx River Catchment, Wright Valley, Antarctica. Sample site 1 = Lower Wright – Glacial Stream; 2 = Onyx River at Lower Wright; 3 = Clarks Stream; 4 = Onyx River at Vanda Weir; 5 = Lake Vanda; LB = Lake Brownworth; BP = Boulder Pavement. Known areas of stream flow are marked by the blue lines. Map Credit: Phil Clunies-Ross

5.2.2 Sample Collection, Preparation and Analysis.

Sampling in the Wright Valley occurred between the 12th December, 2016 and the 2nd January, 2017. Water and glacial SPM were collected from the Onyx River and its tributaries when flow, weather and logistics allowed. A summary of collection data is compiled in **Table 5.1** below. Where possible, the water conductivity, dissolved oxygen, pH and temperature were measured in situ with a Hach HQ40d portable field meter. Raw and filtered water samples were collected into clean 50 ml polypropylene tubes for later analysis in New Zealand. Samples for major ions, trace elements, carbon (DIC, TC, TIC, TOC) and nutrients were collected and analysed as per the procedures described in **Chapter 2, Section 2.2.3**. Raw water was analysed for turbidity using an Orion AQ4500 turbidimeter. Larger quantities of SPM were collected by filtering water through a 47mm diameter 0.45 µm nitrocellulose filter membranes using a Nalgene© 300 ml polysulfone graduated filter holder and a hand-operated PVC vacuum pump. Particles <0.45 µm were isolated on the membrane once an initial layer of sediment had formed during the process. SPM was collected for SEM analysis by filtering water through 0.22 µm Nucleopore membrane filters, which were air dried in clean petri dishes and stored for later analysis. A time integrated mass flux sampler (TIMs) was also used to collect bulk quantities of SPM for XRD analysis from the Clarks Stream and the Lower Onyx River. Diffuse

Gradients in Thin Film (DGT) probes were deployed in the upper and lower Onyx to measure the time integrated concentrations of DGT-labile trace elements and phosphorus. Additional details of the TIMs and DGT deployments are provided in **Appendix A.**

All samples were kept chilled at < 4^0C throughout the duration of their return to a containment laboratory (PC1 – Ministry for Primary Industries) at Lincoln University, New Zealand. Particulate matter was liberated from the 0.47 µm membranes into ultrapure water by sonication before being freeze-dried. The suite of analytical procedures detailed in **Chapters 2-3** were used to determine the character and composition of the water and SPM samples. A summary is presented in **Table 5.1.** The PSD digestions (H_2O_2, NaOH) were only completed with SPM from the Clarks Stream and the Onyx River – Vanda Weir where sufficient quantities were available.

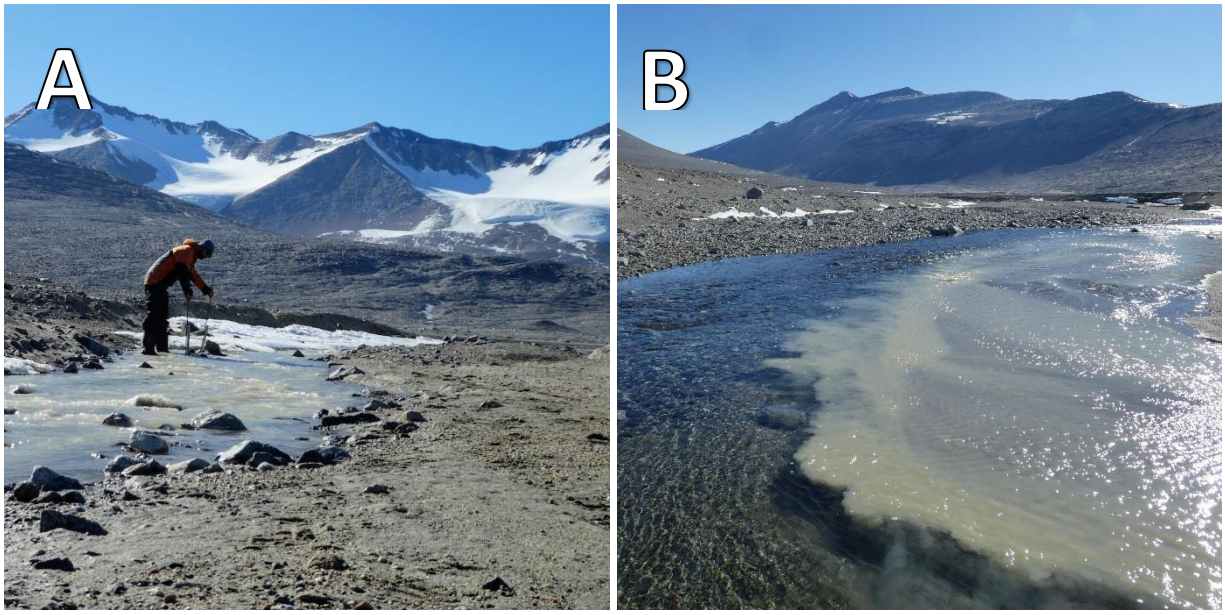

Figure 5.3. A) Sampling Clarks Stream, a small tributary of meltwater from the Clarks Glacier B) The Clarks Stream is the major source of glacial SPM to the Onyx River. This is highlighted by the confluence just west of the Lower Wright Hut. Image Credits: Phil Clunies-Ross

Table 5.1. Summary of analytical procedures used to characterize water and SPM samples in the Onyx River catchment.

Analysis:	Procedure/s:
Water Analysis	
TSS	▪ Concentration determined by filtration of accurately determined quantity of water onto nitrocellulose filter membranes.
DRP + TP	▪ Ascorbic acid method + persulfate digestion
TC/TIC/TC	▪ Combustion and detection by Shimadzu TOC-L.
DIC	▪ IRGA
Major Ions	▪ Major anions by HPIC/. Major Cations by ICP-MS
Trace Elements	▪ ICP-MS
DGT (Metals + P)	▪ Diffuse layers in thin films (DGT). Trace metals (Chelex) and P (HFO) probes.
SPM Analysis	
Particle Size Distribution (PSD)	▪ Laser diffraction with a Horiba LA-950 V2. Samples were analysed: o Untreated o Chemically dispersed with Sodium Hexametaphosphate o Pre-digested with H_2O_2 to remove organic matter o Pre-digested with H_2O_2 and NaOH to remove remaining biogenic particles
Morphology and Mineralogy	▪ Bulk mineralogy with XRD ▪ The mineralogy and morphology was determined with SEM/EDS analysis
Acid-soluble composition	▪ Digestion in hot analytical grade 1+1 HNO_3/HCl before ICP-MS analysis
Organic Carbon Content	▪ Combustion and IR detection
Specific Surface Area (SSA), Cation Exchange Capacity (CEC), Adsorption Potential	▪ Methylene Blue (MB) technique
Weathering Profiles	▪ CIA and WIP
Isoelectric Point (IEP)/Point of Zero Charge (PZC)	▪ The isoelectric point was determined with a ZetaSizer Nano ZS ▪ The immersion technique was used to determine the PZC by pH drift
Statistical Analysis	▪ Performed with XLStat version 19.1

5.3 Results

5.3.1 Water chemistry trends down catchment

A summary of the physical and chemical measurements obtained for the meltwater samples is presented in **Tables 5.2 – 5.4.** All samples were well aerated (no deep lake samples were collected) with no significant variations in pH. The lowest temperatures (2-3^{0}C) were measured in the melt from the L.W Glacier Stream. This water was found to be extremely dilute (conductivity < 30 µS/cm), and typically had a low turbidity. The highest turbidity and SPM concentrations of 7.9 NTU and 11.2 mg/l SPM were associated with high flows on a warm sampling day (12th December). Little variation was detected at the downstream sites, with conductivity, turbidity and SPM concentrations remaining low throughout the sampling periods. Samples collected from Clarks Stream (CS) were found to have a comparably high conductivity (<100 µS/cm), with greater turbidity's and SPM concentrations (**Figure 5.3).**

Table 5.2. Water quality parameters for study sites. Unless a single value is given, a range of 3 sample measurements collected in situ are provided. *Note – SPM concentrations (mg/l) were determined from a single sample due to logistical constraints.

Site	Location (Code)	pH	Temp (°C)	Conductivity (µS/cm)	DO (mg/L)	Turbidity (NTU)	SPM* (mg/L)
1	Lower Wright Glacier Stream (LWGS)	7.3 – 7.4	2.2 – 3.4	14.1 – 25.2	12.2 -13.4	0.7 - 7.9	11.2
2	Upper Onyx R. – L.W Hut (OLW)	7.3 – 7.7	3.0 – 7.3	25.1 – 31.8	12.2 – 13.2	0.3 - 0.5	0.8
3	Clarks Stream (CS)	8.0 – 8.1	9.7 – 9.9	103.5 - 127.5	11.2 - 12.7	180.3 - 257.0	259.0
4	Lower Onyx R. - Vanda Weir (OVW)	7.7 – 7.8	3.3 – 5.3	39.0 – 49.2	12.8 – 13.1	2.0 - 3.5	6.2
5	L. Vanda - SE End (LV)	8.3	2.4	45.3	14.74	0.2	0.5

The concentrations of 'dissolved' major ions and nutrients in the catchment were generally low (**Table 5.3**). The most dilute waters collected from the Lower Wright glacial stream (LWGS). The Clarks Stream (CS) tributary was relatively enriched in major ions, with concentrations typically an order of magnitude higher than the other stream sites. Low concentrations of TOC were detected throughout the catchment but were found to progressively increase with greater distance from the glacial source.

Table 5.3. Typical nutrient and major anion chemistry (mg/L) for study sites. DRP was <DL at all sites.

Site	Na^+	K^+	Mg^{2+}	Ca^{2+}	Cl^-	SO_4^{2-}	NO_3^-	TP	DIC	TOC
1 LWGS	2.3	0.5	0.59	2.0	3.7	1.9	0.4	0.006	10	0.4
2 OLW	2.3	0.5	0.5	2.0	4.2	2.3	0.2	0.005	11	0.3
3 CS	18.7	3.4	1.95	9.5	17.2	8.5	2.6	0.075	45	0.4
4 OVW	4.4	1.2	1.07	4.3	6.2	3.9	0.2	0.005	17	0.6
5 LV	1.7	0.5	0.59	2.7	9.1	10.1	1.2	< DL	9	0.9

The associated concentrations of dissolved trace elements are presented in **Table 5.4**. Low concentrations were detected in samples collected from the Lower Wright glacier stream (LWGS), Onyx River (OLW and OVW) and Lake Vanda (LV). The concentrations detected in the Clarks Stream (CS) sample were typically 1-2 magnitudes of order greater. The increased concentrations of Al (446.5 µg/l), Fe (500.6 µg/l) and Mn (7.9 µg/l) are particularly noteworthy given their role in the formation of reactive SPM surfaces.

Table 5.4. Concentrations of dissolved Trace Metals (µg/l) measured at sample sites by ICP-MS.

Site	Al	Mn	Fe	Cu	Zn	As	Cd	Pb	U
1 LWGS	31.4	1.22	13.4	0.28	0.23	0.04	0.002	0.01	0.020
2 OLW	28.6	0.60	2.1	0.27	0.23	0.06	0.009	0.01	0.014
3 CS	446.5	7.91	500.6	1.36	1.99	0.14	0.013	0.17	0.253
4 OVW	30.5	0.87	24.2	0.23	0.48	0.05	0.008	0.01	0.018
5 LV	13.2	0.25	5.6	0.20	1.82	0.03	0.010	0.02	0.014

Table 5.5. DGT labile concentrations (µg/L) detected in the upper and lower Onyx River over 5 and 7 day deployment times respectively. DL = Detection Limit.

Site	Al	Fe	Mn	PO_4-P
2 OLW	4.2 - 4.5	2.6 - 2.8	1.1 - 1.2	< DL
4 OVW	10 - 11.7	0.3 - 0.4	0.8 - 0.9	< DL

5.3.2 SPM Particle size and Character

Distinct differences in the PSD profiles, SSAs and CECs of the SPM were determined throughout the catchment (**Table 5.5 and Figure 5.4**). The PSD profiles in the upper catchment all had a single mode and demonstrated that particles 1-100 µm in size were prominent in suspension. Particles 1 – 15 µm were found to dominate the volume size distribution, while the number size distributions indicated that particles < 4, 6, and 15 µm in size were the most numerous in the Clarks Stream (CS), Lower Wright glacier stream (LWGS) and the upper Onyx River (OLW) sites respectively. The particle size distributions from the lower Onyx River (OVW) and Lake Vanda (LV) had a distinctly bimodal character, while the number distributions indicated that particles < 0.4 µm in size were the most numerous. The lowest specific surface areas (SSA) of 879 and 999 m^2/g were measured for the Lower Wright glacier stream (LWGS) and upper Onyx River (OLW) SPM respectively. The SPM from the Clarks Stream (CS) and Lake Vanda (LV) were found to have comparable values of 1163 and 1014 m^2/g respectively. The greatest SSA of 1728 m^2/g was determined with SPM collected from the lower Onyx River (OVW). The same trend was observed for the associated CEC's.

Table 5.6. Particle size distributions (PSD's), specific surface areas (SSA's) and cation exchange capacities (CEC's) for SPM samples. The PSD's are presented as the size in which 10% (D10), 50% (D50) and 90% (D90) of particles pass for volume and number analysis. The SSAs and CECs were determined with the methylene blue (mb) technique. The SSA is reported in m^2/g SPM, and CEC in milliequivalents (meq) per 100 g SPM.

Site	Distance	Volume Particle Size (µm)			Number Particle Size (µm)			ζ (mv)	SSA	CEC
	(km)	D_{10}	D_{50}	D_{90}	D_{10}	D_{50}	D_{90}	mv	m^2/g	$m_{eq}/100g$
1 LWGS	0.5	3.57	7.28	15.33	1.66	2.93	6.02	-21.7	879	26.7
2 OLW	5.6	3.03	6.69	14.79	1.41	2.41	14.8	-22.4	999	35.4
3 CS	6.2	2.31	5.02	10.55	1.22	2.01	3.9	-21.9	1163	47.1
4 OVW	32.1	0.43	5.55	18.15	0.11	0.17	0.32	-24.2	1728	104.8
5 LV	33.8	4.09	8.61	15.85	0.16	0.22	0.36	-21.3	1014	35.9

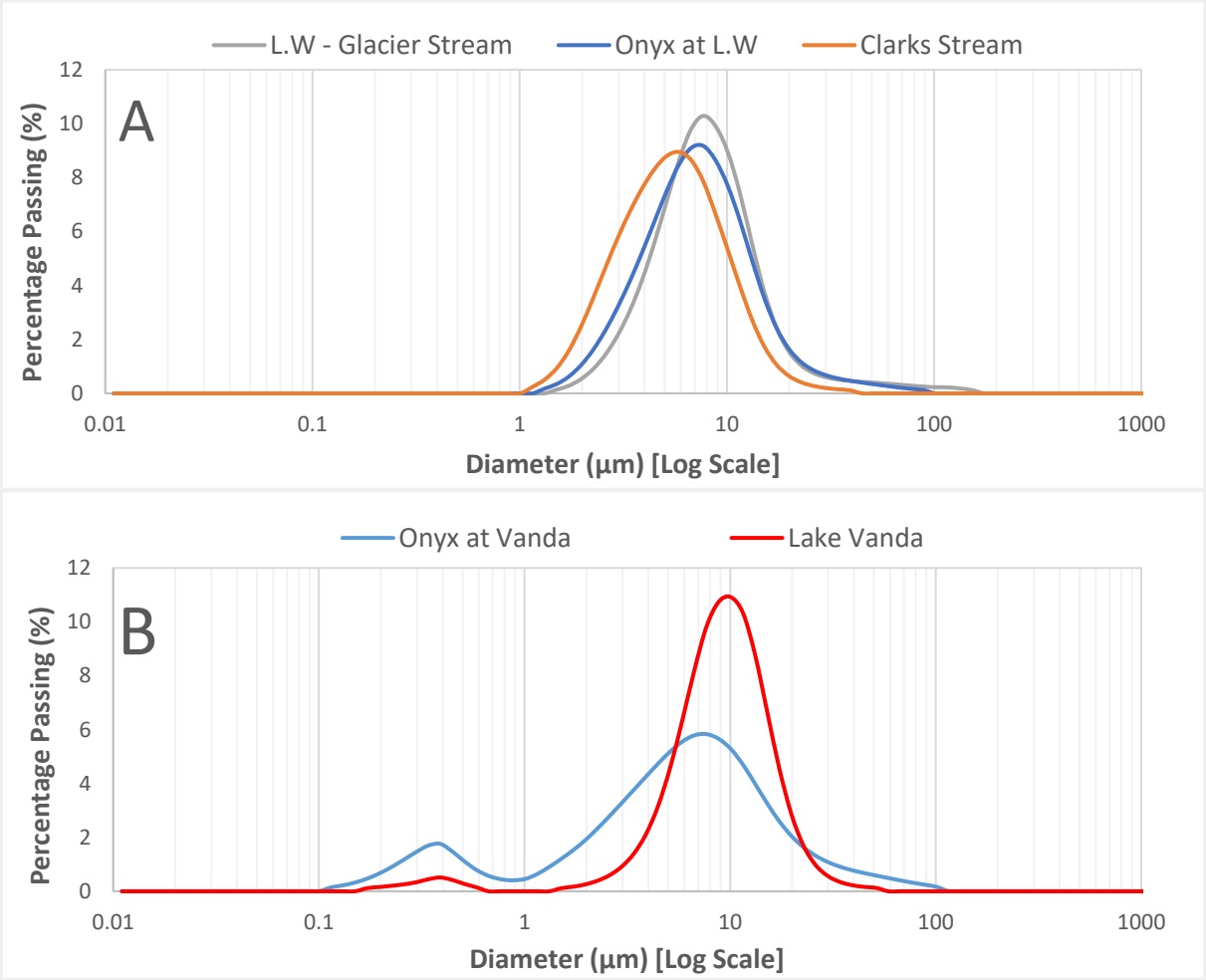

Figure 5.4. Particle size distributions of chemically dispersed SPM ($(NaPO_3)_6$) in the upper Onyx River catchment (a) and lower catchment (b).

The digestion procedures had a profound effect on the PSD D50s for SPM from Clarks Stream and the lower Onyx River (OVW) (**Table 5.7 and Figure 5.5**). The $D_{50's}$ for the Clarks stream SPM were reduced to 4.8 and 3.3 µm for the H_2O_2, and H_2O_2 and NaOH digestion respectively. The effect of the digestions was greater with respect to the Lower Onyx River (OVW) SPM, with the SPM $D_{50's}$ being reduced to 1.7 and 0.59 µm for the H_2O_2, and H_2O_2 and NaOH digestion, respectively.

Table 5.7. PSD Median volumes (D_{50}) for dispersed, and digested SPM collected throughout the Onyx River catchment.

Site	Dispersed	H_2O_2	H_2O_2 + NaOH
3. Clarks Stream	5.02	4.82	3.28
4. Onyx R. – Vanda Weir	5.55	1.7	0.59

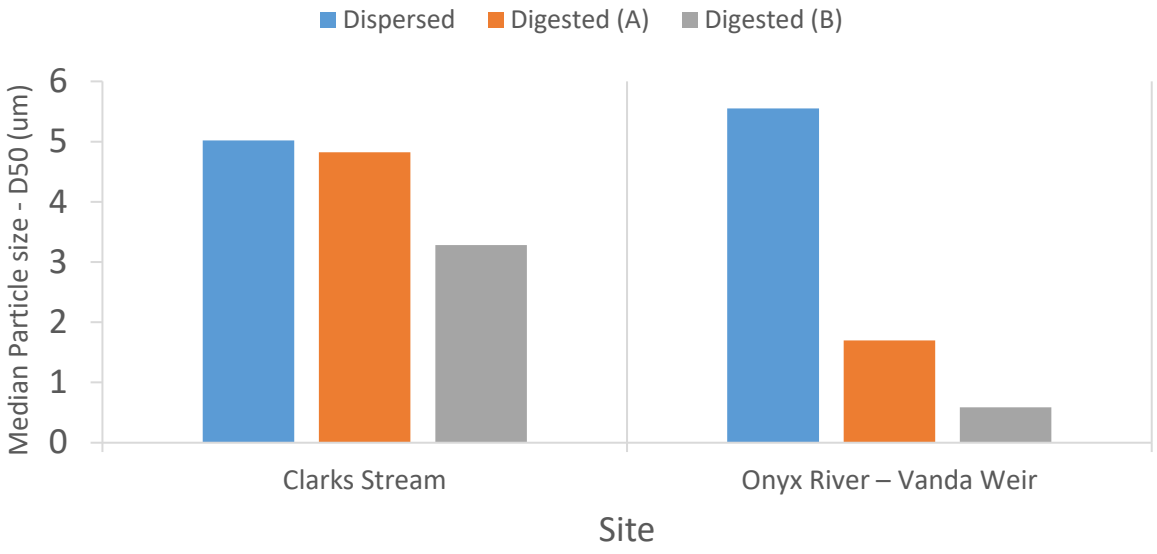

Figure 5.5. Plot of the PSD median volume's (D50) for chemically dispersed ($(NaPO_3)_6$), H_2O_2 treated (A), and NaOH treated (B) SPM collected from Clarks Stream and the Onyx River.

5.3.3 SPM Morphology

SEM imaging corroborates the PSD data, demonstrating that the majority of the SPM constituted single mineral particles. In the upper catchment, the particles were typically 1 – 10 µm in size, with the SPM collected in close proximity to the glacial source (LWGS and CS) a homogenous mix of both angular and rounded particles. Particles isolated from the remaining sites had a greater degree of rounding and smoothness by comparison. The greatest proportion of SPM from the lower Onyx (OVW) and Lake Vanda were < 1 µm in size (**Figures 5.6 -5.8**). Diatoms of various morphology as well as detrital organic matter were common, with the greatest numbers of diatoms identified in the Clarks Stream and Lake Vanda SPM. Atypical spherical particles observed in samples collected from Lake Brownworth were compositionally similar to quartz. Iron-oxide particles (**Figure 5.7 D**) were also detected at the Onyx River sites. Particle aggregates were detected infrequently.

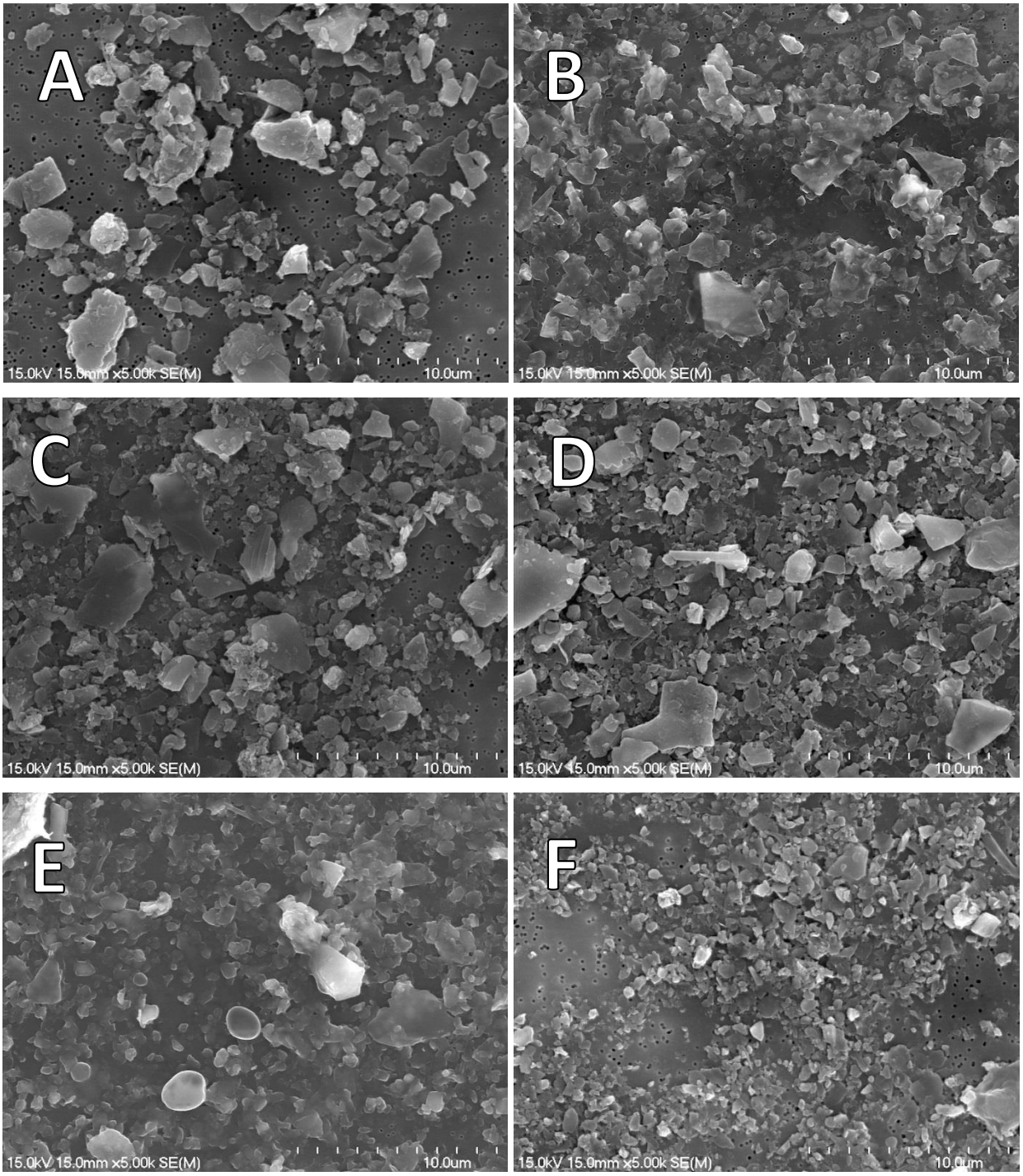

Figure 5.6. SEM images of SPM retrieved from sites progressing down the length of the Onyx River Catchment. 5000x magnification to allow size comparison (full scale bar is 10 μm): (A) SPM from the Lower Wright Glacial Stream; (B) upper Onyx River at Lower Wright Hut; (C) Clarks Stream; (D) Onyx River at Vanda Weir; (E) and (F) Lake Vanda.

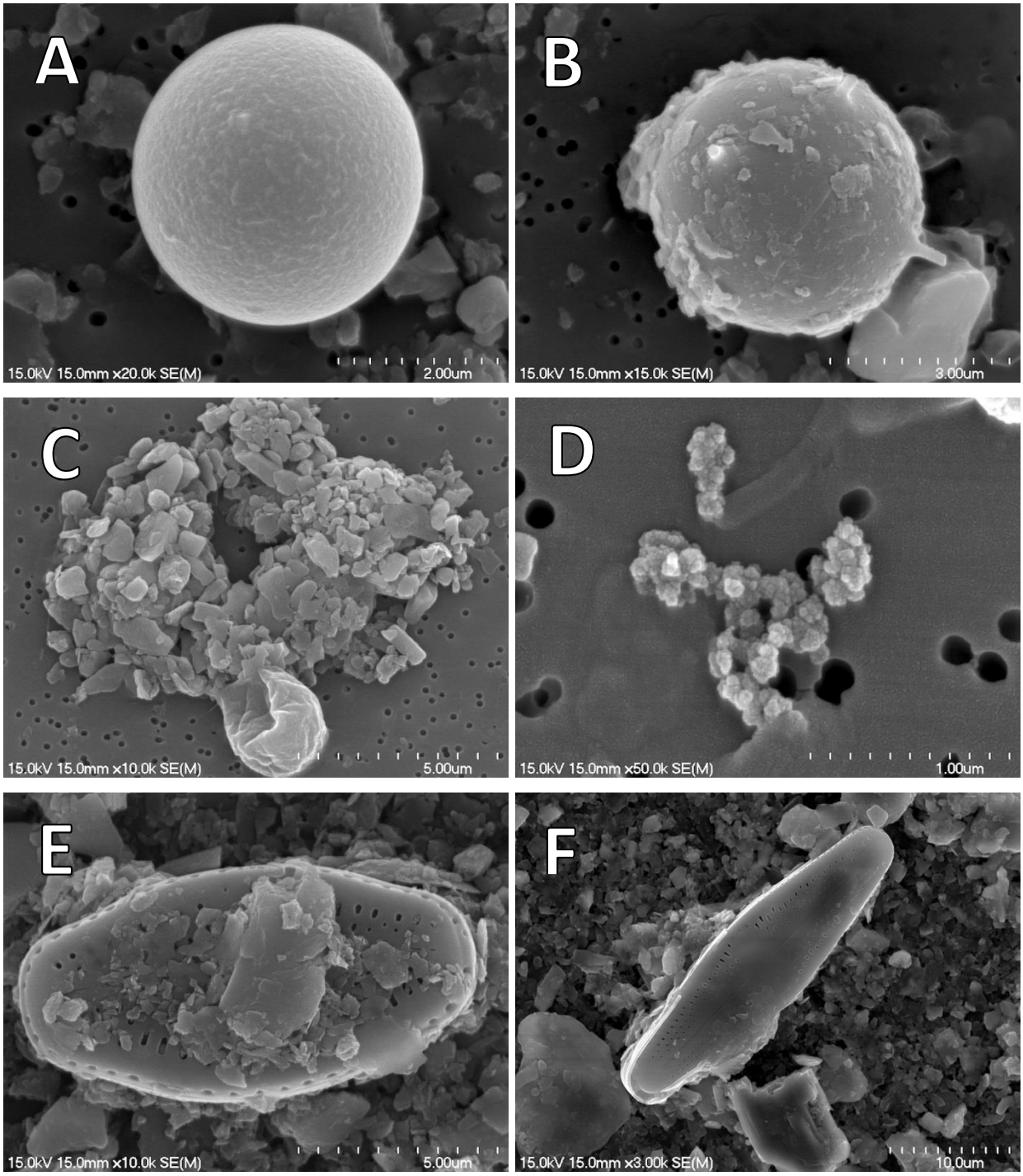

Figure 5.7. SEM images from of particles isolated from the Onyx River Catchment. (A) Spherical particle isolated from Lake Brownworth. Composition unknown (B) Spherical particle, also isolated from Lake Brownworth. Composition similar to quartz; (C) SPM aggregate of fine inorganic particles and organic detritus from the Onyx River at Wright Lower Hut. (D); extremely small particles of hydrous ferric oxide from the Onyx River at Lower Wright Hut. (E) and (F); Diatoms isolated in SPM from the Clarks Stream. Note the variation in scale. 3,000 – 50,000 X magnification. Full scale bar ranging from 1 – 10 µm.

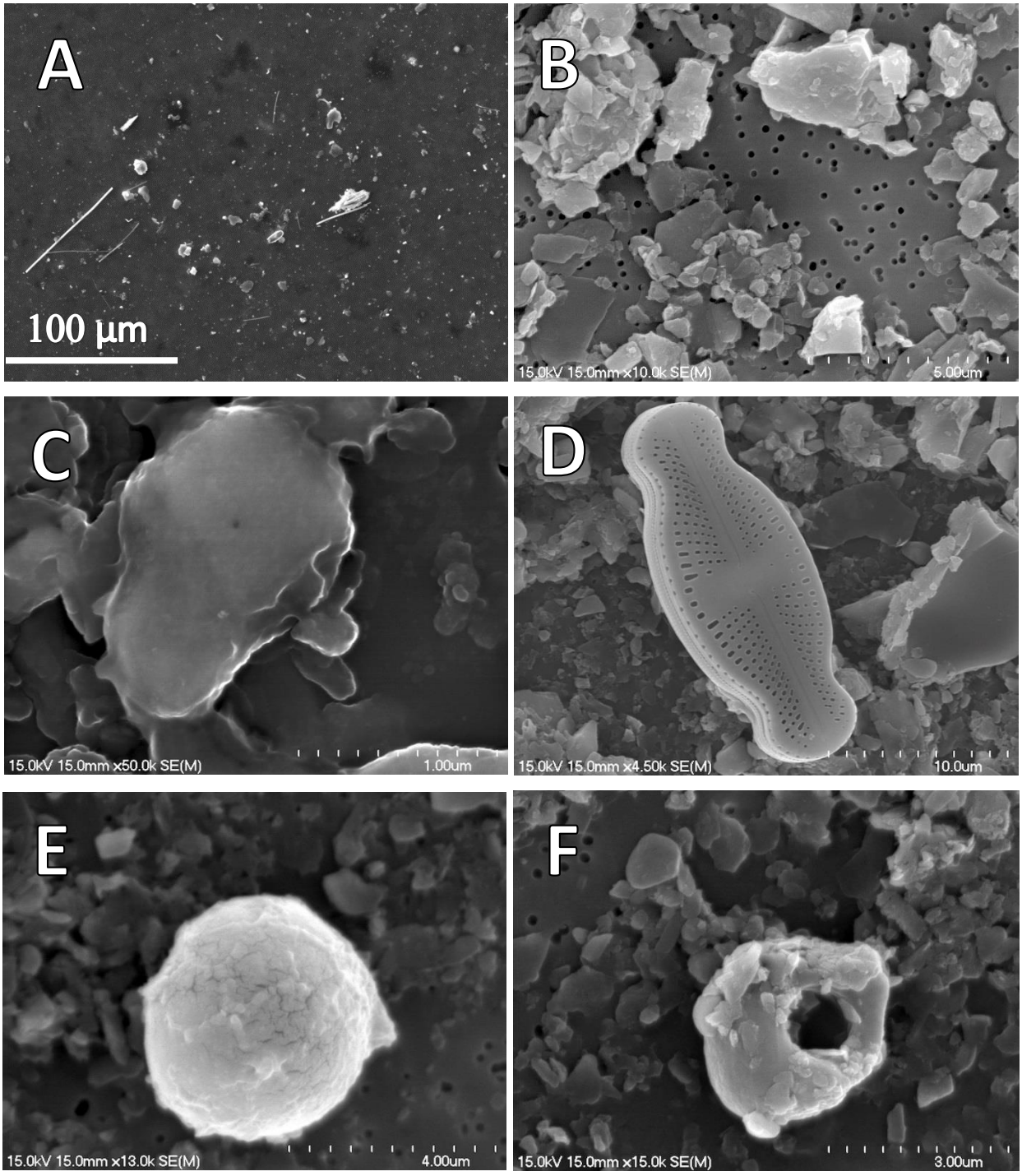

Figure 5.8. SEM images from of particles isolated in the Onyx River Catchment: (A) SPM rich in organic detritus from the upper Onyx River at L.W hut. (B) Rough textured particles from the Lower Wright Glacier Stream (C) Rounded illite particle from the Onyx River at Vanda Weir. (D) Diatom and inorganic particles from the Onyx River at Vanda Weir (E) and (F) Organic rich particles isolated in SPM from Lake Vanda. Note the variation in scale. 13,000 – 50,000 X magnification. Full scale bar ranging from 1 – 100 µm. Image A captured with JEOL JSM 6100 scanning electron microscope at the University of Canterbury.

5.3.4 SPM Composition

SPM mineralogy and composition is summarized in **Table 5.7** and referred to in **Figures 5.6 – 5.9.** The analysis of SPM throughout the catchment by XRD indicated mineralogy to be dominated by mica (illite), montmorillonite, chlorite, quartz and calcite. Diatoms and organic matter were common in the Clarks Stream and Onyx River samples. Pyroxene (diopside) was detected in the Clarks Stream and lower Onyx samples. Minor quantities of epidote, albite, apatite, biotite, titanite, orthoclase and iron-oxide were also detected with SEM/EDS throughout the catchment.

Table 5.8. SPM composition and mineralogy at sites throughout the Onyx River Catchment. Major phases (> 80% particles) identified with combination of XRD and SEM/EDS analysis. Minor phases were not identifiable in the XRD analysis. These were characterized with SEM/EDS mapping and targeted point analysis.

Site	Particles identified (in order of abundance)		Character*
	Major phases identified by XRD and SEM/EDS	**Minor phases observed by SEM/EDS**	
1. LWGS	Mica (illite), montmorillonite, quartz, chlorite	Epidote, albite, apatite	A
3. OLW	Mica (illite), montmorillonite, chlorite, quartz, organic matter	Epidote, albite, apatite, Fe-oxide, titanite, orthoclase	A, B, D
4. CS	Mica (illite), montmorillonite, chlorite, calcite, pyroxene (diopside), quartz, kaolinite, diatoms	Epidote, biotite, albite, orthoclase, organic matter	A, C, D
5. OVW	Mica (illite), montmorillonite, chlorite, calcite, pyroxene (diopside), Quartz, kaolinite, diatoms, organic matter	Epidote, albite, Fe-oxide, orthoclase	A, B, C, D
6. LV	Mica (illite), montmorillonite, chlorite, kaolinite, diatoms, quartz	Epidote, albite, titantite	A, C, D, E
Particle Character Classification System: A = Single Particles; B = Aggregates; C = Diatoms; D = Organic Detritus or Pollen; E = Filamentous algae &/or cyanobacteria			

In general, the proportions of the major inorganic elements did not differ considerably throughout the Onyx River catchment (**Table 5.8**). The exception was the SPM collected from the L.W Glacial Stream, which was found to have a greater proportion of Mg, Fe, Al and Si (weight %) compared to the other sites. The SPM from the Onyx River was found to have a greater organic content (3.4%) that the Clarks Stream sample (1.6%).

Table 5.9. Top: Elemental composition of SPM obtained by 400 x 400 µm scan showing: weight % from SEM/EDS analysis of SPM. TOC (% weight SPM) determined by combustion. Insufficient quantities of SPM were collected from sites 1, 2 and 5 for this analysis.

Site	Na	K	Mg	Ca	Fe	Al	Si	S	TOC (%)
1. LWGS	1.7	2.0	3.5	3.9	7.3	8.0	24.2	0.0	-
2. OLW	1.4	1.0	2.3	1.9	4.7	5.1	14.7	0.0	-
3. CS	1.6	1.8	2.9	2.4	6.6	6.6	18.6	0.1	1.6
4. OVW	1.3	1.4	2.5	1.9	5.6	5.9	15.5	0.0	3.4
5. LV	1.6	1.5	2.5	1.6	5.5	5.6	14.6	0.1	-

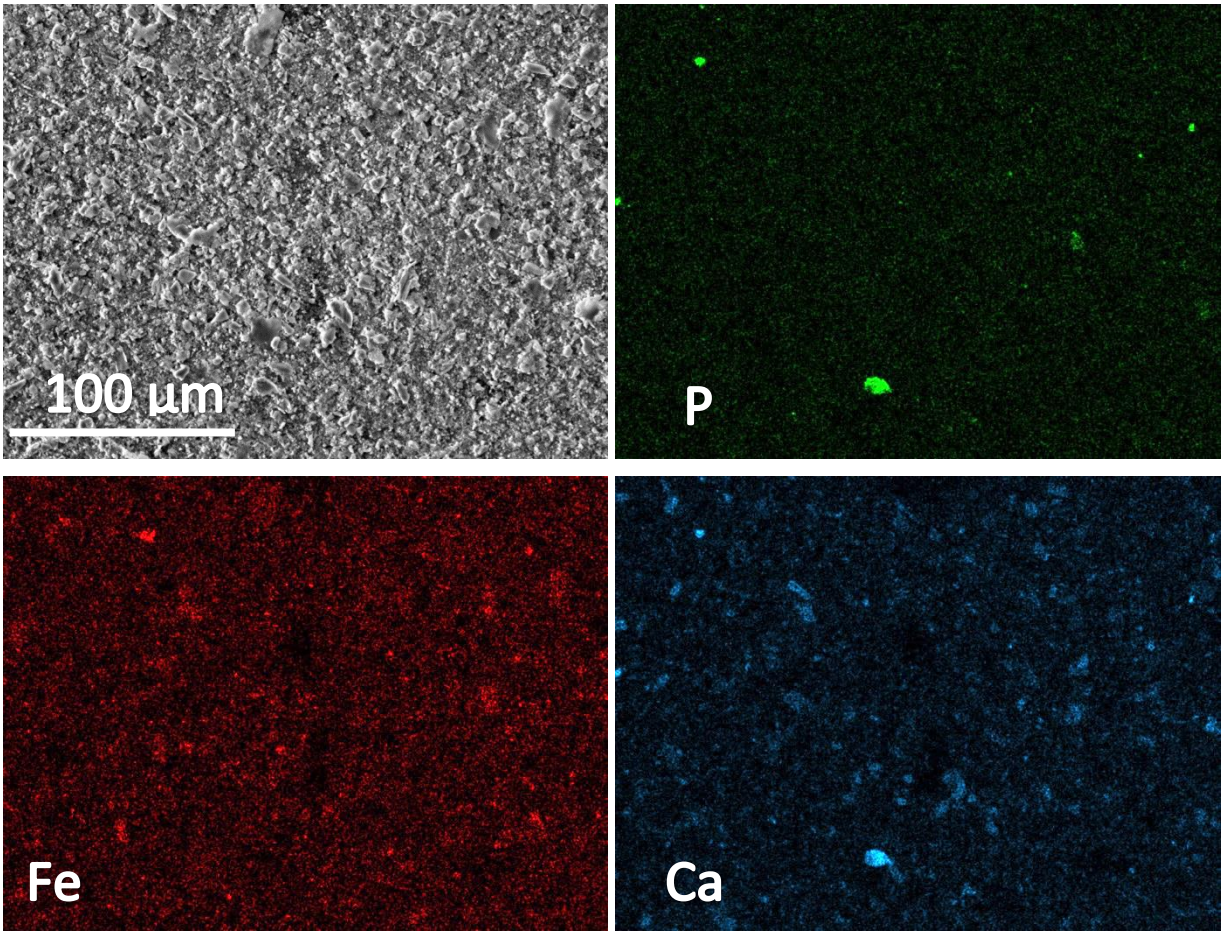

Figure 5.9. SEM/EDS mapping was used to characterise minerals in polar SPM; Minor phases were identified from "elemental hotspots" detected with SEM/EDS. The presence of apatite was identified from the area enriched in both P (green) and Ca (blue). The ubiquitous presence of Fe is shown in red.

The concentrations of metals and trace-elements measured in SPM samples after acid digestion are detailed in **Table 5.9**. Large differences in the acid-soluble concentrations of Al, Fe and Mn were

detected between samples collected in the upper and lower stream catchment. The SPM samples collected from the Lower Wright glacial stream and the upper Onyx River (OLW) had very similar compositions, with relatively low proportions of Al (1.9 – 2%), Fe (1.9 – 2.1) and Mn (297 – 390 mg/kg). However, the SPM from these sites had 20 – 40% greater TP concentrations relative to remainder of the catchment. The SPM from Clarks Stream and the lower Onyx (OVW) had a comparable composition, with greater overall concentrations of Al (2.9 – 3%), Fe (3.2 – 3.4) and Mn (478 – 500 mg/kg). The SPM sample from Lake Vanda was considerably different and was found to have lower concentrations (2-3x) of all elements analysed.

Table 5.10. Composition of SPM in mg/kg dry-weight after digestion in hot concentrated nitric acid. Concentrations of Mo, Cd and Sb were all extremely low or undetectable. Total phosphate measured in mg/kg after autoclave assisted persulphate digestion.

Site	Al (Wt %)	Fe (wt %)	Mn	Cr	Co	Ni	Cu	Zn	As	Pb	U	TP
1 LWGS	1.9	1.9	296.5	50.4	4.3	16	42.2	< DL	< DL	1.4	< DL	819
2 OLW	2	2.1	390.1	< DL	7.1	13.5	32.1	134	< DL	16.2	0.3	775
3 CS	2.9	3.2	499.9	22.2	13.7	25.4	51	161.6	1.5	8.2	1	644
4 OVW	3	3.4	477.9	4.1	12.7	27.8	63.3	172.5	1.2	8.7	1.5	578
5 LV	1	1.3	166.3	< DL	2.9	8.4	20.2	109	< DL	1.3	< DL	600

5.3.5 Weathering Indices

A comparison of the two different CIA and WIP weathering indices, as a function of distance down the catchment, is shown in **Figure 5.10**. There was a general increase in the CIA scores, indicating an increase in mineral weathering, with progressive distance from the glacial source. The SPM from the Clarks Stream tributary was found to have a higher CIA (62) than SPM from the upper Onyx River (61.3). The greatest CIA was determined in SPM from the lower Onyx River (65.4), while the Lake Vanda sample was offset from the trend seen in the Onyx (63.8). The results of the WIP were less coherent than the CIA, but again showed more weathered compositions down-catchment. The lowest WIP scores, indicating the greatest degree of weathering, was determined in the L.W glacial stream (49.7) and upper Onyx River (47.6). The WIP scores determined for Clarks Stream (52.3) and Lake Vanda (56.2) were greater than those in the Onyx River samples.

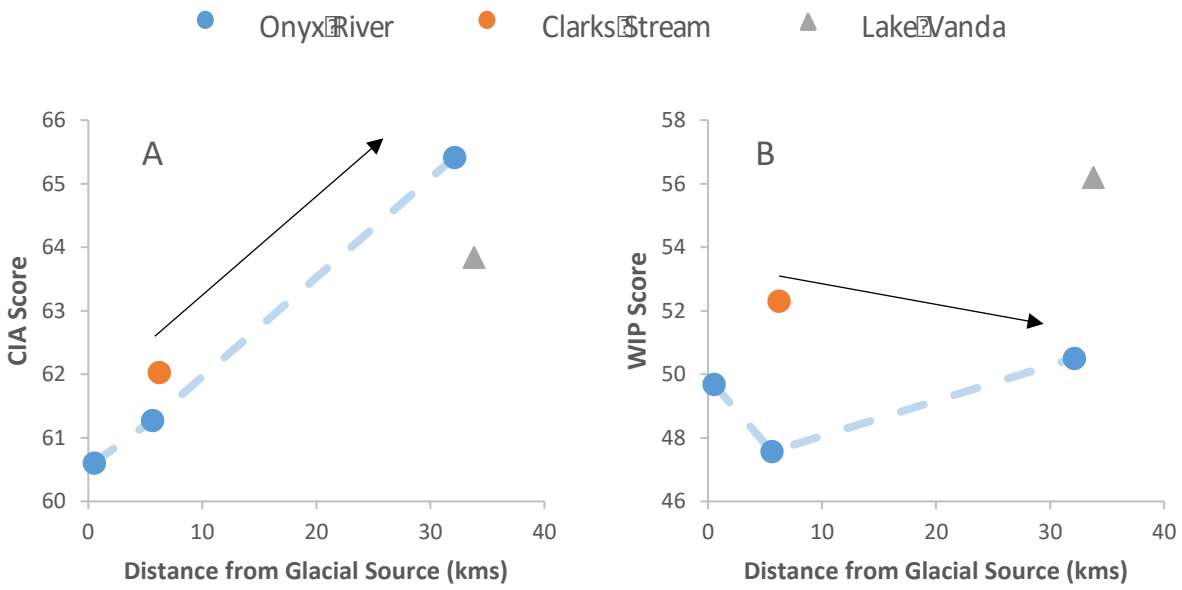

Figure 5.10. Chemical index of alteration (CIA) (A) and Weathering Index of Parker (WIP) (B) scores calculated for SPM collected with progressive distance from the glacial source in the Onyx River Catchment. An increase in weathering is indicated by an increased CIA value. The opposite is true for the WIP, as shown by the arrows.

5.3.6 PZC/IEP DATA

The isoelectric point (IEP) was determined from the pH value in which the zeta potential (ζ) was closest to 0 mv. The Onyx River SPM collected from the Vanda Weir was found to have an IEP of approximately pH 2. The greatest zeta potentials > -45 mV were measured at pH > 6-9 (**Figure 5.11 A**).

An additional point of zero charge (PZC) was determined at pH 6.8 with the immersion technique. This was the point at which the SPM solution was found to have the lowest Δ pH. The greatest pH change was detected with SPM solutions with initial pH values of 5 and 9, in which there was a change of up to ± 1.5 pH units (**Figure 5.11 B**).

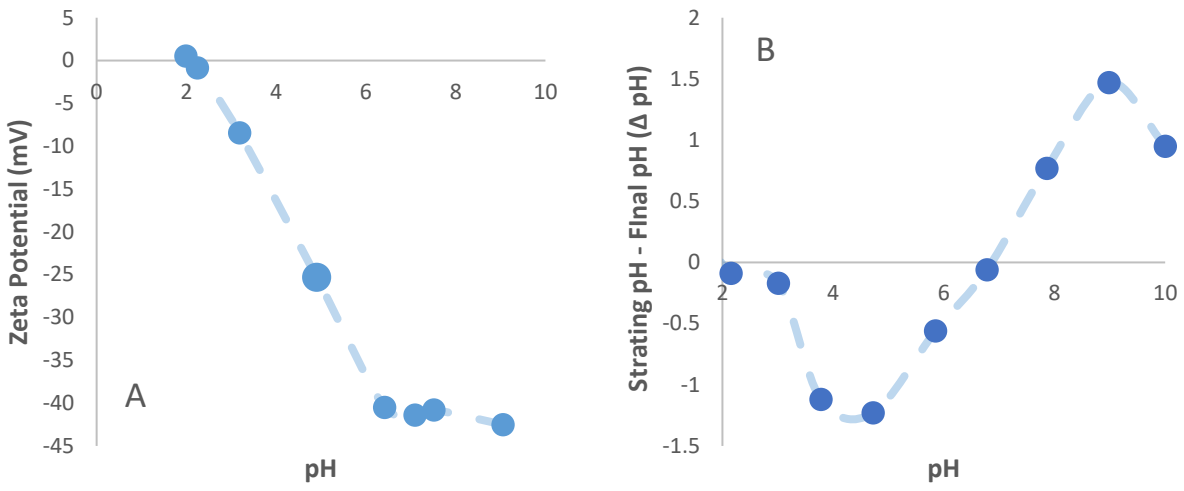

Figure 5.11. (Left) The isoelectic point as determined by zeta potential. (Right) An additional point of zero charge (PZC) was detected at pH 6.8.

5.3.7 Correlation Analysis

Notable correlations between SPM variables were identified using the Pearson correlation coefficient (**Table 5.10)**. These included an increase in TC content with increasing particle size and an increasing SSA with progressive distance from the glacial source. Notable inverse correlations included decreasing TP with increasing distance from the glacial source, and decreases in the acid-soluble concentrations of Al, Fe and Mn with increasing particle size.

Table 5.11. Pearson correlation analysis of the physicochemical characteristics associated with the Onyx River SPM. Strong correlations and inverse correlations are dark green and red respectively.

	km	mg/L	µm	m^2/g	wt %	mg/kg			
Variables	**Distance**	**SPM**	**PSD D50**	**SSA**	**TC**	**Al**	**Fe**	**Mn**	**TP**
Distance	**1.00**								
SPM	-0.35	**1.00**							
PSD D50	0.25	-0.64	**1.00**						
SSA	0.74	-0.49	-0.14	**1.00**					
TC	0.33	-0.54	0.70	0.11	**1.00**				
Al	-0.14	0.54	**-0.98**	0.28	-0.75	**1.00**			
Fe	-0.03	0.53	**-0.97**	0.35	-0.71	**0.99**	**1.00**		
Mn	-0.25	0.55	**-0.99**	0.21	-0.63	**0.97**	**0.96**	**1.00**	
TP	-0.85	-0.19	0.17	-0.57	-0.01	-0.23	-0.34	-0.13	**1.00**

Values in bold are different from 0 with a significance level alpha=0.05

Figure 5.12. Lake Vanda on a beautifully calm morning. The Asgard Range and the Dais are reflected in the moat recently formed by warm temperatures and an influx of meltwater from the Onyx River.

5.4 Discussion

5.4.1 Changing Water Characteristics down Catchment?

The water in the Onyx River was extremely dilute with low concentrations of SPM during the sampling period. The bulk of the flow was sourced from supraglacial melt off the north-eastern snout of the Lower Wright Glacier. However, the significant decline in the SPM concentrations at the upper Onyx River (OLW) site indicated that the majority of the SPM from the Lower Wright glacier stream (LWGS) undergoes sedimentation in Lake Brownworth. The highly SPM-enriched meltwater from the Clarks Stream was the dominant source of SPM to the lower Onyx River (OVW) and Lake Vanda. Chinn and Mason (2015) previously identified that the Clarks Glacier meltwater passes through sand dunes in the streambed, formed during the cooler months by strong westerly winds. The channel becomes partially infilled during this period and, during glacial melt, the sediment is evacuated into the Onyx. The stream flows in a diurnal fashion, commonly in the range of < 10 – 300 L/s (Chinn and Mason, 2015). However, the small contribution to the main Onyx flow may enhance the concentrations of major ions and nutrients for the remainder of the catchment. The weathering of the SPM and surface sediments is also likely to influence the higher concentrations of major ions detected

in the Lower Onyx River (OVW). No significant differences in the concentrations of trace elements were detected. Green et al. (2005) reported comparable results for the Onyx River catchment. They hypothesized that the adsorption of trace metals onto the surfaces of the SPM mediates their dissolved concentrations. The data presented in this study supports this theory. The concentrations of nutrients in the lower Onyx River (OVW) were extremely low, indicative of uptake by aquatic biota in the Boulder Pavement which again has been previously reported (Green et al., 2005; Howard-Williams et al., 1997). Water collected from Lake Vanda was extremely dilute. The water was collected from a drill hole in close proximity to the lake moat, where dilute water from the melting ice cap has likely influenced the results.

The DGT probes provided an additional and complimentary insight into the concentrations of dissolved elements present in the water column. No DGT-labile P was detected despite the lengthy time of deployment, and the concentrations of trace metals were typically lower than the filtered water samples. This data provided a strong indication that both P and trace metal concentrations are mediated by adsorption to SPM and complexation with organic matter. It also indicated that much of the "dissolved" concentrations of both P and trace metals are actually associated with colloidal particles that may pass through 0.45 um filter membranes (Horowitz et al., 1996). In any case, the DGT technique confirmed that the concentration of P is highly influenced by adsorption processes onto SPM. The implications of this finding will be discussed in **Chapter 6**.

5.4.2 Changing SPM Characteristics down Catchment?

No major differences in the bulk mineralogy of the SPM were detected along the length of the catchment. SPM was dominated by clay-sized mica, quartz, montmorillonite and chlorite particles. The mineralogical composition was comparable to surface sediments and soils in the catchment (Green et al., 1993; Marra et al., 2017) and suggests that the mineralogy is conserved amongst the different sized fractions (clay, silt, sand). The differences in the acid-soluble contents of the SPM, particularly between the samples sourced from the Lower Wright and Clarks streams, is likely due to the variability in the geological composition of the soils and sediments in the Wright Valley. The eastern flank of the valleys are blanketed in Ross Sea Drift, which has relatively high concentrations of P-rich basalts and kenytes (Bate et al., 2008; Heindel et al., 2017). This may have contributed to the greater TP content determined in the SPM sourced from the Lower Wright Glacier. It is however extremely difficult to conclusively identify the source of sediments to streams in the McMurdo Dry

Valleys. Aeolian deposition results in a high degree of spatial variability in the MDVs (Bate et al., 2008; Marra et al., 2017; Stumpf et al., 2012). The incorporation of wind-blown material into glaciers may also act as a temporary residence for the sedimentary material, where active weathering of the sediment may occur prior to evacuation by supraglacial stream flows.

Particles were typically found to have a high degree of rounding, which is suggestive of the aelion source of the suspended sediments. However, SPM from the fresh melt from the Lower Wright Glacier was found to have a greater proportion of angular, rough textured particles. This could indicate that a proportion of the particles are generated by glacial abrasion processes. Hambrey and Fitzsimons (2010) demonstrated that the Lower Wright Glacier does generate angular sediments by the re-working of bedrock, drift and aeolian deposits entrained into the glacial ice. However, sand was found to be dominant size fraction and clay sized particles were rare. The results from this study suggests that the polar glaciers of the Wright Valley may in fact generate clay-sized sediments which are evacuated during glacial melt.

The SPM collected from the Onyx River - Vanda Weir site was considerably finer than samples collected from upstream sites. It is likely that the larger particles associated with the SPM in the upper catchment drop out of suspension during the waters ~30km journey to Lake Vanda. The stream channel of the Onyx evolves from a single channel to a braided bed in fine alluvial gravels before reaching the expansive Boulder Garden (Chinn and Mason, 2015). Significant reductions in water velocities occur in these transitions and will promote sedimentation of the larger particles. Despite the dramatic change in particle size, SPM from the lower Onyx was found to have a nearly identical chemical composition to the courser material from Clarks Stream. This supports the hypothesis that the Clarks Stream was the primary source of SPM to Lake Vanda, and that the mineralogy of particles has remained consistent despite the opportunities for sorting and sedimentation to occur. SPM from the Lake Vanda sample was found to be composed of extremely fine, and highly rounded inorganic particles. The mineralogy of the particles was comparable to the stream sites. However, the SPM was found to be depleted in acid-soluble trace elements. The sample site was in close proximity to the melting ice cap, at a shallow depth, and some distance from the Onyx River mouth. It is therefore likely that the SPM is composed of particles from a number of sources (such as resuspended surface sediments and dust incorporated into the melting ice cap).

Organic detritus and diatoms were commonly detected in the SPM. Organic matter was particularly prevalent in upper Onyx River and Lake Vanda samples (**Figure 5.8**). Floating detritus sourced from benthic mats in Lake Brownworth and the Boulder Pavement may be the source of this material. Clarks Stream had the greatest quantities and variety of diatoms. The source of which may be from aeolian deposition into the stream bed (Stanish et al., 2013) or the evacuation of cryoconite holes on the Clarks Glacier. Diatoms were detected in the downstream Onyx River and will be flushed into Lake Vanda where they may proliferate in the water column. The significant reductions in the PSD D_{50} after the H_2O_2 and NaOH digestions indicated that the diatoms and organic detritus had a major influence on the PSD character. Particle aggregates were infrequently detected in the polar SPM, which may be due to the lack of cohesive substances (such as extracellular polymeric substances), and bacteria that are commonly associated with these particles (Droppo, 2001). A lack of aggregation may enhance the surface area of the particles for geochemical weathering and adsorption processes as well as enhancing their ability to remain in suspension in the streams and terminal Lake Vanda.

5.4.3 Does SPM progressively Weather Down Catchment?

Both weathering indices – the CIA and WIP used in this study indicated that active chemical weathering of the SPM does indeed occur during its short residence in the catchment. The CIA demonstrated a clear increase in SPM weathering with progressive distance down the catchment. In basic terms, the CIA is a measure of the conversion of feldspar to clays (Price and Velbel, 2003) and it is most likely that the dissolution of major ions (Ca, Na, K) from reactive components of the SPM (such as feldspar and pyroxene) has contributed to the result. Lyons et al. (2003) and Stumpf et al. (2012) have previously stated that sediments trapped in glacial bodies undergo progressive chemical weathering once released into proglacial streams of the MDVs. Green et al. (2005) also observed the concentrations of major ions to increase in a linear fashion between Lakes Brownworth and Vanda. This was associated with the chemical weathering of sediment and SPM.

The WIP provided an additional and complimentary view of both the SPM source and its degree of weathering. However, the weathering trend was intersected by the SPM source from the Clarks Stream tributary. This SPM was found to have a higher WIP score (and lower degree of chemical weathering) compared to SPM sourced from the Lower Wright Glacier upstream. The degree

of particle weathering through to the lower Onyx River was not clear with this index, indicating that the CIA may be more appropriate to use when multiple sediment sources are present.

5.4.4 Adsorption Potential of the Onyx Catchment SPM

The fine particle character and large SSAs and CECs associated with the SPM indicates that it may have a large capability to adsorb dissolved ions. SPM in the lower Onyx River is predicted to have the greatest adsorption potential, given the finer particle sizes and higher concentrations of acid-soluble Al, Fe and Mn associated with the SPM. The PZC of the SPM (~7) is indicative of an Fe-oxide playing a dominant role as an adsorbing surface (Dzombak and Morel, 1990; Kosmulski, 2014). The adsorption process is therefore predicted to be highly dependent on the biogeochemical conditions encountered (pH, redox, ionic strength) in the catchment. The adsorption and availability of phosphorus (P), a limiting nutrient in the catchment, is investigated in **Chapter 6**.

5.5 Conclusions

The character and composition of meltwater and SPM were described for samples collected throughout the Onyx River catchment during the 2016/17 K802 sampling campaign with Antarctica New Zealand. The major source of meltwater to the catchment was the Lower Wright glacier. This was found to be extremely dilute and had low concentrations of SPM, the majority of which is trapped by sedimentation in Lake Brownworth. The downstream Clarks stream was highly turbid and enriched in both dissolved ions and SPM. It was only a minor contributor of meltwater to the system, but was the dominant source of SPM to the lower catchment during the study period. The SPM throughout the catchment was typically dominated by fine, inorganic particles < 5 µm in size with minor contributions of organic detritus and diatoms. The inorganic particles typically had a high degree of roundness attributable to their aeolian source. However, a small proportion were highly angular and could suggest that the glaciers of the Wright Valley are capable of generating clay-sized particles. The finest particles remained in suspension throughout the meltwaters journey to Lake Vanda and were found to progressively weather down the catchment. The SPM is predicted to have a significant adsorption capability owing to its large SSAs, CECs and concentrations of reactive Fe, Al and Mn oxides. The SPM may play a key role in regulating the biogeochemical cycling and availability of nutrients in the catchment.

5.6 References

Anderson SP. Biogeochemistry of Glacial Landscape Systems. Annual Review of Earth and Planetary Sciences 2007; 35: 375-399.

Bate DB, Barrett JE, Poage MA, Virginia RA. Soil phosphorus cycling in an Antarctic polar desert. Geoderma 2008; 144: 21-31.

Brown GH. Glacier meltwater hydrochemistry. Applied Geochemistry 2002; 17: 855-883.

Canfield DE, Green WJ. Aspects of nutrient behavior in Lake Vanda. Antarctic Journal of the United States 1983; 18: p. 224-226.

Castendyk DN, Obryk MK, Leidman SZ, Gooseff M, Hawes I. Lake Vanda: A sentinel for climate change in the McMurdo Sound Region of Antarctica. Global and Planetary Change 2016; 144: 213-227.

Chinn T, Mason P. The first 25 years of the hydrology of the Onyx River, Wright Valley, Dry Valleys, Antarctica. Polar Record 2015; 52: 16-65.

Denton GH, Prentice ML, Kellogg DE, Kellogg TB. Late Tertiary history of the Antarctic ice sheet: Evidence from the Dry Valleys. Geology 1984; 12: 263-267.

Droppo IG. Rethinking what constitutes suspended sediment. Hydrological Processes 2001; 15: 1551-1564.

Dzombak DA, Morel FMM. Surface Complexation Modeling: Hydrous Ferric Oxide: Wiley, 1990.

Fountain AG, Nylen TH, Monaghan A, Basagic HJ, Bromwich D. Snow in the McMurdo Dry Valleys, Antarctica. International Journal of Climatology 2010; 30: 633-642.

Gooseff MN, McKnight DM, Doran P, Fountain AG, Lyons WB. Hydrological Connectivity of the Landscape of the McMurdo Dry Valleys, Antarctica. Geography Compass 2011; 5: 666-681.

Green WJ, Canfield DE, Shengsong Y, Chave KE, Ferdelman TG, Delanois G. Metal transport and release processes in Lake Vanda: The role of oxide phases. Physical and Biogeochemical Processes in Antarctic Lakes. 59. AGU, Washington, DC, 1993, pp. 145-163.

Green WJ, Canfield DE, Shengsong Y, Chave KE, Ferdelman TG, Delanois G. Metal Transport and Release Processes in Lake Vanda: The Role of Oxide Phases. Physical and Biogeochemical Processes in Antarctic Lakes. American Geophysical Union, 2013, pp. 145-163.

Green WJ, Lyons WB. The Saline Lakes of the McMurdo Dry Valleys, Antarctica. Aquatic Geochemistry 2009; 15: 321-348.

Green WJ, Stage BR, Preston A, Wagers S, Shacat J, Newell S. Geochemical processes in the Onyx River, Wright Valley, Antarctica: Major ions, nutrients, trace metals. Geochimica et Cosmochimica Acta 2005; 69: 839-850.

Hambrey MJ, Fitzsimons SJ. Development of sediment–landform associations at cold glacier margins, Dry Valleys, Antarctica. Sedimentology 2010; 57: 857-882.

Heindel RC, Spickard AM, Virginia RA. Landscape-scale soil phosphorus variability in the McMurdo Dry Valleys. Antarctic Science 2017; 29: 252-263.

Hodson A, Mumford P, Lister D. Suspended sediment and phosphorus in proglacial rivers: bioavailability and potential impacts upon the P status of ice-marginal receiving waters. Hydrological Processes 2004; 18: 2409-2422.

Horowitz AJ, Lum KR, Garbarino JR, Hall GEM, Lemieux C, Demas CR. The effect of membrane filtration on dissolved trace element concentrations. Water, Air, and Soil Pollution 1996; 90: 281-294.

Howard-Williams C, Hawes I, Schwarz A, A. Hall J. Sources and sinks of nutrients in a polar desert stream, the Onyx River, Antarctica. Ecosystem Processes in Antarctic Ice-free Landscapes. Balkema Press, Rotterdam, 1997.

Kosmulski M. The pH dependent surface charging and points of zero charge. VI. Update. Journal of Colloid and Interface Science 2014; 426: 209-212.

Lyons WB, Welch KA, Fountain AG, Dana GL, Vaughn BH, McKnight DM. Surface glaciochemistry of Taylor Valley, southern Victoria Land, Antarctica and its relationship to stream chemistry. Hydrological Processes 2003; 17: 115-130.

Marra KR, Elwood Madden ME, Soreghan GS, Hall BL. Chemical weathering trends in fine-grained ephemeral stream sediments of the McMurdo Dry Valleys, Antarctica. Geomorphology 2017; 281: 13-30.

Maurice PA, McKnight DM, Leff L, Fulghum JE, Gooseff M. Direct observations of aluminosilicate weathering in the hyporheic zone of an Antarctic Dry Valley stream. Geochimica et Cosmochimica Acta 2002; 66: 1335-1347.

McKnight DM, Niyogi DK, Alger AS, Bomblies A, Conovitz PA, Tate CM. Dry Valley Streams in Antarctica: Ecosystems Waiting for Water. BioScience 1999; 49: 985-995.

Nezat CA, Lyons WB, Welch KA. Chemical weathering in streams of a polar desert (Taylor Valley, Antarctica). GSA Bulletin 2001; 113: 1401-1408.

Prestrud Anderson S, Drever JI, Humphrey NF. Chemical weathering in glacial environments. Geology 1997; 25: 399-402.

Price JR, Velbel MA. Chemical weathering indices applied to weathering profiles developed on heterogeneous felsic metamorphic parent rocks. Chemical Geology 2003; 202: 397-416.

Stanish LF, Bagshaw EA, McKnight DM, Fountain AG, Tranter M. Environmental factors influencing diatom communities in Antarctic cryoconite holes. Environmental Research Letters 2013; 8.

Stumpf AR, Elwood Madden ME, Soreghan GS, Hall BL, Keiser LJ, Marra KR. Glacier meltwater stream chemistry in Wright and Taylor Valleys, Antarctica: Significant roles of drift, dust and biological processes in chemical weathering in a polar climate. Chemical Geology 2012; 322: 79-90.

Vincent WF, Laybourn-Parry J. Polar Lakes and Rivers : Limnology of Arctic and Antarctic Aquatic Ecosystems. Oxford University Press, Oxford, 2008.

Webster-Brown JG, Webster KS. Trace metals in cyanobacterial mats, phytoplankton and sediments of the Lake Vanda region, Antarctica. Antarctic Science 2007; 19: 311-319.

6. SPM and Phosphorus Transport in the Onyx River Catchment, Antarctica

6.1 Introduction

The Onyx River catchment supports a diverse range of biota conditioned to the extreme polar conditions. Cyanobacteria, heterotrophic bacteria and diatoms are the dominant primary producers. Many exist in cohesive, perennial mats and can build up a high biomass in the stream beds and benthic environments of Lakes Brownworth and Vanda. Fauna is limited to nematodes, rotifers and tardigrades (Fountain et al., 2014; McKnight et al., 1999). The biological activity is generally extremely low and is primarily driven by water and nutrient availability. Biota in the Onyx River must withstand flow intermittency and desiccation (McKnight et al., 1999), while productivity in the lakes is generally limited by low concentrations of phosphorus (P), nitrogen (N) and carbon (C). Lake Vanda sits at the terminus of the catchment and has been previously stated to be one of the most P-limited ecosystems on the planet (Barrett et al., 2007; Bate et al., 2008; Priscu, 1995).

Bedload sediments have not yet deposited in Lake Vanda (Chinn and Mason, 2015) and SPM has been previously identified to be an important source of P to the lake (Canfield and Green, 1983; Jones-Lee and Lee, 1993). However, the speciation and bioavailability of the SPM P has to date not been well characterized. The quantity of SPM discharged into the catchment is also unclear and has previously only been estimated under a limited range of flows (Chinn and Mason, 2015). Episodic warm weather events can result in the release of significant quantities of both meltwater and SPM from the glaciers that flank the catchment (**Figure 6.8**). However, no attempts have to date been made to estimate these loads and the possible effects they may have on the biological productivity of the system. Anthropogenic forced climate warming is predicted to increase the frequency, duration and volume of glacial melt in the catchment (Castendyk et al., 2016). This is expected to increase nutrient loading, lake levels, and primary production which may ultimately shift the biological structure and diversity of Antarctic aquatic systems (Fountain et al., 1999; Lyons et al., 2006).

The primary aim of this chapter was to determine the role of the Onyx River SPM as a vector for the nutrient P. In order to achieve this aim, it was first necessary to determine the forms of P associated with the SPM. Sequential extractions were undertaken to investigate the speciation and

bioavailability of the P. The adsorption capacity and behaviour of the SPM for P was then investigated with adsorption edge and isotherm experiments, which provided key insights into the phases influencing P adsorption. The quantities of SPM discharged into Lake Vanda over a 20-year period (1996/97 – 2016/17) were predicted with the generation of a SPM-discharge rating curve which was applied to flow data collected by the LTER. The calculated loads and their influence on the biological productivity of the lake will be discussed.

6.2 Methodology

6.2.1 Sample Collection, Preparation and Analysis.

Please refer to **Chapter 5** for a detailed account of the collection and preparation of the Onyx River SPM. It was not possible to collect enough SPM at every site for the experiments conducted in this study. Low concentrations of SPM were typically associated with the meltwater and there were difficulties associated with filtering large volumes of water in the polar field environment. Sufficient quantities for the purposes of this research were collected from Clarks Stream and the lower Onyx River at the Vanda Weir. The focus of this study has been made on the SPM collected from the lower Onyx River, which will ultimately be discharged into Lake Vanda. SPM from the Clarks Stream had a higher proportion of large particles and has been included to provide an insight into the variations that may exist in the different size fractions of the SPM.

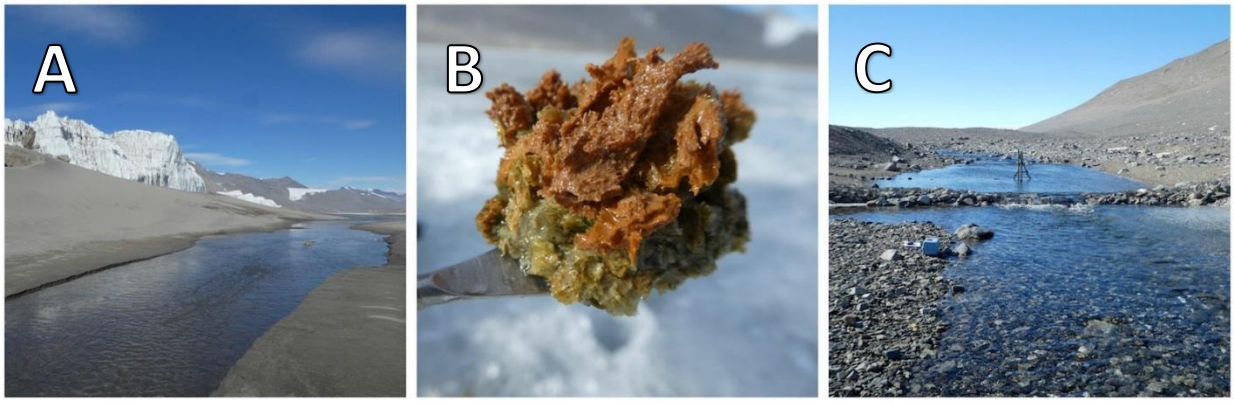

Figure 6.1. A) Melt from the Lower Wright Glacier starts its journey inland. B) A benthic mat from Lake Brownworth. C) The Lower Wright gauge site on the Onyx River, one of two weirs that have been installed on the Onyx River to monitor the flow, temperature and conductivity of the meltwater.

6.2.2 Phosphorus Speciation and Adsorption

A summary of the methods used in this research is provided in **Table 6.1.** A detailed description of the experimental procedures is provided in **Chapter 3, Sections 3.2.3 – 3.2.8**.

Table 6.1. Summary of methods used to determine the phosphorus (P) speciation and adsorption capacity of SPM from the Onyx River catchment. Geochemical modelling was used to assist in the interpretation of the experimental results.

Analysis:	Procedure/s:
Sequential Extractions	▪ Method by Rydin (2000) and Waters (2016) used to characterize P-forms in SPM. Phosphorus fractions liberated with the method include: • "Exchangeable P" – Loosely bound and soluble • "Redox reactive P" – Bound to reactive Fe and Mn oxy/hydroxides • "NaOH reactive P" – Bound to Al oxy/hydroxides, resilient Fe and Mn phases and clay minerals. • "Organic P" – Easily degradable organic P • "HCl-reactive P" - Associated with Ca-phosphates (i.e. apatite), carbonates and refractory oxy/hydroxides • "Residual P" – Associated with highly inert inorganic phases
Phosphorus Adsorption	▪ Adsorption isotherm experiments in the concentration range of 0 – 0.25 mg/l PO_4-P. SPM solution – 100 mg/L in 0.01 M $NaNO_3$ at pH 7. Fitted with Langmuir and Freudlich models to determine adsorption capacity ▪ Adsorption edge experiments with SPM from the Onyx River at Vanda Weir. SPM solution - 100 mg/L in 0.01 M $NaNO_3$. 0.1 mg/l PO_4-P added and pH adjusted in the range of 2-10.
Geochemical Modelling with Visual Minteq 3.1	▪ Used to predict phases implicated in P adsorption processes. ▪ A diffuse layer, surface complexation models (SCMs) was used to predict P adsorption on the SPM. The model assumed HFO to be the sole adsorbing surface. The model was calibrated with the concentration of Fe liberated from the SPM at pH 2 for 24 hours. Parameters applied in the models are detailed in **Appendix F.**

6.2.3 McMurdo LTER Data:

The flow, temperature and conductivity of the Onyx River is monitored as part of the National Science Foundation's Long-term Ecological Research (LTER) Program. Recordings are made at 15-minute intervals by static probes installed at the Lower Wright and Vanda Weirs (**Figure 6.8**). The recorded stage height is used to calculate discharge from an empirically generated rating curve. Calibrated data was generously provided by the LTER for the purposes of this research (J. Singley, personal communication).

6.2.4 SPM and Phosphorus Budgeting.

Rating curves are commonly used to calculate SPM loads when frequent sampling is not practical and/or possible. The curve is established by plotting the concentrations of SPM measured in water samples against their corresponding instantaneous flow measurement. The resulting plot is commonly fit to a power function relationship with regression analysis (Asselman, 2000; Walling, 1977). The model may then be used to predict SPM loading when flow data is available. In the Onyx River catchment continuous flow data from the LTER is readily available and reliable. However, SPM concentration data for a broad range of flows is scarce, primarily due to the practical limitations of working in the polar field environment (T. Chinn, personal communication). Low concentrations (< 10 mg/L) were detected in the Onyx River during the 2016/17 K802 field sampling campaign (**Chapter 5, Section 5.3.1**). This is common under normal, established flow conditions (Chinn and Mason, 2015; Webster-Brown and Webster, 2007). However, the concentrations may increase by several orders of magnitude during flood events (Chinn and Mason, 2015) (**Figure 6.9**) and contribute significant loads of SPM to Lake Vanda.

Despite the lack of comprehensive data, historical streamflow and SPM discharge records from previous sampling campaigns has been used, along with the quality controlled LTER flow data, to estimate the loads of SPM discharged into Lake Vanda over the 20 year period of 1996/97 – 2016/17. An SPM-flow rating curve was generated from historical data mined from the "Hydrological Research Reports" collated by the Antarctic Research Programme from 1970 – 1986. Much of this data was found to be unreliable, with higher/unrealistic concentrations reported than what would normally be expected. However, the detailed records from the 1971 – 72 field season by Hawes (1972) were found to be the most suitable for purpose, with reliable SPM concentration data points (n= 82) spanning a broad range of flows. The additional datasets have been included for comparison but have been excluded from the calculated estimates. The daily mean flow (m^3/s) and suspended sediment discharge (tonnes/day) was transformed and fit to a basic power function (Walling, 1977). The resulting relationship was then applied to the LTER flow data to estimate SPM loads over the 20-year period.

6.3 Results

6.3.1 Sequential Extractions

No appreciable differences were detected between the phosphorus fractions associated with SPM collected from the Clarks Stream and the lower Onyx River (**Table 6.2 and Figure 6.2**). The greatest proportions of SPM P (65 – 66 %) were associated with the HCl-reactive fraction. The remaining P was associated with the NaOH-reactive (15 – 20%) residual (10%), organic (4 – 8%), redox-reactive (1.3 – 1.5%) and exchangeable-P (0 - 0.5%) fractions.

Just 437 and 137 mg/kg of redox-reactive Fe and Mn was released into solution when the Clarks Stream SPM was treated with bicarbonate/dithionite ($NaHCO_3/Na_2S_2O_4$). Concentrations of 354 and 208 mg/g of Fe and Mn were detected for the Onyx River SPM treatment.

Table 6.2. Proportions of P associated with different sequential extraction fractions for glacial SPM collected from the Clarks Stream and the Lower Onyx River. Units in mg/kg. Percentage of total P in brackets.

Site	Exchangeable	Redox-reactive	NaOH-reactive	Organic-P	HCl-P	Res-P	Total
3. CS	2.8 (0.5)	8.9 (1.5)	119.6 (19.8)	24.1 (4.0)	391.3 (65.0)	58.2 (9.6)	604.8
4. OVW	0.0 (0)	7.3 (1.3)	81.8 (14.4)	46.6 (8.2)	373.2 (65.8)	58.2 (10.3)	567.0

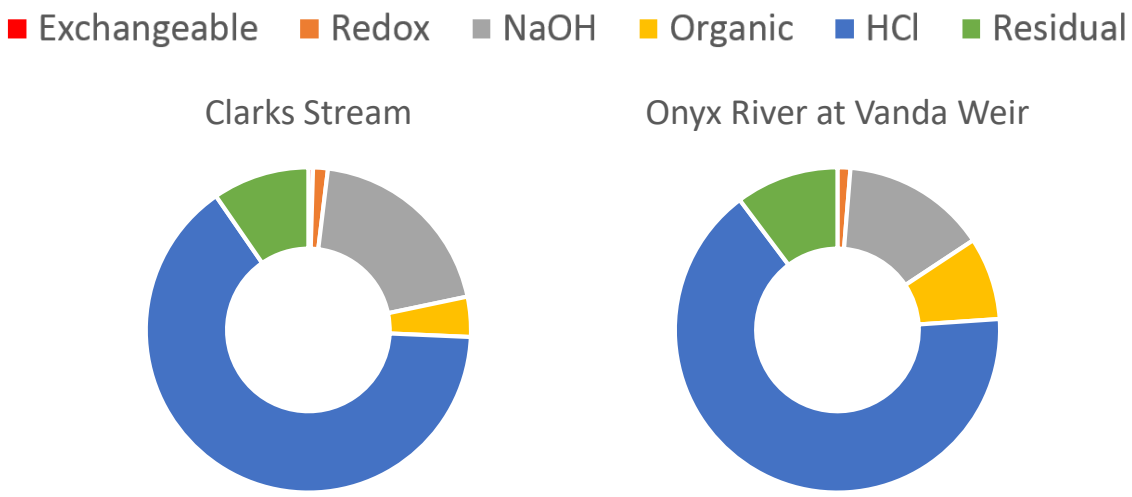

Figure 6.2. Donut graphs presenting the phosphorus (P) fractions associated with SPM from Clarks Stream and the Onyx River.

6.3.2 Adsorption Isotherm

The SPM collected from the Onyx River at the Vanda Weir had a larger adsorption capacity for P (0.28 mg P/g SPM) than the Clarks Stream SPM (0.20 mg P/g SPM) (**Table 6.3 and Figure 6.3**). The affinity of P for the SPM was comparable (K_L = 10.6 – 12.6). The Langmuir isotherm provided an extremely good model fit to the experimental data with high coefficients of determination ($R^2 > 0.99$) for both samples. The Freudlich model also provided a good fit ($R^2 > 0.96$).

Table 6.3. Coefficients of determination (R^2) reported for Freudlich (F) and Langmuir (L) models fitted to the experimental adsorption isotherms for phosphorus (P) onto SPM from the Clarks Stream and Onyx River. The maximum adsorption capacity of the SPM was determined with the Langmuir model (L. Qmax).

Site	Name	Freudlich R^2	Langmuir K_L	Langmuir R^2	Langmuir QMax (mg/g)
1	Clarks Stream	0.97	12.6	1	0.19
2	Onyx River – Vanda Weir	0.98	10.6	0.99	0.28

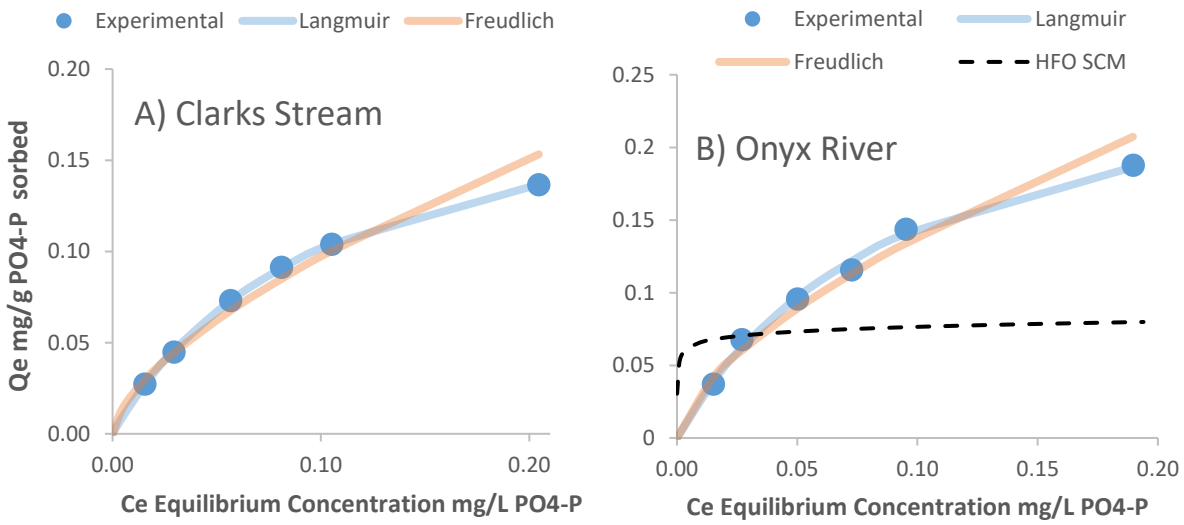

Figure 6.3. Phosphorus adsorption isotherms for SPM collected from Clarks Stream (A) and the Onyx River (B). Ce = equilibrium solution concentration. Qe = mg P adsorbed per g SPM. The solid lines indicate the Langmuir and Freudlich model fits. The dashed line is the modelled adsorption of P, as predicted with the Diffuse Layer surface complexation model assuming HFO to be the only adsorbing surface.

6.3.3 Adsorption Edge

SPM from the lower Onyx River adsorbed P in the pH range of 5-9 (**Figure 6.4**). This was the same range in which the lowest concentrations (< 5 µg/l) of Fe and Al were detected in solution,

indicating no dissolution of these phases. The greatest concentrations (0.15 – 0.22 mg/g) of PO_4-P were adsorbed in the pH range of 4.5 – 7.5. Below pH 4, 0.3 - 0.4 mg/l P was liberated into solution, and progressively higher concentrations of Al (22 – 210 µg/l) and Fe (9-165 µg/l) were detected in solution (indicating the dissolution of these phases). The concentration of calcium increased from 88 to 141 µg/L in the same pH range, indicating the dissolution of a calcium bearing phase.

The adsorption of P, as predicted by the DLM SCM, is presented with the experimental adsorption edge data (**Figure 6.4)**. The modelled adsorption capacity was comparable to the SPM in the pH range of 8 – 10.5 (0.01 – 0.7 mg P/g SPM). However, the model was found to under-predict adsorption by 38 – 49% in the pH range of 5 – 8. Below pH 5, the relationship was obscured by the liberation of P from the SPM into solution.

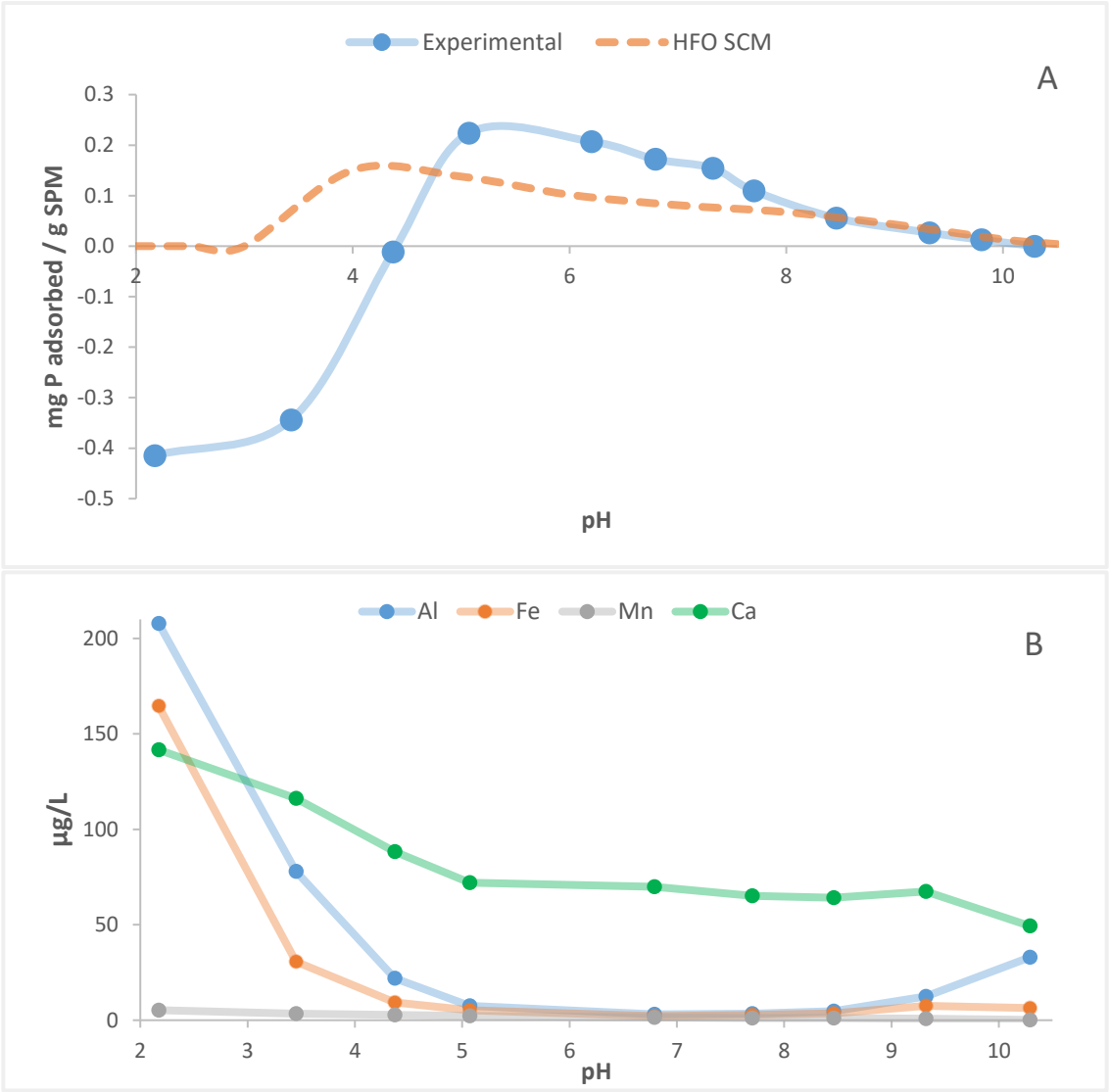

Figure 6.4. A) Adsorption edge profile for P adsorption onto Onyx River SPM. Experiments undertaken in 0.01 mg/l PO_4-P, pH range 2 – 11. B) Concentrations of Al, Fe, Mn and Ca measured in solution after the adsorption edge experiments.

6.3.4 Geochemical Modelling

The experimental concentrations of Al and Fe measured by ICP-MS in the adsorption edge experiment have been plotted with the modelled dissolution curves for gibbsite, ferrihydrite and goethite in **Figure 6.5**. The model predicts the dissolution of gibbsite in the pH range of < 5 and > 10. However, the experimental data did not resemble the modelled curve. Instead, the dissolution of Al from the SPM occurred at a lower pH range of 2 – 4. A small amount was also detected in solution at pH > 9. For Fe, the experimental data shows progressive dissolution at pH < 4. This also did not

resemble the modelled dissolution curves of either ferrihydrite or goethite. Instead, it fit between the two models.

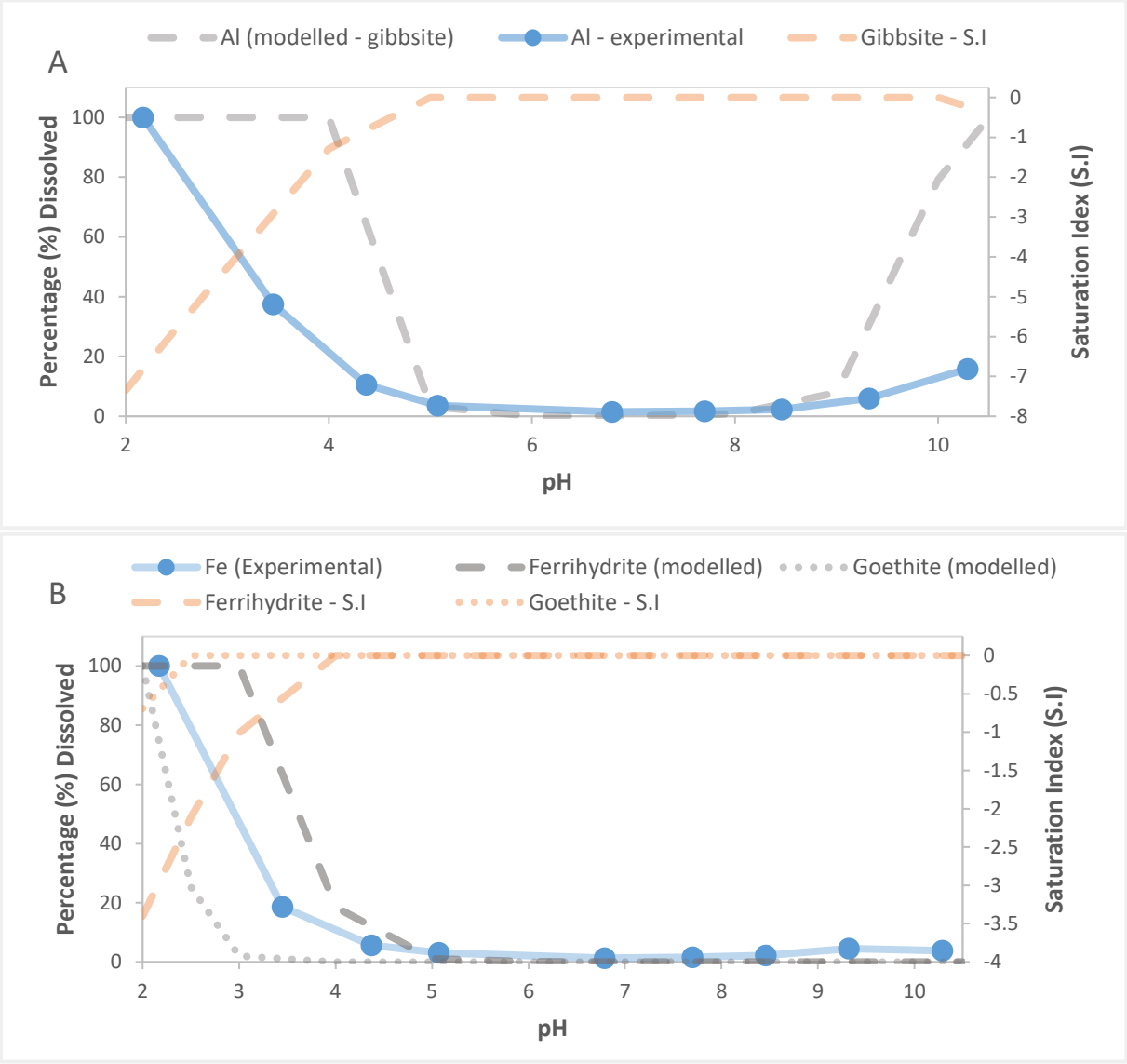

Figure 6.5. The dissolution of gibbsite (top), ferrihydrite and goethite (bottom) were modelled in Visual Minteq 3.1 using the concentrations of "reactive" metal oxides determined by ICP-MS after treatment of the SPM at pH 2 for 24 hours. The dissolution profiles obtained for the experimental data are included for comparison.

6.3.5 SPM and Phosphorus Budget

The SPM-discharge rating curves generated with historical flow and SPM concentration data are presented in **Figure 6.6**. The data sourced from the 1971/72 field season (Hawes, 1972) (blue) was found to provide a good fit to the historical flow and SPM data with a high coefficient of determination ($R^2 = 0.95$). The fit for the remaining data was poor ($R^2 = 0.57$).

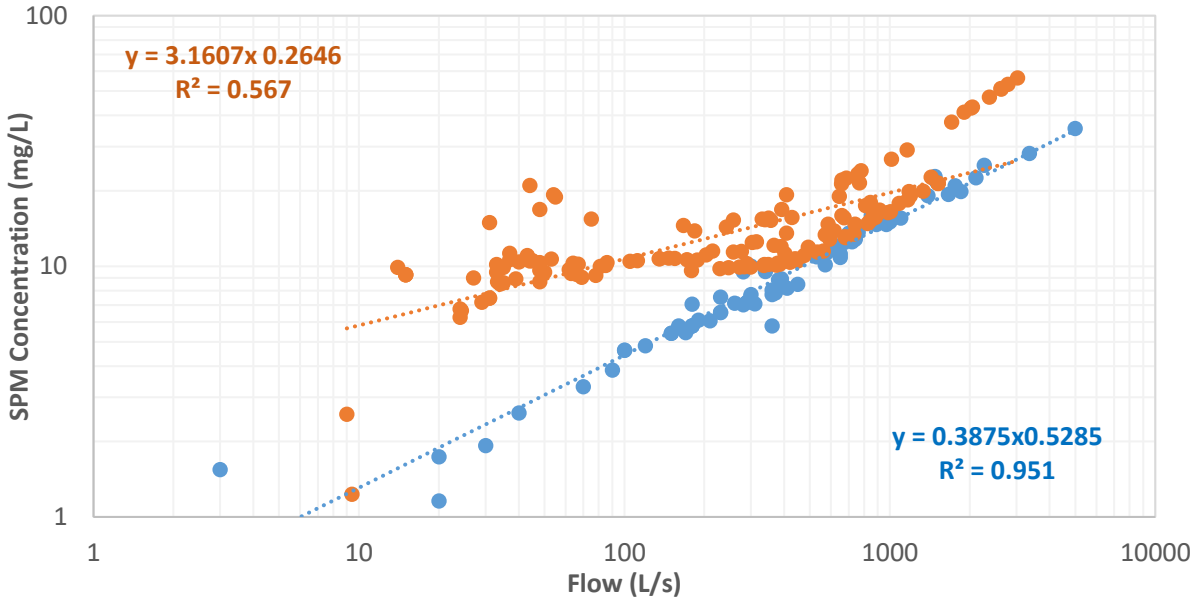

Figure 6.6. SPM-flow rating curve for the Onyx River at Vanda Weir. Graph generated with historical data from the Antarctic Research Programme. Blue points related to data compiled during the 1971/72 melt season (Hawes, 1972). The orange points are an amalgamation of estimates during the 1972 – 1975 period (Chinn and Mason, 2015). Data has been fit with a power function to estimate SPM concentrations and loads with flow data from the LTER.

The seasonal water volumes and predicted SPM loads for the 1996/97 – 2016/17 period are presented in **Table 6.4 and Figure 6.7**. The volume of meltwater discharged into Lake Vanda was highly variable in the period of 1996/97 – 2016/17. The volume for the 2016/17 field season was 2,603,865 m^3, which was the 7th largest in the 20 year period. An associated total of 36.5 tonnes of SPM was predicted with the SPM-flow rating curve. Concentrations ranged from 0 – 19.8 mg/L with a median of 8.7 mg/L. Just 20.7 kg of P was estimated to be associated with the SPM, of which 4.9 kg is predicted to be bioavailable. The volume of meltwater in the 2001/02 and 2008/09 seasons were significantly larger at 21,540,508 and 10,568,900 m^3 respectively. The associated SPM loads were > 20 times the 2016/17 field season, with 908.7 and 796.4 tonnes respectively and correspondingly larger loads of P. Relatively low volumes of meltwater were recorded during the 1997/08, 2000/01 and 2003/04 field seasons with total discharges < 300,000 m^3 and < 2 tonnes of associated SPM.

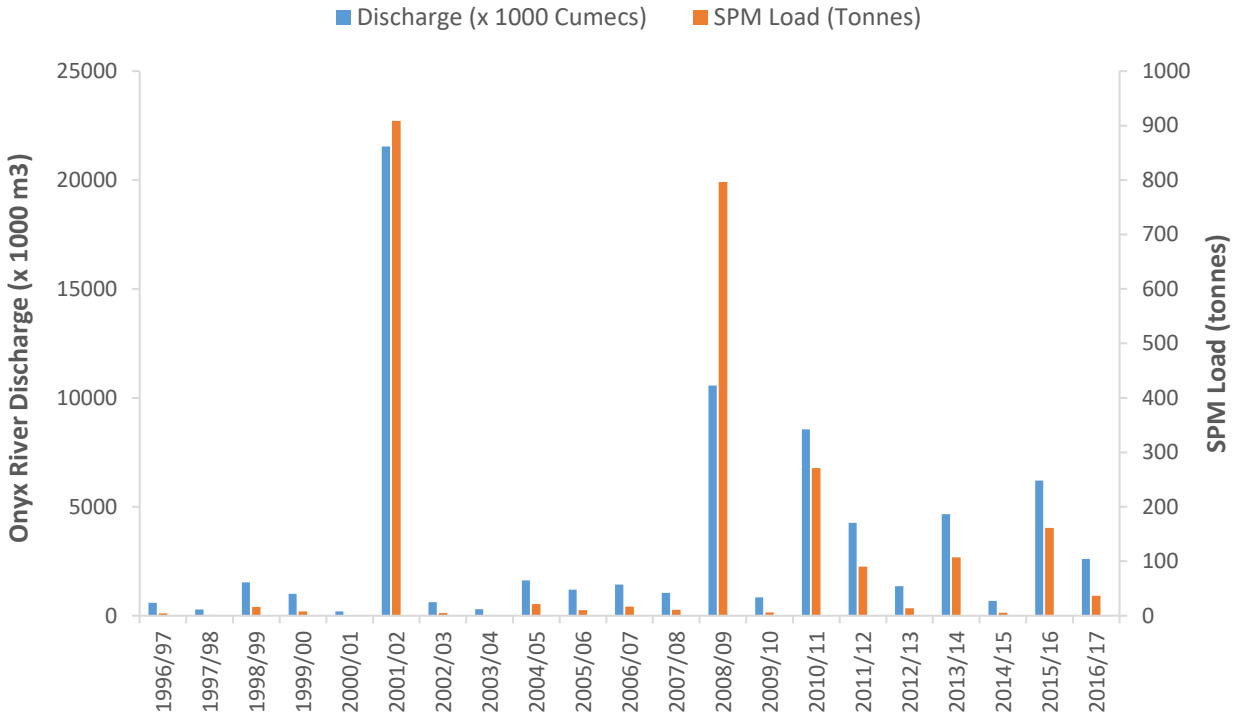

Figure 6.7. Seasonal water volumes and SPM loads (1996/97 – 2016/97) for the Onyx River at the Vanda Weir. Volumes calculated with data provided by the McMurdo LTER (blue). SPM loads are estimates generated with a rating curve generated with historical data from the New Zealand Antarctic Research Programme (orange).

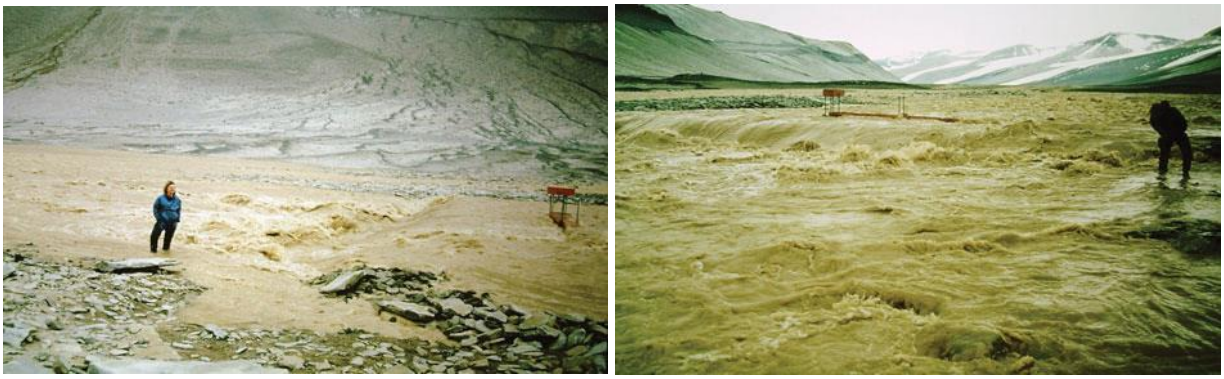

Figure 6.8. Flood at the Onyx River at Vanda Weir during the 1986/87 austral summer. Image Credit: C. Lynch (Chinn and Mason, 2015)

Table 6.4. Twenty year disrcharge record of the Onyx River at Vanda Weir. Total volumes calculated with data provided by the McMurdo LTER. Note* The concentrations and total loads of SPM were predicted using the SPM-discharge rating curve generated with data collected by Hawes (1972). **The associated P loads were estimated with the assumption that the SPM has the same composition as determined in the sequential extraction experiment.

Season	Discharge	SPM concentrations (mg/L)*			SPM Load*	TP**	Bioavailable P**
	Cumecs (x 1000 m^3)	**Mean**	**Median**	**Max**	**Tonnes**	**(kg)**	**(kg)**
2016/2017	2603865	10	8.7	19.8	36.5	20.7	4.9
2015/2016	6200447	13.5	16.6	53.2	161.1	91.3	21.8
2014/15	675163.8	4	3.5	12.1	5.5	3.1	0.7
2013/2014	4668489	10.7	9.1	40.3	107.2	60.8	14.5
2012/13	1355574	6.1	5.6	19.8	13.8	7.8	1.9
2011/2012	4270893	11	9.4	34.6	90.3	51.2	12.2
2010/11	8551563	14.2	7.9	50.4	271.1	153.7	36.7
2009/10	849198	5	4.9	13.5	5.9	3.3	0.8
2008/09	10568900	15.9	10.5	65.5	796.4	451.6	107.9
2007/08	1049292	5.9	4.8	17.2	10.8	6.1	1.5
2006/07	1438213	5.6	4.96	26.9	16.9	9.6	2.3
2005/06	1189557	5.9	5.8	14.5	10.1	5.7	1.4
2004/05	1618198	5.9	4.7	23.2	21.5	12.2	2.9
2003/04	294138.9	3.5	3.2	11.1	1.7	1	0.2
2002/03	618300.9	3.6	3.1	14.2	4.8	2.7	0.7
2001/02	21540508	24.9	21.9	61.5	908.7	515.2	123.1
2000/01	195677.1	1.7	1.1	16.1	1.0	0.6	0.1
1999/00	1008443	5.4	5.3	18.9	7.8	4.4	1.1
1998/99	1534182	6.5	6.6	19.3	15.9	9	2.2
1997/98	288456.3	2.4	1.9	8.7	1.6	0.9	0.2
1996/97	596173.5	4.2	3.9	13.4	4.2	2.4	0.6

6.4 Discussion

6.4.1 SPM: A Vector for Bioavailable Phosphorus?

Suspended particulate matter is predicted to be a primary source of P to the Onyx River catchment. The sequential extractions demonstrated that the SPM P was dominated by the HCl-reactive fraction (65 %). This is most commonly associated with apatite ($Ca_4(PO_4)_3(OH,F)$), which

was identified as a component of the SPM in **Chapter 5, Section 5.3.4**. The liberation of P into solution at pH < 4 during the adsorption edge experiments was also characteristic of the dissolution of apatite. This fraction is not expected to be directly bioavailable to biota in the catchment (Boström et al., 1988). However, the minor proportions associated with the NaOH-reactive (14 – 20%), organic (4-8%), redox-reactive (1.3 – 1.5 %) and exchangeable (< 1%) fractions may be liberated to aquatic biota under favourable conditions (Boström et al., 1988).

The bioavailability of P is primarily mediated by its speciation, which is dependent on the source of the parent material and the influence of in situ processes, such as weathering, biological cycling and sorption processes (Bate et al., 2008). Dissolved reactive phosphate (DRP) is generally considered to be the most readily bioavailable form of P (Boström et al., 1988; House, 2003). However, it's concentrations in the Onyx River catchment are typically extremely low. Previous investigations have reported DRP concentrations ranging from 1 – 33 µg/L (Canfield and Green, 1983; Green and Canfield, 1984). No DRP or DGT-labile P was detected during the 2016/17 sampling period (**Chapter 5, Section 5.3.1**).

It is important to consider the specific organisms and associated mechanisms by which SPM P may be utilized. Algal mats dominate the benthic ecology in the catchment, with metabolic production generally considered to exceed primary production by phytoplankton (Laybourn-Parry and Wadham, 2014). However, the role of nutrients in controlling the growth of benthic mats in Lake Vanda has to date not been well characterized. Hawes et al. (2013) reported high elemental ratios of N:P and hypothesized that the availability of P may constrain the rate of growth, especially in recently flooded parts of the lake where recent establishment of mats has occurred. It is possible that SPM is the primary source of bioavailable P to these organisms. Webster-Brown and Webster (2007) determined that mats incorporated fine SPM in the organic-rich, mucilaginous matrix (**Figure 6.9**). It was later reported that fine sediments exist in banded layers within the mats, with the thickness of the layers determined by the influx of SPM from the Onyx River. The thickest layer was attributed to the climate-driven flood season of 2001-2002 (Hawes et al., 2013). Phototrophic and heterotrophic biota exist in vertically stratified assemblages in these mats, likely due to the variable light availability and geochemical conditions (oxygen concentrations, redox potential, pH) that exist on microscopic scales (Borovec et al., 2010; Stal, 1995). Phosphorus bound to the SPM may be released or recycled under such conditions, where it may be used for metabolic functioning (Borovec et al., 2010). Wood et al.

(2015) demonstrated that the benthic cyanobacteria *Phormidium* produces the conditions necessary for the liberation of P from fine sediments that are commonly incorporated into its own mucilaginous matrix. Photosynthetic respiration can result in an internal pH > 9, and this can liberate adsorbed P due to competitive adsorption with OH^-. The depletion of O_2 from aerobic respiration may also result in the release of P from Fe and Mn oxy/hydroxides that undergo dissolution in reducing conditions. Organic-P associated with the SPM is likely to be recycled in the mat by extracellular enzymatic processes (Correll, 1998; Cottingham et al., 2015). Considering this evidence, it is hypothesized that SPM incorporated into benthic mats may utilize P when:

- Photosynthetic respiration during the long hours of daylight in the austral summer results in a high pH environment (> 9) resulting in the liberation of NaOH-reactive P due to competitive effects with OH^-.
- Reducing conditions may be generated in the lower layers of the mat due to activity by sulphate-reducing resident bacteria, resulting in the reductive dissolution of Fe- and Mn-oxy/hydroxides and the liberation of redox-reactive P.
- Organic-P associated with the SPM is recycled by enzymatic processes.

The ultra-oligotrophic Lake Vanda is also home to a diversity of phytoplankton species (Vincent and Vincent, 1982). The low input of P into the lake has been stated to exert a dominant control on its biomass in Lake Vanda (Priscu, 1995; Vincent and Vincent, 1982). Phosphorus limited phytoplankton exist in the extremely clear upper waters and have low rates of photosynthesis (Howard-Williams and Hawes, 2007). A pronounced increase in activity at ~60m depth corresponds to the deep chlorophyll maximum (DCM). The nutrient rich, anoxic brine that sits below is relatively enriched in DRP (Priscu, 1995). It has been proposed that the diffusion of nutrients by advection fuels the phytoplankton activity in a zone where there is just enough light for photosynthetic activity (Howard-Williams and Hawes, 2007). SPM concentrations in the anoxic waters are high (Webster-Brown and Webster, 2007) and the sulphide rich, anoxic waters will liberate redox-reactive P adsorbed to reactive Fe- and Mn-oxy/hydroxides associated with SPM that has undergone sedimentation.

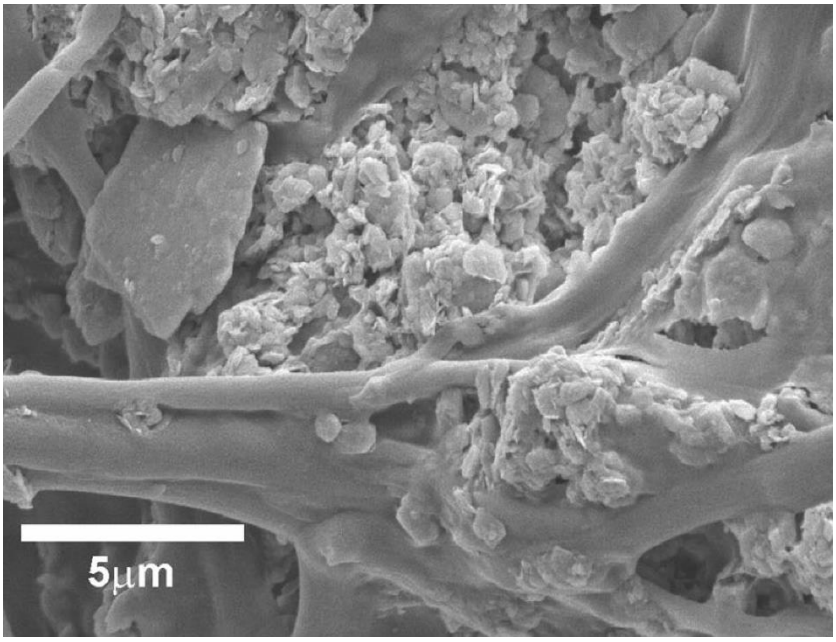

Figure 6.9. SEM image of fine, sub-micron sized particles incorporated into a benthic mat from Lake Vanda. Image credit: Webster-Brown and Webster (2007).

6.4.2 Phosphorus Adsorption onto Polar SPM

The adsorption isotherm and edge experiments demonstrated that the SPM has a reasonable capacity to adsorb DRP under oxic conditions and normal pH conditions (5-8). SPM was previously hypothesized to be an efficient scavenger of dissolved elements in the catchment (Green et al., 1993). Based on the results in this study, it is hypothesized that the SPM adsorbs DRP from the water column in oxic conditions, and may be the primary driver of the notable lack of DRP detected in the catchment during the study period. The finer SPM collected from the lower Onyx River (OVW) had a greater adsorption capacity relative to the coarser Clarks Stream sample. It is likely that the finest fraction will remain in suspension in the terminal Lake Vanda for long periods, where it may actively scavenge P (and other nutrients) from the water column. This process could have a limiting effect on the proliferation of phytoplankton in the water column.

The sequential extractions, adsorption edge experiments and geochemical modelling provided key insights into the phases of the SPM that were implicated in the adsorption processes. Overall, the evidence suggests that Fe-oxides play a major role in the adsorption of P. However, the Fe is expected to be associated with more crystalline phases such as goethite or hematite. It may be present as surface coatings or discrete particles up to 1 μm detected in the SPM (**Chapter 5, Figure 5.7)**. Minor

contributions from amorphous Fe-oxides (such as ferrihydrite), Mn-oxides and the reactive surfaces of clay minerals may augment the adsorption capability.

The sequential extractions provided the first important clues to characterizing these adsorption phases. The BD ($NaHCO_3/Na_2S_2O_4$) extraction procedure reduces reactive Fe- and Mn-oxides. However, low concentrations Fe and Mn were detected in the extractant. Just a tiny proportion of the acid-soluble Fe (1 %) was liberated from the SPM in this process. Ericsson (1984) has previously reported that the BD extraction technique can be inefficient at reducing crystalline phases of Fe. Additional and complimentary evidence was generated during the adsorption edge experiments. The dissolution profile of Fe in the pH range of 2-10 was found to occur at a lower pH that what was modelled for ferrihydrite, and was characteristic of a more crystalline phase (**Figure 6.5)**.

A significant proportion (15 %) of SPM P was found to be associated with the NaOH-reactive fraction. This procedure targets P bound to Al oxides, clay minerals and Fe and Mn oxides resilient to the BD treatment. However, the dissolution profile of Al during the adsorption edge experiments (**Figure 6.5**) was not characteristic of an Al oxide surface (such as gibbsite). It is therefore expected that the P associated with this fraction was predominantly associated with crystalline Fe oxides and the reactive surfaces of the fine, clay sized particles. The adsorption of P onto these surfaces may also be enhanced by the lack of competing ions due to the low ionic strength of the meltwater.

The speciation and bioavailability of Fe in Antarctic glacial meltwaters has important implications for the wider Antarctic region. Melting glaciers are a significant source of Fe to the coastal waters of Antarctica (Lyons et al., 2015; Monien et al., 2017; Raiswell et al., 2006), which is a primary stimulant of primary production in the nutrient rich coastal waters (Martin et al., 1990). However, the relative bioavailability of the Fe may be highly variable and has complicated recent predictions of ecosystem response to increasing glacial melt forced by global climate change. Previous studies have demonstrated that poorly crystalline Fe is more effectively metabolized by aquatic biota for metabolic uptake, with the effective bioavailability decreasing with increasing crystallinity (Raiswell et al., 2008; Wells et al., 1991; Wells et al., 1983). This research indicates that the Fe associated with the Onyx River SPM will not be as readily bioavailable as that generated by alpine glaciers. Additional research will be required to validate this hypothesis.

The Diffuse Layer SCM applied in this research did not accurately predict the adsorption capacity of the SPM. However, it did predict the adsorption character (**Figure 6.4**) in the environmentally relevant pH range of 5 – 10. The assumption of HFO as the sole adsorbing surface has failed to account for the adsorption of P onto the crystalline Fe oxide surfaces that were identified. This model could be optimized by quantifying the crystalline surface and applying it in an assemblage model. Such a calibrated model will be extremely useful in predicting the geochemical behaviour and adsorption characteristics of SPM in the highly variable and evolving conditions of Lake Vanda (Castendyk et al., 2016).

6.4.3 SPM Loading: Variability and Importance

The predicted quantities of SPM transported to Lake Vanda were both extremely limited and highly variable. Loads were typically < 100 t/y. To put this in context, these loads are generally less than streams in New Zealand with a catchment area of < 5 km^2. The alpine, glacier-fed Waitaki River has a predicted sediment yield of 0.34 – 0.69 Mt/y (Hicks et al., 2011).

Significantly greater loads are predicted to be transported to the lake during episodic high flow events. The 2001/02 season was the most notable, with the load of meltwater 1-2 orders of magnitude greater than a typical flow year. This event has been attributed to down valley foehn winds that struck the McMurdo Dry Valleys (MDVs). The resulting two-week period of relatively warm air temperatures (+4°C) resulted in high rates of glacial melt across the valleys. Such events result in the liberation of entrained glacial sediment and the erosion of valley soils which are transported down catchment. In the Taylor Valley, the turbidity associated with the high flows initially limited primary production. However, once this settled a significant increase in both water column nutrient concentrations and primary production was recorded (Foreman et al., 2004). Recently, the flood event has also been linked to long-term changes to the ecological character of the Taylor Valley lakes (Gooseff et al., 2017).

The predicted loads of SPM P in this study were comparable to previous estimates, and this provided a degree of reassurance in the methodology used in this study. Canfield and Green (1983) predicted 22 kg of P entered Lake Vanda during the 1980 - 1981 season. Jones-Lee and Lee (1993) collected samples in the same year and estimated just 10.5 kg of P entered the lake. In any case, the predicted loads are extremely low, especially considering that up to 80% will not be readily

bioavailable based on the sequential extractions in this study. In the 5-year period from 1996/07 – 2000/01, just 16.3 kg of SPM P was predicted to be transported to the lake. However, > 500 kg was predicted to be transported into the lake in the 2001/02 flood, which may have had a profound effect on the biological productivity of the system. However, any such changes have to date not been characterised.

It must be noted that the estimates generated in this study have a high degree of uncertainty due to the variable nature of the glacial melt and the limited data used to generate the rating curve. Extremely high concentrations of SPM (> 100 mg/L) appear to be associated with these flood flows (**Figure 6.9**). However, these are likely to have been under-predicted by the SPM rating curve due to the lack of data at high flows. The greatest predicted SPM concentration was 65.5 mg/L, and it is possible that these estimates are highly conservative. Additionally, the curve does not factor in the higher loads typically associated with the primary melt. This is attributed to the accumulation of aeolian sediments on the glaciers and river beds during winter. These are typically evacuated into the Onyx on first melt (Howard-Williams et al., 1997; Jones-Lee and Lee, 1993). Despite these limitations, the estimates have provided an important insight into the variable and irregular loading of SPM loading. A dedicated field campaign collecting large quantities of samples over a broad range of flows would be required to increase the precision of these estimates.

6.4.4 Future Outlook

The effects of climate change are predicted to have a significant effect on both the hydrology and ecological conditions of proglacial aquatic systems in the MDVs (Castendyk et al., 2016; Lyons et al., 2006). Climate models have predicted significant warming across the Antarctic continent by the end of the century (Steig et al., 2009), and an increased frequency of down-valley, foehn winds that will increase surface air temperatures in the region (Castendyk et al., 2016). This will not only enhance the distribution of aeolian dust onto glacial surfaces, it will also reduce the surface albedo of the ice and enhance melting (Fountain et al., 2014). The combination of effects may enhance both the duration and severity of glacial melt. For the Onyx River catchment, an increasing incidence of flood flows will deliver large quantities of meltwater and SPM to Lake Vanda. This could result in rapid changes to the both the physical (Castendyk et al., 2016) and biogeochemical conditions of the lake. Greater concentrations of bioavailable nutrients are expected to drive primary production (Green and

Lyons, 2009) and rising lake levels will generate new habitats that will be rapidly colonized by microbial mats (Hawes et al., 2013). Based on recent evidence from the Taylor Valley (Gooseff et al., 2017), it may ultimately shift the biological character of the catchment.

6.5 Conclusions

Suspended particulate matter is predicted to be a dominant source of P to the extreme, nutrient limited Onyx River catchment. The sequential extractions indicated that the majority of the SPM P was associated with primary phosphorus containing minerals (such as apatite) and is not expected to be readily bioavailable. Less than 20% was found to be associated with reactive metal oxides (Fe and Mn), clay minerals and organic matter. However, this may be liberated from the particle surfaces for metabolic uptake when incorporated into benthic mats or exposed to the highly reducing conditions present in the bottom waters of Lake Vanda. In oxic waters the SPM is predicted to be an efficient scavenger of dissolved P, due to adsorption by Fe and Mn oxides and the reactive clay surfaces associated with the fine, sub-micron sized particles.

The flux of SPM in the Onyx River catchment was predicted over a 20 year period with the generation of an SPM-discharge rating curve that was applied to flow data collected by the McMurdo Long Term Ecological Research Network (LTER). The predicted SPM loads for the annual melt seasons were highly variable, ranging from 1.0 – 908.7 tonnes. So too were the predicted quantities of P, with loads varying from 0.6 – 515.2 kg of P. High flow events, such as those during the 2001/02 and 2008/09 austral summers, resulted in SPM loads up to three orders of magnitude greater than typical years. As such, the dominant source of P to the catchment is likely to be during these episodic events, which are predicted to have a long-lasting effect on the ecological productivity of the Lake. An increase in the frequency of flood events caused by anthropogenic climate change is predicted to initiate a profound shift in the physicochemical characteristics of Lake Vanda, and its biological structure and diversity.

6.6 References

Asselman NEM. Fitting and interpretation of sediment rating curves. Journal of Hydrology 2000; 234: 228-248.

Barrett JE, Virginia RA, Lyons WB, McKnight DM, Priscu JC, Doran PT, et al. Biogeochemical stoichiometry of Antarctic Dry Valley ecosystems. Journal of Geophysical Research: Biogeosciences 2007; 112

Bate DB, Barrett JE, Poage MA, Virginia RA. Soil phosphorus cycling in an Antarctic polar desert. Geoderma 2008; 144: 21-31.

Borovec J, Sirová D, Mošnerová P, Rejmánková E, Vrba J. Spatial and temporal changes in phosphorus partitioning within a freshwater cyanobacterial mat community. Biogeochemistry 2010; 101: 323-333.

Boström B, Persson G, Broberg B. Bioavailability of different phosphorus forms in freshwater systems. Hydrobiologia 1988; 170: 133-155.

Canfield DE, Green WJ. Aspects of nutrient behavior in Lake Vanda. Antarctic Journal of the United States 1983; 18: p. 224-226.

Castendyk DN, Obryk MK, Leidman SZ, Gooseff M, Hawes I. Lake Vanda: A sentinel for climate change in the McMurdo Sound Region of Antarctica. Global and Planetary Change 2016; 144: 213-227.

Chinn T, Mason P. The first 25 years of the hydrology of the Onyx River, Wright Valley, Dry Valleys, Antarctica. Polar Record 2015; 52: 16-65.

Correll DL. The Role of Phosphorus in the Eutrophication of Receiving Waters: A Review. Journal of Environmental Quality 1998; 27: 261-266.

Cottingham KL, Ewing HA, Greer ML, Carey CC, Weathers KC. Cyanobacteria as biological drivers of lake nitrogen and phosphorus cycling. Ecosphere 2015; 6: 1-19.

Ericsson T. A Mössbauer Study of the Efect of Dithionite/Citrate/Bicarbonate Treatment on a Vermiculite, a Smectite and a Soil. Clay Minerals 1984; 19: 85-91.

Foreman CM, Wolf CF, Priscu JC. Impact of Episodic Warming Events. Aquatic Geochemistry 2004; 10: 239-268.

Fountain AG, Levy JS, Gooseff MN, Van Horn D. The McMurdo Dry Valleys: A landscape on the threshold of change. Geomorphology 2014; 225: 25-35.

Fountain AG, Lyons WB, Burkins MB, Dana GL, Doran PT, Lewis KJ, et al. Physical Controls on the Taylor Valley Ecosystem, Antarctica. BioScience 1999; 49: 961-971.

Gooseff MN, Barrett JE, Adams BJ, Doran PT, Fountain AG, Lyons WB, et al. Decadal ecosystem response to an anomalous melt season in a polar desert in Antarctica. Nature Ecology & Evolution 2017; 1: 1334-1338.

Green WJ, Canfield DE. Geochemistry of the Onyx River (Wright Valley, Antarctica) and its role in the chemical evolution of Lake Vanda. Geochimica et Cosmochimica Acta 1984; 48: 2457-2467.

Green WJ, Canfield DE, Shengsong Y, Chave KE, Ferdelman TG, Delanois G. Metal transport and release processes in Lake Vanda: The role of oxide phases. Physical and Biogeochemical Processes in Antarctic Lakes. 59. AGU, Washington, DC, 1993, pp. 145-163.

Green WJ, Lyons WB. The Saline Lakes of the McMurdo Dry Valleys, Antarctica. Aquatic Geochemistry 2009; 15: 321-348.

Hawes I, Sumner YD, Andersen TD, Jungblut DA, Mackey JT. Timescales of Growth Response of Microbial Mats to Environmental Change in an Ice-Covered Antarctic Lake. Biology 2013; 2.

Hawes J. Report on the 1971-72 Hydrolgical-Glaciological Programme. Department of Science and Industrial Research, 1972.

Hicks DM, Shankar U, McKerchar AI, Basher L, Lynn I, Page M, et al. Suspended sediment yields from New Zealand rivers. Journal of Hydrology (New Zealand) 2011; 50: 81-142.

House WA. Geochemical cycling of phosphorus in rivers. Applied Geochemistry 2003; 18: 739-748.

Howard-Williams C, Hawes I. Ecological processes in Antarctic inland waters: interactions between physical processes and the nitrogen cycle. Antarctic Science 2007; 19: 205-217.

Howard-Williams C, Hawes I, Schwarz A, A. Hall J. Sources and sinks of nutrients in a polar desert stream, the Onyx River, Antarctica. Ecosystem Processes in Antarctic Ice-free Landscapes. Balkema Press, Rotterdam, 1997.

Jones-Lee A, Lee GF. The Relationship Between Phosphorus Load and Eutrophication Response in Lake Vanda. Physical and Biogeochemical Processes in Antarctic Lakes. American Geophysical Union, 1993.

Laybourn-Parry J, Wadham JL. Antarctic lakes. Oxford; New York: Oxford University Press, 2014.

Lyons WB, Dailey KR, Welch KA, Deuerling KM, Welch SA, McKnight DM. Antarctic streams as a potential source of iron for the Southern Ocean. Geology 2015; 43: 1003-1006.

Lyons WB, Laybourn-Parry J, Welch KA, Priscu JC. Antarctic Lake Systems and Climate Change. In: Bergstrom DM, Convey P, Huiskes AHL, editors. Trends in Antarctic Terrestrial and Limnetic Ecosystems: Antarctica as a Global Indicator. Springer Netherlands, Dordrecht, 2006, pp. 273-295.

Martin JH, Fitzwater SE, Gordon RM. Iron deficiency limits phytoplankton growth in Antarctic waters. Global Biogeochemical Cycles 1990; 4: 5-12.

McKnight DM, Niyogi DK, Alger AS, Bomblies A, Conovitz PA, Tate CM. Dry Valley Streams in Antarctica: Ecosystems Waiting for Water. BioScience 1999; 49: 985-995.

Monien D, Monien P, Brünjes R, Widmer T, Kappenberg A, Silva Busso AA, et al. Meltwater as a source of potentially bioavailable iron to Antarctica waters. Antarctic Science 2017; 29: 277-291.

Priscu JC. Phytoplankton nutrient deficiency in lakes of the McMurdo dry valleys, Antarctica. Freshwater Biology 1995; 34: 215-227.

Raiswell R, Benning LG, Tranter M, Tulaczyk S. Bioavailable iron in the Southern Ocean: the significance of the iceberg conveyor belt. Geochemical Transactions 2008; 9: 7.

Raiswell R, Tranter M, Benning LG, Siegert M, De'ath R, Huybrechts P, et al. Contributions from glacially derived sediment to the global iron (oxyhydr)oxide cycle: Implications for iron delivery to the oceans. Geochimica et Cosmochimica Acta 2006; 70: 2765-2780.

Rydin E. Potentially mobile phosphorus in Lake Erken sediment. Water Research 2000; 34: 2037-2042.

Stal LJ. Physiological ecology of cyanobacteria in microbial mats and other communities. New Phytologist 1995; 131: 1-32.

Steig EJ, Schneider DP, Rutherford SD, Mann ME, Comiso JC, Shindell DT. Warming of the Antarctic ice-sheet surface since the 1957 International Geophysical Year. Nature 2009; 457: 459-462.

Vincent WF, Vincent CL. Factors Controlling Phytoplankton Production in Lake Vanda (77°S). Canadian Journal of Fisheries and Aquatic Sciences 1982; 39: 1602-1609.

Walling DE. Assessing the accuracy of suspended sediment rating curves for a small basin. Water Resources Research 1977; 13: 531-538.

Waters AS. Phosphorus dynamics in a shallow, coastal lake system, Canterbury, New Zealand. Waterways Centre for Freshwater Management. PhD. University of Canterbury, University of Canterbury, 2016.

Webster-Brown JG, Webster KS. Trace metals in cyanobacterial mats, phytoplankton and sediments of the Lake Vanda region, Antarctica. Antarctic Science 2007; 19: 311-319.

Wells ML, Mayer LM, Guillard RRL. A chemical method for estimating the availability of iron to phytoplankton in seawater. Marine Chemistry 1991; 33: 23-40.

Wells ML, Zorkin NG, Lewis AG. The role of colloid chemistry in providing a source of iron to phytoplankton. Journal of Marine Research 1983; 41: 731-746.

Wood SA, Depree C, Brown L, McAllister T, Hawes I. Entrapped Sediments as a Source of Phosphorus in Epilithic Cyanobacterial Proliferations in Low Nutrient Rivers. PLOS ONE 2015; 10: e0141063.

7. Conclusions

7.1 Synthesis: The Waitaki Catchment

7.1.1 What was the Character and Composition of SPM in the Glacier-Fed Waitaki Catchment?

In **Chapter 2**, the previously unknown physicochemical characteristics of SPM collected throughout the glacier-fed Waitaki catchment were determined. The SPM was characterised in terms of its mineralogy and morphology, particle size, trace element content and degree of particle weathering. The relative specific surface area (SSA) and cation exchange capacity (CEC) of the SPM was determined with the adsorption of methylene blue, providing a relative measure of the SPM's adsorption capability. Suspended particulate matter collected in close proximity to the glacial source was characteristically dominated by extremely fine inorganic particles (quartz, mica, feldspar) with a low degree of chemical weathering compared to the source rock. The SPM was hypothesized to have the greatest potential adsorption capability - attributable to its relatively high concentrations of reactive surface oxides and a greater SSA and CEC. Major evolutions in SPM character occurred down-catchment. SPM concentrations declined significantly, becoming progressively weathered and enriched in organic matter, diatoms and aggregates. Corresponding reductions in the concentrations of reactive surface oxides, SSAs and CECs were detected. Based on this data, it was predicted that the fresh fine glacial SPM in the upper catchment will be primed for both adsorption and weathering processes. SPM in the lower catchment was predicted to have a lower adsorption capability.

7.1.2 Was the Glacial SPM an Effective Adsorbent of P, Cd and Cu?

In **Chapter 3**, the adsorption capability of the Waitaki catchment SPM for phosphorus (P) was determined. The fresh glacial SPM was found to have a relatively large adsorption capacity for P compared to the organic rich SPM collected down catchment. The enhanced ability was largely attributed to the greater concentrations of reactive Fe oxides associated with the fresh glacial SPM, which was determined to have a dominant influence on the adsorption of P. The novel measure of 'adsorption potential' conceived in this study indicated that the SPM-rich meltwater in the upper

catchment has a significant ability to attenuate dissolved P. However, the adsorption potential rapidly declined down catchment, owing to the lower capacity of the SPM for P and the significantly lower SPM concentrations in the water.

In **Chapter 4,** the adsorption capability of the SPM for Cd and Cu was determined. The fresh glacial SPM was found to have a larger adsorption capacity for Cd relative to the organic rich SPM down catchment. However, the affinity of Cd for the SPM was generally low, with most Cd found to remain in the solution phase. The opposite trend was detected for Cu, which was found to have a relatively high affinity for the SPM. The fresh glacial SPM had the lowest adsorption capability compared to the lower catchment SPM. This was attributed to the significant influence of organic matter in the adsorption of Cu, which was predicted to be a dominant adsorbing phase. The 'adsorption potential' of the Waitaki catchment water for both Cd and Cu was greatest in the upper catchment, and significantly declined down catchment.

The adsorption capability of the SPM varied throughout the Waitaki catchment. This was dependent on both the character of the SPM and the adsorbate. Glacial SPM is predicted to be an effective adsorbent of both P and Cu where appreciable concentrations remain in the water. However, its ability to adsorb Cd was largely restricted by its low affinity for the SPM.

7.1.3 Can Surface Complexation Models Predict the Adsorption of P, Cd and Cu onto the Glacial SPM?

Surface complexation models (SCMs) were successfully used throughout this research to assist in the interpretation of the laboratory experiments, providing key insights into the phases implicated in adsorption. However, the ability of the SCMs to predict the adsorption of Cd, Cu and P onto the SPM had a mixture of success. In **Chapter 3,** a Diffuse Layer SCM, assuming HFO to be the only adsorbing surface, was used to model the adsorption of P. The model provided a good fit to the adsorption character and capacity of the fresh glacial SPM. However, its accuracy declined for the down catchment SPM, which was attributed to the increasingly complexity of the SPM and possible competitive effects.

In **Chapter 4**, the combined Diffuse Layer (DLM) and Stockholm Humic (SHM) models were used to predict the degree of Cd and Cu adsorption onto the Waitaki SPM. The models were found to

under-predict the degree of adsorption onto the glacial SPM for both Cd and Cu. It was hypothesized that additional adsorbing surfaces, including crystalline Fe oxides and the reactive surfaces of clay minerals, may enhance the adsorption capability of the glacial SPM. Additional research will be required to elucidate these mechanisms. The combined model did however predict the adsorption character and capacity of the organic rich SPM in the lower Waitaki. Organic matter was predicted to be the dominant adsorbing phase in these samples.

7.1.3 What are the Implications?

Glacial SPM has proven to have a significant potential to adsorb dissolved P and Cd in natural waters. Much of the adsorption character is attributed to the Fe oxides that are associated with the SPM. For this reason, it is likely that the glacial SPM may also have a significant ability to adsorb various other trace metals (including Cr, Pb, Co, Zn and Ni) that adsorb strongly to reactive Fe oxides (Benjamin and Leckie, 1981; Dzombak and Morel, 1990; Smith, 1999). However, in natural waters the adsorption potential of the glacial SPM will be highly constrained by the concentrations that remain in suspension. In the Waitaki catchment, the glacial influence of the SPM significantly declined with increasing distance from the glacial source. The associated adsorption potential of the water was found to decline to such a point that it was not expected to play an appreciable role in the attenuation of P and Cd. It is therefore expected that biogeochemical cycling of these elements will largely be controlled by adsorption onto surface sediments and uptake by aquatic biota. The rapid development in the region has already resulted in the degradation of the once pristine Lakes Benmore and Aviemore (Gray, 2015), and further development is expected to result in greater loads of nutrients associated with the runoff (Clarke, 2015). The glacial SPM in these lakes is not predicted to play an important role in attenuating these loads. It is also predicted that progressive glacier wasting in the catchment will ultimately reduce the concentrations of glacial SPM discharged into the system. This response, coupled with the warming of the proglacial waters could enhance the process of eutrophication. Such effects should be considered in the management of the catchment.

Glacial SPM may have a greater protective role in non-modified catchments where the glacial influence of the SPM remains high. It may also play a key role in regulating the quality of waters in glacier-fed catchments that are highly stressed by anthropogenic influences. Important examples include glacier-fed rivers originating from the Himalayas (Barnett et al., 2005). Models generated by

Immerzeel et al. (2010) have predicted major decreases of glacial meltwater for the Brahmaputra (−19.6%), Ganges (−17.6%), upper Indus (−8.4%) and Yangtze rivers (−5.2%) by 2050. These rivers provide drinking and irrigation water for 1.4 billion people and flow through densely populated regions in Asia. The SPM in these rivers are commonly enriched in both trace metals and nutrients (Viers et al., 2009), and it is possible that the attenuation of anthropogenic contaminants by the glacial SPM plays a role in regulating their transport and toxicity. A reduction in the flux of glacial SPM, coupled with low flows in the dry season could increase the bioavailable concentrations of contaminants in these systems.

The adsorption capability of SPM in glacier-fed catchments is likely to rapidly evolve with climate change. It is generally expected that the quantities of meltwater and glacial sediments discharged into proglacial environments will be enhanced in the short term by rapid glacial melt. However, the ongoing wasting of glaciers will limit meltwater runoff to proglacial water bodies (Casassa et al., 2009; Milner et al., 2017). It may also limit the ability of the glaciers to generate fine inorganic sediments. Glaciers have been previously stated to be producers of mineral surface area (Anderson, 2007). A reduction in glacial mass may limit their erosive ability and the development of fine clay minerals and/or secondary metal oxides (Hodson et al., 2004). Ultimately, this may result in a significant reduction in the reactive surface area available for adsorption processes in downstream water bodies. These changes are likely to be coupled with an increase in the temperature of downstream waters, and a reduction in the glacial influence on turbidity (Adrian et al., 2009; Sommaruga, 2015) (**Figure 7.1**). This may result in the proliferation of aquatic biota in waters where primary production is normally limited by light availability (Sommaruga, 2015). The development of vegetation in lands exposed by glacial retreat (Milner et al., 2009) may also enhance the concentrations of organic matter in nearby water bodies. Ultimately, the adsorption capability of the SPM is likely to change in coming years.

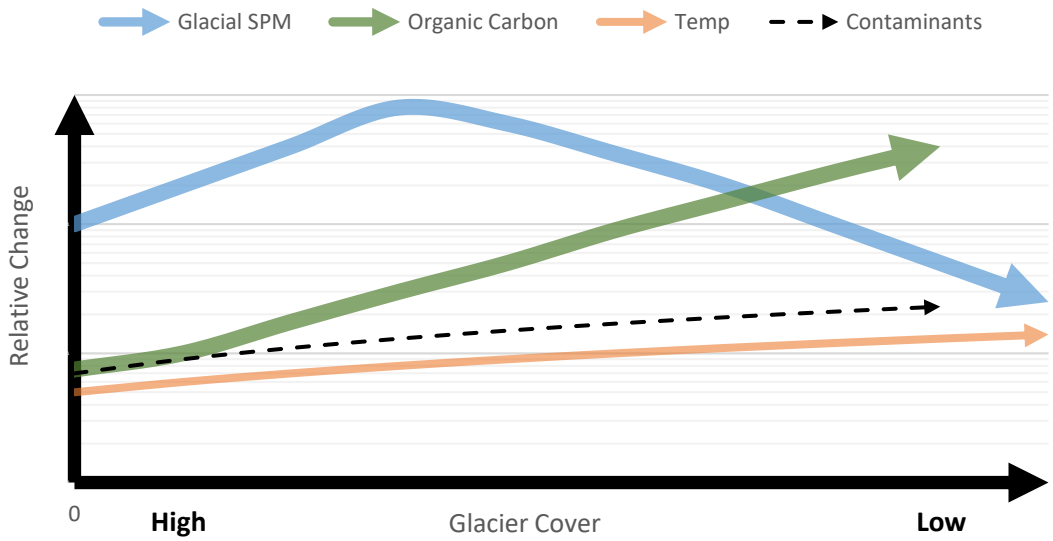

Figure 7.1. A conceptual response curve of the evolution of a glacier-fed water body with decreasing glacial coverage. An enhancement of melting is expected to result in a temporary increase in the discharge of glacial SPM. However, this will decline with decreasing ice mass (blue arrow). A decrease in turbidity and increase in temperature (orange arrow) may enhance the concentrations of organic matter in the water. Anthropogenic development may result in an increase in contaminant loading (black dashed arrow).

7.1.4 Limitations

One of the major difficulties in this study was obtaining enough SPM for analytical procedures in the laboratory. The concentrations in the lower Waitaki catchment were extremely low (consistently < 5 mg/L). In the absence of more modern equipment to automate the collection process (automated pump sampler, continuous-flow centrifugation), large quantities of water were filtered to obtain small quantities of material. Where possible, a time-integrated suspended (TIMs) sediment sampler was deployed to capture SPM from the water column (**Appendix A**). However, this method was found to result in SPM with different size characteristics to the grab samples. For this reason, the SPM collected by the TIMs sampler was not used in the characterisation and adsorption experiments.

The careful use of controls and analytical standards in this research has ensured that the data is of a high quality. Where possible and practical, the water and SPM samples were also analysed in triplicate to ensure analytical accuracy. However, is was not possible to do this for the destructive analytical procedures that required significant quantities of SPM (adsorption experiments, TOC). Optimizing the quantities of SPM collected in the first instance would ensure that replicate

experiments could be carried out for every analytical procedure, and reduce any uncertainty in the data.

The SPM used in this research was collected in stable, base flow conditions in the dry autumn months. However, this research has not considered the temporal variation that may occur throughout the year. For example, in the wet winter months rain runoff will transport significant quantities of particulate matter into the catchment, which may have very different characteristics and adsorption properties to the SPM in base flow conditions. Significant quantities of contaminants (including P, Cd and Cu) are commonly flushed into natural waters during these events (Bibby and Webster-Brown, 2005; Bibby and Webster-Brown, 2006; Webster et al., 2000), and the interaction of these contaminants with the SPM will play a key role in regulating their transport and toxicity. The measure of adsorption potential applied in this research accounts for the differing SPM concentrations that are commonly detected in the catchment. However, it does not account for the variable adsorption capabilities of the SPM.

Another limitation of this work is that it has simplified the process of adsorption to the interactions of the adsorbate with the SPM in a laboratory environment. This has ensured that the data could be compared with previous research. However, in actual fact the speciation of contaminants will be highly dynamic in a natural setting. Dissolved ions will commonly complex with inorganic and organic ligands and this will often change their affinity for the adsorbent (Davis and Leckie, 1978; Mantoura et al., 1978; Vuceta and Morgan, 1978). For example, the complexation of copper by humic substances is well documented and significantly alters its behaviour in the natural environment (Davis, 1984; Mantoura et al., 1978).

7.1.4 Recommendations for Further Research

This research has provided important data on the adsorption capability of the glacial SPM for P, Cd and Cu. It demonstrated how the character and adsorption potential of the SPM evolved throughout the catchment. Such information will be increasingly important in assessing changes in water quality as land-use modification and climate change proceed into the future. Additional studies are recommended to determine the adsorption capability and potential of glacial SPM in other catchments. Such studies could be conducted in glacier-fed catchments with varying degrees of glacier cover. This may identify changes to the physicochemical characteristics of the SPM with decreasing

ice mass. It will also determine if key adsorption processes exist between catchments, and whether models of contaminant adsorption and transport on the glacial SPM can be widely applied or need to be site specific.

It is recommended that future studies use an improved method to collect SPM. Very recently, a new field protocol for collecting SPM has been published by the United States Geological Society. The method uses a portable continuous-flow centrifuge that can be deployed in the field to obtain SPM samples of sufficient quantity and quality for laboratory analysis (Conn et al., 2016). In any case, care must be taken with the collection method to ensure that the SPM is not significantly altered from its natural state and is representative of that occurring in the natural environment.

For surface complexation modelling, it is recommended that future studies use a dedicated, comprehensive suite of analytical procedures to fully characterise the phases implicated in adsorption. In this research, the monitoring of dissolved Fe, Al and Mn in solution during the adsorption experiments provided important data that assisted in the characterisation of adsorption phases in the SPM. However, the technique was not able to conclusively differentiate the speciation/crystallinity of these phases. This could be achieved with sequential extractions techniques that selectively target such fractions (Filgueiras et al., 2002; Gleyzes et al., 2002; Hall et al., 1996). Determining the reactive proportion of organic matter may also be achieved with dedicated extractions (Frimmel, 1998; Schnitzer and Schuppli, 1989). However, the application of this data may be limited given the significant spatial and temporal variation of the organic influence in the natural environment. A standardised method for determining the reactive surfaces present in sediments and SPM would be extremely valuable for guiding future research in the area, and in scenarios where models are used to predict environmental response and guide policy development.

The use of X-ray spectroscopy, including X-ray Absorption Near Edge Structure (XANES) and Extended X-ray Absorption Fine Structure (EXAFS) can provide important information on the speciation and adsorption characteristics of trace elements (Morra et al., 1997; O'Day, 1999). The use of such techniques could provide a comprehensive insight into the molecular scale processes that govern adsorption onto glacial SPM.

7.2 Synthesis: The Onyx River Catchment

7.2.1 What was the Character and Composition of the Polar SPM in the Onyx River Catchment, Antarctica?

In **chapter 5**, the character and composition of SPM collected throughout the Onyx River catchment was described. The SPM was dominated by fine, inorganic particles (mica, smectite, chlorite, quartz) < 5 µm in size with minor contributions of organic detritus and diatoms. The inorganic particles typically had a high degree of roundness which was attributed to their primary aeolian source. The finest particles remained in suspension throughout the meltwaters journey to Lake Vanda and were found to progressively weather down the catchment. The SPM was hypothesised to have a large adsorption capability owing to its fine particle size and contributions of reactive Al, Fe and Mn oxides.

Interestingly, the polar SPM from the Onyx River catchment was found to share a number of similar characteristics to the fresh glacial SPM detected in the Waitaki catchment. In general, both were dominated by extremely fine inorganic particles that had high SSAs and similar concentrations of acid-soluble Fe, Al and Mn. This was a surprising outcome given the significantly different composition, mechanisms of production, and morphology of the particles. However, the specific adsorption phases of the SPM were variable. The Fe oxides associated with the alpine SPM from the Waitaki catchment was characteristic of ferrihydrite, which may be generated during the weathering of sulphide minerals in the freshly eroded rock (Brown, 2002; Tranter, 2007). The dissolution profile for the Onyx River SPM was suggestive of more resilient, crystalline phases such as goethite or hematite. These have been previously identified in polar waters (Raiswell et al., 2008; Raiswell et al., 2006).

7.2.2 Is SPM an appreciable source of P to the catchment?

Suspended particulate matter is predicted to be a dominant source of bioavailable P to aquatic biota in the extreme, nutrient limited Onyx River catchment. Sequential extractions indicated that the majority of the SPM P was associated with primary phosphorus containing minerals (such as apatite) and is not expected to be readily bioavailable. Less than 20% was found to be associated with reactive metal oxides (Fe and Mn), clay minerals and organic matter. The SPM was also found to have a significant adsorption capability. In oxic waters, the SPM is predicted to be an efficient scavenger of

dissolved P, which is primarily mediated by adsorption onto Fe oxides associated with the fine, sub-micron sized particles. This P may be liberated from the particle surfaces for metabolic uptake when incorporated into benthic mats or exposed to the highly reducing conditions present in the bottom waters of Lake Vanda.

The flux of SPM in the Onyx River catchment was predicted over a 20 year period with the generation of an SPM-discharge rating curve that was applied to flow data collected by the McMurdo Long Term Ecological Research Network (LTER). The predicted SPM loads for the annual melt seasons were highly variable, ranging from 1.0 – 908.7 tonnes. So too were the predicted quantities of P, with loads varying from 0.6 – 515.2 kg of P. High flow events, such as those during the 2001/02 and 2008/09 austral summers, resulted in SPM loads up to three orders of magnitude greater than typical years. As such, the dominant source of P to the catchment is likely to be during these episodic events.

7.2.3 Implications

This research has provided much-needed data on the character, composition and adsorption capability of the polar SPM in the Onyx River catchment. When coupled with the streamflow and SPM flux data, it improved the estimates of the delivery of P into the extreme, oligotrophic Lake Vanda. Such data will be increasingly important as these unique aquatic systems respond to a changing climate.

The Onyx River is the primary source of meltwater and nutrients to one of the least productive aquatic systems on Earth, Lake Vanda. Phosphorus is a limiting nutrient in this catchment, which is due to the extremely limited concentrations in the water column and the small quantities of SPM associated with the meltwater. However, it is likely that the episodic flood events have a profound and long-lasting effect on the ecological productivity of the Lake. It is hypothesised that SPM is an important source of P to the benthic mats in the catchment. The vast majority of this SPM is expected to be transported to the catchment during high flow events. These events have been associated with significant warming of the valleys by down valley foehn winds. An increase in the frequency of these events will increase the transport of both meltwater and SPM to the system. Ultimately, this may initiate a shift in the physicochemical characteristics of Lake Vanda, and its biological structure and diversity (Castendyk et al., 2016; Lyons et al., 2006).

7.2.3 Limitations

A primary limitation of this work was that samples of SPM were only able to be collected during the limited sampling period in the 2016/17 melt season. At the time of sampling, the streamflow was already established and SPM concentrations were stable. Therefore, it was not possible to identify if compositional differences in the SPM exist during the "first flush" of the catchment and in high flow events. Sediments in the Wright Valley display significant spatial differences (Bate et al., 2008; Marra et al., 2017; Stumpf et al., 2012), and the speciation and quantities of P content may vary (Bate et al., 2008; Heindel et al., 2017). Coarser sediments associated with flooding flows may also have a lower reactivity. However, for the purposes of this research it was necessary to assume that the physicochemical characteristics and composition of the SPM were constant. This adds a degree of uncertainty to the P load estimates reported in this research.

Another limitation in this study was the limited body of SPM concentration data for the Onyx River. All data was mined from the "Hydrological Research Reports" collated by the Antarctic Research Programme from 1970 – 1986, and much was discarded from the analysis as it was deemed to be unreliable based on recent measurements in the field. The SPM-flow rating curve generated with the remaining data provided the best possible estimates of SPM loading into the catchment. However, the extrapolation of the curve to flows > 5000 L/s is likely to have a high degree of error, owing to the significant concentrations of SPM likely to be associated with these flows.

7.2.4 Recommendations for Future Research

It is recommended that future campaigns in the Wright Valley collect SPM samples for dedicated compositional and SPM concentration analysis across a range of flows. This would include the collection of SPM from initial stream flows and during periods of flood. Given the unpredictability of the flows, it is recommended that future sampling events collect time-stamped SPM samples that could be archived for future analysis. Over time this will result in a sufficiently large dataset in which optimized SPM-flow discharge curves could be constructed. This will aid in tracking the loads of SPM transported into the catchment, which will assist in the interpretation of both hydrological and ecological perturbations.

The specific bioavailability of P associated with the Onyx River SPM could be specifically investigated with the use of dedicated bioassays (Abell and Hamilton, 2013; Boström et al., 1988; Ellis and Stanford, 1988). This information would provide an important insight into the ability of the polar biota to utilise and recycle nutrients associated with the SPM.

7.3 References

Abell JM, Hamilton DP. Bioavailability of phosphorus transported during storm flow to a eutrophic, polymictic lake. New Zealand Journal of Marine and Freshwater Research 2013; 47: 481-489.

Adrian R, O'Reilly CM, Zagarese H, Baines SB, Hessen DO, Keller W, et al. Lakes as sentinels of climate change. Limnology and oceanography 2009; 54: 2283-2297.

Anderson SP. Biogeochemistry of Glacial Landscape Systems. Annual Review of Earth and Planetary Sciences 2007; 35: 375-399.

Barnett TP, Adam JC, Lettenmaier DP. Potential impacts of a warming climate on water availability in snow-dominated regions. Nature 2005; 438: 303.

Bate DB, Barrett JE, Poage MA, Virginia RA. Soil phosphorus cycling in an Antarctic polar desert. Geoderma 2008; 144: 21-31.

Benjamin MM, Leckie JO. Multiple-site adsorption of Cd, Cu, Zn, and Pb on amorphous iron oxyhydroxide. Journal of Colloid and Interface Science 1981; 79: 209-221.

Bibby RL, Webster-Brown JG. Characterisation of urban catchment suspended particulate matter (Auckland region, New Zealand); a comparison with non-urban SPM. Science of the Total Environment 2005; 343: 177-197.

Bibby RL, Webster-Brown JG. Trace metal adsorption onto urban stream suspended particulate matter (Auckland region, New Zealand). Applied Geochemistry 2006; 21: 1135-1151.

Boström B, Persson G, Broberg B. Bioavailability of different phosphorus forms in freshwater systems. Hydrobiologia 1988; 170: 133-155.

Brown GH. Glacier meltwater hydrochemistry. Applied Geochemistry 2002; 17: 855-883.

Casassa G, López P, Pouyaud B, Escobar F. Detection of changes in glacial run-off in alpine basins: examples from North America, the Alps, central Asia and the Andes. Hydrological Processes 2009; 23: 31-41.

Castendyk DN, Obryk MK, Leidman SZ, Gooseff M, Hawes I. Lake Vanda: A sentinel for climate change in the McMurdo Sound Region of Antarctica. Global and Planetary Change 2016; 144: 213-227.

Clarke G. Upper Waitaki limit setting process. Predicting consequences of future scenarios: Lake water quality. Environment Canterbury, 2015.

Conn KE, Dinicola RS, Black RW, Cox SE, Sheibley RW, Foreman JR, et al. Continuous-flow centrifugation to collect suspended sediment for chemical analysis. Techniques and Methods, Reston, VA, 2016, pp. 44.

Davis JA. Complexation of trace metals by adsorbed natural organic matter. Geochimica et Cosmochimica Acta 1984; 48: 679-691.

Davis JA, Leckie JO. Effect of adsorbed complexing ligands on trace metal uptake by hydrous oxides. Environmental Science & Technology 1978; 12: 1309-1315.

Dzombak DA, Morel Fo. Surface complexation modeling: hydrous ferric oxide. New York: Wiley, 1990.

Ellis BK, Stanford JA. Phosphorus bioavailability of fluvial sediments determined by algal assays. Hydrobiologia 1988; 160: 9-18.

Filgueiras AV, Lavilla I, Bendicho C. Chemical sequential extraction for metal partitioning in environmental solid samples. Journal of Environmental Monitoring 2002; 4: 823-857.

Frimmel FH. Characterization of natural organic matter as major constituents in aquatic systems. Journal of Contaminant Hydrology 1998; 35: 201-216.

Gleyzes C, Tellier S, Astruc M. Fractionation studies of trace elements in contaminated soils and sediments: a review of sequential extraction procedures. TrAC Trends in Analytical Chemistry 2002; 21: 451-467.

Gray D. Upper Waitaki catchment flows, water quality and ecology: state and trend. Investigations and Monitoring Group. Environment Canterbury, Christchurch, New Zealand, 2015.

Hall GEM, Vaive JE, Beer R, Hoashi M. Selective leaches revisited, with emphasis on the amorphous Fe oxyhydroxide phase extraction. Journal of Geochemical Exploration 1996; 56: 59-78.

Heindel RC, Spickard AM, Virginia RA. Landscape-scale soil phosphorus variability in the McMurdo Dry Valleys. Antarctic Science 2017; 29: 252-263.

Hodson A, Mumford P, Lister D. Suspended sediment and phosphorus in proglacial rivers: bioavailability and potential impacts upon the P status of ice-marginal receiving waters. Hydrological Processes 2004; 18: 2409-2422.

Immerzeel WW, van Beek LPH, Bierkens MFP. Climate Change Will Affect the Asian Water Towers. Science 2010; 328: 1382.

Lyons WB, Laybourn-Parry J, Welch KA, Priscu JC. Antarctic Lake Systems and Climate Change. In: Bergstrom DM, Convey P, Huiskes AHL, editors. Trends in Antarctic Terrestrial and Limnetic Ecosystems: Antarctica as a Global Indicator. Springer Netherlands, Dordrecht, 2006, pp. 273-295.

Mantoura RFC, Dickson A, Riley JP. The complexation of metals with humic materials in natural waters. Estuarine and Coastal Marine Science 1978; 6: 387-408.

Marra KR, Elwood Madden ME, Soreghan GS, Hall BL. Chemical weathering trends in fine-grained ephemeral stream sediments of the McMurdo Dry Valleys, Antarctica. Geomorphology 2017; 281: 13-30.

Milner AM, Brown LE, Hannah DM. Hydroecological response of river systems to shrinking glaciers. Hydrological Processes 2009; 23: 62-77.

Milner AM, Khamis K, Battin TJ, Brittain JE, Barrand NE, Füreder L, et al. Glacier shrinkage driving global changes in downstream systems. Proceedings of the National Academy of Sciences 2017; 114: 9770-9778.

Morra MJ, Fendorf SE, Brown PD. Speciation of sulfur in humic and fulvic acids using X-ray absorption near-edge structure (XANES) spectroscopy. Geochimica et Cosmochimica Acta 1997; 61: 683-688.

O'Day PA. Molecular environmental geochemistry. Reviews of Geophysics 1999; 37: 249-274.

Raiswell R, Benning LG, Tranter M, Tulaczyk S. Bioavailable iron in the Southern Ocean: the significance of the iceberg conveyor belt. Geochemical Transactions 2008; 9: 7.

Raiswell R, Tranter M, Benning LG, Siegert M, De'ath R, Huybrechts P, et al. Contributions from glacially derived sediment to the global iron (oxyhydr)oxide cycle: Implications for iron delivery to the oceans. Geochimica et Cosmochimica Acta 2006; 70: 2765-2780.

Schnitzer M, Schuppli P. Method for the Sequential Extraction of Organic Matter from Soils and Soil Fractions. Soil Science Society of America Journal 1989; 53: 1418-1424.

Smith KS. Metal sorption on mineral surfaces: an overview with examples relating to mineral deposits. The Environmental Geochemistry of Mineral Deposits. Part B: Case Studies and Research Topics 1999; 6: 161-182.

Sommaruga R. When glaciers and ice sheets melt: consequences for planktonic organisms. Journal of Plankton Research 2015.

Stumpf AR, Elwood Madden ME, Soreghan GS, Hall BL, Keiser LJ, Marra KR. Glacier meltwater stream chemistry in Wright and Taylor Valleys, Antarctica: Significant roles of drift, dust and biological processes in chemical weathering in a polar climate. Chemical Geology 2012; 322: 79-90.

Tranter M. Glacial Chemical Weathering, Runoff Composition and Solute Fluxes. Glacier Science and Environmental Change. Blackwell Publishing, 2007, pp. 71-75.

Viers J, Dupré B, Gaillardet J. Chemical composition of suspended sediments in World Rivers: New insights from a new database. Science of The Total Environment 2009; 407: 853-868.

Vuceta J, Morgan JJ. Chemical modeling of trace metals in fresh waters: role of complexation and adsorption. Environmental Science & Technology 1978; 12: 1302-1309.

Webster JG, Brown KL, Webster KS. Source and transport of trace metals in the Hatea River catchment and estuary, Whangarei, New Zealand. New Zealand Journal of Marine and Freshwater Research 2000; 34: 187-201.

Appendix A – Supplementary Information on Techniques:

A1: Diffuse Gradients in Thin Films (DGTs)

Introduction

The concentrations of dissolved trace metals and nutrients are typically measured with grab samples that are filtered through 0.45 µm filter membranes. This is in line with the current operational procedure to identify the "dissolved" ion of interest (Chapman et al., 1996). However, this fraction may be associated with colloids <0.45 µm in size and/or complexes that are common in natural waters. Additionally, grab samples can fail to account for the temporal variations in water composition, which can vary substantially in glacier-fed catchments (Anderson et al., 2003). This was a consideration in the polar Onyx River catchment, where the flow of the Onyx River is highly dependent on glacial melt and flows can vary by the hour (Chinn and Mason, 2015). The concentrations of dissolved nutrients in this catchment are also extremely low which could affect their detection. For these reasons, the diffusive gradient in thin-films (DGT) technique was applied to study the in-situ concentrations of reactive phosphorus and trace metals in the catchments. The technique involves the use of a passive sampler, which is deployed in-situ for a known period of time. Post-deployment analysis of the probes provides a means to understand the time-weighted average concentration of a solutes, as well as complimentary information on their geochemical behaviour and bioavailability in the environment.

The DGT device has three layers: a resin gel which is selective for the solute of interest; a polyacrylamide hydrogel which serves as a well-defined diffusive layer; and a protective filter membrane (**Figure A1**). These are then sealed in a plastic case so that only the filter is exposed to the water. Once deployed, the gel establishes a steady-state diffusion gradient between the water column and the resin gel. The solute of interest in the water column may pass through the diffusive layer to be irreversibly bound to the adsorbing resin. After a known deployment time, the DGT probes are removed and deconstructed. The solute is eluted (i.e. with acid) and then quantitatively analysed with a sensitive analytical method. The 'DGT-labile' concentration of the solute is then calculated with Fick's first law of diffusion.

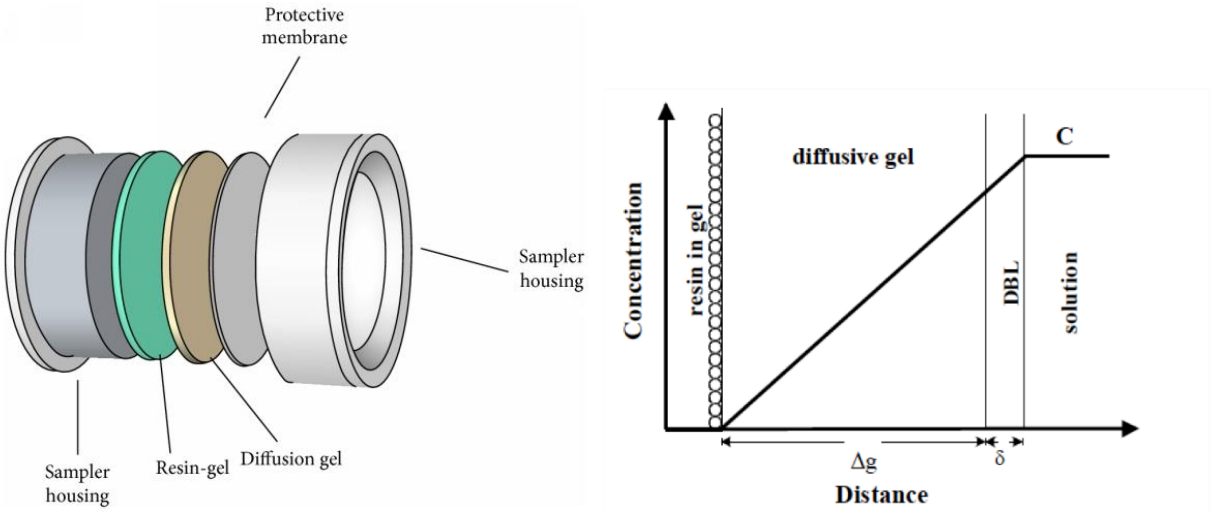

Figure A1. (Left) A DGT probe and its internal components prior to construction. (Right) The principle of the DGT technique – The concentration of the solute (C) decreases across the diffusive gel as the solute approaches the resin gel. The total thickness of the diffusive layer = Δg (gel thickness) + δ (diffusion boundary layer). Image Credits: Left: Knutsson et al. (2014). Right: Wikipedia – DGT theory (Creative Commons).

Methods

DGT probes were constructed in a clean-lab at Lincoln University, New Zealand. The plastic cases were thoroughly acid-washed for 24 hours prior to rinsing with ultrapure H_2O. Polyacrylamide hydrogels of 0.4, 0.8 and 1.6 mm thicknesses were made in the laboratory as per the methods detailed by Zhang et al. (1998) and Zhang and Davison (1995). The resin gels for the phosphate (P) probes were impregnated with ferrihydrite. The resin gels for the trace metal probes were impregnated with a chelating resin (Chelex 100 - Bio-Rad Laboratories). The probes were assembled with acid washed tweezers in a laminar flow cabinet to prevent contamination. These were double-bagged and kept chilled until deployment.

The probes were deployed in triplicate for each gel thickness at the Lower Wright and Vanda Weir sites located on the Onyx River. The probes were held in a custom built plastic frame, which kept the probes aligned and submersed for the duration of the deployment. The probes were deployed for 120.47 hours from 15/12/2016 – 20/12/2016 at the Lower Wright Weir. For the Onyx River at the Vanda Weir, the probes were deployed for 168.89 hours on the dates 22/12/2016 – 29/12/2016.

The temperature of the meltwater was recorded every 10 minutes with the use of two iButtons© (model number DS1922L) attached to the probe holder. The water during this period varied

in temperature from 0.1 – 10.1^{0}C (median = 3.5^{0}C) for the Onyx River at Lower Wright Weir, and 0.1 – 7.2^{0}C for the Onyx River at Vanda Weir (median = 3^{0}C). Despite the low temperatures, the Onyx did not freeze during the deployment period. The median temperature of the river was determined and this value was used to select the diffusion coefficient for the analyte of interest. The diffusion coefficients supplied by DGT Research© (DGTresearch.com) were used for the purposes of this research. Additional probes were transported to Antarctica but were not deployed for later analysis as analytical blanks.

After the probes were removed from the water column, the probes were rinsed with ultrapure H_2O prior to being double bagged and chilled until they could be analysed later in New Zealand. The probes were opened in a laminar flow cabinet, and the resin gels transferred to clean 15 ml polypropylene tubes with acid-washed tweezers. For the P probes, the resin gels were eluted with 10 ml of 0.25 M H_2SO_4. For the trace metal probes, the probes were eluted in 5 ml of 1 M of trace grade HNO_3. After 24 hours, the eluted resin gels were removed prior to analysis of the eluent. Phosphorus concentrations were determined using the ascorbic acid method (APHA, 2005), and trace metals by ICP-MS as described in **Chapter 2, Section 2.2.3**. The absolute mass of the solute of interest was determined with **Equation A1**.

$$\boldsymbol{M = \frac{C_e(V_g + V_e)}{f_e}} \qquad (\boldsymbol{A1})$$

Where M = absolute mass of adsorbate in the resin gel; C_e = measured concentration of adsorbate in the eluent; V_g = gel volume (cm^3); V_e = eluent volume (ml); f_e = elution factor/efficiency. The absolute mass of adsorbate calculated from this equation is then used to calculate the 'DGT-labile' concentration of solute using **Equation A2**:

$$\boldsymbol{C_{DGT} = \frac{M\Delta g}{DtA}} \qquad (\boldsymbol{A2})$$

Where C_{DGT} = is the DGT labile concentration in solution; M = measured mass of solute accumulated on the resin gel during deployment; Δg = total diffusion layer thickness, i.e. the thickness of the gel and filter membrane; D = diffusion coefficient of solute in the diffusion gel and filter; A = exposed area of diffusion gel; and t = time deployed.

When DGTs are immersed in solution, a diffusion boundary layer (DBL) forms at the interface of the filter membrane and the solution phase. This layer may act as an extension of the diffusion layer

Δg, where a non-uniform concentration of the solute forms due to diffusive control. In flowing rivers, the DBL is typically so small it can be largely ignored (Warnken et al., 2006). However, a sufficiently large DBL may form when DGTs are deployed in slow flowing and stagnant waters (i.e. lakes). This may result in an underestimation of the true DGT labile concentrations of solute if it is not accounted for. In this instance, the deployment of DGT probes with different diffusive gel thicknesses can allow for the calculation of the DBL, which can be incorporated into the calculations to provide a more accurate determination of C_{DGT}. A plot of M vs $1/\Delta g$ will be non-linear and there will be error in the value of Δg. In this instance, a plot of $1/M$ vs Δg linearizes the data and allows for an estimation of the DBL thickness (Warnken et al., 2006). In this study, the Onyx River sites were both flowing in the range of 1-2 m^3/s, with a constant flow of water passing the probes. The plots of M vs $1/\Delta g$ were found to be linear, and no correction was necessary.

Results

In general, the DGT-labile concentrations of trace metals and P were lower than the dissolved concentrations measured in the grab samples. The exceptions were the DGT-labile concentrations of Fe (2.6 - 2.8 µg/L) and Mn (1.1 – 1.2 µg/L) measured at the Onyx at Lower Wright weir, which were greater than the dissolved concentrations detected in a filtered sample. Of significant interest to this research was the complete lack of DGT-labile P detected with the probes despite the lengthy deployment.

Table A1. DGT labile concentrations (µg/L) detected in the upper and lower Onyx River over 5 and 7 day deployment times respectively. DL = Detection Limit. The dissolved concentrations determined in filtered (0.45 µm) grab samples are included for comparison.

	DGT Concentrations					
	Al	**Fe**	**Mn**	**Cu**	**Cd**	**P**
Onyx - Lower Wright	4.2 - 4.5	2.6 - 2.8	1.1 - 1.2	0.05 - 0.06	0.0007 - 0.0008	< DL
Onyx - Vanda Weir	20.0 - 20.8	0.4 - 0.7	1.4 - 1.5	0.1 - 0.15	0.0004 - 0.001	< DL
	"Dissolved Concentrations"					
Onyx - Lower Wright	28.6	2.1	0.6	0.27	0.009	< DL
Onyx - Vanda Weir	30.5	24.2	0.87	0.23	0.008	< DL

DGT Discussion

The DGT probes were deployed successfully in the Onyx River despite the extreme nature of the system. The resulting concentrations of DGT-labile trace metals and nutrients were extremely low, and were generally lower than the "dissolved" concentrations typically measured with a single filtered sample. This indicates that much of the dissolved flux is not likely to be readily bioavailable to aquatic biota in the catchment, and provides additional evidence as to why the terminal Lake Vanda is one of the least productive lakes on Earth. Of particular interest to this study was the complete lack of P. The ramifications of this finding are discussed in **Chapter 6**.

DGT Limitations

The DGT probes were prone to issues when deployed for long periods in this research. Upon retrieval from the water column, it was found that a number of probe casings were loose. When opened in the lab, these probes typically found to be contaminated with sediment. These results were excluded from the data analysis. Other possible sources of error include: contamination due to improper manufacture and handling; biofouling of the probes; analytical errors when determining the concentration of solute in the eluent; and the use of an improper diffusion coefficient (Kreuzeder et al., 2015). In this study, care was taken to mitigate such errors. However, there may be some uncertainty in the diffusion coefficient used given the highly variable temperatures in the Onyx River.

DGT Recommendations:

DGT is an excellent technique that provides important information of the speciation, behaviour and bioavailability of trace metals and nutrients in aquatic environments. For this reason, DGT can be applied to determine the time-weighted concentrations of contaminants in both urban and agricultural settings. However, the current design of the probe limits its use by operators that are not highly trained in their handling. Additionally, the current design of the probe makes it prone to failure in applications where it is subjected to turbulence (i.e. flowing rivers). Therefore, it is recommended that the probe design is optimized for easy handling and resilience.

A2: Time-Integrated Mass-flux sampler

Introduction

One of the major difficulties encountered in this research was collecting sufficient quantities of SPM for the characterization and adsorption experiments. In the absence of more modern equipment to automate the collection process (automated pump sampler, continuous-flow centrifugation), large quantities of water were required to be filtered to obtain small quantities of material. This was both extremely time consuming and inefficient. Therefore, the use of a passive sampler was trialled to collect SPM in the field. The Time-Integrated Mass-flux sampler (TIMs) sampler, first developed by Phillips et al. (2000), was built and deployed in both the Waitaki and Onyx River catchments.

The basic concept of the sampler is to slow the velocity of the flowing water to such a degree that sedimentation of SPM occurs. Water enters a narrow inlet and encounters a dramatic increase in surface area (~600x) inside the expansion chamber. A proportion of the SPM will be is entrained in the sampler while water exits through the outlet. The sampler was designed to be streamlined in order to minimise the effect of flow disruption which could bias the particle size distribution (PSD) of SPM collected in the sampler (**Figure A2)**.

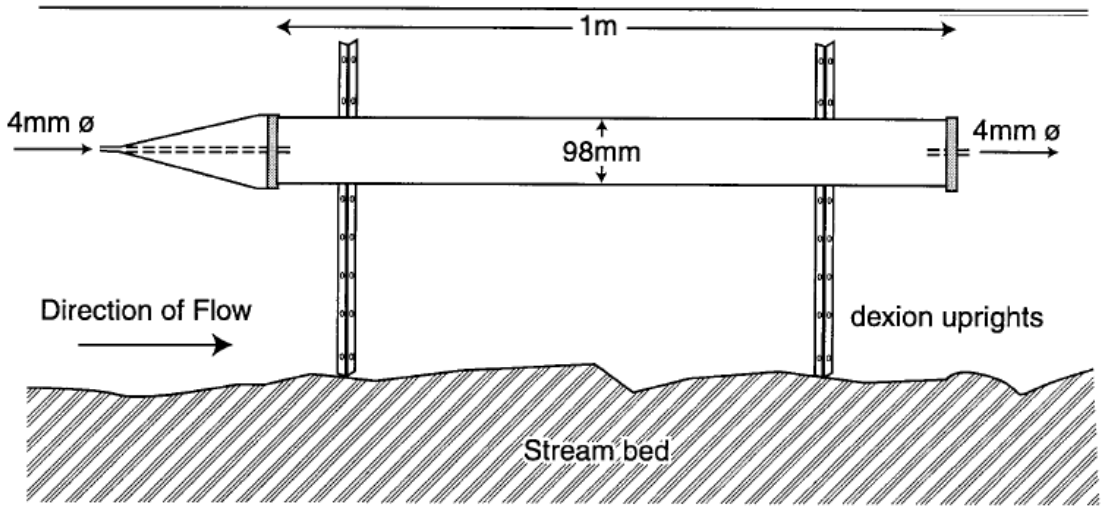

Figure A2. Diagram of Time-Integrated Mass-flux sampler. Image Credit: Copied from Phillips et al. (2000).

Construction:

In this study, a TIMs sampler was made with the assistance of Nick Oliver, a technician in the chemistry department at the University of Canterbury. The sampler was constructed with the dimensions reported by Phillips et al. (2000), using a 1m length of polyvinylchloride (PVC) piping with 150 mm internal width. This was sealed with threaded PVC caps with internal O-rings. Holes were drilled in the centre of the caps and fitted with inlet and outlet tubes that were made on a lathe. These were sealed with silicone sealant. The cone that was fitted to the inlet was formed with a flat sheet of PZC and a vacuum manifold. Adjustable clamps and rods were fitted to the tube so that it could be deployed at variable heights in a riverine environment.

Deployment:

The TIMs sampler was pre-rinsed with river water three times on site, pre-filled with water and assembled prior to deployment. The sampler was placed in the water with the pointed head facing towards the flow. The height was then adjusted to 60% of the water column depth with the adjustable rods, and secured in place with rocks and additional stakes (**Figure A3**). The sampler was left for a period of 5-7 days in the Waitaki and Onyx River catchments. After the deployment period, the captured water was collected in clean, pre-rinsed 20 L plastic containers. For the Waitaki catchment, these were transported back to the lab where the water was filtered through 0.45 µm nitrocellulose filter membranes with a vacuum pump. In the Onyx River catchment, the water was filtered with the assistance of a Nalgene© 300 ml polysulfone graduated filter holder and a hand-operated PVC vacuum pump. The resulting material was sonicated off the membranes and freeze dried at the University of Canterbury for later analysis. The particle size distributions of the particulate matter was determined with a Horiba LA-950V2 laser diffractometer as described in **Chapter 2, Section 2.2.4.1**.

Figure A3 The Time-Integrated Mass-flux sampler (TIMs) sampler, deployed in the Tasman River (Top) and the Clarks Stream and Onyx River (Bottom). Image Credits: Phil Clunies-Ross

Results

The TIMs sampler was able to collect appreciable quantities of SPM from both the Tasman and Onyx Rivers and the Clarks Stream. However, there were significant differences in the PSDs measured between the grab samples and that recovered by the TIMs sampler. In all cases, the TIMs average particle volume was greater than the grab samples. The dramatic differences in the number size distribution indicates that the finest particles were not retained by the TIMs sampler (**Table A2 and Figure A4**)

Table A2. The Particle size distributions (PSD) are presented as the size (µm) in which 50% (D50) of the particles pass for volume and number analysis. The results of the single grab samples, and those obtained by the TIMs sampler are included for comparison.

Site	Volume	Number	Volume	Number
	D50 (µm)			
	Grab samples		TIMs samples	
Tasman River	3.22	0.19	5.80	2.89
Clarks Stream	5.02	2.01	11.96	4.86
Onyx River	5.55	0.17	8.27	2.25

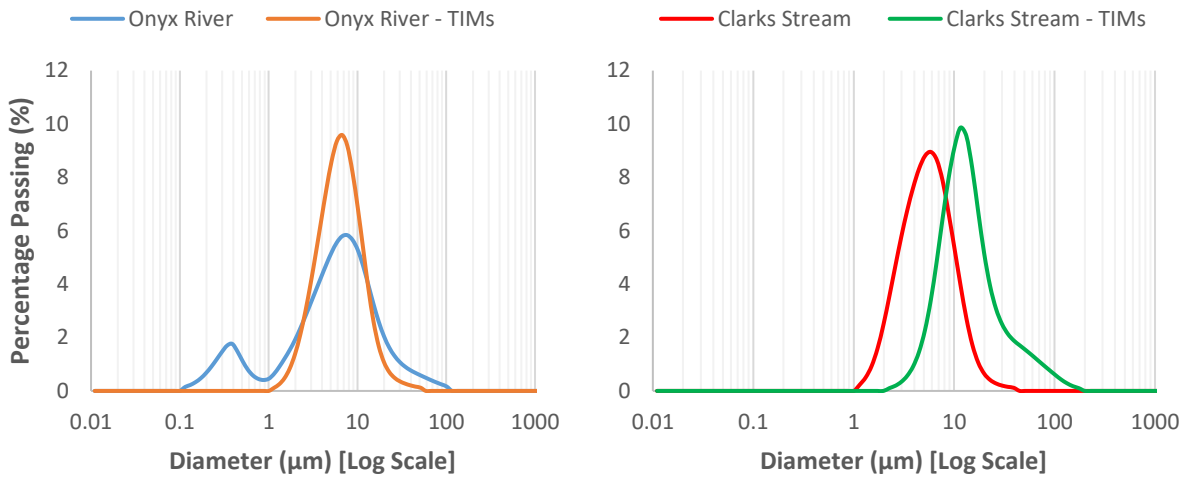

Figure A4. Particle size distributions (PSD) of chemically dispersed SPM ($(NaPO_3)_6$) from the Onyx River and the Clarks Stream in the Wright Valley, Antarctica. The variation in the PSDs between the grab sample SPM and that collected with the TIMs sampler is evident.

Discussion

The use of the TIMs sampler was desirable on account of its practicality and cost, and its ability to collect samples large enough to be useful in this study. However, the significant differences in the particle size distribution of the samples meant they could not be used for many of the geochemical analyses conducted in this research. A number of the samples were used for X-ray diffraction analysis, which provided useful information that was complimentary to the SEM/EDS work undertaken in **Chapters 2 and 5**.

The adsorption ability of the SPM was often highly correlated with its particle size (**Chapter 2)**. Therefore, the use of the TIMs samples could have resulted in significant errors in the experimental data, and a deviation from what is actually occurring in the water column. For this reason, it is not recommended that SPM collected with TIMs samplers be used for adsorption experiments.

Appendix B (Chapter 2)

Trace Metal Recovery

The recovery of trace metals from the PACs-2 marine reference sediment during SPM and sediment digestions (**Chapter 2, Section 2.2.4.2**) are detailed in **Table B3**.

Table B3. Recovery of trace elements for PACs-2 marine reference sediment as determined by ICP-MS.

Element (Atomic Mass)	Reference mg/kg	Recovery - range (%)
Mn (55)	440 ± 19	62.7 – 82.4
Co (59)	11.5 ± 0.3	93.9 - 96.7
Ni (60)	39.5 ± 2.3	81.9 – 100.9
Cu (63)	310 ± 12	85.6 – 98.0
Zn (66)	364 ± 23	86.8 - 114.6
As (75)	26.2 ± 1.5	113.6 – 127.4
Mo (95)	5.43 ± 0.28	80.0 - 88.7
Cd (111)	2.11 ± 0.15	90.1 – 105.0
Sb (121)	11.3 ± 2.6	74.8 – 106.4
Pb (208)	183 ± 8	72.5 – 92.1

Surface Sediment Character and Composition

The character and composition of surface sediments collected throughout the Waitaki catchment were also determined in this research. This was done to investigate its application as an analog in analytical procedures where insufficient SPM was available. A summary of this data is presented below.

Particle Size Distributions and Surface Area

The PSD data generated for the surface bed sediment is presented in **Table B4**. The median volume's (D50's) for the dispersed sediment show a general increase in particle size with progression down the catchment. The lowest D50 of 5.6 µm was measured at the Tasman River, while the largest of 15.6 µm was measured at the Lower Waitaki. A considerable reduction in the D50s was measured after H_2O_2 and NaOH digestions at all sites. The PSD's of the chemically dispersed sediments is presented in Figure 17. All PSD's had a single distinct mode.

Table B4. PSD Median volumes (D50) for untreated, dispersed, and digested surface sediments.

Site	Distance	Dispersed $(NaPO_3)6$	H_2O_2	H_2O_2 + NaOH	SSA (MB)	CEC (MB)
	(km)	D50 (µm)			m^2/g	meq/100g
2	5	5.6	3.5	2.3	**292**	2.8
4	45	7.7	4.2	2.3	**583**	11.3
7	140	12.2	8.8	3	**876**	25.5
8	210	15.6	10.4	4.4	**730**	17.7

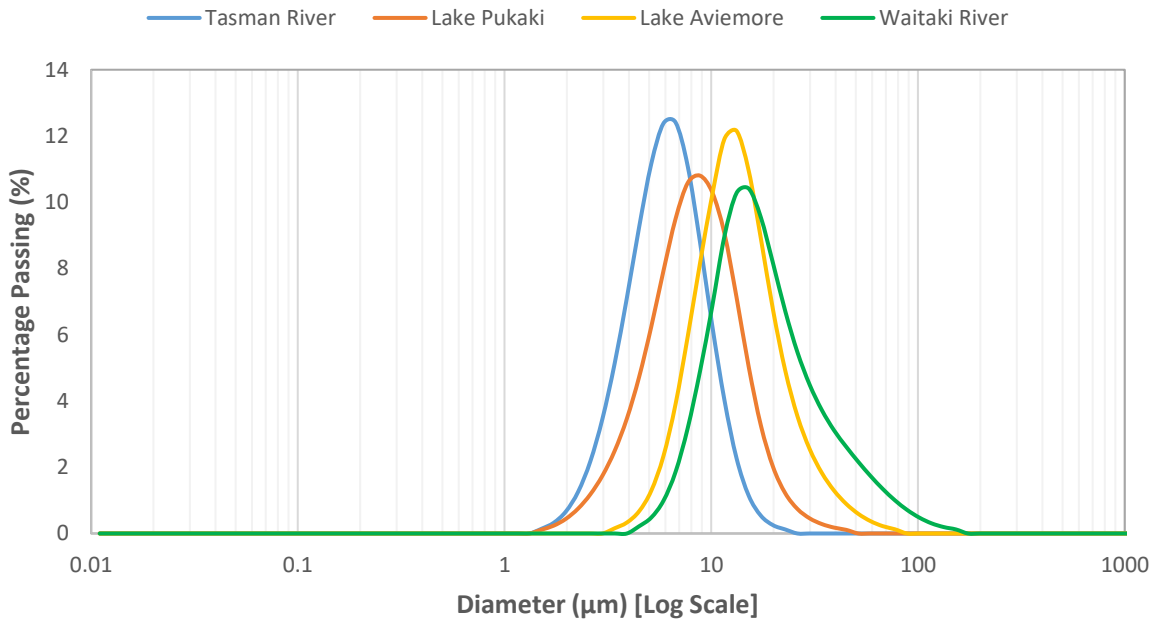

Figure B5 Particle size distributions for chemically dispersed ($(NaPO_3)_6$) surface sediments collected throughout the Waitaki Catchment.

The SEM imaging clearly indicated that a greater proportion of biogenic particles were present in the sediment at all sites below the Tasman River. The surface sediments appear to be similar in character and composition with inorganic particles dominating the character throughout the catchment (**Figure B6**). The elemental composition of the sediments is presented in **Tables B5 - B6**. Little variation in the elemental composition determined by EDS mapping was detected. The CIA and WIP profiles were similar to those in the SPM (**Figure B7**). An increase of ~4 % TOC was measured in sediments in the lower catchment. Higher Mn concentrations were measured in the Lake Aviemore Sediment, while a decrease in the acid-soluble concentrations of Al and Fe was measured in the Lower Waitaki surface sediment. The concentrations of acid-soluble Cu, Zn, Cd and Pb appeared to decline downstream. Comparisons of the surface sediment's composition are shown in Figures 19 and 20.

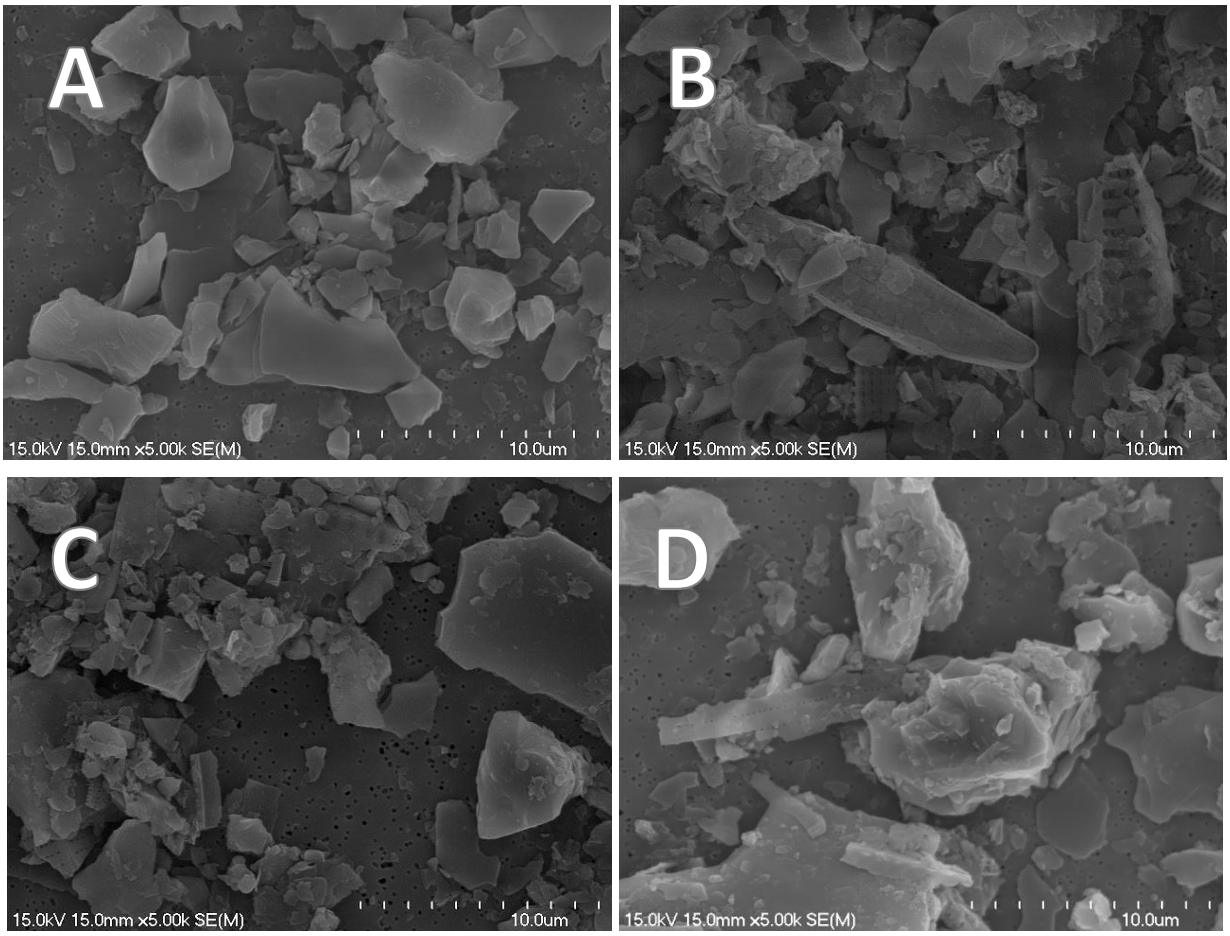

Figure B6. SEM images of surface bed sediments retrieved from sites progressing down the length of the Waitaki Catchment. Consistent 5000x magnification maintained for all images. Full scale bar is 10 μm: (A) Sediment from the Tasman River; (B) Lake Pukaki; (C) Lake Aviemore; (D) Waitaki River.

Table B5 Elemental composition of surface sediments obtained by 400 x 400 µm scan; weight % by EDS mapping analysis of SPM. TOC (% weight SPM) determined by combustion.

Site	Na	K	Mg	Ca	Fe	Al	Si	S	TOC	CIA	WIP
2	1.9	3.9	1.6	0.9	4.7	10	23.3	0.1	6.3	69	62.7
4	1.8	3.2	1.4	0.9	4.4	8.9	23.9	0.1	9	68.8	57.8
7	1.5	2.4	1.4	0.8	5.1	8.4	23.1	0.1	10.3	72.6	46.9
8	1.6	2.7	1.4	0.7	4.3	8.7	23.8	0.1	10.1	71.4	51.1

Table B6 Acid soluble composition of surface sediments in mg/kg after digestion in hot concentrated nitric acid. Total phosphate in mg/kg after autoclave assisted persulphate digestion.

Site	Al_{as}	Mn_{as}	Fe_{as}	Co_{as}	Ni_{as}	Cu_{as}	Zn_{as}	As_{as}	Cd_{as}	Pb_{as}	TP_{as}
2	30607	675	35317	16.5	26	55.7	119.3	14.9	0.31	26.9	368
4	28759	576	29837	13.4	23.2	38.6	102.5	16.3	0.24	26.2	634
7	29283	1126	37725	15.3	19.5	45.1	79.3	14.8	0.11	19.3	987
8	21274	419	24921	8.8	15.7	44.1	63.6	3	0.1	11.9	816

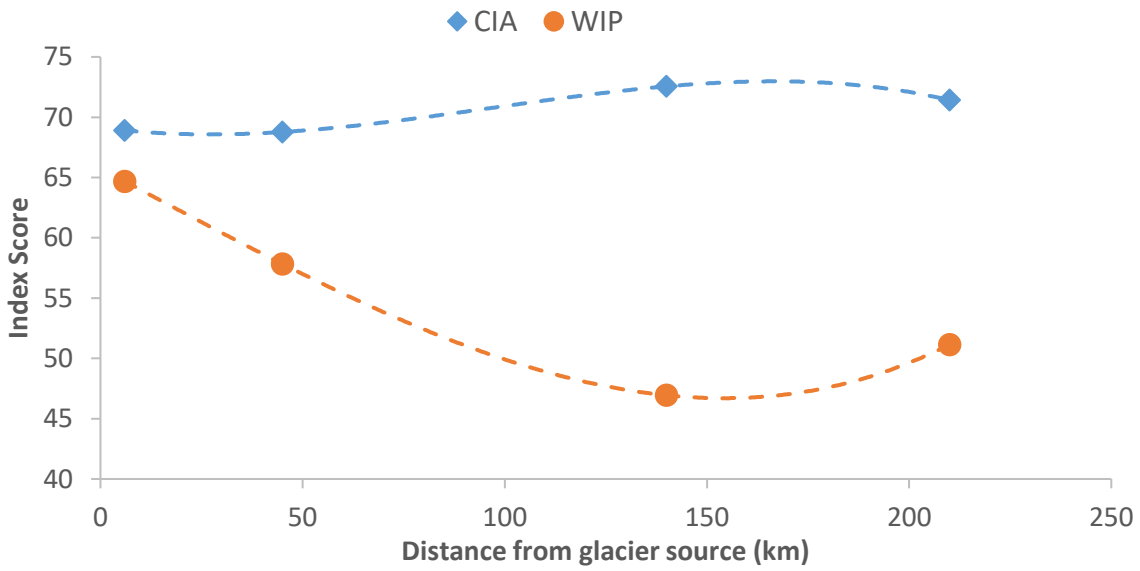

Figure B7 Chemical index of alteration (CIA) and Weathering Index of Parker (WIP) scores calculated for surface sediments collected with progressive distance from the glacial source.

Specific Surface Area

A combination of techniques were trialled to determine the specific surface area of surface sediments collected from the Waitaki catchment, and gauge their suitability for use with the small quantities of SPM available.

The para-nitrophenol method by Theng (1995) and Hedley et al. (2000) was first tested. First, solutions of 10, 20, 30, 40 and 50 mmol PNP were made by dissolving pNP in xylene at 80°C in a water bath. A 2.5 ml aliquot of this solution was each equilibrated with 0.1g of sediment in glass vials and mixed on an end-over-end mixer for 2 hours at constant temperature (20 ± 1°C). The vials were then centrifuged at 500x for 10 minutes. A 25 µl aliquot from each tube was next transferred into 50 ml centrifuge tubes containing 50 ml of deionized water made up to pH 12 with 1M NaOH. All samples were mixed for a further 10 minutes before standing for 20 minutes. The layer of xylene was removed with a pipette and the concentration of the aqueous phase was determined at 400 nm with a HACH DR 6000. The SSA was determined with **Equation B1**:

$$\boldsymbol{SSA = V_m N a_s \cdot 10^{-24}} \qquad (\boldsymbol{B1})$$

Where: V_m (µmol/g) is the surface monolayer binding capacity of pNP; N= Avogadro's number (6.02 $\times 10^{23}$/mol); a_s is the area covered by one pNP molecule (0.424 nm^2). In the case where the isotherm did not plateau, V_m was obtained by applying a Langmuir isotherm **Equation B2**:

$$\frac{\boldsymbol{C}}{\boldsymbol{A}} = \frac{\boldsymbol{1}}{\boldsymbol{K}} + \frac{\boldsymbol{C}}{\boldsymbol{V_m}} \qquad (\boldsymbol{B2})$$

Where: C is the equilibrium concentration on pNP (mM); A is the amount of pNP adsorbed and K is a constant.

The Brunner, Emmett and Teller (BET) method was also trialled at the University of Canterbury with the use of a Micrometrics Gemini 2385. An accurately weighed quantity (~1g) of sediment was dried with a VacPrep Degasser© for 48 hours at 60^0C, and then re-weighed. The SSA was then determined by N_2 gas adsorption and the construction of a BET isotherm with the Gemini 2.01 software.

The methylene blue method, as described in **Chapter 2, Section 2.2.4.3** was tested for comparison. It is clear that the results vary a great deal between the techniques (**Table B7 and Figure B8**). However, similar relative SSA values were measured. The SSA measured by methylene blue increased from 292 - 876 m^2/g with progressive distance down catchment. Interestingly the lowest SSA was measured for the Tasman River surface sediment. The greatest value of 876 m^2/g was measured for surface sediments at Lake Aviemore. A similar trend was measured with para-nitrophenol with SSA's ranging from 9.5 – 21.6 m^2/g. The BET surface area was only measured in samples from the Tasman River and Lake Aviemore. Once again, the SSA at Lake Aviemore was greater (9.2 m^2/g) than at the Tasman River (6.6 m^2/g).

Table B7. The specific surface areas (SSA) for surface bed sediments collected in the Waitaki Catchment determined by methylene blue (MB), pare-nitrophenol (PNP) and the BET method. The cation exchange capacity (CEC) was determined from MB adsorption. "na" is "not analysed".

Site	SSA (MB)	SSA (p-NP)	SSA (BET)
	m^2/g		
2 - L. Tasman	292	9.5	6.6
4 - L. Pukaki	583	14.6	n.a
7 - L. Aviemore	876	18.3	9.2
8 - Waitaki River	730	21.6	n.a

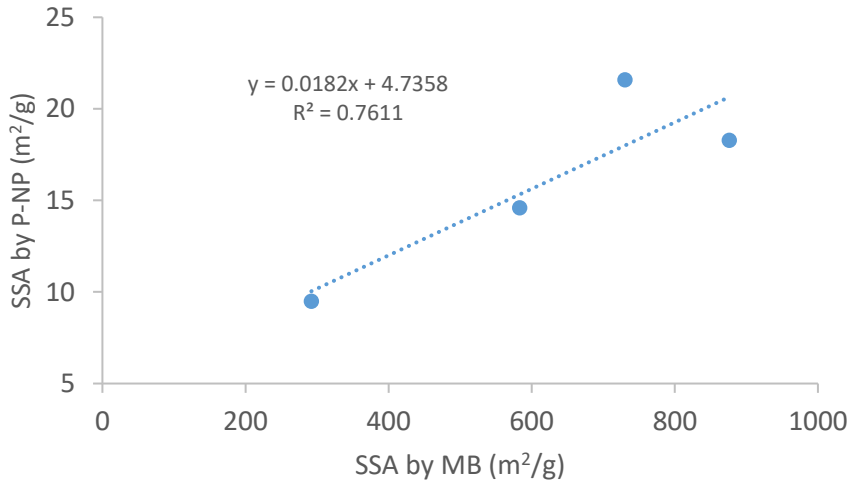

Figure B8 Comparison of specific surface area determined with the methylene blue (MB) technique and by para-nitrophenol (P-NP).

Particle Size Distribution Analysis

The particle size distribution (PSD) of untreated SPM collected from the lower Waitaki catchment is presented in **Figure B9**. Significant discrepancies to the PSDs of SPM treated with sodium hexametaphosphate ($(NaPO_3)_6$ were evident in these samples, and it is highly likely that large flocs were generated during the transport and storage of the SPM prior to analysis.

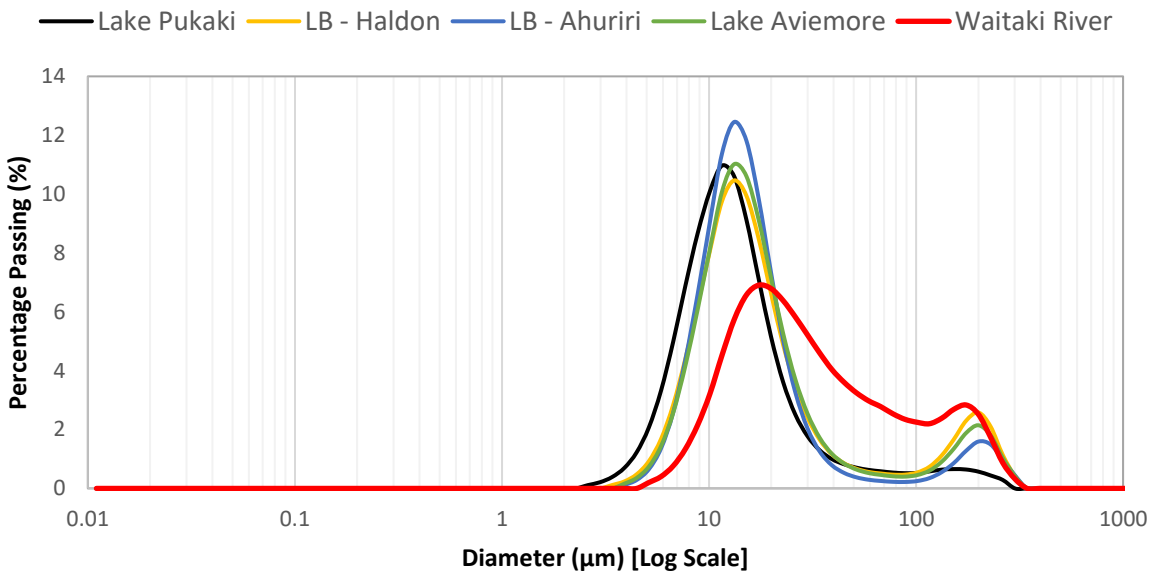

Figure B9. Particle size distributions of untreated SPM in the lower Waitaki Catchment.

Appendix C (Chapter 3)

SPM Concentration/Turbidity Relationship

The relationship between turbidity (NTU) and the concentrations of suspended sediments collected throughout the study were plotted to generate simple linear relationships (**Figure C10**). The inclusion of the high turbidity data resulted in over-predictions of SPM for low turbidity samples (NTU <30). Therefore, a separate relationship was generated to minimize this influence. The resulting relationships were applied to turbidity data sourced from the Environment Canterbury Open Data Portal to estimate the SPM concentrations of the Waitaki catchment water as described in **Chapter 3, Section 3.2.4**. It must be noted that the dataset is limited and could be optimized with the collection of additional samples throughout a range of environmental conditions and seasons.

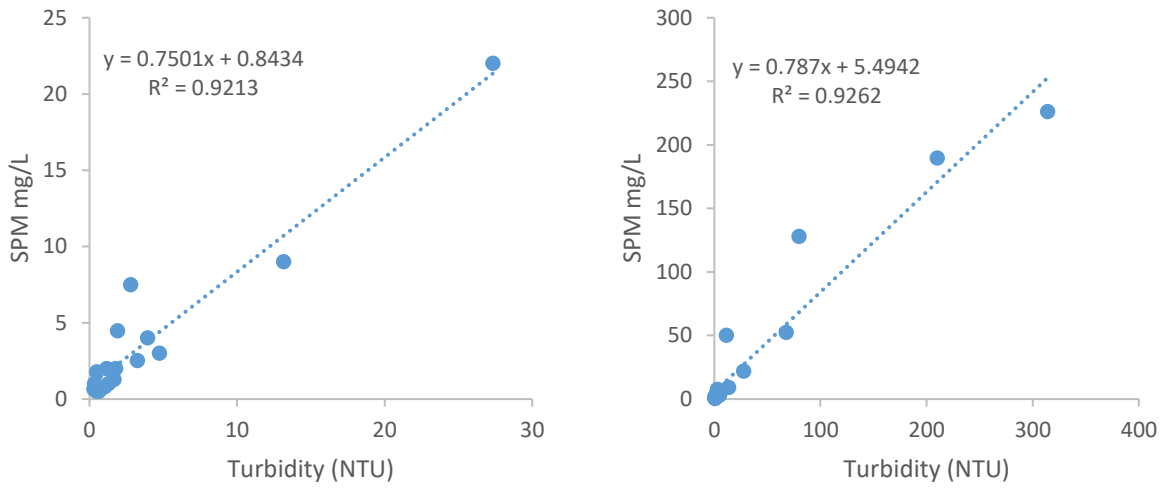

Figure C10 Relationships generated between SPM concentrations (mg/L) and turbidity (NTU) data collected in this study.

Modelling Parameters Applied in Visual Minteq

The following tables detail the modelling parameters that were used in Visual Minteq 3.1 to model the behaviour and adsorption of phosphorus (P) onto SPM in the Waitaki catchment. The natural water quality parameters are detailed in **Table C8.**

Table C8. Major ion chemistry and modelling parameters of water collected in the Waitaki catchment.

	pH	pE	Na	Mg	K	Ca	CO3	Cl	F	SO4	NO3
Glacier Ice	5.65	9	0.17	0.01	0.11	0.24	4.92	0.19	0.04	0.19	0.33
Lake Tasman	7.33	9	1.59	0.44	0.65	9.58	24.09	0.34	0.02	8.19	0.14
Tasman River	6.86	9	1.48	0.50	0.53	8.88	24.58	0.39	0.01	6.05	0.00
L. Pukaki	6.97	9	1.43	0.48	0.59	8.20	24.58	0.47	0.04	5.09	0.10
L. Benmore - Haldon	6.93	9	1.77	0.66	0.58	8.43	31.47	0.46	0.03	4.60	0.07
L. Benmore - Ahuriri	7.55	9	2.13	0.77	0.43	5.97	21.64	0.68	0.04	3.13	0.08
L. Aviemore	7.78	9	1.73	0.62	0.52	7.97	24.58	0.54	0.02	4.41	0.00
Waitaki River	7.52	9	2.85	1.24	0.87	10.73	38.35	0.44	0.04	4.99	0.00

The concentrations of reactive trace metals (Fe, Al, Mn) applied in Visual Minteq were determined after the SPM was treated with HNO_3 at pH 2 for 24 hours. An alternative method was to determine the concentrations of reactive metals from water samples collected in the field. The general method in this instance is to subtract the acid-soluble concentrations from a filtered (0.45 µm) sample

from those determined in an unfiltered sample. When standardized to 100 mg/L (**Table C9**), this was found to grossly overestimate the adsorption capacity of the Waitaki SPM. It is hypothesized that the prolonged acid treatment of the water samples at pH < 2 digests resilient mineral phases that do not necessarily contribute to the adsorption. It is also likely that fine colloidal particles < 0.45 µm pass through the filter membrane and complicate the results. In any case, this method is not recommended for the purposes of modelling the adsorption behaviour and capacity of SPM.

Table C9. Comparison of Methods used to determine the reactive concentrations of trace metals (Fe, Al and Mn) used in geochemical modelling.

	Concentrations of trace metals determined from water samples (Unfiltered minus filtered), and standardised to 100 mg/L for the purposes of geochemical modelling.							**Concentrations liberated from the SPM after acid treatment (pH 2 for 24 hours).**		
Sample Site	**Water Concentrations (ug/l)**				**Standardised - 100 mg/l SPM**			**Concentration at pH 2**		
	Al	**Mn**	**Fe**	**SPM (mg/l)**	**Al**	**Mn**	**Fe**	**Al**	**Mn**	**Fe**
L. Tasman	1786	62.2	2091.4	226	790.3	27.5	925.4	649.1	12.3	667.1
L. Pukaki	73.6	2.5	111.7	4.46	1650.2	54.9	2505.6	549.22	10.5	286.8
L. Benmore – Ahuriri	2.9	3.9	17.7	0.65	446.6	600	2717.1	75.1	53.3	116.9
L. Aviemore	12.2	3.9	27.9	0.55	2222.9	714.4	5076.2	36	8.5	39.1
Waitaki River	13.3	0.9	23.4	1.8	736.5	49.2	1302.7	280.9	12.5	307.5

In **Chapter 3**, the gibbsite surface complexation model (SCM) was not found to adsorb appreciable concentrations of P. They were therefore excluded from the analysis. A comparison of the results determined in the experimental adsorption edge experiments, the HFO SCM and the gibbsite SCM are presented in **Table C10**.

Table C10. Adsorption Capacity of SPM for P, comparing experimental adsorption edge data in the pH range of 6-8 to the modelled adsorption capacity with the Diffuse Layer models with HFO and gibbsite.

Site	**Experimental Data**	**Modelled Data**	
	mg/g	**HFO**	**Gibbsite**
2. L. Tasman	0.14 – 0.27	0.21 - 0.32	0.01
4. L. Pukaki	0.07 – 0.18	0.04 - 0.08	0.004
6. L. Benmore – Ahuriri	0.08 – 0.12	0.04 - 0.06	0.001
7. L. Aviemore	0.03 – 0.1	0.05 - 0.08	0.001
8. Waitaki River	0.09 – 0.21	0.1 - 0.15	0.002

Adsorption Behaviour and Capacity for phosphorus (P): Surface sediments

The adsorption capacity of the surface sediments was determined in parallel with the SPM samples (**Figure C8 and Table C11**). The greatest adsorption capacity was determined in the sediment from the lower catchment Lake Benmore – Ahuriri Arm (0.26 mg/g). The lowest capacity was determined for the Lake Tasman sediment (0.20 mg/g). The different trend to the SPM was attributed to the sedimentation of fine glacial sediments in the down catchment lakes.

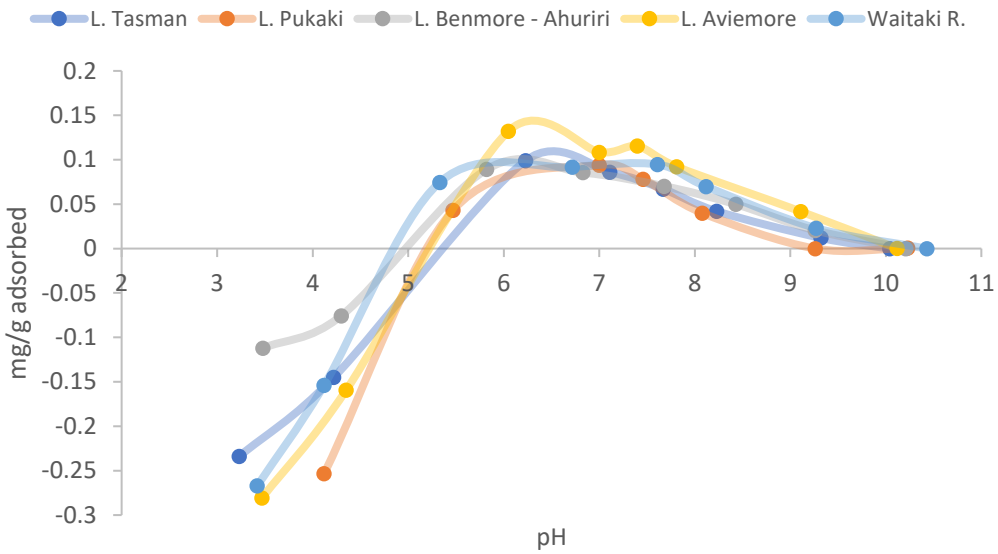

Figure C8 Adsorption edge for the adsorption of P onto surface sediments in the Waitaki catchment.

Table C11 Coefficients of determination (R^2) reported for Freudlich (F) and Langmuir (L) models fitted to the experimental adsorption isotherms for phosphorus (P) onto surface sediments. The maximum adsorption capacity of the SPM was determined with the Langmuir model (L. Qmax).

#	Site Name	SPM		
		Langmuir R^2	**Langmuir QMax (mg P/g SPM)**	**Freudlich R^2**
		Surface Sediments		
2	L. Tasman	0.975	0.195	0.889
4	L. Pukaki	0.963	0.256	0.928
6	L. Benmore - Ahuriri	0.926	0.245	0.985
7	L. Aviemore	0.974	0.211	0.977
8	Waitaki River	0.961	0.207	0.944

Adsorption Potential - Phosphorus

The data used to calculate the adsorption potential of the Waitaki catchment water for P in **Chapter 3, Section 3.3.2** is detailed in **Tables C12 and C13**.

Table C12. Data obtained from the Environment Canterbury (ECan) Open Data Portal was converted to mean, minimum and maximum SPM concentrations.

Site			**ECan Turbidity (NTU)**			**Converted (mg/l) SPM**		
	Distance	# ECan data	Mean	Min	Max	Mean	Min	Max
Lake Tasman	5	8	165.4	27.3	362	135.7	21.3	290.4
Lake Pukaki	45	83	10.9	0.8	61	9.0	1.4	53.5
Ahuriri	125	47	2.3	0.3	13.3	2.6	1.1	10.8
Lake Aviemore	140	38	2.3	0.2	19	2.6	1.0	15.1
Waitaki River	210	39	5.8	1.3	43	5.2	1.8	39.3

Table C13. The SPM concentration data detailed in Table B12 was multiplied by the maximum adsorption capacity of the SPM for P. The resulting 'adsorption potential' of the Waitaki Catchment water is reported in mg P/L.

Site	**mg/g SPM**	**Adsorption Potential (mg P/L)**		
	Langmuir Max	Mean	Min	Max
Lake Tasman	0.27	0.03663	0.00576	0.07840
Lake Pukaki	0.238	0.00215	0.00034	0.01273
Ahuriri	0.205	0.00053	0.00022	0.00222
Lake Aviemore	0.15	0.00039	0.00015	0.00226
Waitaki River	0.187	0.00097	0.00034	0.00736

Appendix D (Chapter 4)

Copper and Cadmium Speciation

The speciation of dissolved copper (Cu) and cadmium (Cd) was modelled in Visual Minteq 3.1 to assist in the interpretation of the experimental results (**Table D14**).

Table D14. Modelled Copper (Cu) and cadmium (Cd) speciation (%) as a function of pH.

	Copper Speciation	**Control Sample**				
pH	**Cu^{2+}**	**$CuCO3_{(aq)}$**	**$CuNO_3^+$**	**$CuOH^+$**	**$Cu(OH)_{2\ (aq)}$**	**$Cu(OH)^{3-}$**
5	97.7	0.0	2.0	0.2		
6	94.7	0.9	2.0	2.2		
7	67.0	15.2	1.4	15.6	0.3	
8	15.6	41.3	0.3	36.4	6.1	0.0
9	1.1	27.9	0.0	25.7	42.7	1.8
10	0.0	2.7		3.9	64.9	28.1
	Cadmium Speciation					
pH	**Cd^{2+}**	**$CdNO_3^+$**	**$CdOH^+$**	**$CdCO3_{(aq)}$**	**$Cd(OH)_{2\ (aq)}$**	
5	97.9	2.0				
6	97.9	2.0				
7	97.9	2.0	0.1			
8	97.3	2.0	0.6	0.1		
9	91.5	1.9	5.4	0.9	0.3	
10	49.9	1.0	29.2	3.1	16.7	
11	2.5	0.1	14.4	0.3	81.9	

Adsorption Potential – Copper and Cadmium

The data used to calculate the adsorption potential of the Waitaki catchment water for Cd and Cu in **Chapter 3, Section 3.3.2** is detailed in **D15 and D16.** The adsorption potential of the SPM for Cd and Cu with a theoretical concentration of 1 µg/L was determined using the Langmuir isotherms in **Chapter 4, Section 4.3.4.**

Table D15. The SPM concentration data detailed in **Table B12** was multiplied by the adsorption capacity of the SPM for Cd. The resulting 'adsorption potential' of the Waitaki Catchment water is reported in µg Cd/L.

Site	**µg/g Cd/g SPM**	**Adsorption Potential (µg Cd/L)**		
		Mean	Min	Max
Lake Tasman	2.1	0.271	0.047	0.589
Ahuriri	4.6	0.015	0.008	0.054
Lake Aviemore	2.9	0.010	0.005	0.047
Waitaki River	2.8	0.017	0.007	0.097

Table D16. The 'adsorption potential' of the Waitaki Catchment water for Cu in µg Cu/L.

Site	µg/g Cu/g SPM	Adsorption Potential (µg Cu/L)		
		Mean	Min	Max
Lake Tasman	42	5.698	0.895	12.196
Ahuriri	55	0.143	0.060	0.595
Lake Aviemore	66	0.171	0.066	0.996
Waitaki River	64	0.332	0.116	2.517

In **Chapter 4**, the gibbsite surface complexation model (SCM) was not found to adsorb any appreciable concentrations of either Cd or Cu. The model was therefore excluded from the chapter. A comparison of the modelled pH_{50} values and adsorption capacities (mg Cd or Cu/g SPM) compared to the experimental data is presented in **Table D17**. It can be seen that the pH_{50} values determined by the model were ~3 pH units greater than what was determined experimentally. The modelled adsorption capacities were also negligible (< 0.1 mg Cd or Cu/g SPM).

Table D17. Modelled pH_{50} and adsorption capacities of the gibbsite SCM model applied in Chapter 4.

	Cadmium pH 50			Copper pH50		
Site	**Experimental**	HAO	mg/g	**Experimental**	HAO	mg/g
L. Tasman	**7.2**	9.8	0.03	**6.6**	7.5	0.009
L. Benmore -Ahuriri	**6.9**	9.8	0.005	**6.2**	7.7	0.002
L. Aviemore	**7**	9.8	0.007	**6.2**	7.5	0.002
Waitaki River	**6.8**	9.8	0.013	**5.5**	7.5	0.004

Appendix E (Chapter 5)

The Onyx River flow, temperature and conductivity recorded at the Vanda Weir during the 2016/17 melt season is presented in **Figure E18**. This data was supplied by the McMurdo LTER.

The first flow was recorded at the Vanda Weir on the 13th December and was < 1000 L/s for the first week. The flow increased, generally remaining between 1000 - 1600 L/s, until the 6th January. After this period, the flow progressively decreased and remained low (< 500 L/s) before ceasing on the 4th February. The highest conductivity, between 80 – 120 µS/cm, was measured in the first two

weeks of flow. It then settled to 40- 60 µS/cm for the remaining period. The temperature was highly variable and diurnal, ranging from 0.5 - 7^{0}C during the flow period.

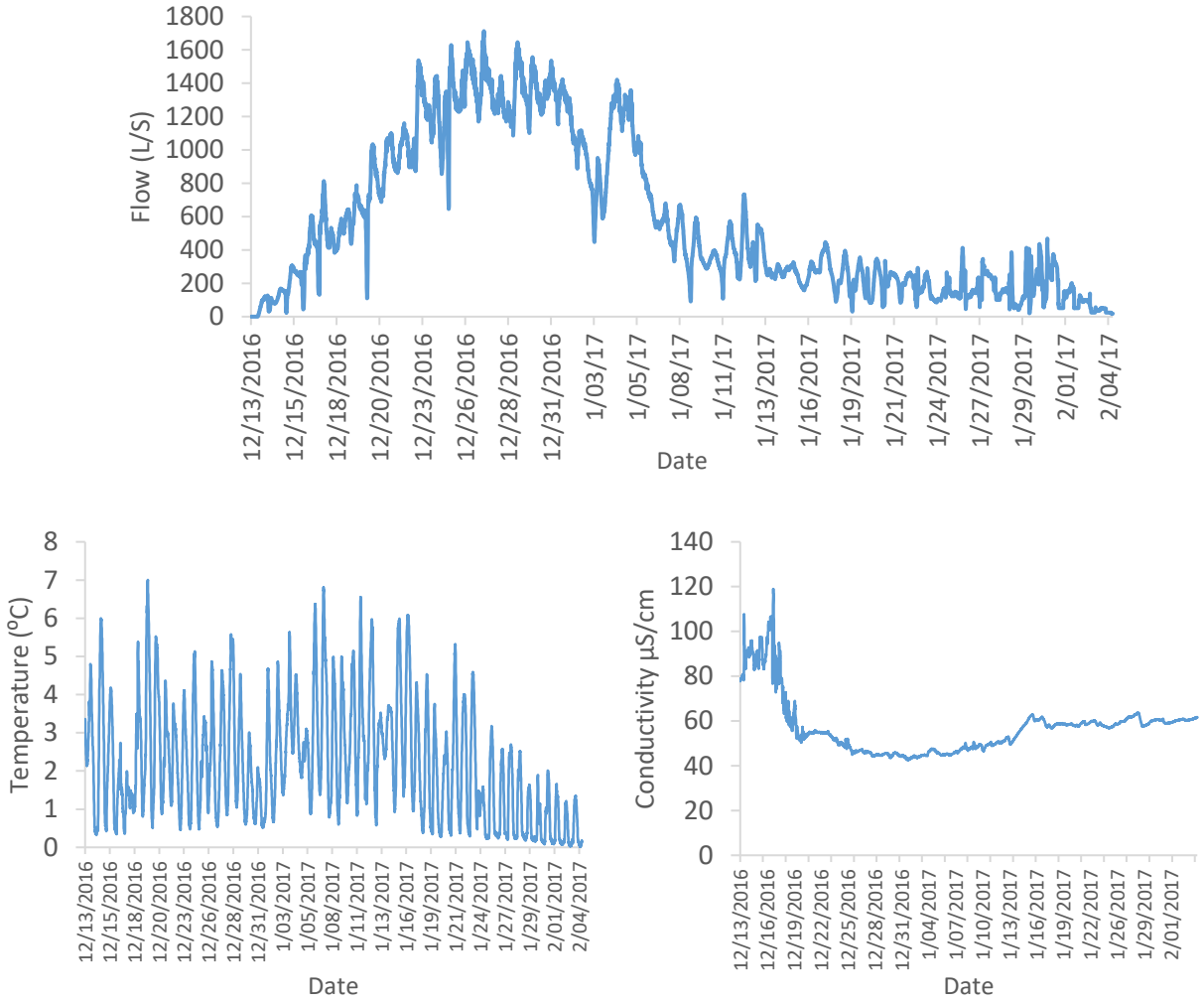

Figure E18. Top – The flow of the Onyx River at the Vanda Weir during the 2016/17 field season. Bottom Left – Temperature of the Onyx River Water. Bottom Right – Conductivity of the Onyx River water. Data recorded every 15 minutes. Calibrated data supplied by the McMurdo LTER.

Appendix F (Chapter 6)

Modelling

The parameters used to model the adsorption of phosphorus (P) onto HFO using the Diffusive Layer Model in Visual Minteq are detailed in **Table E18**. The model, assuming HFO to be the only

adsorbing surface, was generated using the concentration of dissolved Fe. This was connected to the 'possible' formation of ferrihydrite in the software.

Table E18. Parameters used to model the adsorption of P onto the SPM collected from the Onyx River at Vanda Weir.

Site			Molar		(mg/L)	(µg/L)		
	pH	pE	Na	NO3	$CO3^{2-}$	Al	Mn	Fe
Onyx River - Vanda	3 - 10.5	9	0.01	0.01	4.5	271.8	6.5	209.5

Appendix References

Anderson SP, Longacre SA, Kraal ER. Patterns of water chemistry and discharge in the glacier-fed Kennicott River, Alaska: evidence for subglacial water storage cycles. Chemical Geology 2003; 202: 297-312.

APHA. Standard methods for the examination of water and wastewater. American Public Health Association, Washington, D.C., 2005.

Bibby RL, Webster-Brown JG. Trace metal adsorption onto urban stream suspended particulate matter (Auckland region, New Zealand). Applied Geochemistry 2006; 21: 1135-1151.

Chapman DV, Organization WH, Press C. Water quality assessments: a guide to the use of biota, sediments and water in environmental monitoring: E & Fn Spon London, 1996.

Chillrud SN, Pedrozo FL, Temporetti PF, Planas HF, Froelich PN. Chemical Weathering of Phosphate and Germanium in Glacial Meltwater Streams: Effects of Subglacial Pyrite Oxidation. Limnology and Oceanography 1994; 39: 1130-1140.

Chinn T, Mason P. The first 25 years of the hydrology of the Onyx River, Wright Valley, Dry Valleys, Antarctica. Polar Record 2015; 52: 16-65.

Föllmi KB, Hosein R, Arn K, Steinmann P. Weathering and the mobility of phosphorus in the catchments and forefields of the Rhône and Oberaar glaciers, central Switzerland: Implications for the global phosphorus cycle on glacial–interglacial timescales. Geochimica et Cosmochimica Acta 2009; 73: 2252-2282.

Hedley CB, Saggar S, Theng BKG, Whitton JS. Surface area of soils of contrasting mineralogies using para-nitrophenol adsorption and its relation to air-dry moisture content of soils. Soil Research 2000; 38: 155-168.

Knutsson J, Rauch S, Morrison GM. Estimation of Measurement Uncertainties for the DGT Passive Sampler Used for Determination of Copper in Water. International Journal of Analytical Chemistry 2014; 2014: 7.

Kreuzeder A, Santner J, Zhang H, Prohaska T, Wenzel WW. Uncertainty Evaluation of the Diffusive Gradients in Thin Films Technique. Environmental Science & Technology 2015; 49: 1594-1602.

Phillips JM, Russell MA, Walling DE. Time-integrated sampling of fluvial suspended sediment: a simple methodology for small catchments. Hydrological Processes 2000; 14: 2589-2602.

Theng BKG. On measuring the specific surface area of clays and soils by adsorption of para-nitrophenol: use and limitations. Clays: Controlling the Environment, Proceedings of the 10th International Clay Conference, Adelaide, Australia, CSIRO Publications, Melbourne, 1995, pp. 302-308.

Warnken KW, Zhang H, Davison W. Accuracy of the Diffusive Gradients in Thin-Films Technique: Diffusive Boundary Layer and Effective Sampling Area Considerations. Analytical Chemistry 2006; 78: 3780-3787.

Webster-Brown JG, Dee TJ, Hegan AF. Metal removal via particulate material in a lowland river system. Water Sci Technol 2012; 66: 1439-45.

Zhang H, Davison W. Performance Characteristics of Diffusion Gradients in Thin Films for the in Situ Measurement of Trace Metals in Aqueous Solution. Analytical Chemistry 1995; 67: 3391-3400.

Zhang H, Davison W, Gadi R, Kobayashi T. In situ measurement of dissolved phosphorus in natural waters using DGT. Analytica Chimica Acta 1998; 370: 29-38.

Zulfiqar U, Subhani T, Wilayat Husain S. Towards tunable size of silica particles from rice husk. Journal of Non-Crystalline Solids 2015; 429: 61-69.